# CHARACTERISATION OF PHOSPHATIDYLTHREONINE IN HUMAN BLOOD

Ali A Y Gh H H M Hajeyah

A thesis submitted to Cardiff University in partial fulfilment of the requirements
for the degree of

Doctor of Philosophy (PhD)


September 2022

# ACKNOWLEDGMENTS

The work presented herein is the culmination of three years of research. None of this would have been possible without the support and guidance of my supervisors: Prof. Valerie O'Donnell and Prof. Peter Collins. Another catalyst for this work was the generous scholarship from Kuwait University. I am also grateful to Prof. Yugo Iwasaki (Chubu University) for providing lipid standards and Dr. Majd Protty for the clinical cohort samples.

My thanks are also extended to:

- My parents and three brothers.
- My friends.
- The Cardiff Lipidomics Group.
- Dr. Vince Jenkins.
- Dr. Zaheer Yousef.
- Hala Mohammed and the Kuwait Cultural Office in London.

# SUMMARY

Phosphatidylthreonine (PT) is an anionic phospholipid that was previously reported in animal tissues, cell cultures, bacteria, and protozoa, but not human tissues. PT is a structural analogue of phosphatidylserine (PS), a phospholipid with a recognised role in blood coagulation. This thesis investigates the occurrence of PT in human blood and its potential roles in blood coagulation and coronary artery disease.

Using liquid chromatography–tandem mass spectrometry (LC-MS/MS), I demonstrated the presence of PT in human blood, platelets, extracellular vesicles (EV), and leukocytes. PT was enriched in the inner membrane leaflet of resting platelets but was externalised into the outer leaflet in response to thrombin activation. Additionally, total platelet PT decreased in response to thrombin activation. These findings suggest roles for PT in platelet activation and aggregation. Next, I investigated the ability of PT to support coagulation *in vitro* using coagulation assays. PT supported coagulation through enhancement of prothrombinase activity but not extrinsic tenase activity. This suggests that PT functions in the propagation but not initiation of coagulation, contrasting with PS which functions in both processes. Last, I measured PT in platelets, EVs, and leukocytes from a clinical cohort of coronary artery disease. PT was significantly higher in platelets and EVs from the disease groups compared to healthy volunteers, suggesting a link between PT and coronary artery disease.

In summary, PT is a native lipid in human blood cells, possesses procoagulant properties *in vitro*, and its levels are significantly higher in platelets and EVs from coronary artery disease patients compared to healthy volunteers. However, many aspects of PT's biochemistry are unknown, including its metabolism, functions *in vivo*, and involvement in vascular disease.

# ABBREVIATIONS

| | |
|---|---|
| ACS | Acute coronary syndrome / acute coronary syndrome patient group |
| ADP | Adenosine diphosphate |
| ATP | Adenosine triphosphate |
| $Ca^{2+}$ | Calcium ion |
| CAD | Coronary artery disease / coronary artery disease patient group |
| CAT | Calibrated automated thrombinography |
| $cPLA_2$ | Cytosolic phospholipase $A_2$ |
| CTI | Corn trypsin inhibitor |
| Da | Dalton (unified atomic mass unit) |
| ER | Endoplasmic reticulum |
| ESI | Electrospray ionisation |
| EV | Extracellular vesicle |
| FA | Fatty acid / fatty acyl |
| HC | Healthy control group |
| HETE | Hydroxyeicosatetraenoic acid |
| HILIC | Hydrophilic interaction chromatography |
| HpETE | Hydroperoxyeicosatetraenoic acid |
| $iPLA_2$ | Calcium-independent phospholipase $A_2$ |
| IS | Internal standard |
| LC-MS/MS | Liquid chromatography tandem mass spectrometry |

| | |
|---|---|
| LUV | Large unilamellar vesicle |
| LysoPL | Lysophospholipid |
| LysoPS | Lysophosphatidylserine |
| LysoPT | Lysophosphatidylthreonine |
| *m/z* | Mass-to-charge ratio |
| MLV | Multilamellar vesicle |
| MRM | Multiple reaction monitoring |
| MS | Mass spectrometry |
| $MS^n$ or MS/MS | Tandem mass spectrometry ($n$ = 2 or 3) |
| NHS-biotin | N-hydroxysuccinimide biotin |
| NL | Neutral loss |
| PA | Phosphatidic acid |
| PAR | Protease-activated receptor |
| PC | Phosphatidylcholine |
| PE | Phosphatidylethanolamine |
| PG | Phosphatidylglycerol |
| PI | Phosphatidylinositol |
| PL | Phospholipid (glycerophospholipid) |
| PPP | Platelet poor plasma |
| PS | Phosphatidylserine |
| PSS | PS synthase |
| PT | Phosphatidylthreonine |

| | |
|---|---|
| PTS | Phosphatidylthreonine synthase |
| PUFA | Polyunsaturated fatty acid |
| RBC | Red blood cell |
| RF | Risk factor patient group |
| RP | Reversed phase chromatography |
| *sn*-1/*sn*-2 | Stereospecific numbering system |
| TF | Tissue factor |
| UVPD | Ultraviolet photodissociation |

# TABLE OF CONTENTS

# CHAPTER 1 General Introduction

## 1.1 Phospholipids and membrane asymmetry

Lipids are hydrophobic or amphipathic small biomolecules which function in membrane structure, energy storage, and as chemical messengers. The LIPID MAPS consortium currently recognizes eight classes of lipids: fatty acyls, glycerolipids, glycerophospholipids, sphingolipids, sterol lipids, prenol lipids, saccharolipids, and polyketides (1). Glycerophospholipids (shortened to phospholipids, PL), consist of a glycerol backbone, two acyl or alkyl chains, and a head group of phosphate linked to an alcohol. In mammalian tissues, common PL head group modifications include choline, ethanolamine, serine, and inositol (**Figure 1.1**). Fatty acids (FA) at the *sn*-1 position are typically saturated, while those at the *sn*-2 position are unsaturated. Double bonds in FAs occur at different positions along the hydrocarbon chain and could exist in a cis or trans configuration, with the cis configuration predominating in mammalian tissues (2).

Phospholipids are major constituents of cell membranes, along with cholesterol, sphingomyelin, and proteins. PL species are asymmetrically distributed between the plasma membrane's inner and outer leaflets, with phosphatidylserine (PS) and phosphatidylethanolamine (PE) enriched in the inner leaflet, while phosphatidylcholine (PC) predominates in the outer leaflet (3). This asymmetric distribution is regulated by membrane proteins that transport PLs between the inner and outer leaflets (**Figure 1.2**). These include flippases (move PLs inwards), floppases (move PLs outwards), and scramblases (bidirectional) (3). Changes to PL asymmetry in membranes mediates apoptosis and blood coagulation. In the former, externalised PS on apoptotic cells constitutes an "eat-me" signal which is recognized by macrophages for efferocytosis, whereas in the latter externalised PS binds coagulation factors, enabling them to form complexes and ultimately support thrombus formation (4, 5).

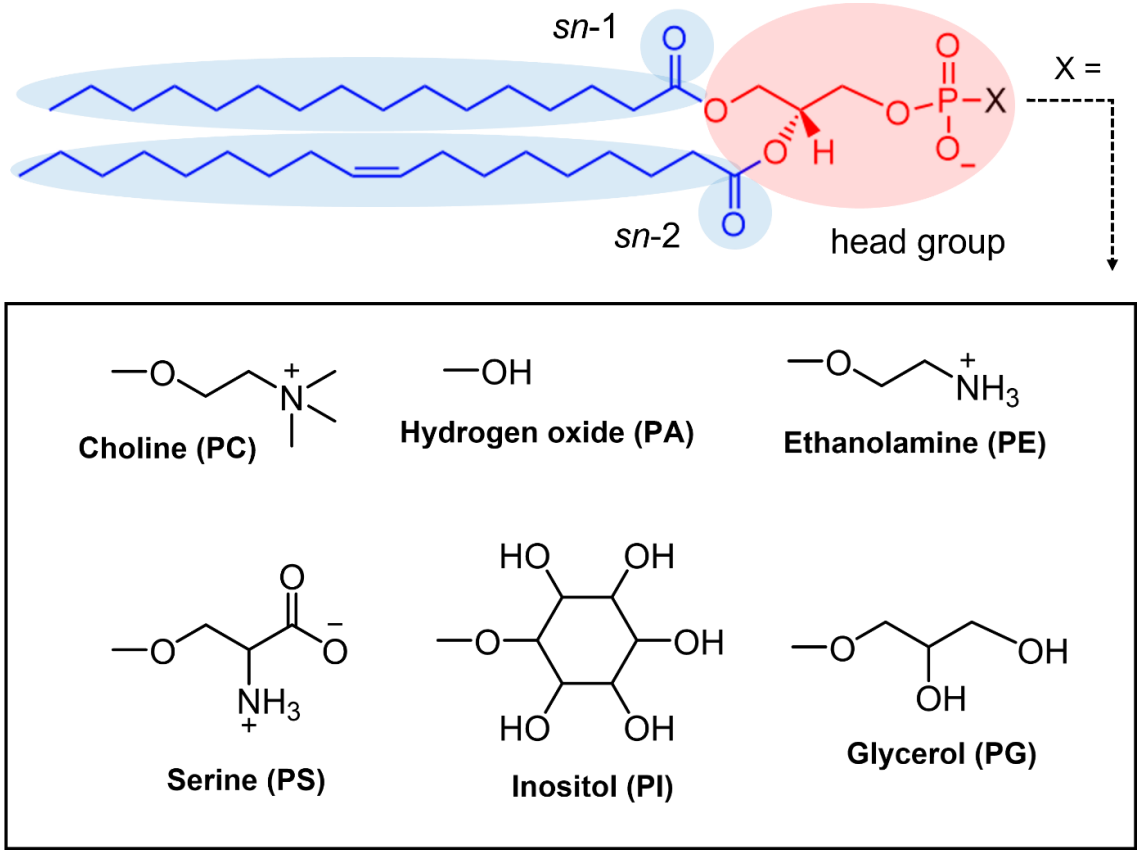


**Figure 1.1 – General structure of a glycerophospholipid and common mammalian head groups**

Phospholipids comprise a polar head group (red) and two nonpolar tails (blue). The phosphate head group can be modified with several moieties. Choline and ethanolamine contain positively charged groups, while serine is zwitterionic at pH 7.35. Fatty acids are attached to the *sn*-1 and *sn*-2 positions of the glycerol backbone. PC: phosphatidylcholine, PA: phosphatidic acid, PE: phosphatidylethanolamine, PS: phosphatidylserine, PI: phosphatidylinositol, PG: phosphatidylglycerol.

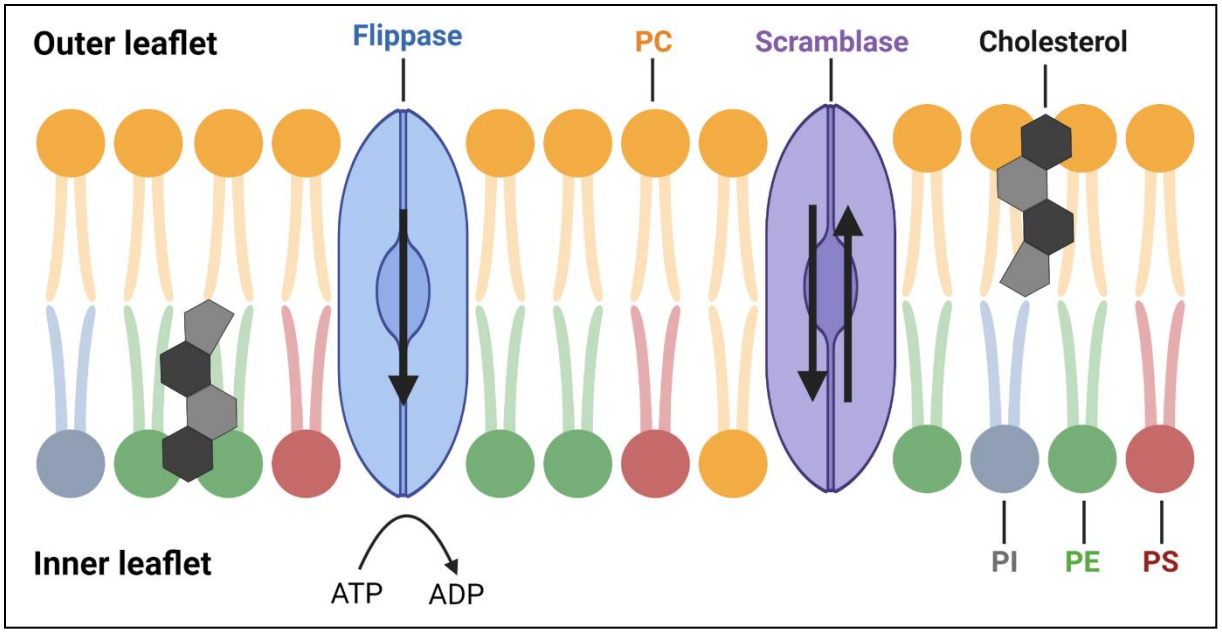


**Figure 1.2 – Cartoon representation of the plasma membrane, highlighting the asymmetric distribution of phospholipids and some membrane proteins involved in maintaining it**

Flippases (e.g., aminophospholipid translocase) catalyse an ATP-dependent inwards movement of PE and PS. Scramblases catalyse the bidirectional movement of phospholipid along their concentration gradient. Floppases (not depicted) catalyse an ATP-dependent outwards movement of PC. PC: phosphatidylcholine, PE: phosphatidylethanolamine, PS: phosphatidylserine, PI: phosphatidylinositol, ATP: adenosine triphosphate, ADP: adenosine diphosphate. Figure created using BioRender.com.

## 1.2 Blood coagulation

Coagulation is a process by which blood changes from a liquid to a gel to support haemostasis. It is tightly regulated through a balance of procoagulant and anticoagulant biomolecules. Deficiencies in coagulation factors lead to excessive bleeding, such as in haemophilia, while uncontrolled coagulation results in vascular blockage and thrombosis (6). The coagulation system consists of a series of proteins (coagulation factors) that are activated in series to amplify a signal that eventually leads to the formation of an insoluble mesh that stops bleeding.

Traditionally, coagulation has been described by a cascade model (**Figure 1.3**) in which two pathways, termed the extrinsic (or tissue factor) pathway and the intrinsic (or contact) pathway, may be activated separately then converge at a common pathway (7). The extrinsic pathway is initiated by tissue factor (TF), a membrane protein found in subendothelial tissue and normally not found in circulation (7). Damage to the endothelial wall releases TF into circulation, which then binds and activates factor VII into VIIa (7). The association of TF and VIIa constitutes the extrinsic tenase complex which converts factor X into Xa, a component of the common pathway. On the other hand, the intrinsic pathway is initiated by factor XII, prekallikrein, and high-molecular weight kininogen. Contact of blood with negatively charged surfaces (e.g., glass and diatomite) activates XII into XIIa, which converts prekallikrein into kallikrein. Here, a positive feedback loop is initiated because kallikrein activates XII (6, 8). The XIIa generated then activates factor XI into XIa, which in turn converts factor IX into IXa. The association of factors IXa and VIIIa forms the intrinsic tenase complex which converts factor X into Xa (7). The common pathway involves the formation of the prothrombinase complex, an association between factors Xa and Va, which converts factor II (prothrombin) into IIa (thrombin). Thrombin then converts factor I (fibrinogen) into Ia (fibrin) and activates factor XIII into XIIIa. Fibrin is insoluble in water and spontaneously polymerises, and factor XIIIa crosslinks fibrin, stabilising it (9).

The cascade model of coagulation poorly predicts the clinical manifestations of individual coagulation factor deficiencies. For example, a deficiency in factor XII is not associated with a bleeding tendency, while deficiencies in factors VIII and IX result in haemophilia A and B, respectively, despite XII activation being considered as the initiator of the intrinsic pathway (6). This suggests inaccuracies in the traditional (intrinsic/extrinsic pathway) model. A cell-based

model of coagulation has been proposed to explain these observations (10). The model emphasises the interactions of coagulation factors with TF-bearing cells and platelets and comprises three stages: initiation, amplification, and propagation (**Figure 1.4**). In the initiation stage, TF (on the surface of subendothelial cells) released into circulation binds factor VII and activates it, then the complex of TF and VIIa generates factor Xa, which subsequently generates small amounts of factor IIa (thrombin). In the amplification stage, thrombin activates factors VIII, XI, and V through proteolytic cleavage at specific sites. Additionally, thrombin activates platelets through their protease-activated receptors (PARs) (detailed in **Section 1.4**). The propagation stage occurs on the surface of activated platelets and involves the generation of very large amounts of thrombin. Factor XIa converts factor IX into IXa, which forms a complex with factor VIIIa (intrinsic tenase) that converts factor X into Xa. This is followed by the formation of the prothrombinase complex (Xa:Va) which generates thrombin. Generated thrombin activates factors I (fibrinogen) and XIII, forming crosslinked fibrin, and amplifies its own generation by activating factors VIII, XI, and V (11). These coagulation reactions occur on membrane surfaces such as those of platelets and TF-expressing cells. There, membrane phospholipids like PS bind clotting factors to facilitate the assembly of the tenase (intrinsic and extrinsic) and prothrombinase complexes.

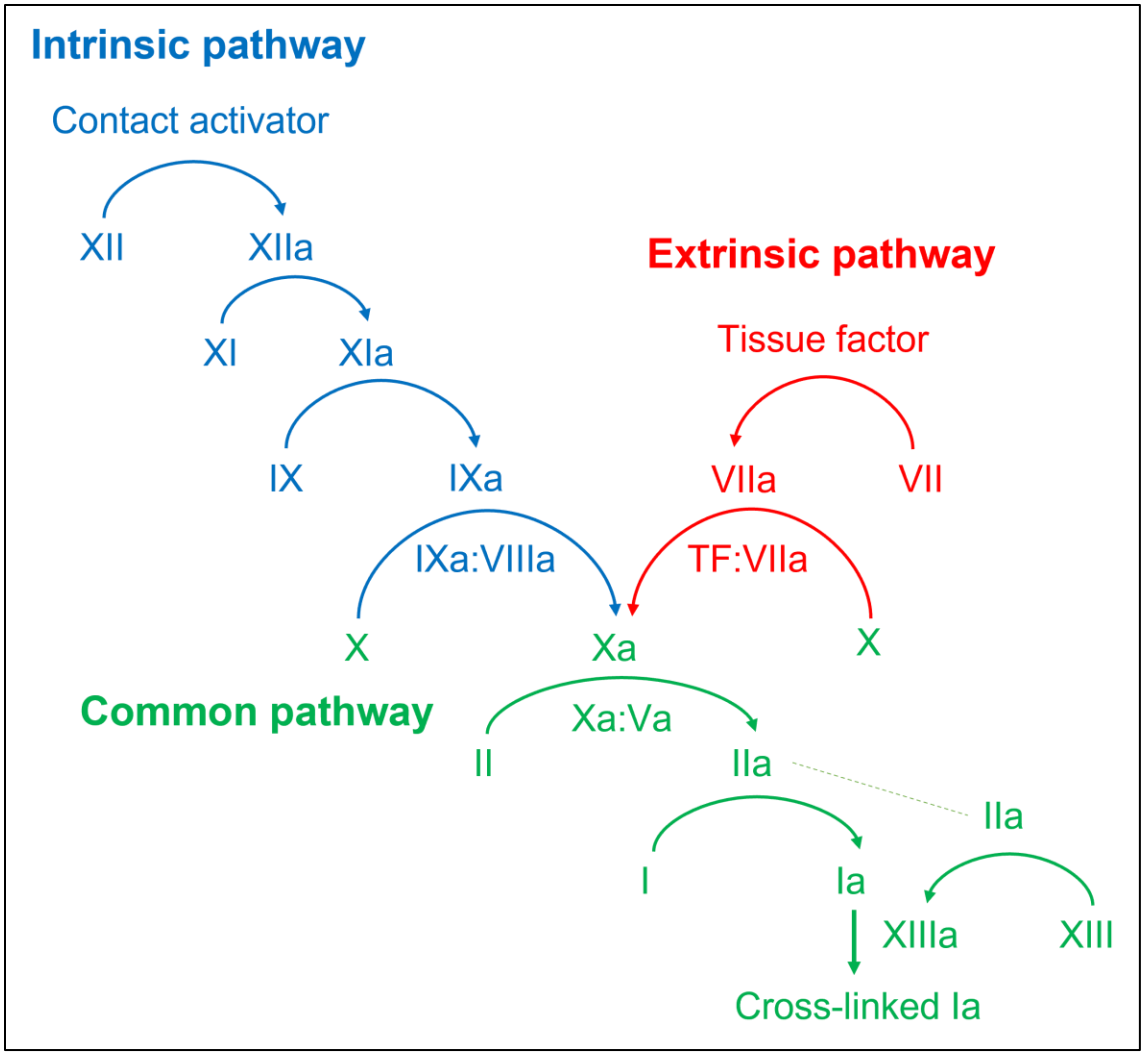


**Figure 1.3 – Simplified diagram of the cascade model of coagulation**

The cascade model describes two pathways that may be activated separately: the intrinsic pathway (blue) and the extrinsic pathway (red), then converge into a common pathway (green). Note, most of these reactions occur on membrane surfaces and require calcium ions (not depicted).

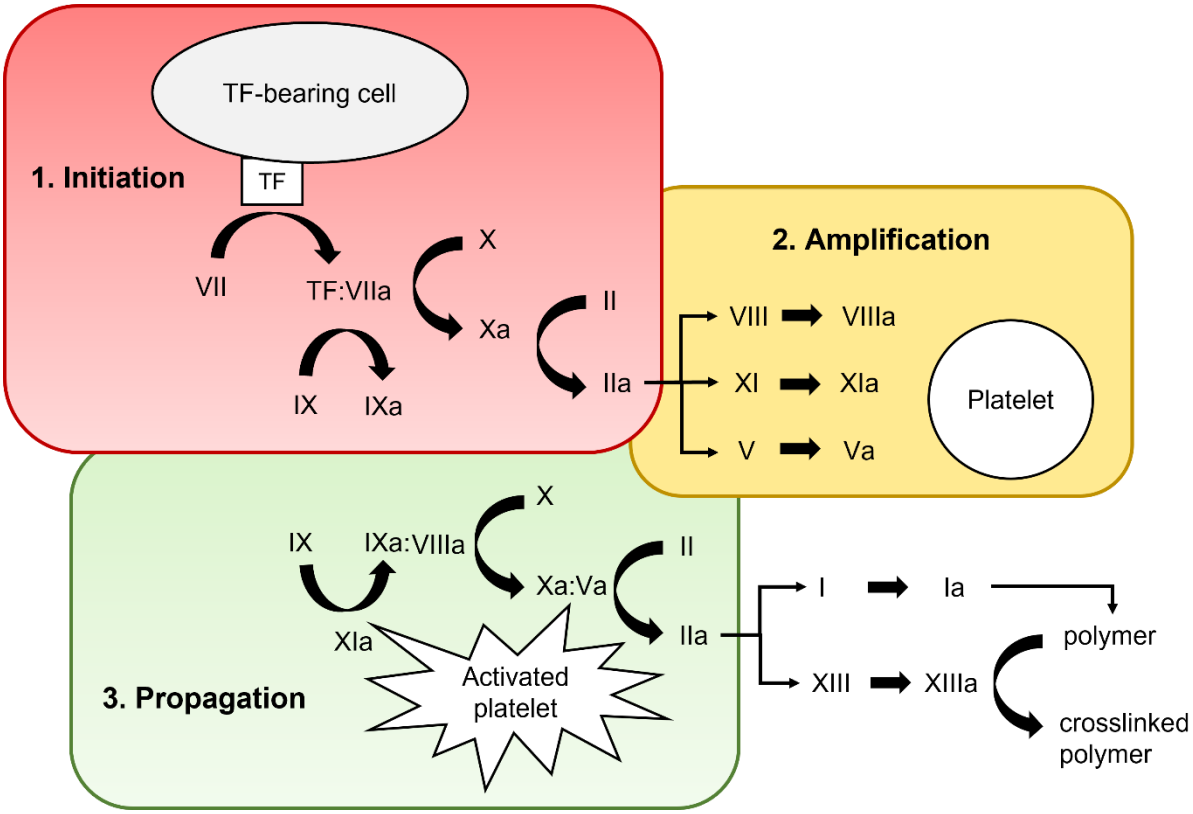


**Figure 1.4 – Simplified illustration of the cell-based model of coagulation**

The cell-based model of coagulation comprises three stages: initiation, amplification, and propagation. The initiation stage occurs on the surface of TF-bearing cells and involves the formation of small amounts of thrombin (IIa). In the amplification stage, thrombin activates factors VIII, XI, V through proteolytic cleavage, as well as platelets through their protease-activated receptors. The propagation stage occurs on the surface of activated platelets and involves the generation of massive amounts of thrombin through the prothrombinase complex (Xa:Va) by a positive feedback mechanism. This is supported by factors XIa and VIIIa (made in the amplification stage) through the production of Xa. Generated thrombin activates factors I (fibrinogen) and XIII, leading to the formation of crosslinked Ia (fibrin) polymer. Furthermore, thrombin amplifies its own generation by activating factors VIII, XI, and V (amplification stage).

## 1.3 Metabolism of phosphatidylserine

PS is an anionic PL that functions in coagulation (structure in **Figure 1.1**) (12). It possesses a net negative charge at physiological pH (7.35) and constitutes up to 10% of total lipids in mammalian cells (13). PS in human cells is synthesized by two distinct phosphatidylserine synthase (PSS) enzymes, PSS1 and PSS2, through base-exchange reactions. Both isoforms are integral membrane proteins embedded in mitochondria-associated membranes, distinct regions of the endoplasmic reticulum (ER) (14). PSS1 and PSS2 mRNAs (in mice) are widely expressed in tissues, with PSS1 mRNA most abundant in kidney, brain, and liver, while PSS2 mRNA is enriched in testes and brain (15, 16). PSS1, but not PSS2, is a housekeeping enzyme, i.e., it is present in virtually all human cells (17). PSS1 converts both PC and PE to PS *in vitro*, but prefers PC as a substrate *in vivo*, while PSS2 only converts PE to PS (18). Notably, PSS2 exhibits a preference for PE with FA 22:6 in the *sn*-2 position (18, 19).

PS can be metabolized in several ways depending on its site. In mitochondria, PS is converted to PE by PS decarboxylase (20). PS in the inner plasma membrane leaflet can be hydrolysed by cytosolic phospholipase $A_2$ ($cPLA_2$) releasing 1-acyl-lysophosphatidylserine (1-acyl-lysoPS) and a FA, typically a polyunsaturated fatty acid (PUFA) that can be oxygenated into oxylipins. In plasma, PS on cell surfaces can be hydrolysed by a secreted PS-specific phospholipase $A_1$ into 2-acyl-lysoPS (21). However, this enzyme is expressed in rat but not human platelets (22). Therefore, the relevance of this pathway in human physiology is unclear.

## 1.4 Platelet activation and blood coagulation

Coagulation reactions occur on PS-containing surfaces such as those of activated platelets and extracellular vesicles (EVs). Platelets are anucleate, discoid shaped blood cells (2–4 μm in diameter) derived from megakaryocytes, that have a lifespan of 7–10 days in the circulation (23). Platelets contain three types of granules: alpha granules, dense granules, and lysosomes. Of note, alpha granules contain adhesion proteins (e.g., P-selectin and von Willebrand factor) and coagulation factors (e.g., factors V and IX), whereas dense granules contain divalent cations ($Ca^{2+}$ and $Mg^{2+}$), polyphosphates, bioactive amines, and nucleotides. Platelets can be activated by several ligands including thrombin, adenosine diphosphate (ADP), and thromboxane $A_2$ (24).

Thrombin signals using protease-activated receptors (PAR), which are activated by proteolytic cleavage. In human platelets, PAR1 and PAR4 account for the thrombin response (25). On the other hand, ADP activates platelets through purinergic P2Y receptors, which are targeted by antiplatelet drugs for the treatment of acute coronary syndrome (ACS). The downstream effects of these receptors (PAR and P2Y) include an increase in cytosolic $Ca^{2+}$ concentration. This activates several proteins including cytosolic phospholipase $A_2$ ($cPLA_2$), gelsolin, calpain, and scramblase. $cPLA_2$ releases arachidonic acid from the *sn*-2 positions of membrane PLs to serve as precursors for the biosynthesis of oxylipins such as 12-hydroxyeicosatetraenoic acid (HETE) and thromboxane $A_2$, the latter of which is secreted to stimulate the activation of other platelets (26). Gelsolin and calpain cleave actin filaments, leading to membrane blebbing and release of procoagulant EVs. Scramblase facilitates PS and PE externalisation to the outer leaflet of the plasma membrane, where they can interact with clotting factors (27). Scramblase function is also required for EV release, as evident by the impaired release of EVs from platelets in Scott syndrome (a disorder with defective scramblase) patients (28). However, the exact details of the involvement of scramblase in EV release are unclear.

To summarize, activated platelets support coagulation through a multitude of mechanisms. These include the secretion of coagulation factors and platelet activators (ADP and thromboxane $A_2$), the externalisation of PS to support coagulation reactions on their surfaces, and the release of procoagulant EVs. Consequently, measurement of PS in platelets and EVs could be useful in understanding the pathophysiology of vascular disease but remains poorly explored (more details in **Section 1.6**).

## 1.5 Binding of coagulation factors to membrane phosphatidylserine

Coagulation factors bind membrane PS via one of two domains: a Gla domain or a C2-like discoidin domain (shortened to C2 domain) (**Figure 1.5**). Gla domains are rich in gamma-carboxyglutamyl residues which strongly bind $Ca^{2+}$ ions (**Figure 1.5A**). Calcium binding facilitates the proper folding of the domain and correctly orients the protein on the PS-containing membrane (29). Gla domains are found in factors II, VII, IX, and X, and bind PS with varying affinities (12, 30). For example, factor VII binds PA more strongly than PS (31). Gla domains

also contain a conserved stretch of hydrophobic residues in the shape of the Greek letter ω, termed the "omega loop". involved in membrane binding (32). Importantly, the binding of Gla domains to PS is greatly enhanced by PE (12).

The C2 domains of coagulation factors Va and VIIIa bind PS independently of $Ca^{2+}$ (33, 34). However, $Ca^{2+}$ ions are required for the assembly of factor Va's subunits and consequently its function in the prothrombinase complex (35). The C2 domain of factor Va binds PS through three spikes that are enriched in hydrophobic and positively charged residues (36) (**Figure 1.5B**).

In a physiological context, optimal binding of coagulation factors to membranes requires externalised PS and PE on the surfaces of platelets, leukocytes, and EVs. As previously noted, PS and PE are normally found in the inner plasma membrane leaflet. However, upon cell activation, the lipids are externalised through the activation of scramblase and inhibition of aminophospholipid translocase (3, 27). Coagulation factors have been shown to concentrate in cap structures on the surface of activated platelets (37). This suggests that PS and PE are colocalised in membrane microdomains to support protein binding. This colocalization could be due to both lipid classes (PS and PE) being externalised by scramblase. One prediction of this hypothesis is that externalised PS and PE would be found in the vicinity of scramblase, but this requires experimental proof.

Other phospholipids such as PA, PI, PG, and enzymatically oxidized phospholipids have also been shown to enhance the ability of PS to support coagulation (30, 38). The "anything but choline" hypothesis predicts that any phospholipid, expect PC due to its bulky head group, can synergize with PS to enhance coagulation (30).

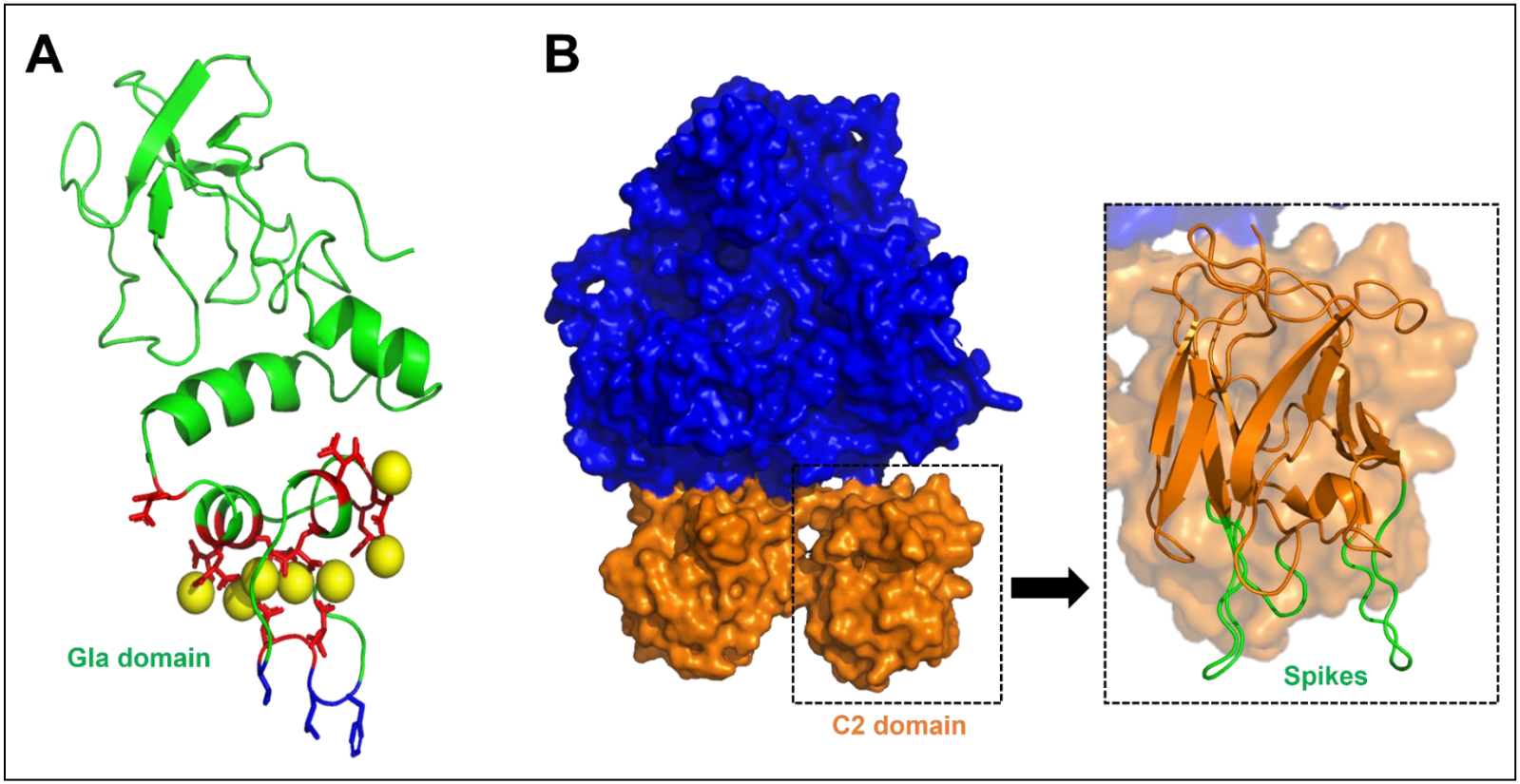


**Figure 1.5 – Structures of PS-binding domains in coagulation factors**

(A) Ribbon diagram of the Gla domain of bovine prothrombin (PDB ID: 2PF2). The Gla domain binds seven calcium ions (yellow) through its γ-carboxyglutamyl residues (red). The calcium ions facilitate the proper folding of the domain and bridge the protein to the negatively charged PS in the membrane. Hydrophobic residues (blue) in the omega loop facilitate membrane binding. (B) Surface representation of human factor Va (PDB ID: 7KXY) with overlayed ribbon diagram of the C2 domain of human factor V (PDB ID: 1CZS). The C2 domain (orange) contains three spikes (green) that are enriched in hydrophobic and positively charged residues, allowing PS binding. Figures were generated using PyMOL2 (Schrödinger, Inc) and structures from the protein data bank (PDB) (39).

## 1.6 Thrombosis and coronary artery disease

Thrombosis occurs when a blood clot forms inside a blood vessel. This restricts normal blood flow to tissues and organs, resulting in damage. Coronary artery disease (CAD) is characterized by the build-up of plaques in the coronary artery wall, leading to its narrowing. Thrombus formation in CAD patients could result in partial or complete occlusion of the coronary artery, manifesting as acute coronary syndrome (ACS), which is a medical emergency. Following ACS, patients remain at high risk of developing recurrent cardiovascular events, at least partly due to platelet dysfunction (40-42).

Platelets in CAD patients undergo a higher rate of turnover compared to healthy individuals (43, 44). This leads to a higher fraction of immature platelets in the circulation of patients (45). These platelets have been termed “reticulated platelets” and exhibit a larger size, higher RNA content, and contain higher amounts of rough ER, mitochondria, and granules (both alpha and dense granules) compared to mature platelets (45-49). Generally, immature platelets have been shown to be more reactive than mature platelets, and have been implicated in not only CAD, but also diabetes (50). There are currently no studies comparing the lipidomes of immature and mature platelets. Similarly, there are no comprehensive reports on the lipid composition of EVs in health versus CAD. As noted previously, activated platelets shed procoagulant EVs into circulation, and CAD patients exhibit higher EV counts compared to healthy individuals (51-54). This could translate to a higher proportion of procoagulant lipids in the circulation of CAD patients. As such, measurement of procoagulant lipids (e.g., PS) in EVs could be useful in understanding the higher risk of thrombosis in CAD.

The role of lipid membranes in driving pathological thrombosis is not utilized in medicine for the screening or prevention of cardiovascular events. Medical intervention usually involves antiplatelet drugs (e.g., aspirin) or anticoagulants which inhibit coagulation factors (e.g., rivaroxaban). Insight into the involvement of procoagulant lipids in thrombosis could lead to the development of novel treatments that target lipids.

## 1.7 History of phosphatidylthreonine research

Phosphatidylserine (PS) has and continues to be the target of extensive research. This is evident by the term "phosphatidylserine" yielding more than 19,000 results on the Web of Science search engine. In contrast, other another phospholipid with an amino acid head group, phosphatidylthreonine (PT), has been neglected despite its discovery in 1957. As of September 2022, a search for "phosphatidylthreonine" using the Web of Science yields 12 results, none of which describes research on human tissues. PT is a structural analogue of PS, differing by a single methyl group in PT compared to PS (**Figure 1.6**). This raises the question whether PT, like PS, is found in human blood and if so, whether it also functions in blood coagulation or other biological processes where PS is involved. First, I provide a comprehensive timeline of PT research and highlight current gaps in knowledge (**Figure 1.7**).

The existence of PT was first hinted by Rhodes and Lea in 1957, where the authors analysed the PL composition of chicken egg (55). Acid hydrolysis of egg PL and derivatization with 1-fluoro-2,4-dinitrobenzene generated two acidic compounds, as judged by paper chromatography. One was identified as serine and the other was proposed to be threonine (55). In 1958, Igarashi *et al*. detected a threonine-containing PL in tuna muscle using acid hydrolysis and 2,4-dinitrophenylhydrazine derivatization (56). Notably, the proposed structure contained hexadecanoic acid (FA 16:0) and octadecenoic acid (FA 18:1) chains. Shortly after, a chemical synthetic route for PT was described by Baer and Eckstein (57).

In 1966, Porcellati *et al*. found that radiolabelled L-serine ethanolamine phosphate and L-threonine ethanolamine phosphate were incorporated into the PL pool by microsomes from reptilian brain tissue (58). They identified the serine-containing PL as phosphatidylserine (PS) using ninhydrin derivatization and thin-layer radioautography. However, attempts to identify the threonine-containing PL were unsuccessful. They proposed that L-threonine ethanolamine phosphate is hydrolysed by an esterase, releasing L-threonine which gets incorporated into PLs.

The first description of PT in mammalian cells was in 1977. Mark-Malchoff *et al*. observed that cultured hamster embryo fibroblasts exhibit a decrease in PC and PE, and an increase in PT content upon polyoma virus transformation (59). They identified PT through its products from acid hydrolysis, enzymatic hydrolysis by phospholipase C, and alcoholysis. While untransformed

cells contain far higher amounts of serine compared to threonine in their PL pools, polyoma transformed cells exhibit equal amounts of serine and threonine. Later work by the same group confirmed the occurrence of PT in several polyoma-transformed cell lines as a major component, as well as in other cell lines and rodent organs (liver, kidney) as a minor component (60). The mechanism behind the increase in PT after polyoma transformation is not understood.

Identification of PT in these older studies had mostly been done using indirect methods such as hydrolysis and derivatisation followed by colorimetric detection. The first direct evidence of PT was in 1998 by Mitoma *et al.* (61). They detected PT in rat hippocampal neurons using preparative thin-layer chromatography and secondary ion mass spectrometry. Under normal conditions, astrocytes support the survival of hippocampal neurons by providing L-serine for the synthesis of PS and sphingolipids (62). Here, hippocampal neurons incubated without astrocytes (source of L-serine) had greatly reduced levels of PS, but instead synthesized PT (61). Using rat brain microsomes, the authors showed that L-threonine and L-serine are binding competitors, but L-threonine (Km: 16 mM) has a lower affinity for the enzyme compared to L-serine (Km: 0.11 mM). This indicated that PT is synthesized by PSS through a base-exchange reaction. However, it is unknown which PSS isoform synthesized PT.

Shortly after, in 2002, Heikinheimo and Somerharju reported the metabolism of PT in baby hamster kidney cells (63). Using stable isotope labelling and electrospray ionization mass spectrometry (ESI-MS), they demonstrated that PT is readily transported into mitochondria but inefficiently decarboxylated into phosphatidylisopropanolamine. This contrasts with PS which is decarboxylated faster than it is transported to mitochondria (63). This was the first time ESI-MS had been used to analyze PT, through neutral loss (NL) scans of 101 Da in the negative ion mode.

In the 2010s, the adoption of benchtop MS technology in biology supported the discovery of PT in cultured murine macrophages, murine and porcine organs, bacteria, and parasitic protozoans including *Toxoplasma gondii*, *Eimeria falciformis*, and *Neospora caninum* (64-68). Of note, PT is a major component in parasitic protozoans and is synthesized by a dedicated enzyme, phosphatidylthreonine synthase (PTS). In *T. gondii*, PT functions in calcium homeostasis and virulence, and deletion of the PTS gene impairs virulence by disrupting motility, egress, and invasion (67, 69). However, the biological functions of PT in animals are unclear. The only clues

come from studies showing that lysophosphatidylthreonine (lysoPT) induces murine mast cell degranulation at concentrations $1/10^{th}$ that of lysoPS (70, 71). Thus, intact PT could be a precursor for a lipid mediator (lysoPT) involved in cell activation. Recently, an enzymatic synthesis route for PT was reported, using an engineered phospholipase D enzyme that catalyses a base-exchange reaction, replacing choline with L-threonine (72). This will facilitate functional studies.

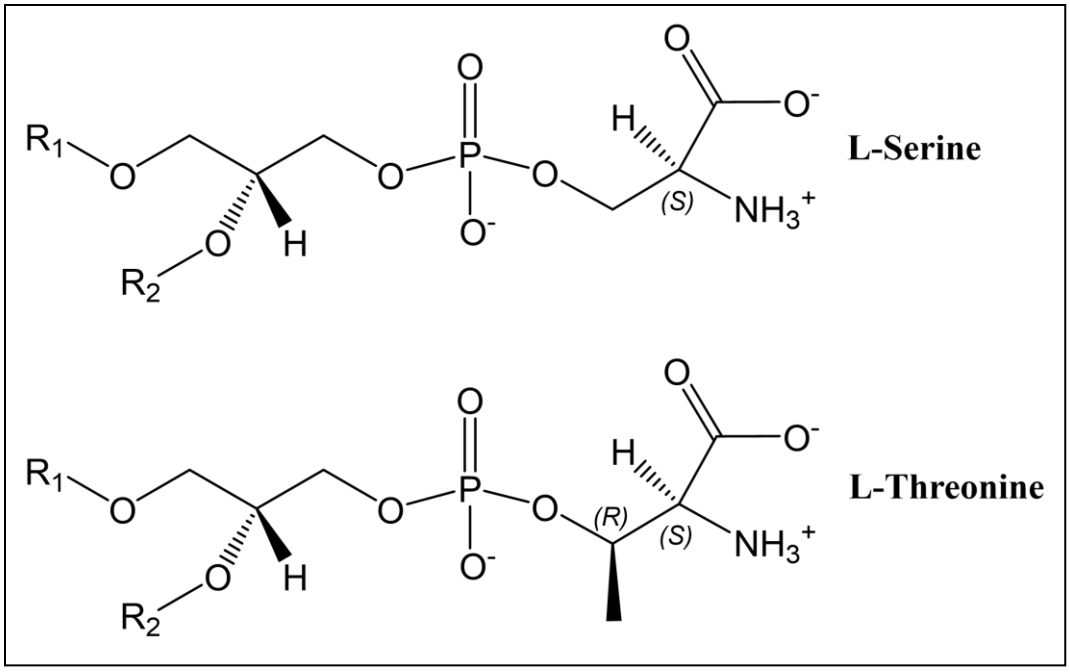


**Figure 1.6 – Chemical structures of PS and PT head groups**

Phosphatidylserine (PS) contains a phospho-L-serine (2S) head group (top), whereas phosphatidylthreonine (PT) contains a phospho-L-threonine (2S, 3R) head group (bottom). Charge states of functional groups are shown for physiological pH (7.35), where both lipids exhibit a net negative charge. $R_1$ and $R_2$ = *sn*-1 and *sn*-2 fatty acids, respectively.

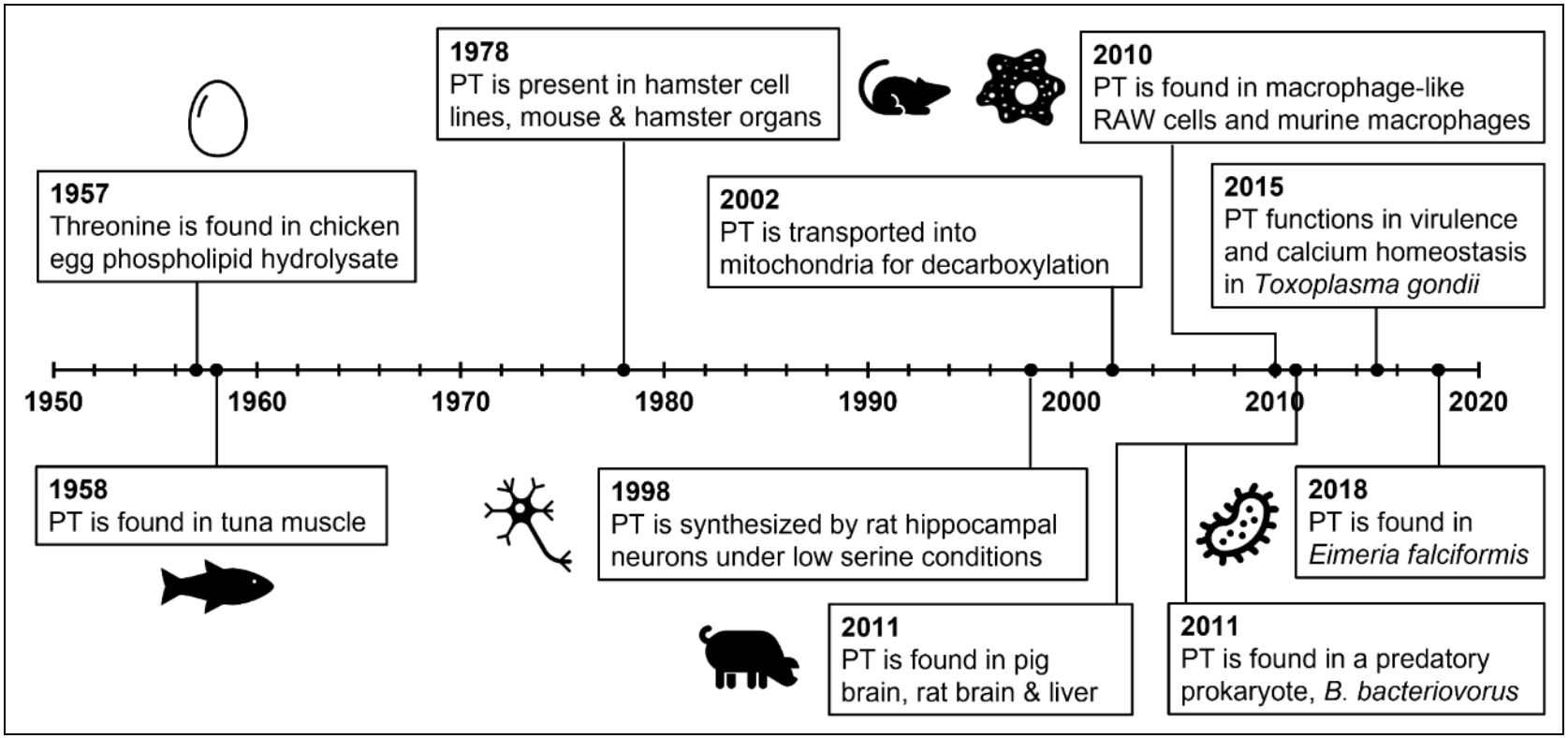


**Figure 1.7 – Timeline of PT research from 1957 to 2018, highlighting key milestones**

PT: phosphatidylthreonine.

## 1.8 Mass spectrometry-based lipidomics

MS is a powerful analytical technique that measures the mass-to-charge ratio (*m/z*) of ions. Mass spectrometers have three components: an ion source, a mass analyser, and a detector. The ion source generates charged species (ions) from analytes before their entry into the mass analyser. Several ion source types have been developed, which vary in their ionisation methods. Modern ionisation methods include electrospray ionisation (ESI), atmospheric pressure chemical ionisation, and matrix assisted laser desorption ionisation. These "soft" ionisation methods are suitable for biological samples because they do not cause extensive fragmentation of ions, in contrast to hard ionisation methods such as electron ionisation (73). In ESI, ions are produced by passing a liquid through a high-voltage capillary at high temperature (74). This creates charged droplets (aerosol) that rapidly evaporate, generating gas-phase ions. Positive or negative ions could be generated using ESI depending on the polarity of the applied voltage. The mass analyser filters ions based on their *m/z* allowing the separation of ions prior to detection. Types of mass analysers include quadrupole, time-of-flight, and quadrupole ion trap analysers. A quadrupole analyser consists of four parallel rods. The voltage of the rods can be controlled, and the resulting radiofrequency selectively stabilises or destabilises the trajectory of ions passing through the quadrupole depending on their *m/z* (74). Detectors amplify the signal from the ions through electron multipliers or photomultipliers.

Modern mass spectrometers combine two or more mass analysers (tandem mass spectrometry, MS/MS), allowing for more complex experiments to be carried out. For example, a linear series of three quadrupole analysers makes up a triple quadrupole mass spectrometer . Here, the first quadrupole (Q1) is used to filter ions (precursor ions) based on their *m/z*. The second quadrupole (Q2) is a collision cell, filled with inert gas. Collision of precursor ions with energized gas causes fragmentation of precursor ions into product ions. The third quadrupole (Q3) passes product ions of specified *m/z* values into the detector (75). Three types of MS/MS techniques will be used in my thesis: neutral loss (NL) scanning, multiple reaction monitoring (MRM), and $MS^n$ scans. In a NL scan, Q1 and Q3 scan ions at a specified offset (e.g., 87 Da), while Q2 acts a collision cell. In this scan mode, ions that pass through Q1 and lose a neutral fragment of 87 Da are transmitted through Q3 and detected. This method is useful for detecting PL classes which lose specific

neutral fragments (upon collision with gas) such as PE, PG, PI and PS (73). In MRM, a precursor ion is selected in Q1, fragmented in Q2, and a specific product ion is selected in Q3 for detection. The signal is proportional to the amount of the analyte and the method is highly sensitive and specific (depending on the product ion monitored), making MRM ideal for quantitation, especially when combined with chromatographic separation. $MS^n$ scans such as $MS^2$ and $MS^3$ provide structural information on the precursor ion. In an $MS^2$ scan, a precursor is selected in Q1 for fragmentation in Q2, then the product ions are passed through Q3 into the detector. In an $MS^3$ scan, a precursor ion is selected in Q1 for fragmentation in Q2, then products ions are passed into a linear ion trap where a specific ion is isolated (second precursor) for further fragmentation. The resulting fragments are then passed into the detector.

Mass spectrometry (MS) will be used in this thesis in the context of lipidomics, which is the large-scale study of lipids and lipid pathways. MS-based lipidomic approaches can be classified according to the presence or absence of chromatographic separation before MS analysis. Methods without chromatography include shotgun lipidomics and MS imaging. Details of MS imaging are outside the scope of this thesis. In shotgun lipidomics, lipid extracts are directly infused into the mass spectrometer and lipids are identified through NL scans, precursor ion scans, and MRM. Additionally, spiking samples with internal standards (e.g., deuterated forms of target analytes) enables quantification. One disadvantage of shotgun lipidomics is that biological lipid extracts produce highly complex spectra, which hinders the identification of low abundance species. This is exacerbated by the occurrence of lipids with the same elemental composition and mass (isomers). To address this problem, liquid chromatography (LC) can be coupled to MS (LC-MS), adding an extra dimension of separation. LC separates analytes based on their interactions with a mobile phase (solvent system) and a stationary phase (column). LC methods typically employed in lipidomic analysis include reversed phase (RP) chromatography (nonpolar column, elution with organic solvent) and hydrophilic interaction (HILIC) chromatography (polar column, elution with water).

MS-based lipidomic approaches can also be classified according to their analytical coverage into targeted and untargeted approaches. Targeted lipidomics seeks to quantify levels of specific individual lipids (either in absolute terms or relative terms between biological groups), facilitated by the sensitive MRM method described earlier in combination with internal standards. This type

of approach is hypothesis driven. In contrast, untargeted lipidomics investigates global lipid changes and aims to identify as many lipid species as possible in the sample, using high-resolution instruments and lipid databases. This approach is used in hypothesis generation. Lipids of interest that are identified in untargeted lipidomics are then interrogated using a targeted approach. In my thesis I will use targeted MS in combination with hydrophilic interaction chromatography (HILIC) separation to analyse phosphatidylthreonine in human blood.

The LIPID MAPS consortium has proposed nomenclature guidelines for the reporting of MS-derived lipid structures (1). The recommended shorthand notation for PLs consists of an abbreviation for the lipid class, followed by the number of carbon atoms in their FAs and the number of double bonds separated by a colon (e.g., PC 36:1 or PS 38:4). If known, FAs are depicted separately following the class abbreviation (PC 18:0_18:1 or PC 18:0/18:1). An "_" between FAs denotes unknown *sn*-positions, while "/" indicates known *sn*-positions (*sn*-1/*sn*-2). This nomenclature will be used throughout this thesis.

## 1.9 Hypothesis and aims

Given that PT has been described in animal cell lines/tissues, and is proposed to be synthesized by PSS, and that PSS is present in human cells, I hypothesize that PT is present in human tissue, specifically circulating blood cells. In this thesis, I will investigate this using targeted LC-MS/MS analysis. Due to the structural similarities between PS and PT, and the essential role of PS in blood coagulation, I hypothesize that PT also functions in coagulation by interacting with coagulation factors. I will test this using coagulation assays *in vitro*. Lastly, I will measure PT levels in platelets, extracellular vesicles, and leukocytes from a clinical cohort of coronary artery disease. This could establish a link between PT and vascular disease.

In other words, the aims of this thesis are:

(i) To identify PT molecular species in human blood, platelets, leukocytes, and extracellular vesicles.

(ii) To investigate the effects of thrombin activation on the level and membrane distribution of PT in platelets.

(iii) To investigate the procoagulant properties of PT *in vitro*, i.e., to determine whether PT promotes coagulation in vitro and through which coagulation protein complex.

(iv) To investigate whether PT levels in platelets, leukocytes, and extracellular vesicles are altered in coronary artery disease patients compared to healthy volunteers

# CHAPTER 2 Experimental Methods

## 2.1 Materials

PC 18:0/18:0, PS 18:0/20:4(5Z,8Z,11Z,14Z), PS 18:0/18:1(9Z), PE 18:0/18:1(9Z) and SPLASH® LIPIDOMIX® Mass Spec Standard (SPLASH mix, contains 5 µg/mL PS 15:0/18:1-D7) were from Avanti Polar Lipids (Alabama, USA). PT 16:0/18:1(9Z) and PT 18:0/18:1(9Z) were gifts from Yugo Iwasaki (Nagoya University & Chubu University), synthesized as described previously (72). Biotinylated-PS 14:0/14:0 was a gift from Majd Protty, synthesized as described previously (76). Recombinant corn trypsin inhibitor (CTI), recombinant human tissue factor (TF, full length), and human factor Va were from Haematologic Technologies (Vermont, USA). Human coagulation factors (II, IIa, Xa, X, VIIa) and thrombin chromogenic substrate S-2238 (Pefachrome TH 8198) were from Enzyme Research Laboratories (Indiana, USA). Factor Xa chromogenic substrate S-2765 was from Quadratech Diagnostics (Cooksbridge, UK). LiposoFast polycarbonate membranes (pore size: 100 nm) were from Avestin (Ottawa, Canada). HPLC-grade solvents, N-hydroxysuccinimide biotin (NHS-biotin), sulfo-NHS-biotin, and phosphate-buffered saline (PBS, pH 7.4) were from Thermo Fisher Scientific (Massachusetts, USA). Thrombin calibrator (thrombin in complex with alpha-2-macroglobulin, T-cal) was from Stago (Asnières-sur-Seine, France). Thrombin fluorogenic substrate (Z-Gly-Gly-Arg-AMC) was from Bachem (Bubendorf, Switzerland). Plastic microcuvettes were from BrandTech (Connecticut, USA).

The following materials were from Sigma-Aldrich (Missouri, USA): HPLC-grade L-serine, HPLC-grade L-threonine, L-lysine, calcium chloride ($CaCl_2$), acetaminophen, butylated hydroxytoluene (BHT), diethylenetriamine pentaacetate (DTPA), trisodium citrate, citric acid, glucose, sodium chloride (NaCl), potassium chloride (KCl), sodium bicarbonate ($NaHCO_3$), disodium hydrogen phosphate ($Na_2HPO_4$), magnesium chloride hexahydrate ($MgCl_2\,6H_2O$), 4-(2-hydroxyethyl)-1-piperazineethanesulfonic acid (HEPES), tris(hydroxymethyl)aminomethane (Tris), bovine serum albumin (BSA), ethylenediaminetetraacetic acid (EDTA), sodium azide, triethylamine, dimethyl sulfoxide (DMSO), trypan blue, and bovine thrombin.

## 2.2 Buffers

- Acid citrate dextrose (ACD): 85 mM trisodium citrate, 65 mM citric acid, and 100 mM glucose (pH 5.4).
- Tyrode's buffer: 134 mM NaCl, 12 mM $NaHCO_3$, 2.9 mM KCl, 0.34 mM $Na_2HPO_4$, 1 mM $MgCl_2\,6H_2O$, 10 mM HEPES, and 5 mM glucose (pH 7.35).
- Buffer A: 10 mM HEPES and 10 mM NaCl (pH 7.35).
- Buffer B: 20 mM HEPES and 140 mM NaCl (pH 7.35).
- Coagulation buffer: 20 mM Tris, 150 mM NaCl, and 0.05 % (w/v) BSA (pH 7.35).
- Buffer C: 20 mM HEPES, 0.02 % (w/v) sodium azide, and 0.6 % (w/v) BSA (pH 7.35).
- Antioxidant buffer: PBS (137 mM NaCl, 2.7 mM KCl, 8 mM $Na_2HPO_4$, and 2 mM $KH_2PO_4$, pH 7.4), 100 µM DTPA, 100 µM BHT and 75 µM acetaminophen.

## 2.3 Blood collection and preparation of platelet poor plasma

Blood donations were approved by the Cardiff University School of Medicine Ethics Committee (16/02 - Study: 8). Blood (20 mL) from three healthy volunteers was drawn by venepuncture using 21-gauge butterfly needles into syringes containing 3.2 % trisodium citrate (9:1 v/v) and 50 µg/mL CTI. 200 µL aliquots of whole blood were snap frozen in liquid nitrogen and stored at -80 °C. Plasma was prepared from freshly collected whole blood using a single centrifugation step (17,000 *g*, 5 min, 4 °C). The supernatant was transferred into a new Eppendorf tube, snap frozen in liquid nitrogen, and stored at -80 °C.

To make platelet poor plasma (PPP), blood from healthy volunteers was drawn by venepuncture using 21-gauge butterfly needles into syringes containing trisodium citrate (final: 0.32 % w/v) and CTI (final: 20 µg/mL) then transferred into falcon tubes. PPP was prepared from whole blood using two centrifugation steps (1730 *g*, 10 min, 21 °C). PPP from 25 donors was pooled, aliquoted and frozen at -80 °C.

## 2.4 Platelet isolation and thrombin activation

Blood (50 mL) was drawn from healthy volunteers by venepuncture using 21-gauge butterfly needles into a syringe containing ACD (8.1:1.9 v/v blood:ACD) then transferred into a falcon tube for centrifugation (250 *g*, 10 min, 22 °C, no brake). The platelet rich plasma was transferred to a new falcon tube using a Pasteur pipette without disturbing the sedimented cells and centrifuged (1000 *g*, 10 min, 22 °C, no brake). The supernatant was decanted, and the platelet rich pellet was gently resuspended in 10 mL Tyrode's buffer and ACD (9:1 v/v) using a Pasteur pipette. After that, the platelets were centrifuged (1000 *g*, 10 min, 22 °C, no brake), the supernatant was decanted, and the platelet rich pellet was resuspended in 1 mL of Tyrode's buffer. Platelets were counted using a haemocytometer with trypan blue (for contrast), and platelet concentration was adjusted to 2 x $10^8$/mL with Tyrode's buffer.

One set of 1 mL aliquots of platelets was left on the bench at 21 °C (unstimulated platelets). Another set was recalcified with calcium chloride (1 mM), incubated at 37 °C for 5 min, then activated with bovine thrombin (0.2 U/mL) at 37 °C for 30 min (thrombin activated platelets).

## 2.5 NHS-biotin derivatization of platelets

200 µL aliquots of unstimulated and thrombin activated platelets were treated with either sulfo-NHS-biotin (11 mM in PBS) or NHS-biotin (20 mM in DMSO). For sulfo-NHS-biotin derivatization, samples were incubated with the reagent for 10 min at 21 °C, then the reaction was quenched by the addition of L-lysine (50 mM) and incubation for 10 min at 21 °C. PBS was then added to the sample to make 1 mL in preparation for lipid extraction. For NHS-biotin derivatization, samples were incubated with the reagent for 10 min at 21 °C, then PBS was added to make 1 mL for lipid extraction.

## 2.6 Lipid extraction of whole blood, plasma, and blood cells

200 µL aliquots of whole blood (or plasma) were removed from -80 °C and gradually brought to 4 °C. 800 µL of antioxidant buffer was added to samples (total volume: 1 mL) then they were

vortexed for 30 s. Samples were then added into glass extraction vials containing 2.5 mL of hexane:isopropanol:1 M acetic acid (30:20:2) and vortexed for 1 min. In some samples, 20 µL of SPLASH mix was added as an internal standard. After that, 2.5 mL hexane was added, and samples were vortexed for 1 min then centrifuged (526 *g*, 5 min, 4 °C) to separate the organic and aqueous layers. The organic layers were transferred to new tubes, and the aqueous layers were reextracted using 2.5 mL of hexane and repeating the procedure above. The organic layers from the two extractions were combined, dried using a RapidVap vacuum evaporation system (Labconco, Missouri, USA), and the dry lipid films were reconstituted in 200 µL methanol (purification) or 400 µL methanol (other experiments).

## 2.7 Lipid extraction of NHS-biotin derivatized samples

Lipids in biotinylated platelets were extracted using a modified Bligh and Dyer method. In a glass extraction vial, 1 mL of sample was mixed with 2.5 mL ice-cold methanol, then 1.25 mL of chloroform was added to make a monophase. 20 ng of biotinylated-PS 14:0/14:0 (internal standard) was added, then samples were vortexed for 1 min and incubated on ice for 30 min. After incubation, 1.25 mL of chloroform was added and samples were vortexed for 1 min, then 1.25 mL of HPLC-grade water was added and samples were vortexed for 1 min. Samples were centrifuged (526 *g*, 5 min, 4 °C) to separate the organic and aqueous layers. The bottom organic layers were collected into new tubes, and the upper aqueous layers were reextracted with 2.5 mL chloroform, vortexed for 1 min and centrifuged (526 *g*, 5 min, 4 °C). The organic layers from the two extractions were combined, dried using a RapidVap vacuum evaporation system (Labconco), and the dry lipid films were reconstituted in 100 µL methanol. Extracts were transferred into MS vials for analysis.

## 2.8 NHS-biotin derivatization of blood lipid extracts

100 µL of lipid extract was dried by nitrogen and reconstituted in 330 µL of chloroform/methanol (2:1) containing 1% triethylamine (catalyst) before the addition of 2.18 mg of solid NHS-biotin (19.4 mM). The mixture was vortexed for 30 s then incubated at 22 °C for 2

h. Following this, the mixture was dried by nitrogen and reconstituted in 500 µL methanol then vortexed for 30 s. The sample was then centrifuged (526 *g*, 5 min, 20 °C) to precipitate excess NHS-biotin. The supernatant was transferred into a new vial and centrifuged again (526 *g*, 5 min, 20 °C). The supernatant was transferred into an MS vial for analysis.

## 2.9 Processing of samples (platelets, extracellular vesicles, and leukocytes) from a clinical cohort

This project used lipid extracts of platelets, extracellular vesicles, and leukocytes which had been obtained for a separate study, from a cohort of coronary artery disease patients. Ethical permission was obtained from Health and Care Research Wales (HCRW, IRAS 243701) and the designated research ethics committee (REC reference 18/YH/0502). The cohort consists of four groups: healthy controls (HC, n=24), risk factors with no significant coronary artery disease (RF, n=23), significant coronary artery disease (CAD, n=19), and acute coronary syndrome (ACS, n=24). Further details on the cohort are available in Dr. Majd Protty's PhD thesis (54). Blood samples were collected by Dr. Majd Protty, who then isolated platelets, extracellular vesicles, and leukocytes using published methods. Lipids were extracted using the methods described previously (**Sections 2.6 & 2.7)**, and extracts were stored at -80 °C until use. For this project, extracts from platelets, extracellular vesicles, and leukocytes were mixed 1:1 with methanol containing SPLASH mix (final concentration of PS 15:0/18:1-D7: 0.05 ng/µL). Samples were analysed using LC-MS/MS as described below (**Section 2.10**).

## 2.10 Targeted HILIC LC-ESI-MS/MS of phospholipids

Hydrophilic interaction chromatography (HILIC) liquid chromatography–tandem mass spectrometry (LC-MS/MS) analysis was carried out on a 6500 QTRAP mass spectrometer (Sciex, Massachusetts, USA) coupled with a Nexera XR HPLC system (Shimadzu, Kyoto, Japan). Lipids were separated on an Xbridge Amide column (3.5 µm, 4.6 x 150 mm, Waters Corporation, Massachusetts, USA) using solvent A (50:50 water/acetonitrile, 10 mM ammonium formate, 0.1% formic acid) and solvent B (5:95 water/acetonitrile, 10 mM ammonium formate,

0.1% formic acid). Gradient: 0–10 min 100%–80% B; 10–25 min 80%–20%B; 25–26 min 20%–100% B; 26–30 min 100% B. Flow rate was 0.6 mL/min, and the column temperature was maintained at 45 °C. The eluate from 10–16 min of chromatography was introduced into the ESI(-) source for MS analysis.

PT species were first detected using neutral loss scans of 101 Da with the following parameters: scan speed: 1000 Da/s, scan range: m/z 600–900, declustering potential (DP): -60 V, collision energy (CE): -36 V, cell exit potential (CXP): -32 V, entrance potential (EP): -10 V. Fatty acid compositions of PT species were determined by $MS^3$ scans with the following parameters: scan speed: 1000 or 10,000 Da/s, first precursor: $[M-H]^-$, second precursor: $[M-H-101]^-$, scan range: m/z 100–900, CE ramp: -36 to -46 V, DP: -60 V, EP: -10 V.

Later, analysis of PT was carried out via multiple reaction monitoring (MRM). For initial experiments on whole blood, 10 PS and PT species (five for each class) were analysed along with one internal standard (**Table 2.1**). Three MRM transitions were monitored per lipid, monitoring the loss of head group and the two fatty acyl negative ions. For later experiments, only head group transitions were used, and 10 more PS and PT species were added in the analysis of the platelets, leukocytes, and extracellular vesicles. The final MRM transition list contains 10 PS and 10 PT species with one internal standard (**Table 2.2**).

The following instrument (6500 QTRAP) parameters were used: Source/gas: curtain gas flow (CUR): 35, temperature (TEM): 500, ion source gas 1 (GS1): 40, ion source gas 2 (GS2): 30, and ion spray voltage (IS): -4500 V. Detector: single channel electron multiplier (CEM): 2200.

The HILIC-LC method was also used to partially purify PS and PT by diverting the LC output into a collection tube at the appropriate elution time. The collected fraction was then dried using nitrogen, reconstituted in methanol, and stored at -80 °C until further analysis.

## 2.11 Accurate mass MS/MS of phospholipids

High mass accuracy measurements were performed using a SYNAPT XS Q-TOF mass spectrometer (Waters Corporation) coupled with an Acquity UPLC system (Waters Corporation), using the same HILIC-LC setup described above. $MS^1$ and $MS^2$ scans of PT and

PS species were collected in the negative polarity using the resolution mode. $MS^1$ settings: scan time: 1 s, range: m/z 400–900. $MS^2$ settings: scan time: 1 s, range: m/z 50–1000, CE: -31 V. ESI settings: capillary voltage: 2400 V, cone voltage: 25 V, source offset: 4 V, source temperature: 120 °C, desolvation temperature: 500 °C, cone gas: 20 L/h, desolvation gas: 1000 L/h, nebulizer: 6.5 Bar. Leucine enkephalin (554.2615 Da) was used as a LockSpray calibrant for mass correction and was sprayed at 10 s intervals with a scan time of 1 s.

## 2.12 Determination of fatty acid *sn*-positions

1 µg PT 18:0/18:1(9Z) standard or 150 µL of whole blood lipid extract (in methanol) were hydrolysed using 300 µL 0.2 M HCl in methanol/water and incubation at 40 °C for 30 min. After incubation, sample was flushed with nitrogen to remove HCl gas then dried by RapidVap (45° C, 35 mbar). The dry film was reconstituted in 150 µL acidic methanol (0.1 mM formic acid, pH 4.0) for analysis. Hydrolysis products (lysoPS and lysoPT species, 20 µL injection volume) were separated using the HILIC-LC method described above (**Section 2.10**) with eluate from 13.5–17 min introduced into the ESI(-) source and detected using MRM (**Table 2.3**). Ratios of 1-acyl/2-acyl lysophospholipids were used to determine their *sn*-positions.

## 2.13 LC-MS/MS of biotinylated lipids

Biotinylated lipids from whole blood extracts were separated using the HILIC-LC method described above (**Section 2.10**) and detected using MRM (**Table 2.4**).

Biotinylated lipids from platelet extracts were analysed using a more sensitive reversed phase (RP)-LC-MS/MS method, carried out on a 6500 QTRAP mass spectrometer (Sciex) coupled with a Nexera XR HPLC system (Shimadzu). Lipids were separated on an Ascentis C18 column (5 µm, 2.1 x 150 mm, Sigma Aldrich) using isocratic elution with methanol, 0.2 % (w/v) ammonium acetate (2.6 mM) for 25 min. Flowrate was 0.4 mL/min, and the column temperature was maintained at 22 °C. The eluate from 1–9 min of chromatography was introduced into the ESI(-) source, and MS detection was done by MRM. (**Table 2.5**).

The following instrument (6500 QTRAP) parameters were used: Source/gas: curtain gas flow (CUR): 35, temperature (TEM): 500, ion source gas 1 (GS1): 40, ion source gas 2 (GS2): 30, and ion spray voltage (IS): -4500 V. Detector: single channel electron multiplier (CEM): 2200.

## 2.14 Analysis of amino acid head groups

1 µg PT 16:0/18:1(9Z) standard or 100 µL of purified PS-PT fraction were hydrolysed using 200 µL 3 M HCl in methanol/water (1:1) and incubation at 100 °C for 1 h. The hydrolysate was dried using nitrogen gas and reconstituted in 200 µL (standard) or 80 µL (sample) acetonitrile/water (1:1) + 0.1% formic acid for analysis. Solutions of L-serine and L-threonine (0.1 ng/µL) were made in acetonitrile/water (1:1) + 0.1% formic acid to confirm chromatographic separation and compare retention times.

LC-MS/MS analysis of amino acids was carried out on a 4000 QTRAP mass spectrometer (Sciex) coupled with a Nexera XR HPLC system (Shimadzu). Amino acids were separated on an Xbridge Amide column (3.5 µm, 4.6 x 150 mm, Waters Corporation) using solvent A (50:50 water/acetonitrile, 10 mM ammonium formate, 0.1% formic acid) and solvent B (5:95 water/acetonitrile, 10 mM ammonium formate, 0.1% formic acid). Gradient: 0–15 min 100%–0% B; 15–16 min 0%–100%B; 16–20 min 100% B. Flow rate was 0.6 mL/min, and the column temperature was maintained at 45 °C. The eluate was introduced into the ESI(+) source, and MS detection was done by MRM. (**Table 2.6**). Injection volume was 20 µL.

The following instrument (4000 QTRAP) parameters were used: Source/gas: CUR: 20, TEM: 500, GS1: 40, GS2: 30, and IS: 4500 V. Detector: CEM: 2300.

## 2.15 LC-MS/MS data collection and processing

Data was collected using Analyst Software (version 1.7, Sciex) or MassLynx (version 4.2, Waters Corporation). Peaks (5:1 signal to noise (S:N) ratio, with at least 6 points across) were manually integrated using MultiQuant Software (Sciex). Area (cps) values were used to quantify amino acids using calibration curves (**Appendix 9.1**). Ratio (A/IS, cps) values for each analyte

were calculated by dividing the area of the analyte by the area of the internal standard. A/IS values were used to quantify lipids using calibration curves (**Appendix 9.2**). Lipid % externalization in platelets was calculated by dividing the A/IS values from sulfo-NHS-biotin samples by the AR values from NHS-biotin samples. Representative chromatograms and the complete set of MS/MS spectra for measured analytes are available in **Appendices 9.3–9.10**.

## 2.16 Preparation of liposomes by membrane extrusion

Liposomes (large unilamellar vesicles, LUVs) were made from PC 18:0/18:0, PE 18:0/18:1(9Z), PS 18:0/18:1(9Z), and PT 18:0/18:1(9Z) in buffer (A or B) using the extrusion method (compositions in **Table 2.7**). Lipids were added to a glass vial then the solvent was evaporated using a RapidVap vacuum evaporation system (Labconco) with shaking at 45 °C and 30 mbar. Buffer (A or B) was added to the dry lipid samples, and the tubes were vortexed for 30 s then subjected to 10 freeze-thaw cycles (30 s freezing and 30 s thawing) with agitation using liquid nitrogen and a water bath at 60 °C. For tissue factor (TF)-bearing liposomes, TF was included in the buffer, and the thawing step (of the freeze-thaw cycles) was carried out at 37° C. The liposomes were then extruded through a 100-nm pore membrane (Avestin) 19 times to generate uniformly sized liposomes.

## 2.17 Turbidimetric calcium binding assay

Spectrophotometric analysis was done using a UVIKON 923 double beam UV/VIS spectrophotometer (Agilent Technologies, formerly BioTek Instruments, Vermont, USA). 200 µL of liposomes (1 mM), prepared as in **Section 2.16**, were added to a plastic microcuvette and initial absorbance was measured at 400 nm (using buffer A as a reference blank). Samples were titrated with 2 mM $CaCl_2$ (in buffer A) and changes in absorbance at 400 nm were monitored. Titration consisted of 10 additions of 2 µL $CaCl_2$. Each addition was followed by mixing (pipetting up and down), 1 min incubation, and absorbance measurement (using buffer A as a reference blank). Experiments were done using two technical replicates for each sample.

## 2.18 Prothrombinase (FXa:FVa) assay

In a 96-well plate, 20 µL liposomes (25 µM, in buffer B) were mixed with 20 µL coagulation buffer containing (final concentrations) FII (200 nM), FVa (3.0 nM), FXa (10 nM), and 1 mM $CaCl_2$ then incubated at 21 °C for 5 min. The reaction was stopped by the addition of 10 µL EDTA (7 mM, in water). Next, 20 µL chromogenic substrate S-2238 (0.8 mM, in water) was added to each well and absorbance at 405 nm was monitored for 50 minutes (in kinetic mode) using a CLARIOstar Plus microplate reader (BMG Labtech, Ortenberg, Germany). Relative prothrombinase activity values were calculated by determining the slope of the absorbance curves from 0 – 10 min using Excel (version 2201, Microsoft Corporation, Washington, USA). All liposomes preparations were made in triplicate, and each was tested twice (two technical replicates).

## 2.19 Calibrated automated thrombinography (CAT)

In a 96-well plate, 20 µL TF-liposomes (10 µM liposomes, in buffer B, 50 pM TF) or T-cal (calibrator) were mixed with 80 µL pooled CTI-PPP and incubated at 37 °C for 10 min. After incubation, 20 µL buffer C containing calcium (20 mM) and fluorogenic thrombin substrate (5 mM) was added to samples and fluorescence was measured for 60 min using a Fluoroskan Ascent microplate fluorometer (Thermo Fischer Scietific). Peak thrombin and lag time were automatically calculated by the Thrombinoscope software (Stago) using the calibrator reference curve. All liposomes preparations were made in triplicate.

## 2.20 Extrinsic tenase (TF:FVIIa) assay

In a 96-well plate, 20 µL TF-liposomes (25 µM, in buffer B, 1 nM TF) were mixed with 20 µL coagulation buffer containing (final concentrations) FX (500 nM), FVIIa (25 nM), and 2.5 mM $CaCl_2$, then immediately 20 µL chromogenic FXa substrate S-2765 (0.93 mM, in water) was added to each well and absorbance at 405 nm was monitored for 40 minutes (in kinetic mode) using a CLARIOstar Plus microplate reader (BMG Labtech). Relative tenase activity values

were calculated by determining the slope of the absorbance curves from 0 – 10 min using Excel (version 2201, Microsoft Corporation). All liposomes preparations were made in triplicate.

## 2.21 Statistical analysis

Statistics were done using SPSS Statistics (version 27, IBM Corp, New York, USA) or Excel (version 2201, Microsoft Corporation). For cohort samples (four groups), statistical significance was determined using the Kruskal-Wallis H test. Lipids in unstimulated vs. thrombin activated platelets were analyzed using paired t-tests. Pearson correlation coefficients were calculated for PS and PT pairs for species detected in more than six samples and a P value $< 0.05$ was considered significant. For coagulation assays, statistical significance was determined using t-tests (pairwise comparisons) or one-way ANOVA and post-hoc Tukey tests (more than two groups).

**Table 2.1 – Negative mode MRM transitions used in the analysis of PS and PT species in whole blood extracts**

| Analyte | Q1 (m/z) | Q3 (m/z) | Dwell time (ms) | DP (volts) | CE (volts) | CXP (volts) |
|---|---|---|---|---|---|---|
| PS 33:1[D7] | 753.5 | 666.5 | 75 | -60 | -36 | -32 |
| PS 15:0_18:1[D7] | 753.5 | 288.2 | 75 | -60 | -46 | -32 |
| PS 15:0_18:1[D7] | 753.5 | 241.2 | 75 | -60 | -46 | -32 |
| PS 36:1 | 788.6 | 701.6 | 75 | -60 | -36 | -32 |
| PS 18:0_18:1 | 788.6 | 281.2 | 75 | -60 | -46 | -32 |
| PS 18:0_18:1 | 788.6 | 283.2 | 75 | -60 | -46 | -32 |
| PT 36:1 | 802.6 | 701.6 | 75 | -60 | -36 | -32 |
| PT 18:0_18:1 | 802.6 | 281.2 | 75 | -60 | -46 | -32 |
| PT 18:0_18:1 | 802.6 | 283.2 | 75 | -60 | -46 | -32 |
| PS 38:4 | 810.6 | 723.6 | 75 | -60 | -36 | -32 |
| PS 18:0_20:4 | 810.6 | 303.2 | 75 | -60 | -46 | -32 |
| PS 18:0_20:4 | 810.6 | 283.2 | 75 | -60 | -46 | -32 |
| PT 38:4 | 824.6 | 723.6 | 75 | -60 | -36 | -32 |
| PT 18:0_20:4 | 824.6 | 303.2 | 75 | -60 | -46 | -32 |
| PT 18:0_20:4 | 824.6 | 283.2 | 75 | -60 | -46 | -32 |
| PS 40:6 | 834.6 | 747.6 | 75 | -60 | -36 | -32 |
| PS 18:0_22:6 | 834.6 | 327.2 | 75 | -60 | -46 | -32 |
| PS 18:0_22:6 | 834.6 | 283.2 | 75 | -60 | -46 | -32 |
| PS 40:5 | 836.7 | 749.7 | 75 | -60 | -36 | -32 |
| PS 18:0_22:5 | 836.7 | 329.2 | 75 | -60 | -46 | -32 |
| PS 18:0_22:5 | 836.7 | 283.2 | 75 | -60 | -46 | -32 |
| PS 40:4 | 838.7 | 751.7 | 75 | -60 | -36 | -32 |
| PS 18:0_22:4 | 838.7 | 331.2 | 75 | -60 | -46 | -32 |
| PS 18:0_22:4 | 838.7 | 283.2 | 75 | -60 | -46 | -32 |
| PT 40:6 | 848.6 | 747.6 | 75 | -60 | -36 | -32 |
| PT 18:0_22:6 | 848.6 | 327.2 | 75 | -60 | -46 | -32 |
| PT 18:0_22:6 | 848.6 | 283.2 | 75 | -60 | -46 | -32 |
| PT 40:5 | 850.7 | 749.7 | 75 | -60 | -36 | -32 |
| PT 18:0_22:5 | 850.7 | 329.2 | 75 | -60 | -46 | -32 |
| PT 18:0_22:5 | 850.7 | 283.2 | 75 | -60 | -46 | -32 |
| PT 40:4 | 852.7 | 751.7 | 75 | -60 | -36 | -32 |
| PT 18:0_22:4 | 852.7 | 331.2 | 75 | -60 | -46 | -32 |
| PT 18:0_22:4 | 852.7 | 283.2 | 75 | -60 | -46 | -32 |

**Table 2.2 – Negative mode MRM transitions used for the analysis of PS and PT in platelets, extracellular vesicles, and leukocytes (cohort samples)**

| Analyte | Q1 (m/z) | Q3 (m/z) | Dwell time (ms) | DP (volts) | CE (volts) | CXP (volts) |
|---|---|---|---|---|---|---|
| PS 33:1[D7] | 753.5 | 666.5 | 100 | -60 | -36 | -32 |
| PS 34:1 | 760.5 | 673.5 | 100 | -60 | -36 | -32 |
| PS 36:1 | 788.6 | 701.6 | 100 | -60 | -36 | -32 |
| PS 36:2 | 786.5 | 699.5 | 100 | -60 | -36 | -32 |
| PS 38:3 | 812.5 | 725.5 | 100 | -60 | -36 | -32 |
| PS 38:4 | 810.6 | 723.6 | 100 | -60 | -36 | -32 |
| PS 38:5 | 808.5 | 721.5 | 100 | -60 | -36 | -32 |
| PS 40:3 | 840.6 | 753.6 | 100 | -60 | -36 | -32 |
| PS 40:4 | 838.7 | 751.7 | 100 | -60 | -36 | -32 |
| PS 40:5 | 836.7 | 749.7 | 100 | -60 | -36 | -32 |
| PS 40:6 | 834.6 | 747.6 | 100 | -60 | -36 | -32 |
| PT 34:1 | 774.5 | 673.5 | 100 | -60 | -36 | -32 |
| PT 36:1 | 802.6 | 701.6 | 100 | -60 | -36 | -32 |
| PT 36:2 | 800.5 | 699.5 | 100 | -60 | -36 | -32 |
| PT 38:3 | 826.5 | 725.5 | 100 | -60 | -36 | -32 |
| PT 38:4 | 824.6 | 723.6 | 100 | -60 | -36 | -32 |
| PT 38:5 | 822.5 | 721.5 | 100 | -60 | -36 | -32 |
| PT 40:3 | 854.6 | 753.6 | 100 | -60 | -36 | -32 |
| PT 40:4 | 852.7 | 751.7 | 100 | -60 | -36 | -32 |
| PT 40:5 | 850.7 | 749.7 | 100 | -60 | -36 | -32 |
| PT 40:6 | 848.6 | 747.6 | 100 | -60 | -36 | -32 |

**Table 2.3 – Negative mode MRM transitions used for the analysis of lysoPT and lysoPS generated by mild acid hydrolysis of PT and PS from whole blood lipid extract**

| Analyte | Q1 (m/z) | Q3 (m/z) | Dwell time (ms) | DP (volts) | CE (volts) | CXP (volts) |
|---|---|---|---|---|---|---|
| LysoPS 17:1 | 508.3 | 421.3 | 50 | -40 | -28 | -19 |
| LysoPS 18:1 | 522.3 | 435.3 | 50 | -40 | -28 | -19 |
| LysoPS 18:0 | 524.3 | 437.3 | 50 | -40 | -28 | -19 |
| LysoPT 18:1 | 536.3 | 435.3 | 50 | -40 | -28 | -19 |
| LysoPT 18:0 | 538.3 | 437.3 | 50 | -40 | -28 | -19 |
| LysoPS 20:4 | 544.3 | 457.3 | 50 | -40 | -28 | -19 |
| LysoPT 20:4 | 558.3 | 457.3 | 50 | -40 | -28 | -19 |
| LysoPS 22:6 | 568.3 | 481.3 | 50 | -40 | -28 | -19 |
| LysoPS 22:5 | 570.3 | 483.3 | 50 | -40 | -28 | -19 |
| LysoPS 22:4 | 572.3 | 485.3 | 50 | -40 | -28 | -19 |
| LysoPT 22:6 | 582.3 | 481.3 | 50 | -40 | -28 | -19 |
| LysoPT 22:5 | 584.3 | 483.3 | 50 | -40 | -28 | -19 |
| LysoPT 22:4 | 586.3 | 485.3 | 50 | -40 | -28 | -19 |

**Table 2.4 – Negative mode MRM transitions used in HILIC-LC-MS/MS analysis of biotinylated PT and PS**

| Analyte | Q1 (m/z) | Q3 (m/z) | Dwell time (ms) | DP (volts) | CE (volts) | CXP (volts) |
|---|---|---|---|---|---|---|
| PS 33:1[D7] | 753.5 | 666.5 | 100 | -60 | -36 | -32 |
| PT 34:1 | 774.5 | 673.5 | 100 | -60 | -36 | -32 |
| PS 36:1 | 788.6 | 701.6 | 100 | -60 | -36 | -32 |
| PT 36:1 | 802.6 | 701.6 | 100 | -60 | -36 | -32 |
| PS 38:4 | 810.6 | 723.6 | 100 | -60 | -36 | -32 |
| PT 38:4 | 824.6 | 723.6 | 100 | -60 | -36 | -32 |
| PS 40:6 | 834.6 | 747.6 | 100 | -60 | -36 | -32 |
| PS 40:5 | 836.7 | 749.7 | 100 | -60 | -36 | -32 |
| PS 40:4 | 838.7 | 751.7 | 100 | -60 | -36 | -32 |
| PT 40:6 | 848.6 | 747.6 | 100 | -60 | -36 | -32 |
| PT 40:5 | 850.7 | 749.7 | 100 | -60 | -36 | -32 |
| PT 40:4 | 852.7 | 751.7 | 100 | -60 | -36 | -32 |
| PS 33:1[D7] Biotin | 979.5 | 666.5 | 100 | -300 | -48 | -21 |
| PT 34:1 Biotin | 1000.5 | 673.5 | 100 | -300 | -48 | -21 |
| PS 36:1 Biotin | 1014.6 | 701.6 | 100 | -300 | -48 | -21 |
| PT 36:1 Biotin | 1028.6 | 701.6 | 100 | -300 | -48 | -21 |
| PS 38:4 Biotin | 1036.6 | 723.6 | 100 | -300 | -48 | -21 |
| PT 38:4 Biotin | 1050.6 | 723.6 | 100 | -300 | -48 | -21 |
| PS 40:6 Biotin | 1060.6 | 747.6 | 100 | -300 | -48 | -21 |
| PS 40:5 Biotin | 1062.7 | 749.7 | 100 | -300 | -48 | -21 |
| PS 40:4 Biotin | 1064.7 | 751.7 | 100 | -300 | -48 | -21 |
| PT 40:6 Biotin | 1074.6 | 747.6 | 100 | -300 | -48 | -21 |
| PT 40:5 Biotin | 1076.7 | 749.7 | 100 | -300 | -48 | -21 |
| PT 40:4 Biotin | 1078.7 | 751.7 | 100 | -300 | -48 | -21 |

**Table 2.5 – Negative mode MRM transitions used in RP-LC-MS/MS analysis of biotinylated PT and PS in platelets**

| Analyte | Q1 (m/z) | Q3 (m/z) | Dwell time (ms) | DP (volts) | CE (volts) | CXP (volts) |
|---|---|---|---|---|---|---|
| PS 28:0 Biotin | 904.4 | 591.4 | 100 | -300 | -48 | -21 |
| PS 36:1 Biotin | 1014.6 | 701.6 | 100 | -300 | -48 | -21 |
| PS 36:2 Biotin | 1012.5 | 699.5 | 100 | -300 | -48 | -21 |
| PS 38:3 Biotin | 1038.5 | 725.5 | 100 | -300 | -48 | -21 |
| PS 38:4 Biotin | 1036.6 | 723.6 | 100 | -300 | -48 | -21 |
| PS 40:6 Biotin | 1060.6 | 747.6 | 100 | -300 | -48 | -21 |
| PT 36:1 Biotin | 1028.6 | 701.6 | 100 | -300 | -48 | -21 |
| PT 36:2 Biotin | 1026.5 | 699.5 | 100 | -300 | -48 | -21 |
| PT 38:3 Biotin | 1052.5 | 725.5 | 100 | -300 | -48 | -21 |
| PT 38:4 Biotin | 1050.6 | 723.6 | 100 | -300 | -48 | -21 |
| PT 40:6 Biotin | 1074.6 | 747.6 | 100 | -300 | -48 | -21 |

**Table 2.6 – Positive mode MRM transitions used in amino acid HILIC-LC-MS/MS analysis.**

| Analyte | Q1 (m/z) | Q3 (m/z) | Dwell time (ms) | DP (volts) | CE (volts) | CXP (volts) |
|---|---|---|---|---|---|---|
| Serine | 106.0 | 60.0 | 200 | 11 | 15 | 10 |
| Threonine | 120.1 | 74.1 | 200 | 21 | 15 | 4 |

**Table 2.7 – Liposome compositions used for the different assays. Buffer A: 10 mM HEPES, 10 mM NaCl, pH 7.35. Buffer B: 20 mM HEPES, 140 mM NaCl, pH 7.35**

| Assay | [Lipid] | Composition # | PC 18:0/18:0 mol % | PE 18:0/18:1(9Z) mol % | PS 18:0/18:1(9Z) mol % | PT 18:0/18:1(9Z) mol % | [Tissue factor] | Buffer |
|---|---|---|---|---|---|---|---|---|
| Calcium binding assay | 1 mM | 1 | 60 | 40 | 0 | 0 | none | A |
| | | 2 | 60 | 30 | 10 | 0 | | |
| | | 3 | 60 | 30 | 0 | 10 | | |
| Prothrombinase assay | 25 μM | 4 | 60 | 40 | 0 | 0 | none | B |
| | | 5 | 60 | 30 | 10 | 0 | | |
| | | 6 | 60 | 30 | 0 | 10 | | |
| | | 7 | 59.86 | 30 | 10 | 0.14 | | |
| | | 8 | 59.72 | 30 | 10 | 0.28 | | |
| | | 9 | 90 | 0 | 10 | 0 | | |
| | | 10 | 95 | 0 | 0 | 5 | | |
| | | 11 | 90 | 0 | 0 | 10 | | |
| | | 12 | 85 | 0 | 0 | 15 | | |
| Calibrated automated thrombinography | 10 μM | 13 | 60 | 40 | 0 | 0 | 50 pM | B |
| | | 14 | 60 | 30 | 10 | 0 | | |
| | | 15 | 60 | 30 | 0 | 10 | | |
| | | 16 | 59.86 | 30 | 10 | 0.14 | | |
| Extrinsic tenase assay | 25 μM | 17 | 80 | 20 | 0 | 0 | 1 nM | B |
| | | 18 | 80 | 0 | 20 | 0 | | |
| | | 19 | 80 | 0 | 0 | 20 | | |

# CHAPTER 3 Structural characterisation of PT in human blood

## 3.1 Introduction

As outlined in **Section 1.7**, phosphatidylthreonine (PT) had previously been reported in several animal cell lines and tissues, but not in human tissues. Thus, in this chapter, I will investigate the presence of PT in human blood and structurally characterise PT species using mass spectrometry (MS). Liquid chromatography is commonly coupled with MS because it introduces an additional dimension of separation by retention time. Reversed phase (RP) chromatography is widely used for lipid analysis. However, anionic PLs like PS (and presumably PT) resolve poorly on RP columns, which reduces sensitivity. To overcome this, hydrophilic interaction chromatography (HILIC) will be employed before MS/MS analysis.

I will use several approaches to structurally characterise PT in human blood, including acid hydrolysis, chemical derivatisation, and MS/MS. The PT head group exhibits a neutral loss of 101 Da in the negative mode (63). Similarly, FA carboxylate ions are produced in negative mode MS/MS (73). As such, PT species will be detected using neutral loss scanning (of 101 Da) and their FA compositions will be determined using MS/MS.

Determination of FA *sn*-positions will be achieved using mild acid hydrolysis followed by MS analysis of lysophospholipids (lysoPL). Mild acid hydrolysis of PL produces equal amounts of 1-acyl and 2-acyl lysoPLs, which in aqueous solutions undergo acyl migration until an equilibrium of 9:1 (1-acyl to 2-acyl) is reached (77). Acyl migration is slower in acidic conditions, and the two lysoPL isomers readily separate using liquid chromatography (78). This will allow for the determination of *sn*-positions by calculating the ratio of 1-acyl to 2-acyl lysoPLs.

The identity of the PT head group will be further characterised using amino acid analysis and amine derivatisation. A lipid extract containing PT will be hydrolysed using strong acid then analysed HILIC LC-MS/MS in the positive mode for threonine (79). The proposed primary amine of PT will be confirmed using derivatisation with NHS-biotin followed by MS/MS analysis of derivatised lipids, as previously described for PS (76).

## 3.2 Results

### 3.2.1 Targeted LC-MS/MS reveals candidate PT ions in whole blood extract

A HILIC LC-MS/MS method described in the literature was optimised and used for PS and PT analysis (80). Modifications from the published method include a higher flow rate (0.6 mL/min compared to 0.2 mL/min) and a different gradient for elution (**Experimental Methods 2.10**) .

Whole blood lipid extracts were analysed using targeted HILIC LC-MS/MS as described in **Experimental Methods**. Negative mode neutral loss scanning of 101 Da showed five candidate PT ions: *m/z* 802.6, 824.7, 848.6, 850.7, and 852.7 (**Figure 3.1A**). Based on the *m/z* values of the precursors, the ions were putatively identified as PT 36:1, PT 38:4, PT 40:6, PT 40:5, and PT 40:4, respectively, noting they are 14 Da larger than the corresponding PS species. Candidate ions were also observed using multiple reaction monitoring (MRM) of product ions resulting from the loss of 101 Da from precursors (**Figure 3.1B**). The putative PT species eluted earlier than the corresponding PS species in HILIC-LC, which is consistent with the presence of an additional hydrophobic methyl group. However, the methyl group could be attached at different sites on the serine backbone, giving rise to threonine, N-methyl serine, or serine methyl ester (**Figure 3.2**).

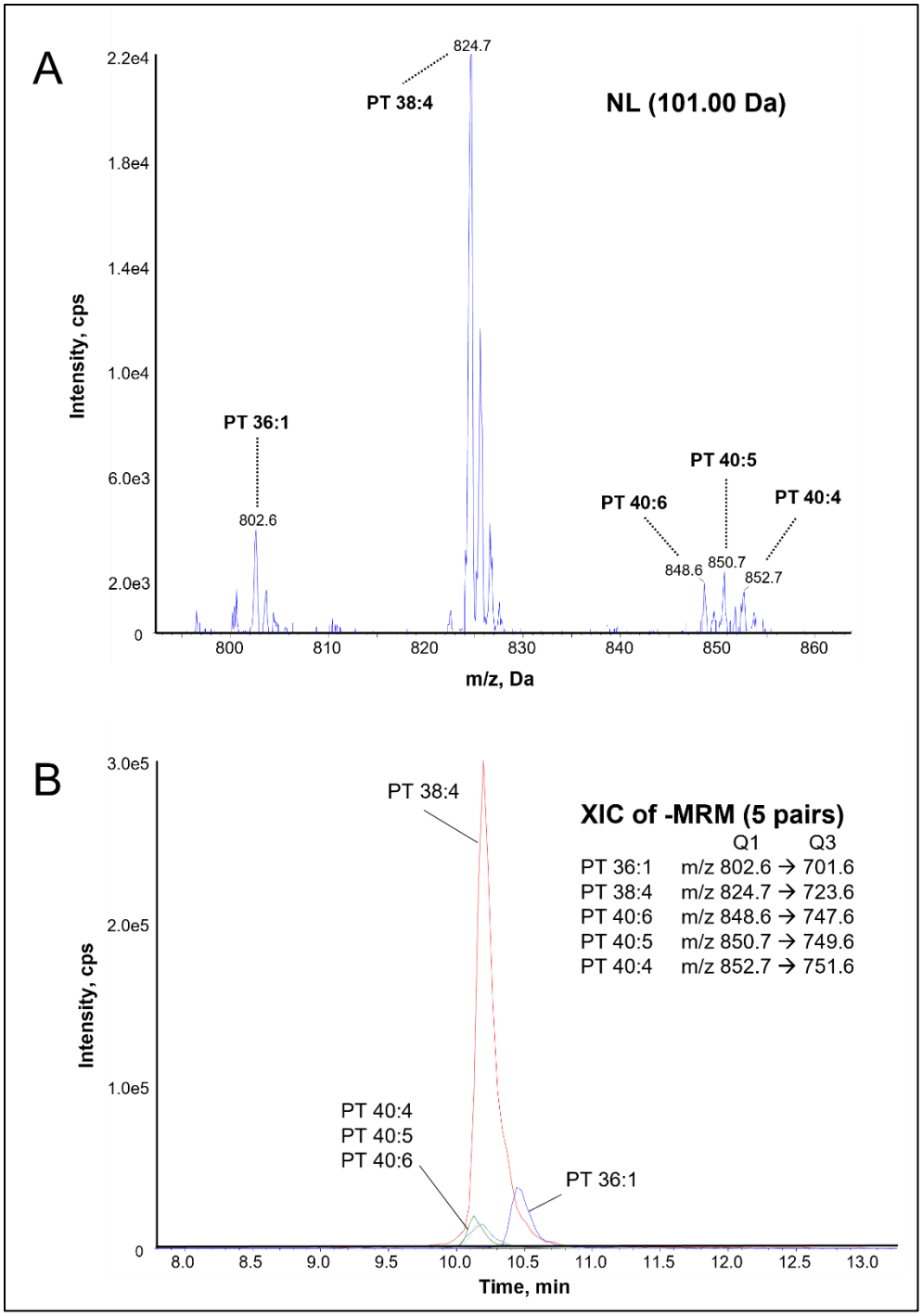


**Figure 3.1 – Detection of candidate PT ions in whole blood lipid extract**

Lipids were extracted from whole blood and analysed using targeted HILIC LC-MS/MS as described in **Experimental Methods**. (A) Neutral loss scan of 101 Da spectrum showing five ions that are above the baseline. (B) Extracted ion chromatograms of five potential PT species, detected using multiple reaction monitoring.

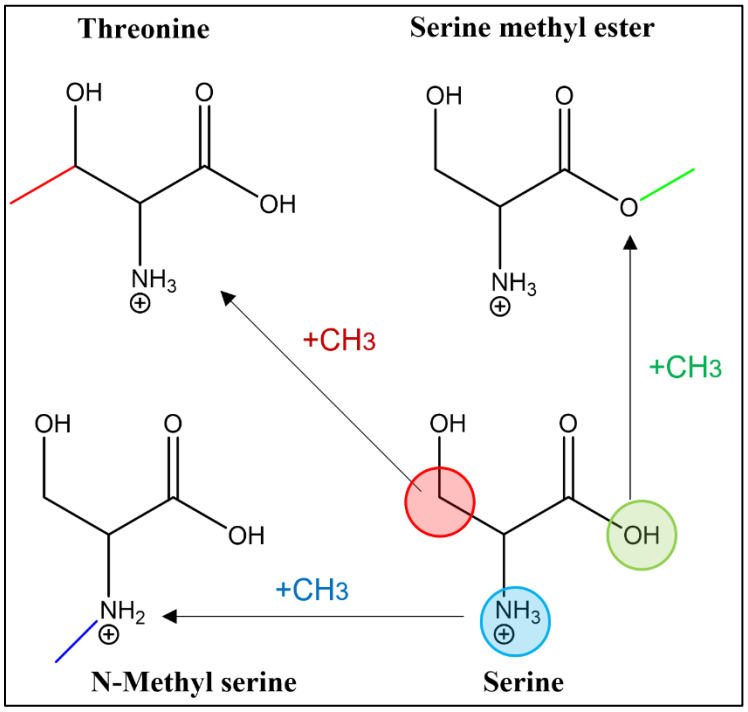


**Figure 3.2 – Structures of serine and isomers of threonine**

Methyl groups could be attached to serine at different sites resulting in different isomers such as threonine, serine methyl ester, and N-methyl serine, among other compounds (not shown).

### 3.2.2 Acid hydrolysis of PT releases threonine

A fraction containing PS and putative PT was purified from whole blood lipid extract using HILIC chromatography then hydrolysed with 3 M HCl at 100 °C for 1 hour (**Experimental Methods**). HILIC LC-MS/MS analysis of the hydrolysate showed the release of serine and threonine (**Figure 3.3A**), which were not present before hydrolysis. The serine and threonine peaks coeluted with L-serine and L-threonine standards, and the threonine peak also coeluted with threonine released from the hydrolysate of a PT standard (**Figure 3.3B**). An MRM transition of *m/z* 120.1 → 74.1 was used for the detection of threonine because the product ion (*m/z* 74.1) is specific to threonine and is not produced by N-methyl serine nor serine methyl ester (66). Hydrolysis of the sample released 32-fold more serine than threonine (**Figure 3.3C**). Representative chromatograms of amino acid standards are available in **Appendix 9.3**.

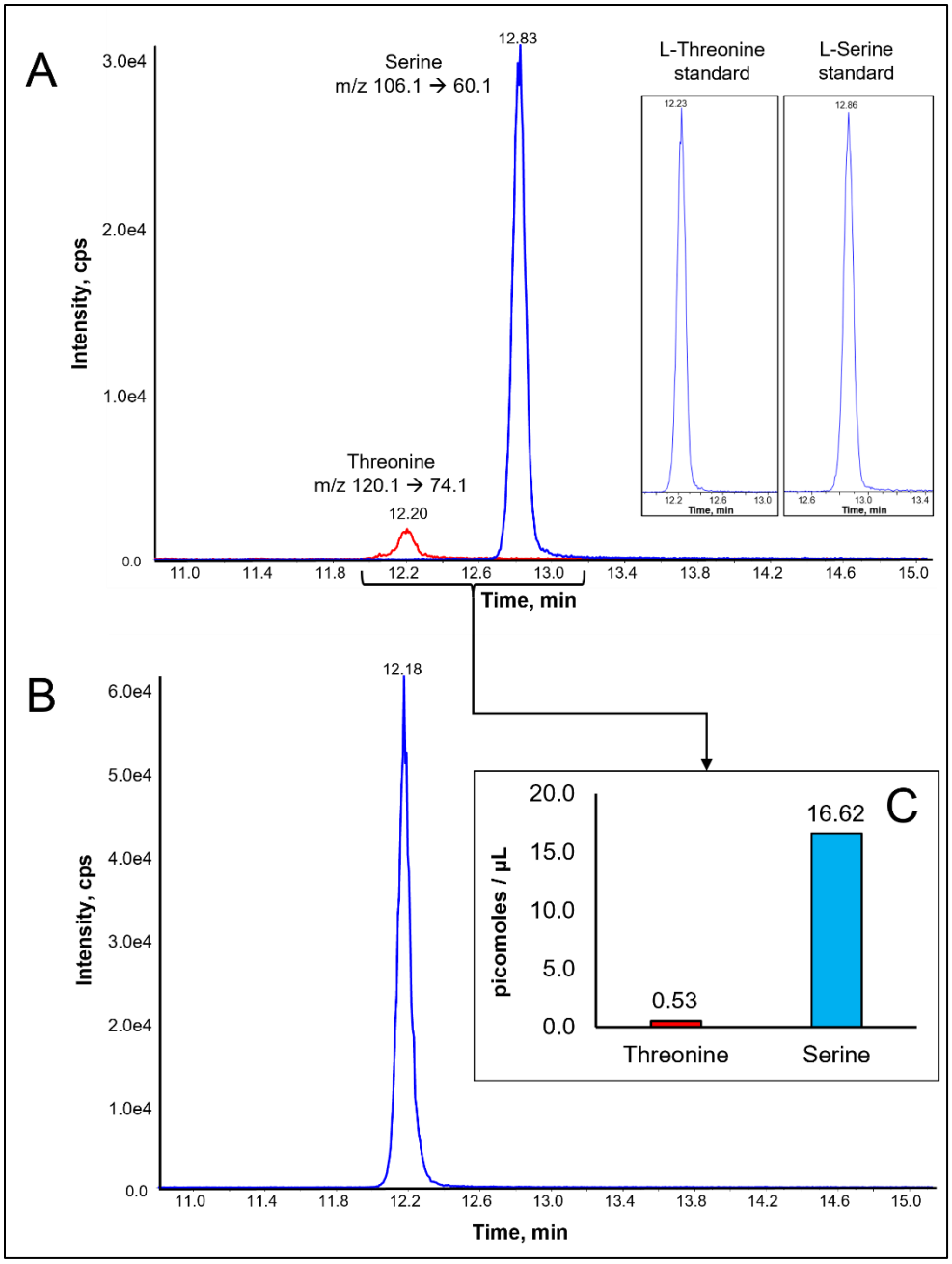


**Figure 3.3 – Detection of serine and threonine in the acid hydrolysate of PS and PT from whole blood using LC-MS/MS**

PS and PT were purified from whole blood lipid extract using HILIC LC, hydrolysed in 3 M HCl at 100 °C for 1 h, then analysed using targeted HILIC LC-MS/MS as described in **Experimental Methods**. (A) Extracted ion chromatograms of serine and threonine in the sample, showing coelution with L-serine and L-threonine standards. (B) Extracted ion chromatogram of threonine released from the acid hydrolysis of PT 16:0/18:1(9Z) standard. (C) Quantification of serine and threonine released from the hydrolysis of PS and PT in whole blood extract. Amino acids were quantified using calibration curves (**Appendix 9.1**).

### 3.2.3 $MS^2$ and $MS^3$ spectra identify fatty acids in PT

Fatty acid compositions of the five identified PT species were determined using LC-MS/MS in the negative ion mode. PS and PT coeluted in the HILIC method employed. Consequently, $MS^2$ scans of PT ions also showed product ions from coeluting odd-chained PS species, specifically product ions resulting from neutral loss of 87 Da from the precursor (**Figure 3.4A**). To avoid this, $MS^3$ scans were collected instead of $MS^2$. Fragments resulting from the threonine head group loss ($[M-H-101]^-$) were selected as second precursors for further fragmentation (**Figure 3.4B**). The five PT species were characterised as follows: PT 18:0_18:1, PT 18:0_20:4, PT 18:0_22:6, PT 18:0_22:5, and PT 18:0_22:4 (**Figures 3.4, 3.5 & 3.6**).

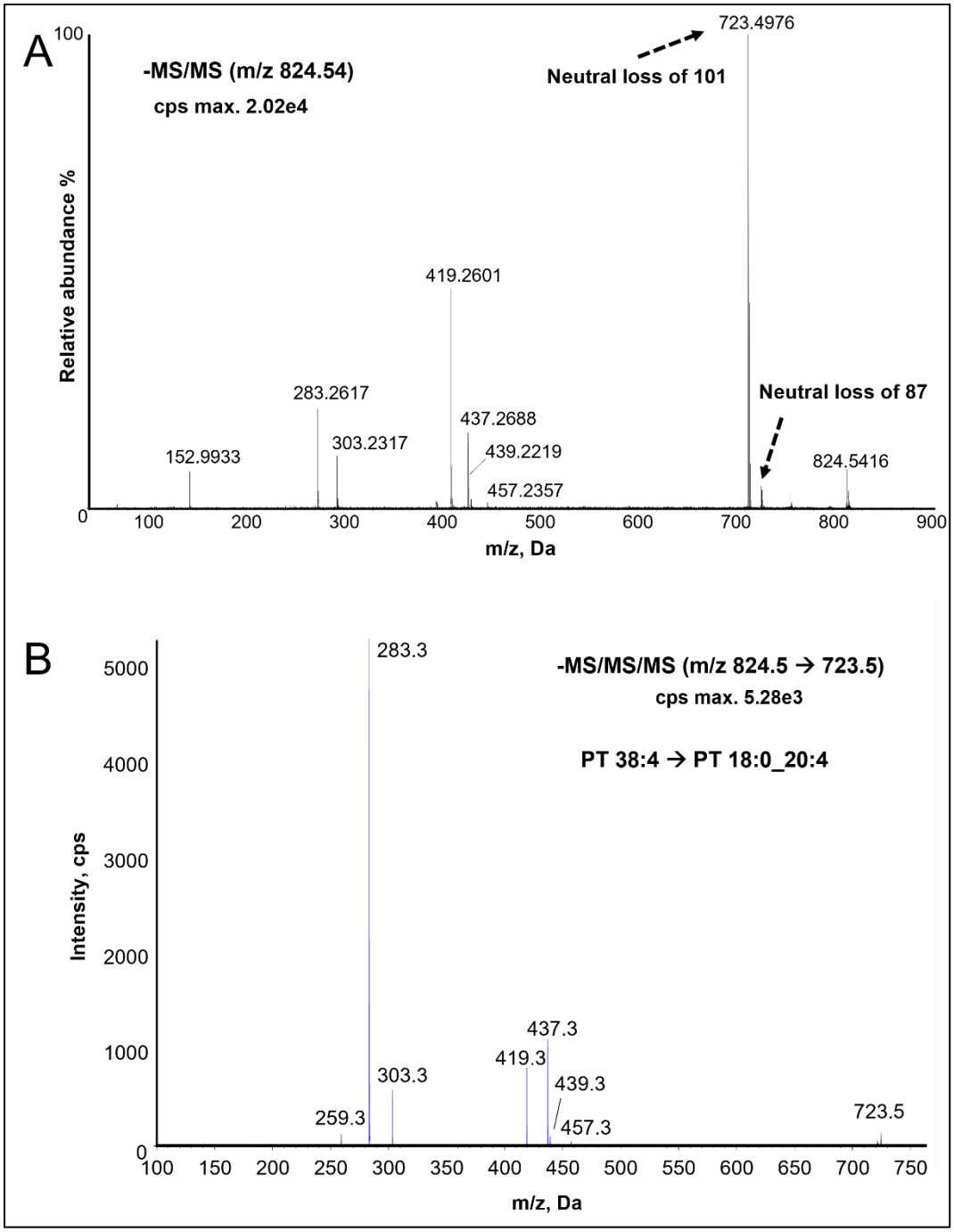


**Figure 3.4 – Identification of PT fatty acyl chains using $MS^2$ and $MS^3$ scans**

Whole blood lipid extracts were analysed using targeted HILIC LC-MS/MS as described in **Experimental Methods**. (A) Accurate mass $MS^2$ scan of *m/z* 824.54 showing head loss fragments from two isomeric species: PT 38:4 (neutral loss of 101 Da) and PS 39:4 (neutral loss of 87 Da). (B) $MS^3$ scan of PT 38:4 with *m/z* 824.5 as first precursor and *m/z* 723.5 as second precursor. Both spectra show *m/z* 283 (FA 18:0) and *m/z* 303 (FA 20:4), identifying the structure as PT 18:0_20:4.

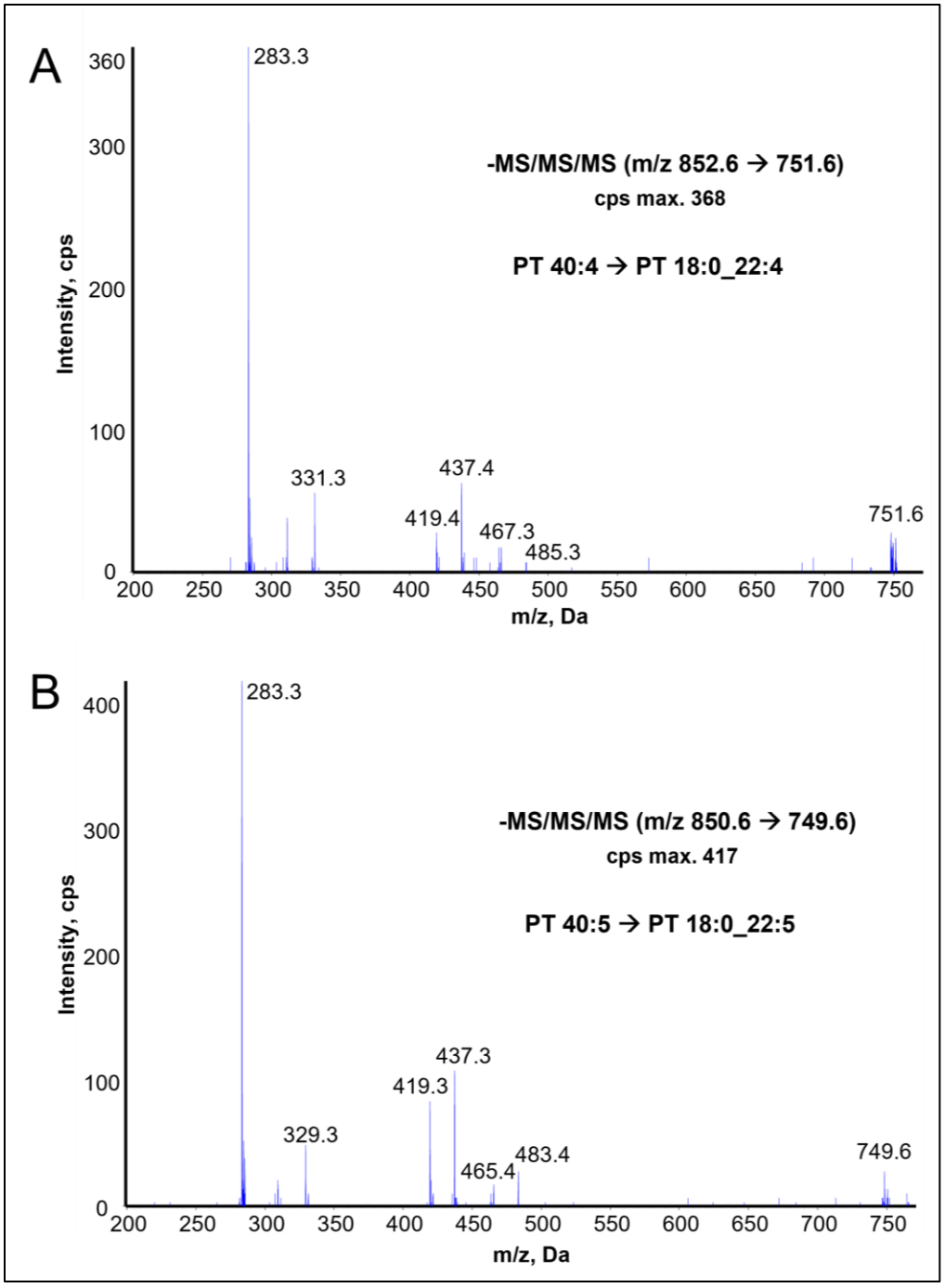


**Figure 3.5 – MS$^3$ scans of PT 40:4 and PT 40:5**

Whole blood lipid extracts were analysed using targeted HILIC LC-MS/MS as described in **Experimental Methods**. (A) MS$^3$ scan of PT 40:4 with *m/z* 852.6 as first precursor and *m/z* 751.6 as second precursor. Spectrum shows *m/z* 283 (FA 18:0) and *m/z* 331 (FA 22:4), identifying the structure as PT 18:0_22:4 (B) MS$^3$ scan of PT 40:5 with *m/z* 850.6 as first precursor and *m/z* 749.6 as second precursor. Spectrum shows *m/z* 283 (FA 18:0) and *m/z* 329 (FA 22:5), identifying the structure as PT 18:0_22:5.

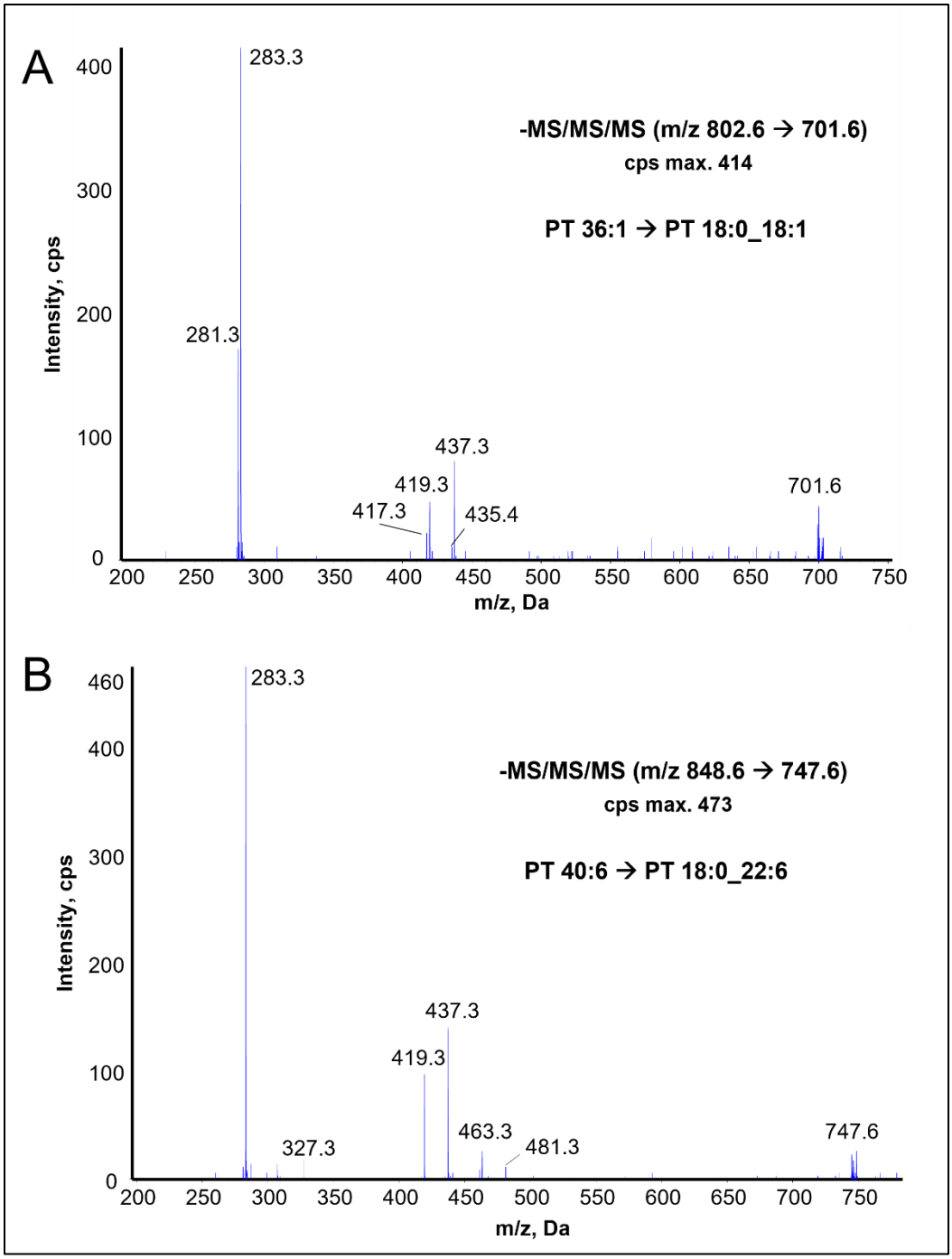


**Figure 3.6 – MS$^3$ scans of PT 36:1 and PT 40:6**

Whole blood lipid extracts were analysed using targeted HILIC LC-MS/MS as described in **Experimental Methods**. (A) MS$^3$ scan of PT 36:1 with *m/z* 802.6 as first precursor and *m/z* 701.6 as second precursor. Spectrum shows *m/z* 283 (FA 18:0) and *m/z* 281 (FA 18:1), identifying the structure as PT 18:0_18:1 (B) MS$^3$ scan of PT 40:6 with *m/z* 848.6 as first precursor and *m/z* 747.6 as second precursor. Spectrum shows *m/z* 283 (FA 18:0) and *m/z* 327 (FA 22:6), identifying the structure as PT 18:0_22:6.

### 3.2.4 Mild acid hydrolysis determines fatty acid *sn*-positions in PT

Next, FA *sn*-positions in PT species were determined using acid hydrolysis (0.3 M HCl, 40 °C, 30 min) of whole blood lipid extracts followed by LC-MS/MS of lysoPT. Ratios of 1-acyl/2-acyl lysoPT generated by acid hydrolysis were used to determine the *sn*-position of FAs (**Figures 3.7 & 3.8)**. A 9:1 (1-acyl/2-acyl) ratio indicates the FA was in the *sn*-1 position before hydrolysis. In contrast, a ratio of ~1:1 indicates the FA was in the *sn*-2 position but underwent partial migration to the *sn*-1, slowed by reconstitution in acidic methanol (containing 0.1 mM formic acid). The *sn*-1 positions were occupied by FA 18:0, whereas the *sn*-2 positions were occupied by unsaturated FAs: 18:1, 20:4, 22:6, 22:5 and 22:4. The final structure assignments were as follows: PT 18:0/18:1, PT 18:0/20:4, PT 18:0/22:6, PT 18:0/22:5, and PT 18:0/22:4.

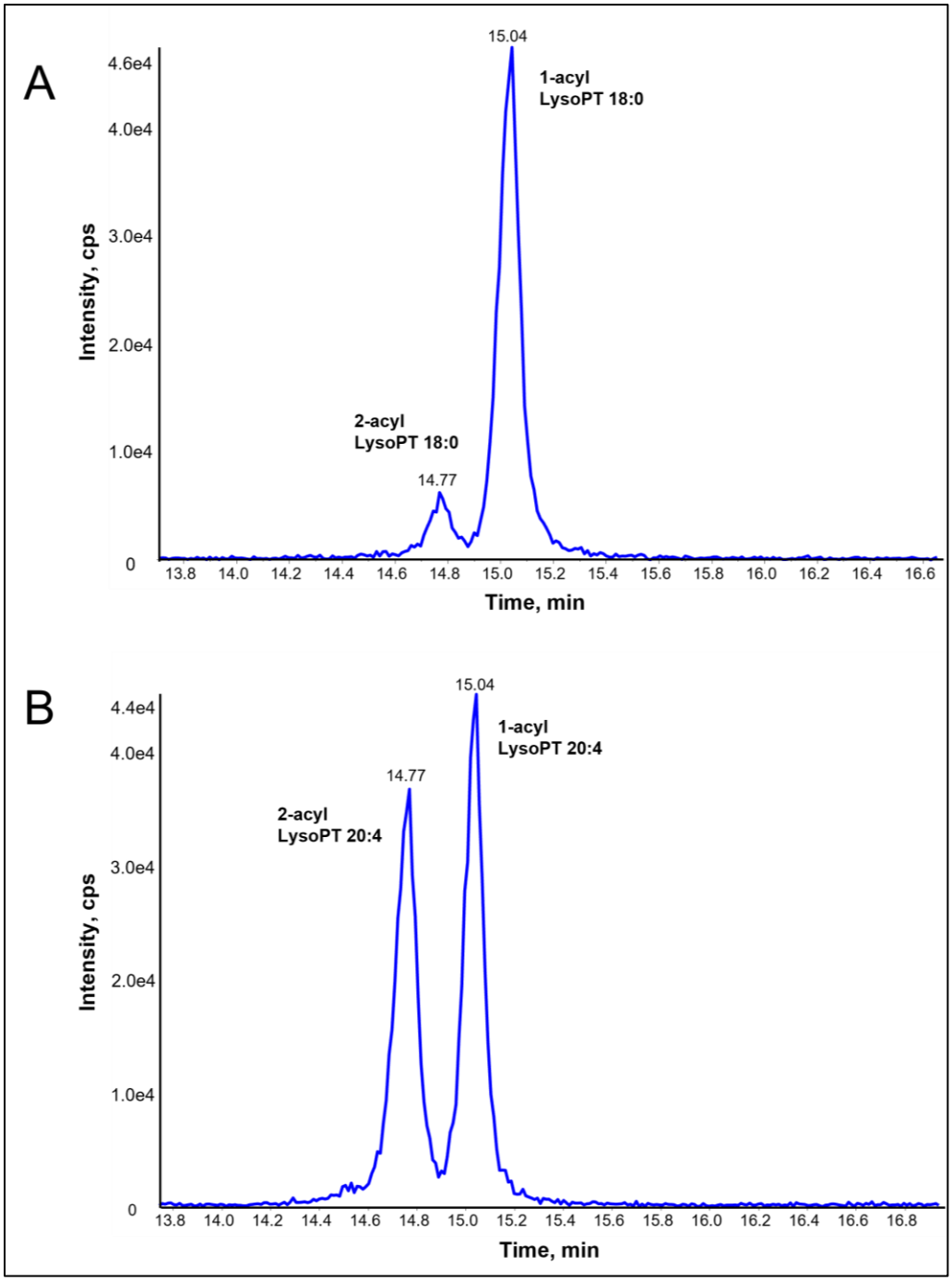


**Figure 3.7 – LysoPT generated by mild acid hydrolysis identifies the *sn*-position of FAs**

Whole blood lipid extracts were hydrolysed using dilute acid (0.2 M HCl, 40 °C, 30 min) then analysed using targeted LC-MS/MS as described in **Experimental Methods**. (A) Extracted ion chromatogram of lysoPT 18:0 shows higher amounts of the 1-acyl isomer compared to the 2-acyl isomer, suggesting FA 18:0 was at the *sn*-1 position. (B): Extracted ion chromatogram of lysoPT 20:4 shows comparable amounts of 1-acyl and 2-acyl isomers, suggesting FA 20:4 was at the *sn*-2 position.

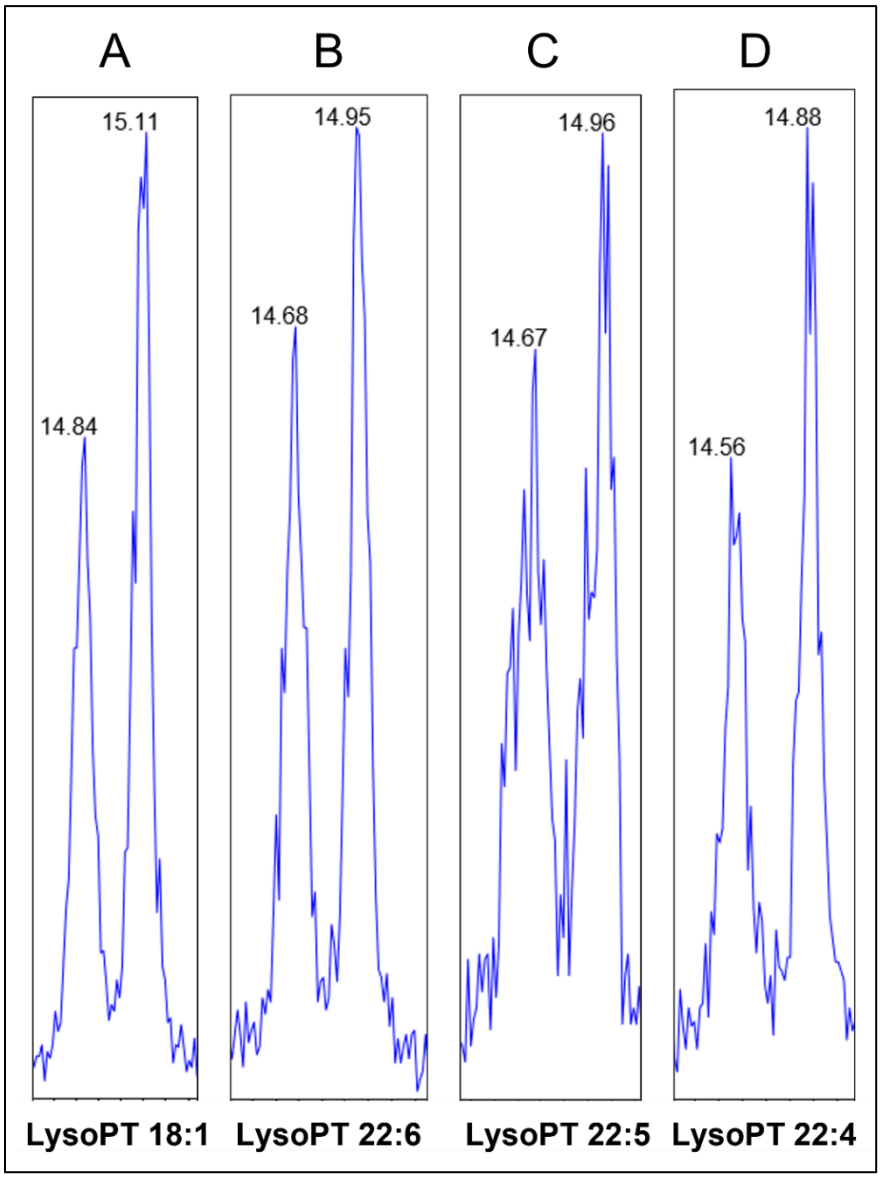


**Figure 3.8 – Extracted ion chromatograms of lysoPT generated by mild acid hydrolysis**

Whole blood lipid extracts were hydrolysed using dilute acid (0.2 M HCl, 40 °C, 30 min) then analysed using targeted LC-MS/MS as described in **Experimental Methods**. The 2-acyl isomer elute earlier than the 1-acyl. (A) Extracted ion chromatogram of lysoPT 18:1 shows comparable amounts of the 1-acyl isomer compared to the 2-acyl isomer, suggesting FA 18:1 was at the *sn*-2 position. (B): Extracted ion chromatogram of lysoPT 22:6 shows comparable amounts of 1-acyl and 2-acyl isomers, suggesting FA 22:6 was at the *sn*-2 position. (C): Extracted ion chromatogram of lysoPT 22:5 shows comparable amounts of 1-acyl and 2-acyl isomers, suggesting FA 22:5 was at the *sn*-2 position. (D): Extracted ion chromatogram of lysoPT 22:4 shows comparable amounts of 1-acyl and 2-acyl isomers, suggesting FA 22:4 was at the *sn*-2 position.

### 3.2.5 PT contains a primary amine group

PT in whole blood lipid extract was derivatised with NHS-biotin by drying, reconstitution in 2:1 chloroform/methanol containing 1% (v/v) triethylamine and NHS-biotin (19.4 mM), and incubation at 22 °C for 2 h (reaction scheme in **Figure 3.9C**) . Lipid extracts were analysed before and after hydrolysis using targeted HILIC LC-MS/MS. Biotinylated PT species were only detected after derivatisation, and the reaction proceeded to completion (i.e., PT was only detected in the derivatised form) (**Figures 3.9A & 3.9B**). These results indicate that PT contains a primary amine group, supporting the evidence from amino acid analysis.

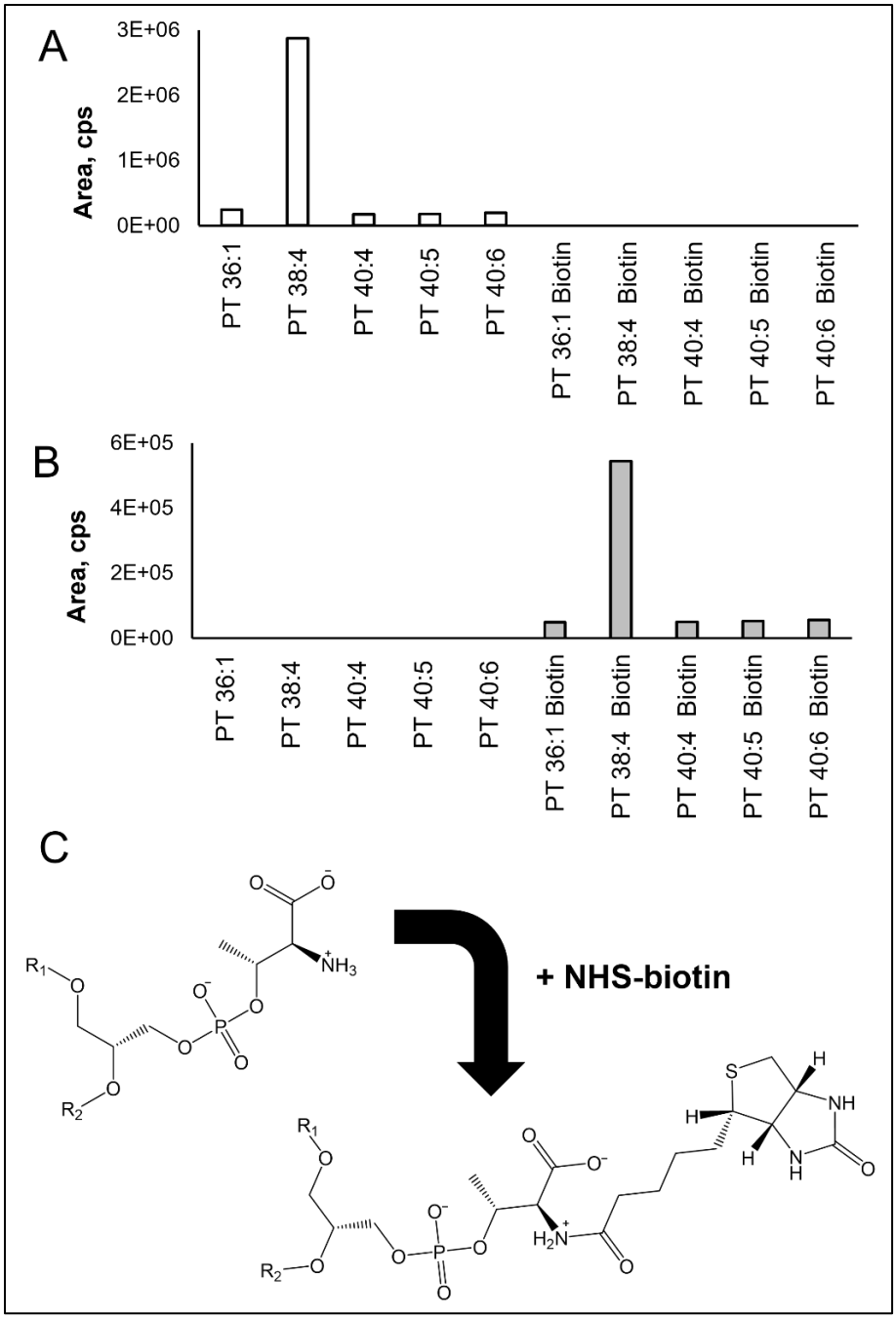


**Figure 3.9 – PT in whole blood contains a primary amine group**

Blood lipid extract was dried then derivatised by reconstitution in 2:1 chloroform/methanol containing 1% (v/v) triethylamine and NHS-biotin (19.4 mM) and incubation at 22 °C for 2 h. Derivatised samples were analysed using targeted HILIC LC-MS/MS analysis as described in **Experimental Methods**. (A) PT in sample before derivatisation. (B) PT-biotin in sample after derivatisation. Data represented as area values (area under the curve). (C) Derivatisation reaction using NHS-biotin, showing the structures of the underivatized (top left) and derivatised PT head groups (bottom right). $R_1$ and $R_2$ = *sn*-1 and *sn*-2 fatty acids, respectively.

### 3.2.6 Quantification of PT and PS in whole blood

PT and PS species were quantified in whole blood or plasma lipid extracts from three genetically unrelated donors using targeted HILIC-LC-MS/MS (**Figure 3.10**). PS 15:0/18:1[D7] (in SPLASH mix) was added to samples as an internal standard (IS) during lipid extraction. Analyte/IS values were used to quantify PS and PT species using calibration curves of PS 18:0/20:4 or PT 16:0/18:1 versus PS 15:0/18:1[D7], respectively (**Appendix 9.2**). In whole blood, PS 38:4 and PT 38:4 were the most abundant lipids in their classes. However, the second most abundant PS was PS 40:6, whereas for PT it was PT 36:1. Collectively, PT levels were approximately 100-fold lower than PS. PS 38:4 and PS 36:1 were 70 to 80-fold higher than their corresponding PT species, whereas PS 40:6, PS 40:5, and PS 40:4 were all >200-fold higher than their corresponding PT species. In other words, the greatest fold differences between PS and PT were observed in species containing 22-carbon FAs. Plasma PS levels were 485-fold lower than those in whole blood (**Figure 3.10**), while PT was likely below the limit of detection for plasma.

These results demonstrate that PS and PT are predominantly found in the cellular component of blood, and PT concentration is 100-fold lower than PS.

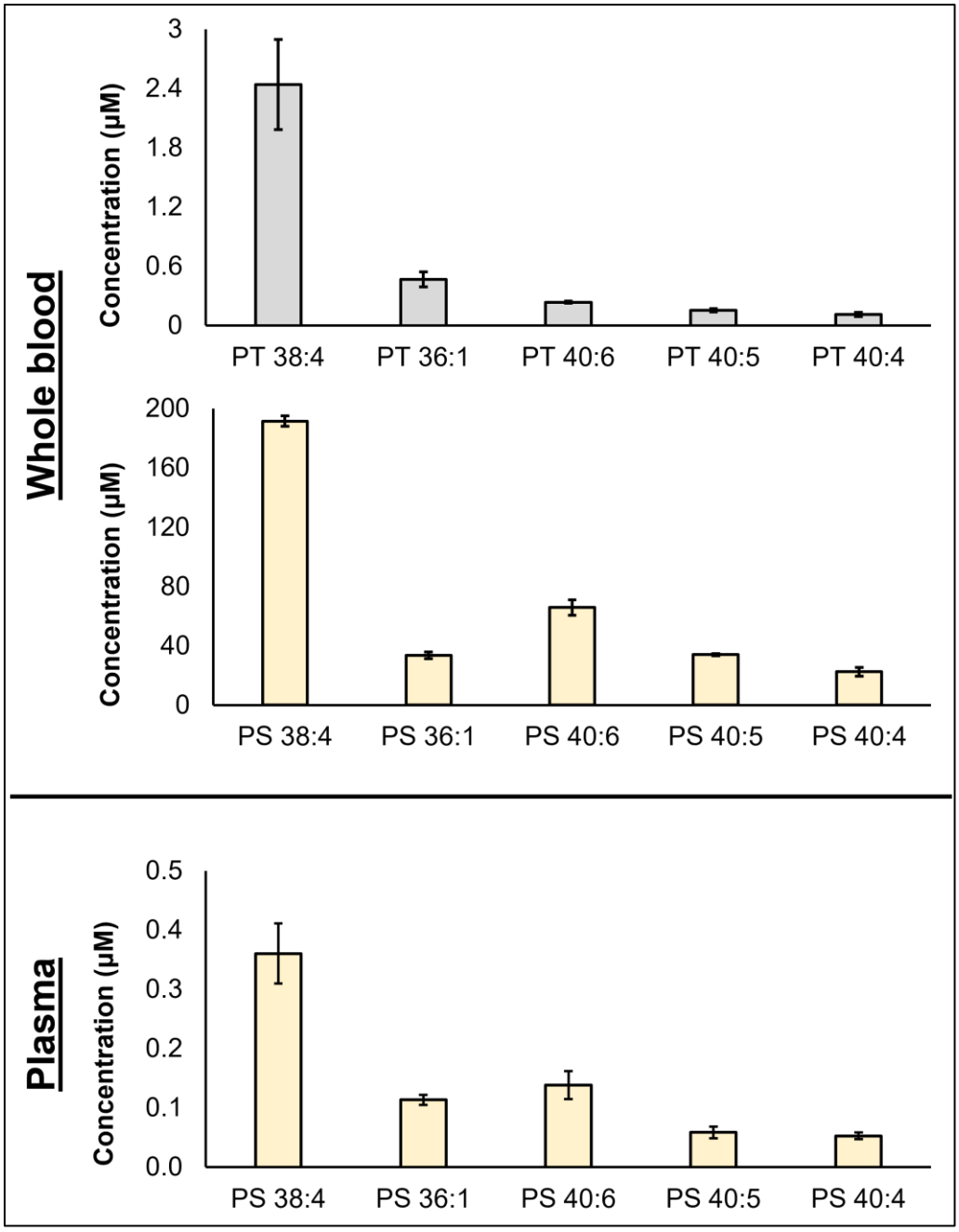


**Figure 3.10 – PT and PS levels in whole blood and PS levels in plasma from three genetically unrelated donors.**

Lipids from whole blood or plasma were extracted and analysed using targeted HILIC LC-MS/MS as described in **Experimental Methods**. Ratios of analytes to internal standard (A/IS, cps) were calculated and used to quantify lipids based on calibration curves (**Appendix 9.2**). Data are represented as mean ± SEM (n = 3). PT was not detected in plasma.

## 3.3 Discussion

In this chapter, I demonstrated the presence of PT in human blood using LC-MS/MS. PT was initially detected using neutral loss scanning of 101 Da, which is not specific for threonine and would also show isomeric species such as N-methyl serine and serine methyl ester. Acid hydrolysis and amino acid analysis were used to further characterise the head group. The MRM transition used for the detection of threonine in the hydrolysate (*m/z* 120.1 → 74.1) is specific for threonine, eliminating N-methyl serine and serine methyl ester as possibilities. PT was successfully derivatised by NHS-biotin, which suggests it contains a primary amine group. The PT head group is most likely to be L-threonine (with 2S,3R stereochemistry) because it is the most abundant threonine isomer in mammalian tissues (81).

In mammalian cells, PS is synthesized by PSS1 and PSS2. The former uses PC as a substrate, while the latter prefers PE with FA 22:6 in the *sn*-2 position (18). It is unknown which isoform synthesizes PT in mammalian cells. Given the high abundance of PS 40:6 compared to PT 40:6, it may be that PSS1 synthesizes both PS and PT, while PSS2 only synthesizes PS or more PS than PT compared to PSS1. This hypothesis requires further investigation with purified/recombinant human enzymes. Alternatively, differences in PS and PT profiles could be due to differential head group and FA preferences of acyltransferases during PL acyl chain remodelling. However, it is unknown which (if any) acyltransferases add FA 22:6 to lysoPS, while several enzymes are known to add FA 22:6 to lysoPC and lysoPE (82). Therefore, it is likely that the rate-limiting step of PS 40:6 biosynthesis is the PSS base-exchange reaction. This may also be the case for PS 40:5 and PS 40:4.

PT was not detected in plasma. This is probably due to the lipid being below the limit of detection. Detection of PT in plasma using the method described in this thesis would not be possible if it was present in plasma at 1/100$^{th}$ the concentration of PS. On the other hand, PS was detectable in plasma, but levels were 485-fold lower than in whole blood. These results indicate that PT, like PS, is predominantly found in the cellular compartment of blood. The PS in plasma could be from contaminating blood cells or extracellular vesicles, as the plasma was prepared using a single centrifugation step. Lipoproteins are unlikely to be the source of PS as several reports failed to detect PS in lipoprotein fractions, but this possibility cannot be ruled out (83-85).

Note, red blood cells (RBC) are the most abundant cells in blood. As such, the lipid profiles determined here likely reflect those of RBCs with minor contributions from platelets and leukocytes. In support of this, the PS profile determined here is consistent with a previous report by Leidl *et al*., in which PS 38:4 and PS 40:6 were the two most abundant PS species in RBCs (86).

Amino acid analysis of blood lipid hydrolysate (purified PS/PT fraction) showed 32-fold more serine than threonine. The fold difference is inconsistent with the direct analysis, where PS was 100-fold more abundant than PT. Several explanations are possible. First, only five PS and PT species were quantified. There exist other PS and presumably PT species that were not quantified here. Second, PS and PT coelute in the chromatographic method used. As such, PT detection could have been hampered by the more abundant PS due to ion suppression effects. This would result in the underestimation of PT levels. Last, the stabilities of serine and threonine in strong acid may be different, and no deuterated standards were used to account for degradation during acid hydrolysis. As such, serine levels could have been underestimated.

Having characterised the PT profile of whole blood, the next logical step would be to investigate the PT profiles of blood cells such as platelets, leukocytes, as well as extracellular vesicles (EV) derived from those cells. The presence of PT in these cell types would be a first step in investigating a potential role for PT in coagulation.

## 3.4 Conclusion

In conclusion, PT is present in the cellular component of blood at approximately 1/100$^{th}$ the concentration of PS. The head group of PT contains a primary amine group which can be derivatised with NHS-biotin. This will facilitate the investigation of the lipid's distribution in the inner and outer leaflets of cells. The PS and PT profiles of whole blood are very similar, with both classes being enriched in FA 20:4 in the *sn*-2 position. However, PS is more enriched in 22-carbon FAs compared to PT, suggesting differences in metabolism of PS and PT. It is recommended to investigate the presence of PT in human platelets, EVs, and leukocytes. This will be the aim of the next chapter.

# CHAPTER 4 PT in platelets, leukocytes, and extracellular vesicles

## 4.1 Introduction

In **Chapter 3**, I showed that phosphatidylthreonine (PT) is present in human blood and speculated that it may function in supporting coagulation. It is highly likely that PT could also be present in individual circulating blood cells (platelets, leukocytes), as it is proposed to be synthesized by PSS enzymes, of which one isoform is a housekeeping protein (17). In this chapter, I will characterise PT and PS molecular species in platelets, leukocytes, and EVs, and investigate their metabolism in thrombin-activated platelets. Platelet PS is enriched in FA 20:4 and may serve as a source of free FAs in activated platelets after hydrolysis by $cPLA_2$ (86). It is unclear whether the PT profile (molecular species composition) of platelets, EVs, and leukocytes are identical to their PS profiles. Another question is whether PT, like PS, is asymmetrically distributed in the membrane and is externalised by platelets in response to thrombin. I will investigate these questions using an LC-MS/MS approach. Traditionally, PS externalisation had been studied qualitatively using annexin V, a protein that binds PS, in combination with fluorescence microscopy or flow cytometry (87). An LC-MS/MS method was developed to quantitatively study PS externalisation (76). Here, cells are treated with membrane-impermeable biotin (sulfo-NHS-biotin) to label external PS or a membrane-permeable analogue (NHS-biotin) to label total PS, then biotinylated lipids are extracted and analysed using LC-MS/MS (76, 88). The derivatisation reaction with NHS-biotin labels primary amine groups, and the resulting derivatives can be detected using LC-MS/MS by monitoring characteristic MS/MS transitions, e.g., *m/z* $[M-H]^- \rightarrow [M-H-313]^-$ for biotinylated PS. The ratio of external PS to total PS gives the % externalisation. I previously showed that PT, like PS, can be derivatised with NHS-biotin. As such, this method will be used to study PT externalisation in platelets.

## 4.2 Results

### 4.2.1 PT profile of platelets

Platelet lipid extracts from the clinical cohort (n = 24, healthy volunteers) were spiked with internal standard (IS) and analysed using HILIC LC-MS/MS, as described in **Experimental Methods**. 10 PS and 10 PT species were measured using MRM transitions corresponding to head group loss (**Table 2.2**). Due to coelution of PS and PT in the LC method employed, FA transitions are not suitable for MS detection due to interference from isomeric species. Representative chromatograms are in **Appendix 9.7**. Absolute quantification of PT was not possible in cohort samples because the IS was added post extraction.

The platelet PT profile matched the PS profile with some differences (**Figure 4.1A**). The most abundant PT lipid was PT 36:1 followed by PT 38:4, while the opposite was observed for PS. PS 36:1 was 71-fold more abundant than PT 36:1, while PS 38:4 was 171-fold more abundant than PT 38:4 (**Figure 4.1A**). PS species were always more abundant than their corresponding PT species, and the greatest fold differences were observed in species with 40:6 (263-fold), 40:5 (252-fold), and 40:4 (260-fold) compositions (**Figure 4.1A**). As a percentage of total lipid in the class, PT is more enriched in shorter chain species (34C and 36C, total carbon chain length) species than PS, while PS is more enriched in longer chain (38C and 40C) species (**Figure 4.1B**).

$MS^3$ was used to determine the FA compositions of PS and PT species in platelets (**Table 4.1,** examples in **Figure 4.2**, complete set in **Appendix 9.9**). PT FA compositions were similar to PS. However, more PS FA composition combinations (compared to PT) were identified due to the higher abundance of PS. PT 40:3 could not be characterised due to its low level. Notably, PS 40:3, 40:4 and 40:5 had considerable amounts of species with two 20-carbon FAs (e.g., PS 20:1_20:4), comparable to species with one 18-carbon FA and one 22-carbon FA (e.g., PS 18:0_22:5), as indicated by intensity of FA ions. This was also observed for PT 40:4 and PT 40:5.

To summarize, these results show that PT is present in platelets, with PT 18:0_18:1 and PT 18:0_20:4 as the most abundant species, making up the bulk of PT in platelets. The PT profile closely matches that of PS, but PT is less enriched in longer chain (38C and 40C) species.

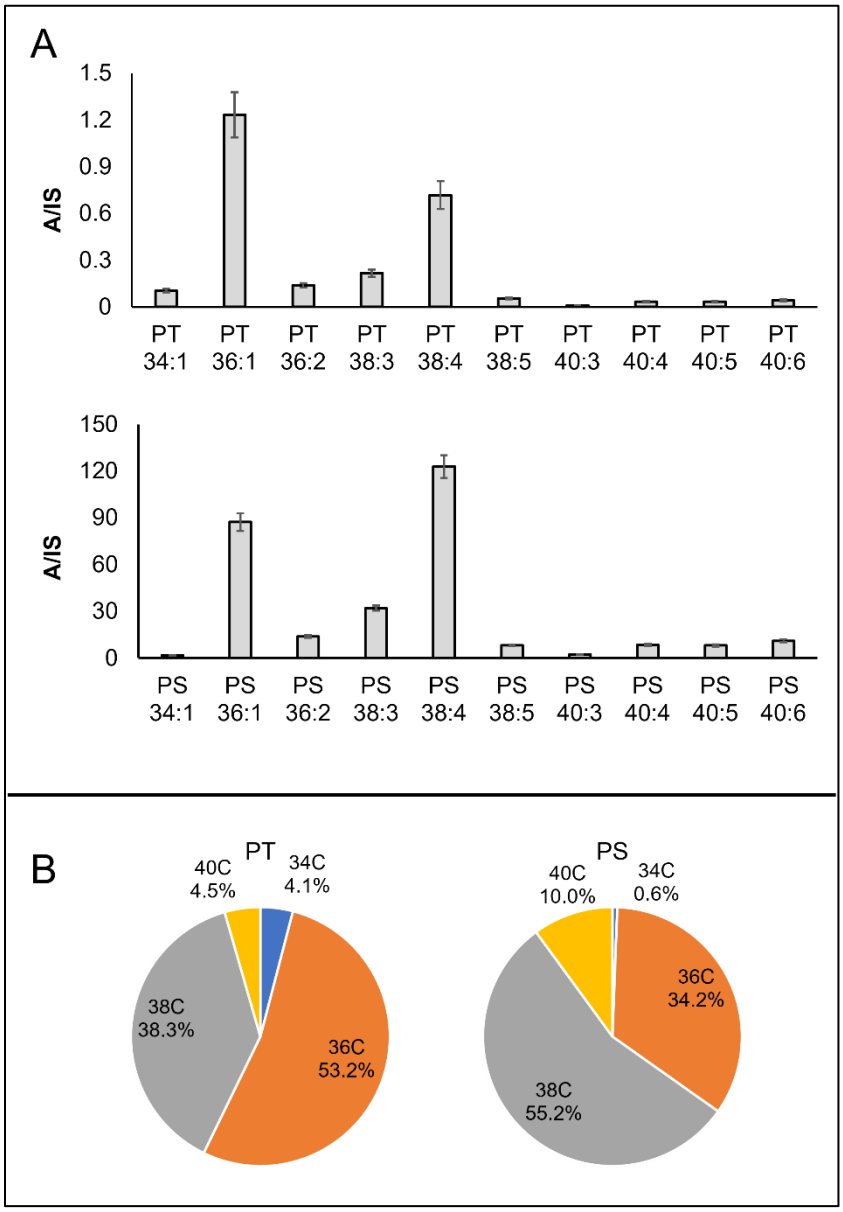


**Figure 4.1 – PT and PS profiles of platelets from healthy volunteers**

Platelet lipid extracts from healthy volunteers were spiked with an internal standard (IS, PS 15:0/18:1[D7]) then analysed using targeted HILIC-LC-MS/MS as described in **Experimental Methods**. Analyte peaks were integrated and ratios of analytes to internal standards (A/IS) were calculated. Bar graph data are represented as mean ± SEM (n = 24). For pie charts, A/IS values of species with the same FA carbon number were summed and used to calculate percentages (mean of n = 24). **(A)** Bar graphs showing relative levels of PT and PS species in platelets. **(B)** Pie charts showing the percentage composition of PS and PT in terms of FA carbon number (34C: 34-carbon, etc). Absolute quantification was not possible because IS was added after extraction.

**Table 4.1 – Fatty acid (FA) compositions of PS and PT species in platelets**

| Lipid | FA composition |
|---|---|
| PS 34:1 | 16:0_18:1 & 16:1_18:0 |
| PS 36:1 | 18:0_18:1 |
| PS 36:2 | 18:1_18:1 & 18:0_18:2 |
| PS 38:3 | 18:0_20:3 |
| PS 38:4 | 18:0_20:4 |
| PS 38:5 | 18:1_20:4 |
| PS 40:3 | 18:0_22:3 & 18:1_22:2 & 20:0_20:3 |
| PS 40:4 | 18:0_22:4 & 18:1_22:3 & 20:0_20:4 |
| PS 40:5 | 18:0_22:5 & 18:1_22:4 & 20:1_20:4 |
| PS 40:6 | 18:0_22:6 & 18:1_22:5 & 20:2_20:4 |
| PT 34:1 | 16:0_18:1 |
| PT 36:1 | 18:0_18:1 |
| PT 36:2 | 18:1_18:1 & 18:0_18:2 |
| PT 38:3 | 18:0_20:3 |
| PT 38:4 | 18:0_20:4 |
| PT 38:5 | 18:1_20:4 |
| PT 40:3 | N/A (low signal) |
| PT 40:4 | 18:0_22:4 & 20:0_20:4 |
| PT 40:5 | 18:0_22:5 & 20:1_20:4 |
| PT 40:6 | 18:0_22:6 |

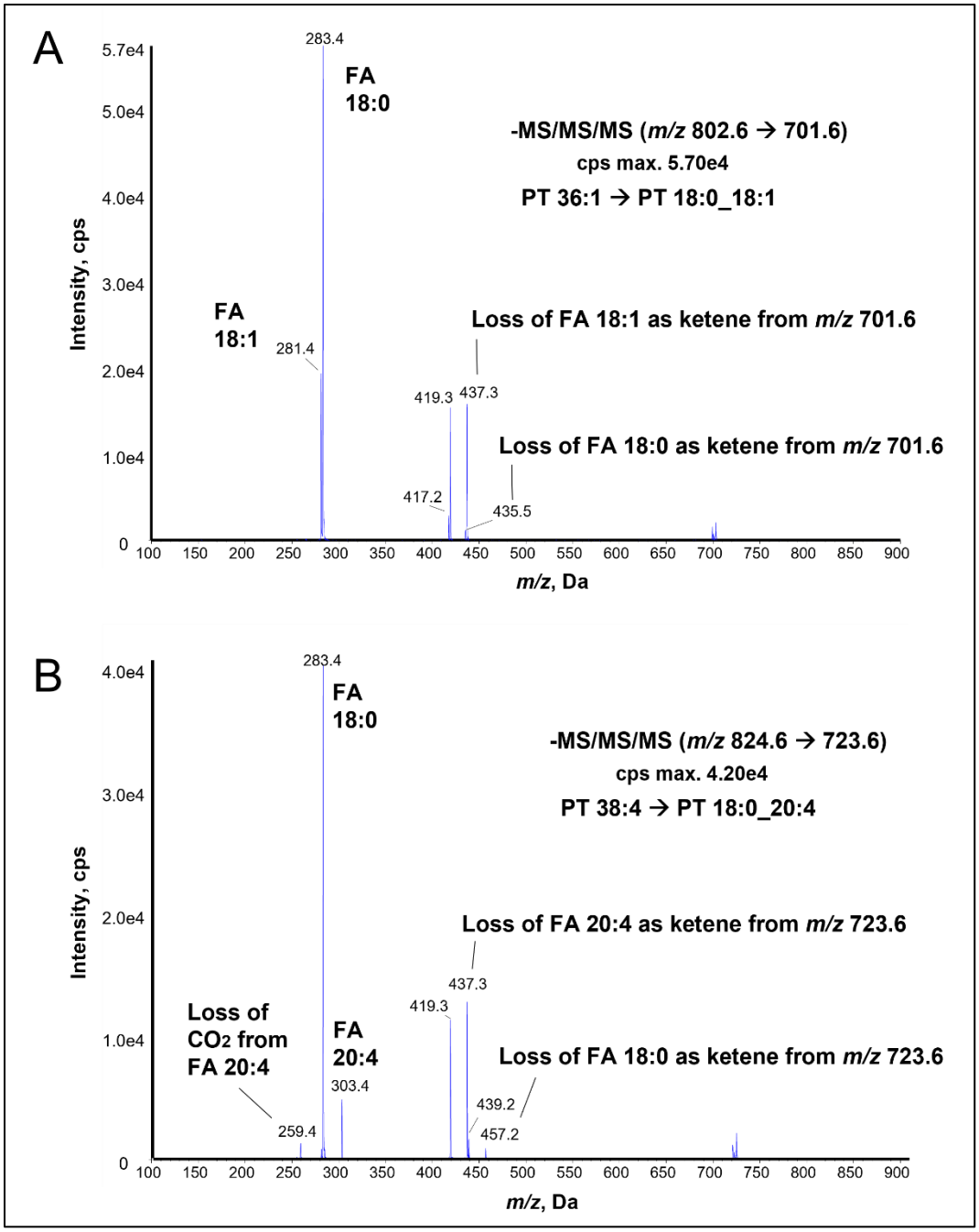


**Figure 4.2 – MS$^3$ spectra of PT 36:1 and PT 38:4 in platelets**

Platelet lipid extracts were analysed using targeted HILIC LC-MS/MS as described in **Experimental Methods**. **(A)** MS$^3$ scan of PT 36:1 with *m/z* 802.6 as first precursor and *m/z* 701.6 as second precursor. The ions at *m/z* 283.4 and *m/z* 281.4 are of FA 18:0 and FA 18:1, respectively. **(B)** MS$^3$ scan of PT 38:4 with 824.6 as first precursor and *m/z* 723.6 as second precursor. The ions at *m/z* 283.4 and *m/z* 303.4 are of FA 18:0 and FA 20:4, respectively. The ion at *m/z* 259.4 is the result of $CO_2$ loss (-44 Da) from FA 20:4 (*m/z* 303.4).

### 4.2.2 Platelet PT is externalised in response to thrombin

Externalisation of PS and PT were investigated using a previously published method (88). Briefly, resting and bovine thrombin activated platelets were treated with NHS-biotin or sulfo-NHS-biotin to derivatise primary amines, then derivatised lipids were extracted and analysed using RP LC-MS/MS, as described in **Experimental Methods**. Five PS and PT and their biotinylated derivatives were analysed based on their higher abundance, relative to other species: 36:1, 36:2, 38:3, 38:4, 40:6 (MRM transitions in **Table 2.5**).

Three PT species were detected after biotinylation with both NHS-biotin and sulfo-NHS-biotin: PT 36:1, PT 38:4, and PT 40:6. In resting platelets, less than 2% of PT lipids were in the outer membrane leaflet, while in thrombin activated platelets % externalisation was much higher, with PT 38:4 reaching 8.6% (**Figure 4.3**). Percentage of externalised PT was higher in activated platelets compared to resting platelets. Externalised PT 40:6 was not detected in resting platelets, likely due to being below the limit of detection. However, it was detected after thrombin activation. PS 36:1, PS 38:4, and PS 40:6 showed similar results, with higher % externalisation after thrombin activation. These results demonstrate that PT, like PS, is enriched in the inner membrane leaflet of platelets and is externalised in response to thrombin.

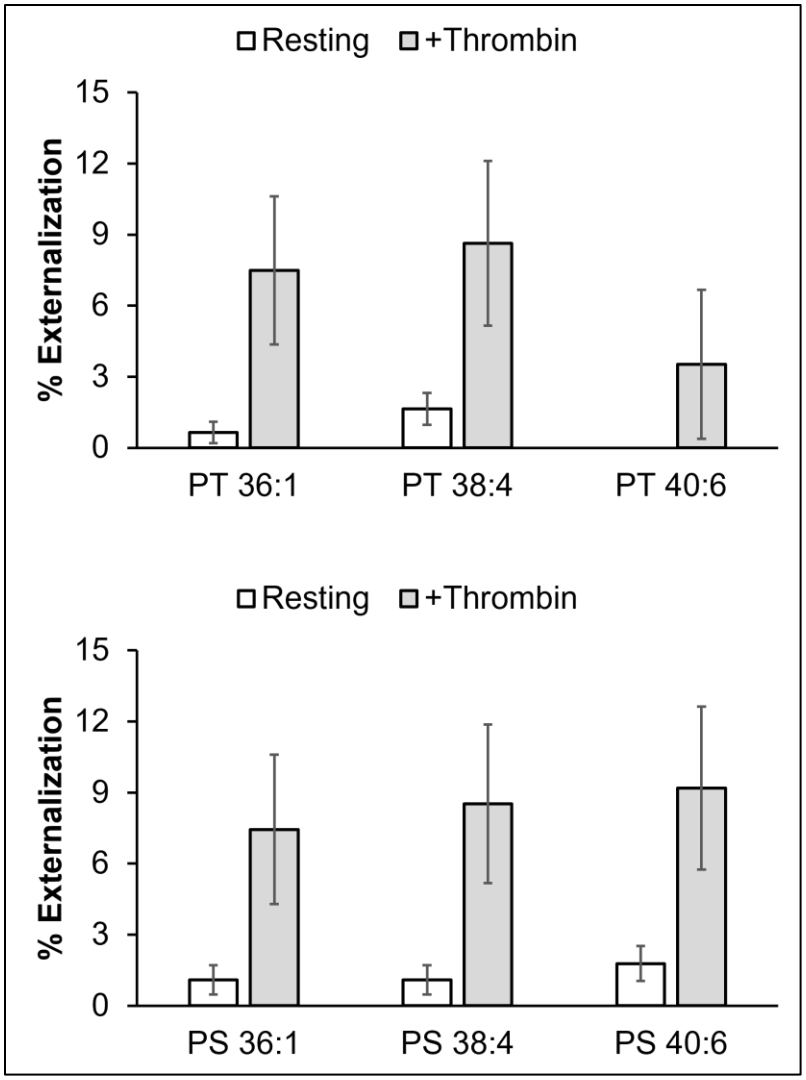


**Figure 4.3 – PT and PS are externalised by thrombin-activated platelets**

Resting or thrombin-activated (0.2 U/mL at 37 °C for 30 min) platelets were derivatized with NHS-biotin or sulfo-NHS-biotin, then lipids were extracted and analysed using RP-LC-MS/MS as described in **Experimental Methods.** Ratios (A/IS, cps) were calculated by dividing analyte signals by the IS (biotinylated-PS 14:0/14:0). Percentage (%) externalisation values for individual lipid species were calculated by dividing the A/IS values from sulfo-NHS-biotin by those from NHS-biotin. Data are represented as mean ± SEM (platelets from healthy volunteers n = 5, three recruited for this study and two from the clinical cohort HC group).

### 4.2.3 Platelet PT decreases in response to thrombin

Next, PT and PS were measured in resting and thrombin-activated platelets from healthy volunteers in the clinical cohort (0.2 U/mL at 37 °C for 30 min) using HILIC LC-MS/MS, as described in **Experimental Methods**.

First, PT and PS levels were found to decrease in platelets in response to thrombin activation (**Figures 4.4A & 4.4B**). The greatest decreases in PS were observed for the 40C species, followed by 38C, and finally 36C. As for PT, the greatest decreases were observed in PT 40:3 followed by PT 38:4, PT 40:4, and PT 38:3, and the smallest reduction upon activation was in PT 34:1. All measured species except PS 34:1 decreased in response to thrombin.

To investigate whether PS and PT are metabolized by the same metabolic pathway, Pearson correlations were calculated for PS and PT pairs in resting and activated platelets (**Figure 4.5**). No negative correlations were observed. In resting platelets, PS species were, in general, strongly correlated with each other. Similarly, PT species were strongly correlated with each other. PS-PT pairs showed a spectrum of correlations from weak to strong. The weakest correlations were between 34C/36C PT species and 38C/40C PS species. In activated platelets, intraclass (PS-PS and PT-PT) correlations were strong but interclass (PS-PT pairs) correlations were weaker than in resting platelets.

Collectively, the results indicate that platelet PT levels, like PS, decrease in response to thrombin activation. This suggests that PT is enzymatically metabolized by platelets, but the exact pathway and products are unknown. The positive correlations between PS and PT indicate a similar enzymatic origin for the two lipid classes. However, stronger intraclass compared to interclass correlations indicate subtle differences in the metabolism of PS and PT.

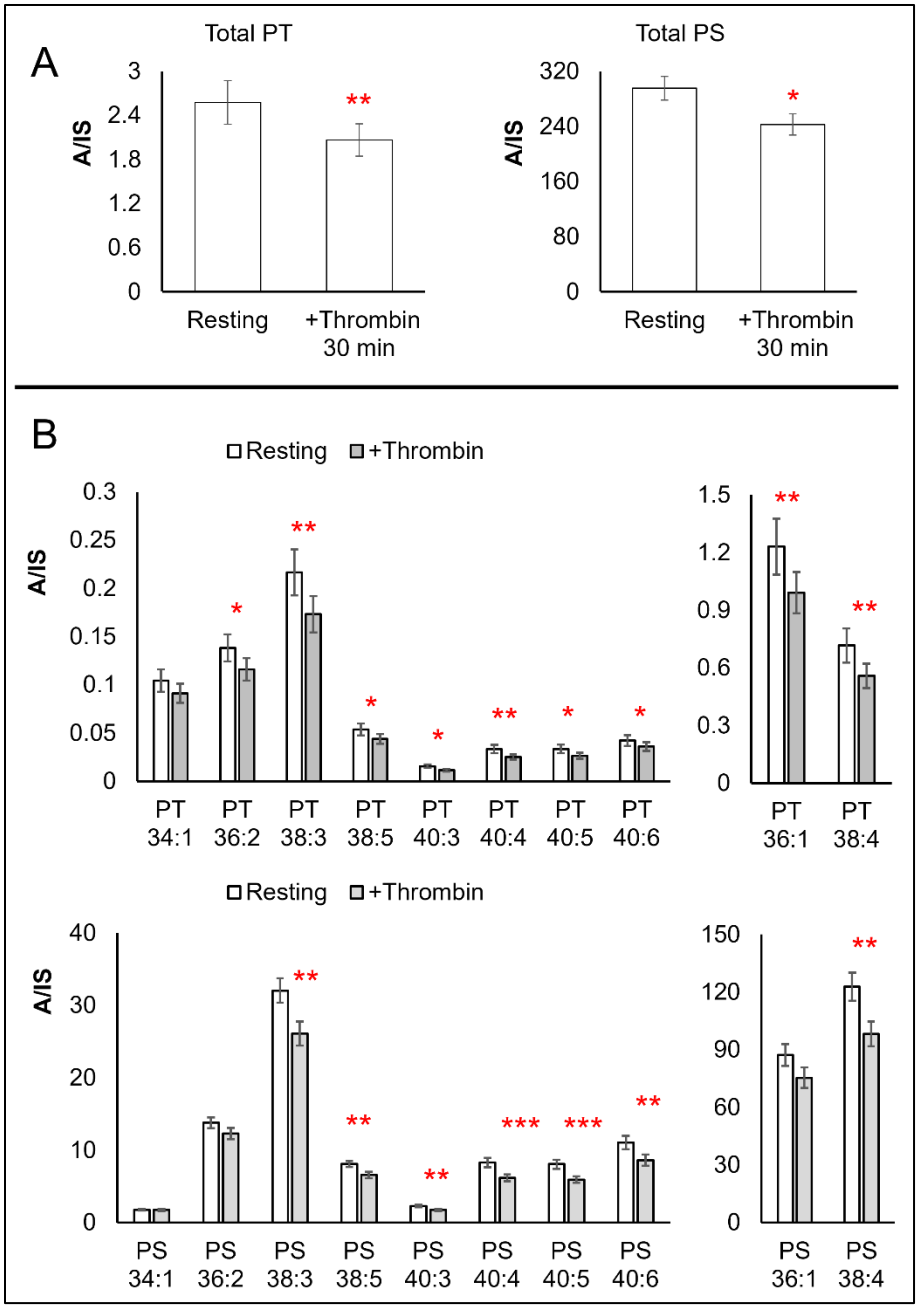


**Figure 4.4 – Platelet PT and PS decrease in response to thrombin**

Lipids from resting or thrombin-activated (0.2 U/mL at 37 °C for 30 min) platelets were extracted and analysed using HILIC-LC-MS/MS as described in **Experimental Methods.** Ratios of analytes to internal standard (A/IS, cps) were calculated by dividing analyte signals by the IS (PS 15:0/18:1[D7]). To calculate total levels, A/IS values of individual species were summed up. Data are represented as mean ± SEM (n = 24). High abundance species are shown on a separate scale. Statistical significance was determined using paired t-tests (*: $P < 0.05$, **: $P < 0.01$, ***: $P < 0.001$). **(A)** Total PT and PS levels in resting and thrombin-activated platelets. **(B)** Levels of individual PT and PS species in resting and thrombin-activated platelets.

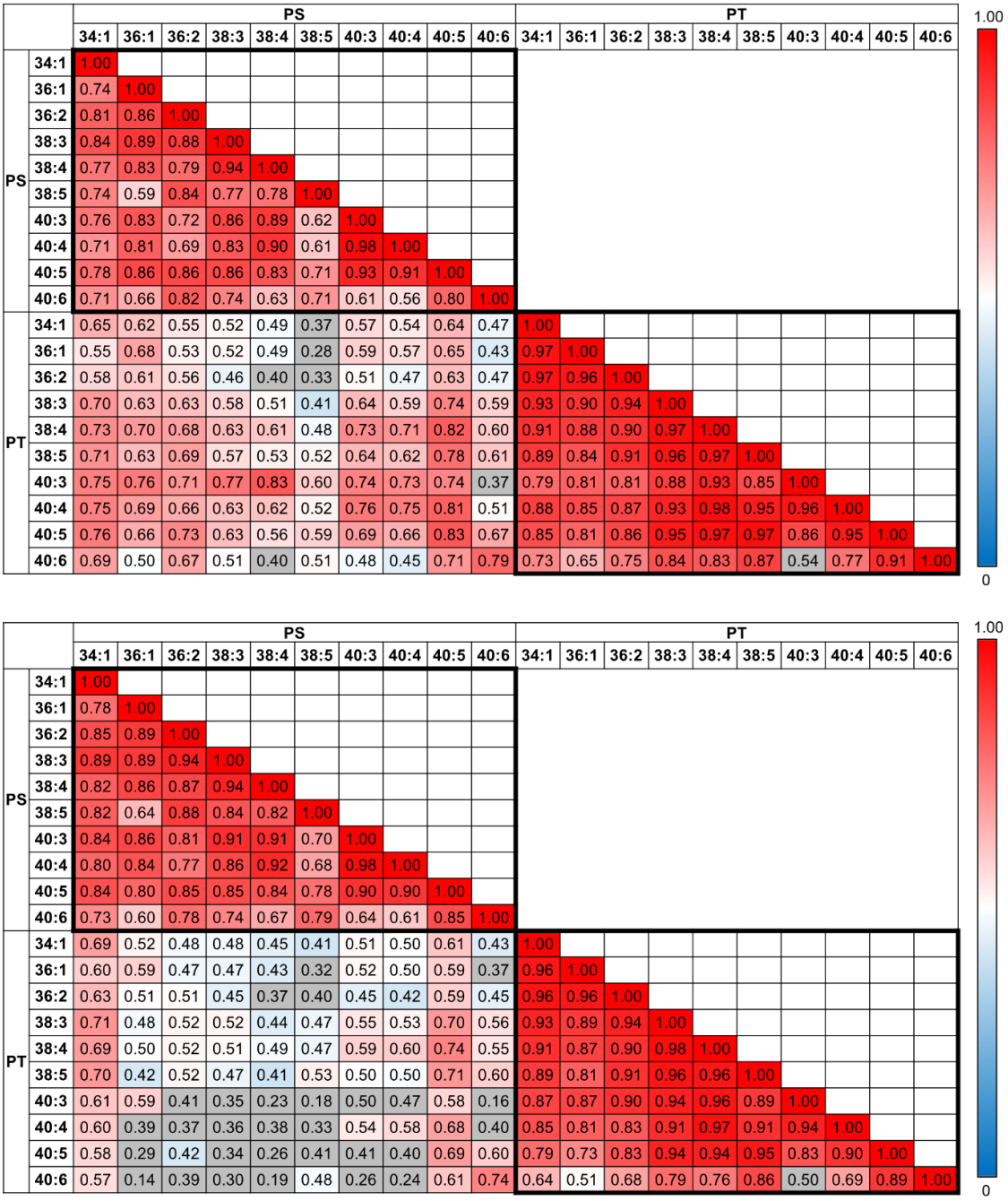


**Figure 4.5 – Pearson correlations between PS and PT species in platelets**

Pearson correlations between PS and PT pairs in resting platelets (top) and thrombin activated platelets (bottom). A/IS values were used to calculate Pearson correlations between pairs. Correlation coefficient values (r) are shown on a scale from 1 (red) to 0 (blue), where r > 0.7 = strong correlation, 0.5 < r < 0.7 = moderate correlation, 0.3 < r < 0.5 = weak correlation, and r < 0.3 = no correlation. Statistically insignificant values are in grey. Pearson correlations were carried out using SPSS.

### 4.2.4 PT profile of extracellular vesicles

Lipid extracts of extracellular vesicles (EV) from healthy volunteers (n = 24, from the clinical cohort) were analysed using targeted HILIC-LC-MS/MS, as described in **Experimental Methods**.

The PT profile of EVs matched their PS profile with minor differences (**Figure 4.6A**). Specifically, the most abundant PT lipid was PT 36:1 followed by PT 38:4, while the opposite was observed for PS. PS 36:1 was 91-fold more abundant than PT 36:1, while PS 38:4 was 126-fold more abundant than PT 38:4. As a percentage of total lipid in the class, PT is more enriched in shorter chain species (34C and 36C) species than PS, while PS is more enriched in longer chain 40C species compared to PT (**Figure 4.6B**). The two classes had comparable percentage amounts of 38C species.

The PS and PT profiles of EVs resemble those of platelets in terms of the most abundant species in each class (**Section 4.2.1**). This is consistent with the general view that most EVs in blood from healthy people are platelet-derived (51).

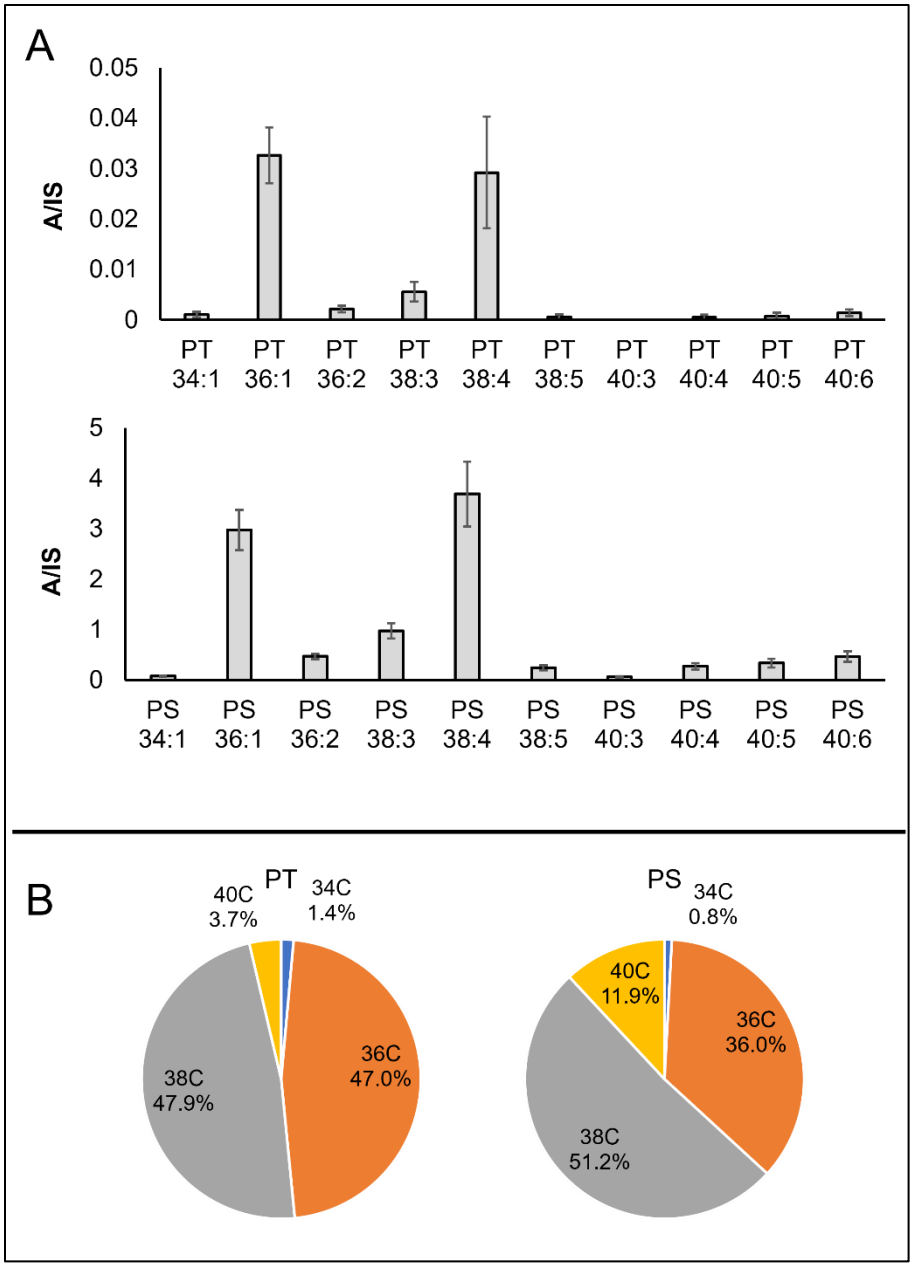


**Figure 4.6 – PT and PS profiles of extracellular vesicles (EV) from healthy volunteers**

EV lipid extracts from healthy volunteers were spiked with an internal standard (IS, PS 15:0/18:1[D7]) then analysed using targeted HILIC-LC-MS/MS as described in **Experimental Methods**. Analyte peaks were integrated and ratios of analytes to internal standards (A/S) were calculated. Bar graph data are represented as mean ± SEM (n = 24). For pie charts, A/IS values of species with the same FA carbon number were summed and used to calculate percentages (mean of n = 24). **(A)** Bar graphs showing relative levels of PT and PS species in EVs. **(B)** Pie charts showing the percentage composition of PS and PT in terms of FA carbon number (34C: 34-carbon, etc).

### 4.2.5 PT profile of leukocytes

Lipid extracts of leukocytes from healthy volunteers (n = 24, from the clinical cohort) were analysed using targeted HILIC-LC-MS/MS, as described in **Experimental Methods**.

The PS and PT profiles of leukocytes were very similar (**Figure 4.7A**). PS 36:1 and PT 36:1 were the most abundant species in their respective classes, followed by PS 38:4 and PT 38:4. The third most abundant lipids in their respective classes were PS and PT 40:5. PS 36:1 level was 85-fold that of PT 36:1, PS 38:4 level was 129-fold that of PT 38:4, and PS 40:5 level was 199-fold that of PT 40:6. As a percentage of total in the class, PT is more enriched in 36C species than PS, while PS is more enriched in longer chain (38C and 40C) species compared to PT (**Figure 4.7B**).

$MS^3$ was used to determine the FA compositions of PS and PT species in leukocytes (**Table 4.2**, complete set in **Appendix 9.10**). PT FA compositions were similar to PS. However, more PS FA composition combinations (compared to PT) were identified due to higher abundance. PT 38:5, 40:3, 40:4, and 40:6 could not be characterised due to their low levels. Of note, PS 38:5 comprised three species, including an unusual composition of 16:0_22:5 (**Table 4.2**). Additionally, PS 40:3, 40:4, 40:5, and 40:6 comprised three FA combinations including minor amounts of species with two 20-carbon FAs (e.g., PS 20:0_20:4), in addition to the more abundant species containing 18-carbon and 22-carbon FAs.

To summarize, these results show that PT is present in leukocytes, with PT 18:0_18:1 and PT 18:0_20:4 as the most abundant species. The PT profile closely matches that of PS, but PT is less enriched in longer chain (38C and 40C) species.

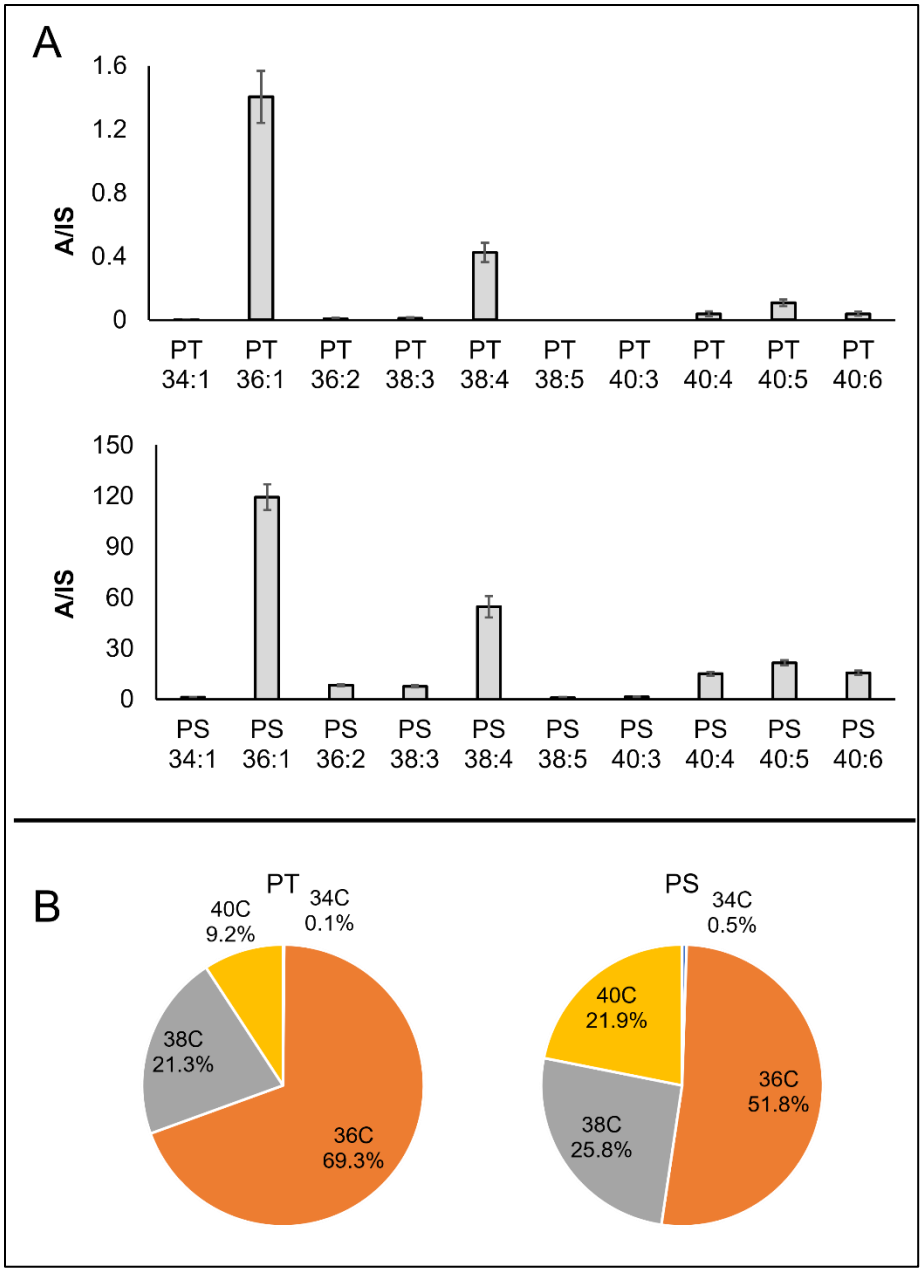


**Figure 4.7 – PT and PS profiles of leukocytes from healthy volunteers**

Leukocyte lipid extracts from healthy volunteers were spiked with an internal standard (IS, PS 15:0/18:1[D7]) then analysed using targeted HILIC-LC-MS/MS as described in **Experimental Methods**. Analyte peaks were integrated and ratios of analytes to internal standards (A/IS) were calculated. Bar graph data are represented as mean ± SEM (n = 24). For pie charts, A/IS values of species with the same FA carbon number were summed and used to calculate percentages (mean of n = 24). **(A)** Bar graphs showing relative levels of PT and PS species in leukocytes. **(B)** Pie charts showing the percentage composition of PS and PT in terms of FA carbon number (34C: 34-carbon, etc).

**Table 4.2 – Fatty acid (FA) compositions of PS and PT species in leukocytes**

| Lipid | FA composition |
|---|---|
| PS 34:1 | 16:0_18:1 & 16:1_18:0 |
| PS 36:1 | 18:0_18:1 |
| PS 36:2 | 18:1_18:1 & 18:0_18:2 |
| PS 38:3 | 18:0_20:3 |
| PS 38:4 | 18:0_20:4 |
| PS 38:5 | 18:1_20:4 & 18:0_20:5 & 16:0_22:5 |
| PS 40:3 | 18:0_22:3 & 18:1_22:2 & 20:0_20:3 |
| PS 40:4 | 18:0_22:4 & 18:1_22:3 & 20:0_20:4 |
| PS 40:5 | 18:0_22:5 & 18:1_22:4 & 20:1_20:4 |
| PS 40:6 | 18:0_22:6 & 18:1_22:5 & 20:3_20:3 |
| PT 34:1 | 16:0_18:1 |
| PT 36:1 | 18:0_18:1 |
| PT 36:2 | 18:1_18:1 |
| PT 38:3 | 18:0_20:3 |
| PT 38:4 | 18:0_20:4 |
| PT 38:5 | N/A (low signal) |
| PT 40:3 | N/A (low signal) |
| PT 40:4 | N/A (low signal) |
| PT 40:5 | 18:0_22:5 |
| PT 40:6 | N/A (low signal) |

## 4.3 Discussion

In this chapter, I investigated the relative levels of 10 PT and 10 PS molecular species in human platelets, extracellular vesicles (EV), and leukocytes, as well as changes to PT and PS following thrombin activation of platelets. These species had already been determined to be the dominant isoforms in platelets in preliminary experiments. The same species were also monitored in leukocytes and extracellular vesicles allowing a direct comparison.

Platelet PS is known to be enriched in FA 20:4, with the majority being in PS 38:4 (86). This is consistent with my results, where PS 38:4 (PS 18:0_20:4) was the most abundant PS species, followed by PS 36:1 (PS 18:0_18:1) (**Figure 4.1A**). FA 20:4 was also a constituent of PS 38:5, 40:4, 40:5 and 40:6 (**Table 4.1**). PS and PT are presumed to be synthesized by the same base-exchange reaction catalysed by PS synthase (PSS) enzymes, of which two isoforms with different substrate specificities are known in humans (18). If PT is generated by the same isoforms as PS, one might expect that PT would also be enriched in FA 20:4. Indeed, PT was enriched in FA 20:4, found predominantly in PT 38:4, but also in PT 38:5, 40:4 and 40:5. However, unlike PS, the most abundant species was PT 36:1. Platelet PS was more enriched in 38C and 40C species compared to PT, while PT is more enriched in 34C and 36C (**Figure 4.1B**). This suggests differences in the metabolism of PS and PT. PSS1 synthesizes PS through serine base-exchange with PC, while PSS2 uses diacyl PE (particularly with FA 22:6) as a substrate (18). One possible explanation for the differences in PS and PT profiles could be due to the isoforms' (PSS1 and PSS2) ability to accept threonine as a substrate to make PT. Platelet PC is enriched in shorter chain species (34C and 36C), while diacyl PE is dominated by longer chain species (38C and 40C) (86). It may be that PT is synthesized predominantly from the PC pool, whereas PS is synthesized from both PC and PE pools. This would explain the higher abundance of shorter chain species in PT and the higher abundance of longer chain species in PS. I hypothesize that PSS1 synthesizes PT more efficiently compared to PSS2. This would account for the high fold differences between PS and PT in 40C species, as PSS2 prefers PE with FA 22:6 (and potentially other 22-carbon PUFA) as a substrate. One way to test this would be to isolate pure PSS1 and PSS2 enzymes and carry out *in vitro* assays with serine and threonine as substrates.

The platelet lipidome is dynamic and undergoes specific changes following thrombin activation. These include the hydrolysis of PUFA (particularly FA 20:4) from PL pools, the oxygenation of released PUFA into oxylipins, and the esterification of oxylipins back into PL to form enzymatically oxidized PL (26, 89, 90). Platelet PC, PE, and PI (containing FA 20:4) all decrease in response to thrombin activation, but PI 38:4 is proposed to be the major precursor of FA 20:4 for the biosynthesis of oxylipins (26, 89). While PS externalisation in activated platelets is well-known, changes in PS levels are less studied. An early study showed that thrombin activated platelets incorporated external labelled glycerol into PS, but this was transient with maximal rates in the first two minutes (91). Furthermore, this experiment did not directly measure endogenous PS biosynthesis because exogenous glycerol was used. In contrast, a later study reported no changes in total platelet PS after a 1 min activation with thrombin (89). Similarly, a recent study reported no significant changes in a panel of PS species after a 5 min incubation with thrombin (26). The study had monitored lipid changes after 5 min following thrombin activation, which is an early timepoint. Changes in platelet PS at later timepoints of thrombin activation are unexplored.

Here, I monitored 10 PS species during a 30-minute activation in platelets from 24 healthy volunteers (**Figure 4.4B**). All, except PS 34:1, decreased in response to thrombin, and the greatest percentage (%) decreases were observed in 40C species. The products are unknown but could include lysoPS since a previous study demonstrated that collagen-activated platelets generate 1-acyl-lysoPS through $PLA_2$ (92). Therefore, it is likely that 1-acyl-lysoPS is also generated by thrombin-activated platelets. This would release FA for the biosynthesis of oxylipins. PS may also be hydrolysed at the *sn*-1 position by a phospholipase $A_1$, generating 2-acyl-lysoPS and a FA, but the enzyme responsible is secreted by activated platelets and can only access externalised PS (21). Additionally, the enzyme is expressed in rat but not in human platelets (22).

To summarize, platelet PS levels were reduced following a 30 min thrombin activation, likely due to phospholipases activity. This may indicate a role for lysoPS at late stages of thrombin activation and, by extension, blood coagulation. Specifically, degradation of PS into lysoPS at later timepoints could serve to remove PS, limiting coagulation. LysoPS species are increasingly being recognized as mediators, exhibiting bioactivities through interactions with specific

receptors including GPR34, P2Y10, GPR174, and TLR2 (93, 94). However, the field is still at its infancy. The data presented herein provides indirect evidence that lysoPS is implicated in blood coagulation. To further explore this, it is recommended to monitor platelet PS and lysoPS at several timepoints following thrombin activation, and experiments should be carried out in the presence and absence of phospholipase inhibitors. The functions of 1-acyl-lysoPS and 2-acyl-lysoPS in blood coagulation could be investigated with migration-resistant analogues (lysoPS analogues that do not undergo acyl migration) and mouse models, in which the lipids are injected into mice at physiologically relevant concentrations and their effects monitored.

Platelet PT also decreased in thrombin-activated platelets after 30 min (**Figure 4.4B**). It is possible that PT was metabolized by activated platelets into lysoPT through the action of phospholipases. Previous work by Iwashita *et al*. demonstrated that lysoPT, synthesized as a lysoPS analogue, induces murine mast cell degranulation at a concentration $1/10^{th}$ that of lysoPS (70). My results suggest lysoPT may be endogenously made, which would hint towards a biological function in inflammation. However, the generation of lysoPT *in vivo* requires further investigation, which is possible through targeted lipidomic analysis. Unfortunately, cohort samples used in this chapter were extracted using acidified hexane isopropanol, which is unsuitable for the analysis of acidic lysoPLs due to poor extraction efficiency. Additionally, analysis of lysoPS is already challenging using current methods and lysoPT is expected to occur at $1/100^{th}$ the concentration of lysoPS, making it even harder to detect. Therefore, optimization of the extraction method is necessary before trying to detect lysoPT in activated platelets.

My hypothesis that PT functions in coagulation by interacting with coagulation factors is dependent on PT being enriched in the inner membrane leaflet of platelets then externalised upon activation. Thus, I compared the membrane distributions of PT and PS in resting and thrombin-activated platelets, using an LC-MS/MS method that involves primary amine derivatisation (88). Despite PT being, on average, 100-fold less abundant than PS, the two most abundant PT species in platelets, PT 36:1 and PT 38:4, were readily detected in the external leaflets of both resting and activated platelets (**Figure 4.3**). The results demonstrate that PT, like PS, is asymmetrically distributed in the plasma membrane, being enriched in the inner leaflet, and is externalised by platelets in response to thrombin activation. In resting platelets, PS and PE are maintained in the inner leaflet through the action of an aminophospholipid translocase, which transports the lipids

inwards. In activated platelets, influx of calcium reversibly inhibits this enzyme, and activates a scramblase, which moves phospholipids down their concentration gradient across the two leaflets, leading to externalisation of PS and PE. The membrane distribution of PT is likely controlled by the same mechanisms. This could be tested by incubating platelets with PT and measuring % externalisation at different timepoints. Additionally, platelets could be isolated from patients with Scott syndrome, then activated with thrombin while monitoring the % externalisation of PT, as described previously for PS and PE (88). Inability of platelets from Scott syndrome patients to externalize PT would suggest the involvement of scramblase (TMEM16F) in PT externalization.

Platelet-derived EVs make up the majority of microparticles in healthy circulation and can support thrombin generation on their surface through externalised PS (51, 52). As EVs are predominantly derived from the plasma membrane of platelets, it is expected that their lipidome mirrors that of their source. That was indeed the case for their PS profile (**Figures 4.1** & **4.6**). In both platelets and EVs, PS 38:4 and PS 36:1 were the two most abundant species, followed by PS 38:3 and PS 36:2. PT was also detected in EVs, with PT 36:1 and PT 38:4 as the two most abundant species, closely matching the profile of platelets. These results demonstrate that EVs contain PT species, which are likely derived from platelets.

PT was also detected in leukocytes, with PT 36:1 as the predominant species (~69% of total PT), followed by PT 38:4 and PT 40:5. The PT profile matched the PS profile, but like in platelets, PT was less enriched in 40C species compared to PS. Note, these lipid profiles likely reflect those of neutrophils, as they constitute the majority (~60%) of circulating leukocytes, with major contributions from lymphocytes (~30%) and minor contributions from other cells (in decreasing order: monocytes, eosinophils, and basophils). The leukocyte PS profile reported here matches previously published data by Leidl *et al*., where PS 36:1 was the PS lipid in neutrophils, lymphocytes, and monocytes (86). However, small discrepancies in the ratios were observed, likely because Leidl *et al*. isolated pure fractions of monocytes, lymphocytes, and granulocytes for lipidomic analysis, while I analysed a mixture of leukocytes in their native ratios, in which neutrophils and lymphocytes predominate. The authors argued that neutrophils are less enriched in PS 38:4 compared to PS 36:1 because the cells kill pathogens through the generation of superoxide (86). As such, having lower amounts of PUFA-containing PL may serve to minimize

lipid peroxidation. This seemingly applies to neutrophil PT too. That said, analysing PT in pure monocytes, lymphocytes, and granulocytes would be interesting, as the different cell types possess distinctive PS profiles. This could also apply to their PT profiles and would assist in elucidating PT functions.

Since this was an existing set of samples, generated for other studies, no internal standard had been included for PS analysis during the extraction of platelets, EVs, and leukocytes. As such, absolute quantification of PT was not possible. Instead, PT was measured relative to PS and produced MS signals approximately 100-fold lower than PS. PS constitutes around 10 mol% of total lipids in blood cells (86). Therefore, PT theoretically makes up 0.1 mol% of total lipids in blood cells.

## 4.4 Conclusion

In conclusion, PT is present in human platelets, EVs, and leukocytes. It is enriched in the inner membrane leaflet of resting platelets and is externalised in response to thrombin. It is unknown if PT asymmetry is maintained by the same mechanisms as PS and PT. PT appears to be metabolised during platelet activation, presumably due to the action of phospholipases. The PT profiles of platelets and EVs are similar, with both enriched in PT 36:1 and PT 38:4. In contrast, leukocytes are more enriched in PT 36:1. The PT profiles of all three cells/particles match their PS profiles, but PT is less enriched in 22-carbon FAs species (e.g., 40:6). The reason behind this is unknown but could be due to differences in substrate preferences of PS synthases. The occurrence of PT in blood cells and its externalisation (and metabolism) by platelets in response to thrombin suggest a role in blood coagulation or platelet activation and inflammation . This will be investigated using *in vitro* coagulation assays in the next chapter.

# CHAPTER 5 Investigating the procoagulant properties of PT *in vitro*

## 5.1 Introduction

In **Chapters 3** and **4**, I demonstrated that phosphatidylthreonine (PT) is present in platelets and is externalised in response to thrombin. Given the role of PS in coagulation, it becomes relevant to determine whether PT can play a similar role. To test this, I will investigate the ability of PT liposomes to support coagulation *in vitro*. Liposomes are synthetic spherical vesicles comprised of lipid bilayers. They can be classified based on size and number of bilayers into multilamellar (MLV) or unilamellar vesicles, with the latter group encompassing large (LUV) and small unilamellar vesicles (SUV). MLVs can be prepared by drying lipids (premixed in desired ratios) then hydrating the lipid film with an aqueous solution using agitation. LUVs can be prepared from MLVs through freeze-thawing (cycles) and extrusion through polycarbonate filters with defined pore sizes. SUVs can be prepared from MLVs by sonication, but SUVs are unstable due to their high curvature, causing them to fuse into larger vesicles. Therefore, LUVs (hereafter referred to as liposomes) containing PT were prepared and used for the experiments. A diameter of 100 nm was chosen for the liposomes because of its similarity to physiological conditions as platelet-derived extracellular vesicles range from 100 nm to 1000 nm in size (95).

PS in liposomes binds calcium ions via its negatively charged phosphate and carboxyl groups, which can be measured through an increase in absorbance at 400 nm, proposed to be due to aggregation of liposomes (96, 97). PT is anionic at physiological pH and is thus expected to bind calcium ions, which would be evident by an increase in absorbance upon calcium titration. PT-containing liposomes will be titrated with calcium to investigate binding.

In this chapter, the ability of PT to support coagulation will be tested using three assays: a prothrombinase assay, calibrated automated thrombinography (CAT), and an extrinsic tenase assay.

(i) Prothrombinase: liposomes are incubated with purified human factors Xa, Va, II, and calcium. The liposomes provide a surface for the assembly of the prothrombinase

(FXa:FVa) complex, which converts factor II to thrombin. After a 5 min incubation, the reaction is quenched using EDTA, then thrombin activity is assayed using a chromogenic substrate, which upon hydrolysis by thrombin releases a dye that absorbs light at 405 nm (yellow colour). As such, the intensity of the colour is proportional to the amount of thrombin generated.

(ii) CAT: This assay measures thrombin generation in plasma incubated with liposomes, an excess of calcium, and a fluorogenic thrombin substrate. Here, coagulation is initiation by the addition of TF-liposomes, leading to the assembly of the extrinsic tenase complex (TF:FVIIa). Generated thrombin is quantified through continuous monitoring of fluorescence and comparison with a calibrator (98). Plasma containing corn trypsin inhibitor (CTI) was used in the CAT assay to study the effect of PT on the extrinsic pathway, as CTI blocks the intrinsic pathway (99).

(iii) Extrinsic tenase: The extrinsic tenase assay involves the incubation with TF-liposomes with factors VIIa, X, and calcium, leading to the formation of the extrinsic tenase complex (TF:FVIIa). This complex generates factor Xa, which is assayed using a chromogenic substrate.

## 5.2 Results

### 5.2.1 PT liposomes bind calcium ions

Liposomes were generated containing PC/PE 6:4 (mol%), PC/PE/PS 6:3:1 (mol%), or PC/PE/PT 6:3:1 (mol%) using membrane extrusion and titrated with $CaCl_2$ while monitoring absorbance at 400 nm, as described in **Experimental Methods**. The experiments were carried out at physiological blood pH (~7.4), in which PS and PT carry a net negative charge, while PC and PE are neutral (100).

Titration of PC/PE liposomes with calcium ions resulted in a decrease in absorbance (**Figure 5.1**), due to the dilution of lipids. By contrast, liposomes containing PS or PT exhibited an increase in absorbance upon titration with calcium ions (**Figure 5.1**). PT liposomes behaved similarly to PS liposomes, indicating PT also binds calcium ions.

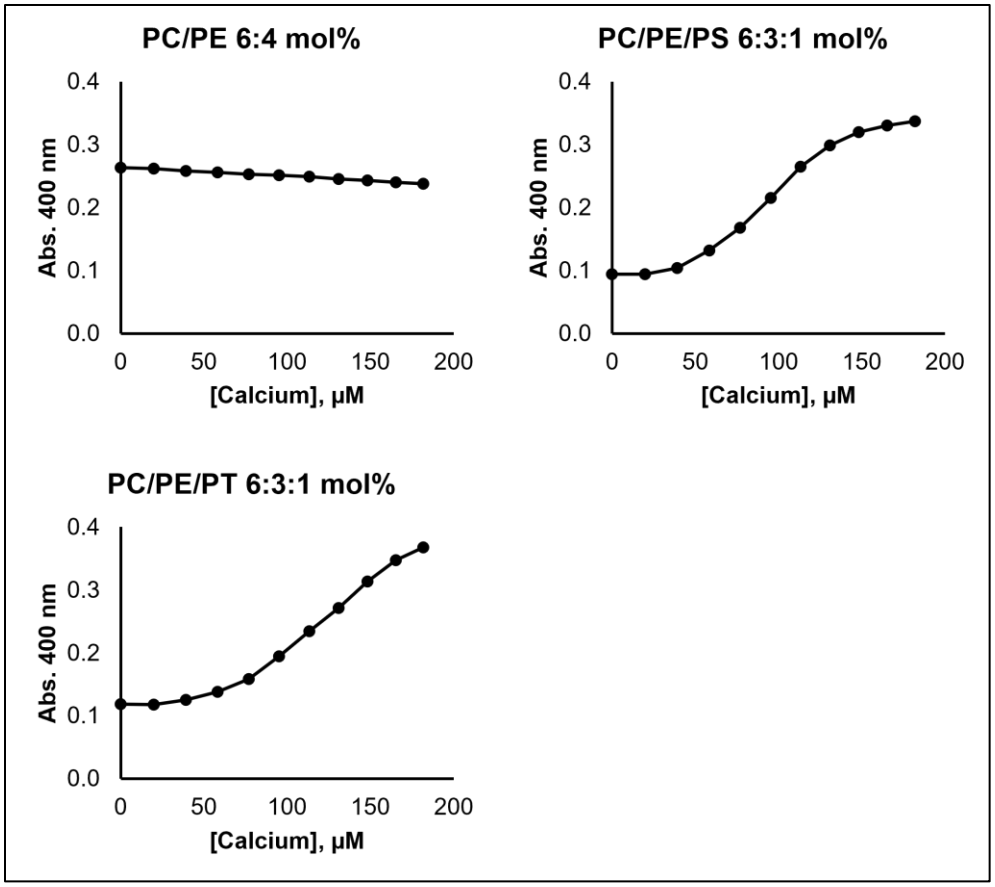


**Figure 5.1 – PS and PT liposomes bind calcium ions.**

Liposomes of different compositions were prepared by membrane extrusion as described in **Experimental Methods**. Liposomes (1 mM, in 10 mM HEPES and 10 mM NaCl, pH 7.35) were titrated with 2 mM calcium chloride (in buffer) and absorbance at 400 nm was measured 1 min following calcium addition and mixing. Each datapoint represents the average of two technical replicates.

### 5.2.2 PT supports prothrombinase (FXa:FVa) activity *in vitro*

Liposomes were prepared by membrane extrusion and assayed for their ability to support prothrombinase activity as described in **Experimental Methods**.

Substituting PS or PT for PE in PC/PE 6:4 (mol%) liposomes significantly enhanced their prothrombinase activity (**Figure 5.2A**). In liposomes containing only PC and PT, the prothrombinase activity was proportional to the amount (mol%) of PT (**Figure 5.2B**). Addition of PE to PC/PT liposomes further enhanced their ability to support prothrombinase activity, although the increase did not reach statistical significance (**Figure 5.2D**). PT supported prothrombinase activity to the same extent as PS in both the presence and absence of PE (**Figures 5.2E & 5.2F**).

In platelets, PT 36:1 is approximately 70-fold less abundant than PS 36:1, as demonstrated in **Chapter 4**. Next, liposomes containing a physiological ratio of PS and PT, specifically 10% PS and 0.14%, were tested and compared to liposomes containing PS but not PT. Liposomes containing 0.14% PT enhanced the activity of PC/PE/PS liposomes (**Figure 5.2C**). Additionally, the effect was greater with 0.28% PT.

Collectively, these results demonstrate that PT liposomes support prothrombinase activity *in vitro*. PT supports prothrombinase activity in a dose-dependent manner, and its activity is enhanced by PE. Furthermore, PT can substitute for PS for the assembly of the prothrombinase complex and exhibits comparable activity to PS. Lastly, physiological amounts of PT enhance the activity of PS liposomes.

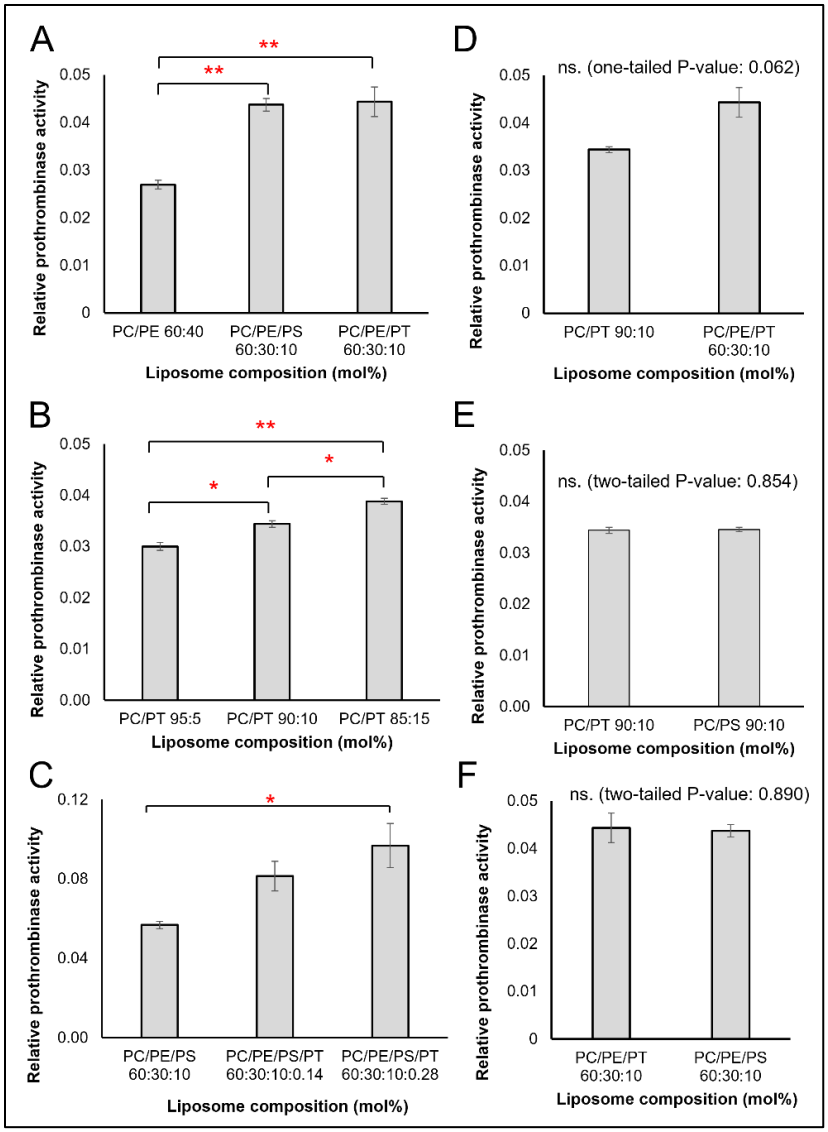


**Figure 5.2 – PT liposomes support prothrombinase activity *in vitro***

Liposomes of different compositions were prepared by membrane extrusion as described in **Experimental Methods**. Liposomes were incubated with buffer containing factor II (200 nM), factor Va (3.0 nM), factor Xa (10 nM), and 1 mM $CaCl_2$ at 21 °C for 5 min. The reaction was stopped by the addition of EDTA (7 mM), then S-2238 (0.8 mM) was added and absorbance at 405 nm was monitored for 50 minutes. Prothrombinase activity values were calculated by determining the slope of the absorbance curves from 0 – 10 min. Data are represented as mean ± SEM (n = 3, independent replicates). **(A)** Substitution of PE with PS or PT enhances prothrombinase activity. **(B)** PT supports prothrombinase activity in a dose-dependent manner. **(C)** Physiological PT level enhances prothrombinase activity of PC/PE/PS liposomes. **(D)** PE enhances the prothrombinase activity of PC/PT liposomes. **(E)** Comparison of PC/PT and PC/PS liposomes. **(F)** Comparison of PC/PE/PT and PC/PE/PS liposomes. Statistical significance was determined using One-way ANOVA followed by Tukey tests for three groups, or student's t-test for pairwise comparisons (*: $P < 0.05$, **: $P < 0.01$).

### 5.2.3 PT poorly supports thrombin generation in PPP

TF-bearing liposomes were prepared using membrane extrusion and assessed for their ability to support thrombin generation in PPP and extrinsic tenase activity *in vitro*, as described in **Experimental Methods**.

PT liposomes were tested using CAT in CTI-treated PPP. CTI blocks the contact pathway of coagulation (99). Thus, this assay measures the contribution of the extrinsic tenase (TF:FVIIa) complex to thrombin generation. PC/PE/PT (6:3:1, mol%) liposomes poorly supported thrombin generation compared to PC/PE/PS (6:3:1, mol%) liposomes, as indicated by the lower peak thrombin and higher lag time with PT liposomes (**Figure 5.3**). Additionally, replacement of 10 % PE with the same amount of PT did not enhance thrombin generation, suggesting PE was responsible for the activity of PC/PE/PT liposomes. Similarly, addition of 0.14 % of PT to PC/PE/PS liposomes had no effect on thrombin generation.

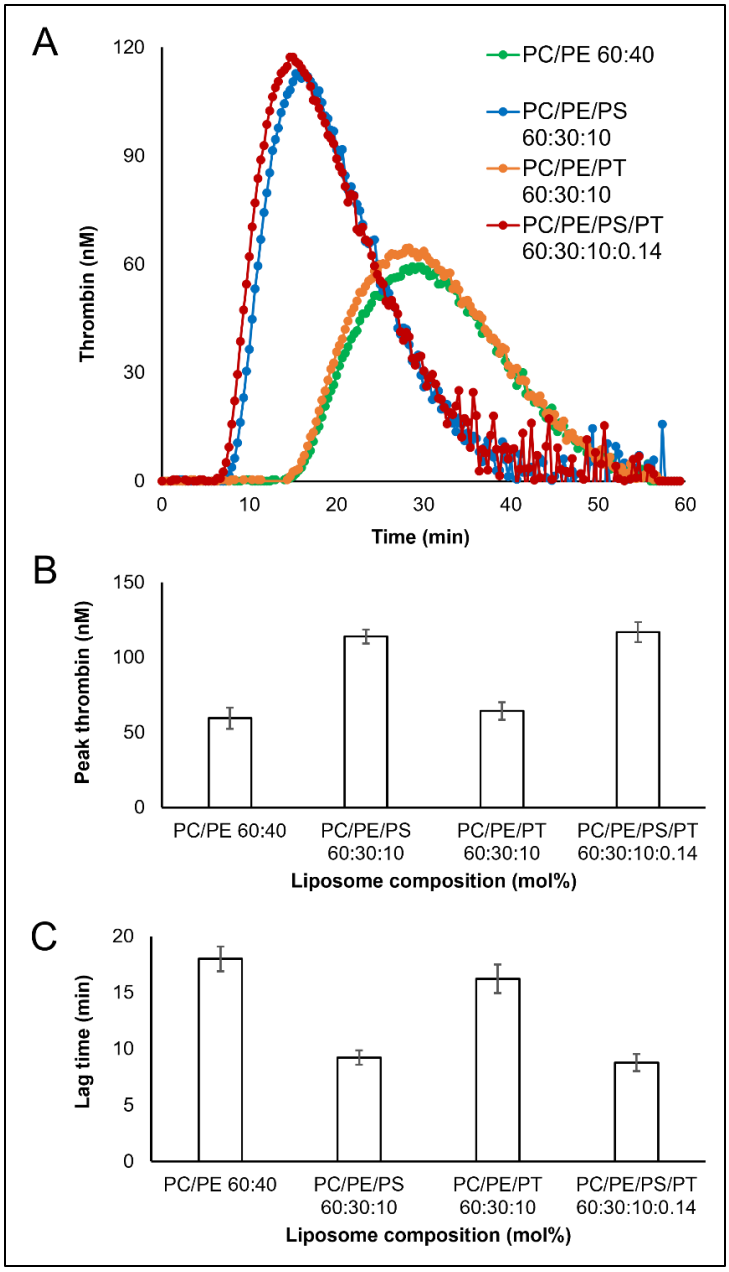


**Figure 5.3 – PT liposomes poorly thrombin generation in PPP**

TF-bearing liposomes of different compositions were prepared by membrane extrusion as described in **Experimental Methods**. Liposomes (50 pM TF) were incubated with pooled PPP (containing CTI) at 37 °C for 10 min, then buffer containing calcium (20 mM) and fluorogenic substrate (Z-Gly-Gly-Arg-AMC, 5 mM) was added and fluorescence was monitored for 60 min. Thrombin generation was quantified automatically by the Thrombinoscope software using a calibrator that was run parallel to the samples. (A) Traces showing thrombin generation capacity of different liposome compositions (average of triplicates). (B) Peak thrombin. (C) Lag time. Data in bar graphs are represented as mean ± SEM (n = 3, independent replicates).

### 5.2.4 PT poorly supports extrinsic tenase (TF:FVIIa) activity *in vitro*

Next, liposomes were tested using a chromogenic extrinsic tenase assay that used recombinant enzymes rather than plasma. This eliminates interference from natural anticoagulants present in plasma. Here, binary compositions of lipids (PS, PT, or PE) with PC were tested to investigate the effects of PS and PT without interference from PE. PC/PT (8:2, mol%) liposomes, like PC/PE (8:2, mol%), poorly supported extrinsic tenase activity compared to PC/PS (8:2, mol%) liposomes (**Figure 5.4**).

These results suggest that PT cannot substitute for PS in the assembly (or activity) of the extrinsic tenase complex, as evident by the inability of PT-containing liposomes to support extrinsic tenase assay in either tested assay.

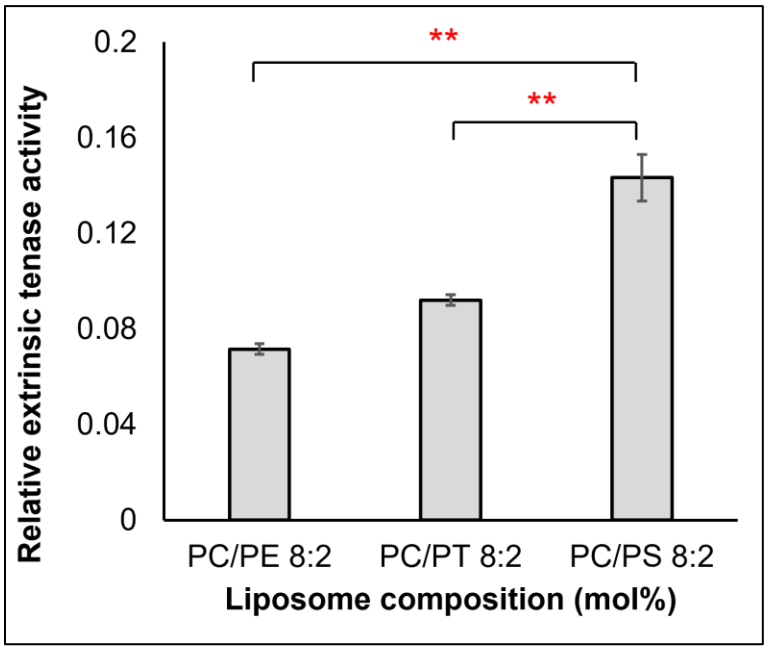


**Figure 5.4 – PT liposomes poorly support extrinsic tenase activity *in vitro***

Liposomes of different compositions were prepared by membrane extrusion as described in **Experimental Methods**. Liposomes with embedded TF (1 nM) were mixed with buffer containing factor X (500 nM), factor VIIa (25 nM), and 2.5 mM $CaCl_2$, then S-2765 (0.93 mM) was added and absorbance at 405 nm was monitored for 40 minutes. Relative tenase activity values were calculated by determining the slope of the absorbance curves from 0 – 10 min. Data are represented as mean ± SEM (n = 3, independent replicates). Statistical significance was determined using one-way ANOVA and Tukey tests (**: $P < 0.01$).

## 5.3 Discussion

In this chapter, I investigated the ability of PT to support coagulation *in vitro* using liposomes and biochemical assays. First, a calcium binding assay was employed, where liposomes are titrated with calcium ions. Binding of calcium ions to PS result in an increase in absorbance at 400 nm, as reported previously in the literature (96, 97). PT liposomes also exhibited an increase in absorbance upon the addition of calcium ions, indicating that the phosphothreonine head group binds calcium ions (**Figure 5.1**). This suggests that the additional methyl group in PT compared to PS does not hinder calcium binding. That said, the turbidimetric assay used here is qualitative. There may be differences in the thermodynamics of the interactions between calcium and PS or PT. Curiously, calorimetric measurements have previously demonstrated that the interaction of calcium with PS is endothermic, and is instead entropically driven through the liberation of water molecules from the hydration shells of the ion and the lipid (96). The methyl group in PT (not found in PS) confers a hydrophobic character, a larger size, and presumably a larger hydration shell. As such, the binding of calcium to PT could, in theory, liberate more water molecules (higher entropy), meaning PT could bind calcium ions better than PS. This idea could be investigated using techniques such as calorimetry and nuclear magnetic resonance. The latter may also be used to characterise the conformational differences between PS and PT in the presence of calcium ions.

The prothrombinase complex consists of a 1:1 complex between FXa and FVa, which assembles on a membrane surface in the presence of calcium. FVa acts as a cofactor for FXa by enhancing the binding between FXa and its substrate, FII (101). The binding of FXa to FVa is affected by calcium concentration, with optimal binding at 1-2 mM $Ca^{2+}$ (102). However, at $Ca^{2+}$ concentrations above ~1.16 mM, FXa forms inactive dimers on PS membranes (103). Under such conditions, FVa competes with FXa dimerization to form the active prothrombinase complex (104). In this chapter, the prothrombinase assay was carried out in the presence of 1 mM $Ca^{2+}$ to prevent the formation of FXa dimers. Additionally, this calcium concentration is close to physiological ionised calcium level in plasma, which ranges from 1.15 to 1.30 mM (105).

Under the chosen experimental conditions, PT liposomes supported prothrombinase activity just as effectively as PS liposomes, both in the presence and absence of PE. Additionally, the

prothrombinase activity was proportional to the mol% of PT in PC/PT liposomes. While the amount of PT used (5-15 mol%) is much higher than physiological levels, the experiments demonstrated that PT, if concentrated in membrane domains to achieve high local concentrations, could theoretically substitute for PS in supporting the assembly and activity of the prothrombinase (FXa:FVa) complex. Furthermore, PC/PE/PT liposomes supported prothrombinase activity better than PC/PT liposomes. PE has been shown to improve the affinity of coagulation factors to PS membranes (12, 106). A similar mechanism may operate here, with PE enhancing the binding of FXa or FVa to PT liposomes. Note, the binding of FXa and FII to membranes is calcium-dependent through their Gla domain, while FVa binds directly to membranes through its C2 domain, with calcium only being required for the assembly of FVa's subunits (35, 107). The mechanistic details behind PT's ability to support prothrombinase activity remain unclear. It is not known if PT binds FXa, FVa, or both.

The addition of physiologically relevant amounts of PT (0.14%) to PC/PE/PS liposomes enhanced their ability to support prothrombinase activity. Curiously, the enhancement effect of 0.14% PT to PC/PE/PS (6:3:1, mol%) liposomes was greater than the enhancement of 5% PT to PC/PT (90:10, mol%) liposomes. This suggests that the enhancement is due to a complex synergistic effect, rather than a simple additive effect, but the exact details are unknown. This could be investigated by testing the activity of liposomes containing varying compositions of PS/PT and measuring kinetic parameters.

The extrinsic tenase complex consists of membrane-embedded TF and FVIIa. The binding of FVIIa to membrane PS is calcium-dependent and mediated by a Gla domain, but the enzyme is inactive in the absence of TF (108, 109). FVIIa undergoes a conformational change upon binding TF, allowing it to bind its substrate, FX. In this chapter, PT was found to poorly support factor X activation through extrinsic tenase compared to PS. In the literature, inactive TF in the absence of PS is termed "encrypted TF", and externalised PS in activated cells is proposed to "decrypt" TF by promoting a conformational change (110, 111). One possible explanation for the inability of PT to support extrinsic tenase activity is that PT, unlike PS, cannot decrypt TF into the active form. A second possible explanation is that PT poorly binds FVIIa. In this regard, it is possible that PT may poorly bind Gla domains in general. This would suggest that the ability of PT to support prothrombinase activity is through the recruitment of FVa. However, Gla domains of

different proteins exhibit differential affinities to membrane lipids, and this may also influence their interactions with PT (31, 112). Therefore, it is recommended to investigate the binding of PT to individual coagulation factors. This could be conducted using lipid nanodiscs and surface plasmon resonance (12).

Collectively, the *in vitro* assays demonstrate that PT supports coagulation effectively through the prothrombinase complex but poorly through extrinsic tenase. PT can completely substitute for PS in the prothrombinase assay, and physiological amounts of PT enhance the ability of PS liposomes to support prothrombinase activity. By contrast, PT cannot substitute for PS in supporting the activity of the extrinsic tenase complex. This suggests that PT may be involved in the common pathway of coagulation but not in the tissue factor pathway. The ability of PT to support coagulation through the intrinsic tenase complex (contact pathway) was not investigated here and constitutes a future goal. Additionally, *in vivo* experiments are required to establish what role PT may play in regulating coagulation.

## 5.4 Conclusion

In conclusion, PT binds calcium ions and can promote coagulation *in vitro* by supporting the activity of the prothrombinase complex. Specifically, physiological amounts of PT enhanced the ability of PS liposomes to support prothrombinase activity, and this suggests a role for PT in the propagation of coagulation. However, PT poorly supported the activity of the extrinsic tenase complex. The reason behind this is unclear but could be due to the differential affinity of PT for binding coagulation factors. To address this, it is recommended to investigate the direct binding of PT to coagulation factors using surface plasmon resonance.

# CHAPTER 6 Exploring the impact of coronary artery disease on PT and PS levels of platelets, EVs, and leukocytes

## 6.1 Introduction

In **Chapters 3, 4** & **5**, I demonstrated that PT is present in blood cells and platelets, and that it can promote coagulation *in vitro* by supporting prothrombinase activity. In **Chapter 4**, PT levels were investigated in cells from healthy volunteers. Next, I will investigate whether PT levels are altered in circulating cells from people with coronary artery disease (CAD). As outlined previously (**Section 1.6**), CAD is characterised by higher EV counts, which could suggest increased procoagulant lipid levels in the circulation of CAD patients compared to healthy individuals. Thus, it would be useful to compare procoagulant lipid levels (e.g., PS and PT) in circulating cells from CAD patients and healthy volunteers.

PT measurements will be carried out on a cohort that had been recruited for a previous study and consists of acute coronary syndrome patients (ACS, n = 24) and three groups representing a spectrum of atherosclerosis: healthy controls (HC, n = 24), risk factor but no significant obstruction (RF, n = 23), and significant coronary artery disease (CAD, n = 19) (54). In a previous study using the same cohort, Protty measured and quantified three PS molecular species (PS 36:1, PS 36:2, and PS 38:4) in platelets, leukocytes, and EVs (54). Here, I will measure relative levels of 10 PS molecular species in the cohort groups and compare them to PT levels.

## 6.2 Results

### 6.2.1 PT and PS are significantly higher in platelets from coronary artery disease patients

An internal standard (IS, PS 15:0/18:1-D7) was added to platelet lipid extracts (from the clinical cohort groups, n = 90 total samples) which were then analysed using targeted HILIC LC-MS/MS, as described in **Experimental Methods**. 10 PS and 10 PT species were measured using an MRM method using transitions in **Table 2.2**. Total PS and PT were estimated by summing A/IS values of individual species in the respective classes. Absolute quantification was not possible because the IS was added post extraction.

Total PT and PS in platelets (normalized to cell count) were higher in RF, CAD, and ACS groups compared to HC, with total PT showing statistically significant changes in CAD and ACS compared to HC (**Figure 6.1**). Next, individual molecular species were investigated. All PT species were higher in platelets from disease groups (RF, CAD, ACS) compared to HC (**Figure 6.2**). Notably, PT 34:1 and PT 40:4 were significantly higher in platelets from ACS patients compared to HC, while PT 36:1 and PT 40:3 were significantly higher in CAD and ACS compared to HC. All PS species, except PS 38:5, showed an upwards trend in disease groups (**Figure 6.3**). Notably, PS 40:3 and PS 40:4 were significantly higher in ACS compared to HC, while PS 36:1 was significantly higher in CAD and ACS compared to HC.

These results demonstrate the elevation of PT and PS in platelets from disease groups compared to healthy volunteers. This suggests a metabolic dysregulation of PT and PS in coronary artery disease which results in increased levels of PS and PT in platelets of CAD patients compared to healthy volunteers. However, it is unclear if these increased lipids levels result from higher rates of generation or reduced rates of clearance.

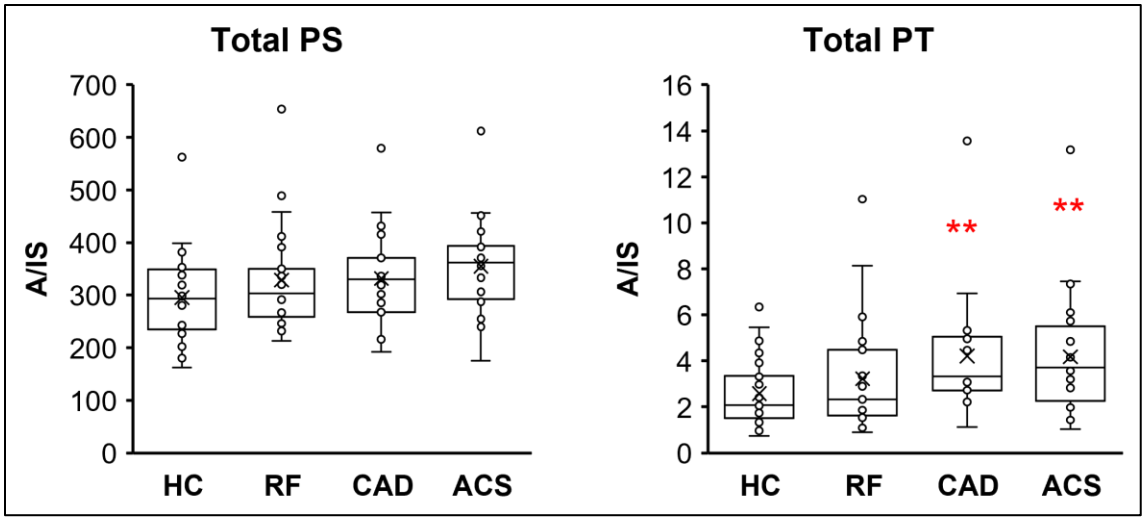


**Figure 6.1 – Platelet total PS and PT trend upwards in coronary artery disease patients**

Internal standard (IS, PS 15:0/18:1-D7) was added to platelet lipid extracts from the clinical cohort then samples were analysed using targeted HILIC-LC-MS/MS, as described in **Experimental Methods**. Ratios of analytes to IS (A/IS, cps) were calculated for individual PS and PT species, then A/IS values were added up to estimate total PS and PT. Data are represented as whisker plots. HC: healthy controls (n = 24), RF: risk factor (n = 23), CAD: coronary artery disease (n = 19), ACS: acute coronary syndrome (n = 24). Statistical significance was determined using the Kruskal-Wallis H test (**: $P < 0.01$).

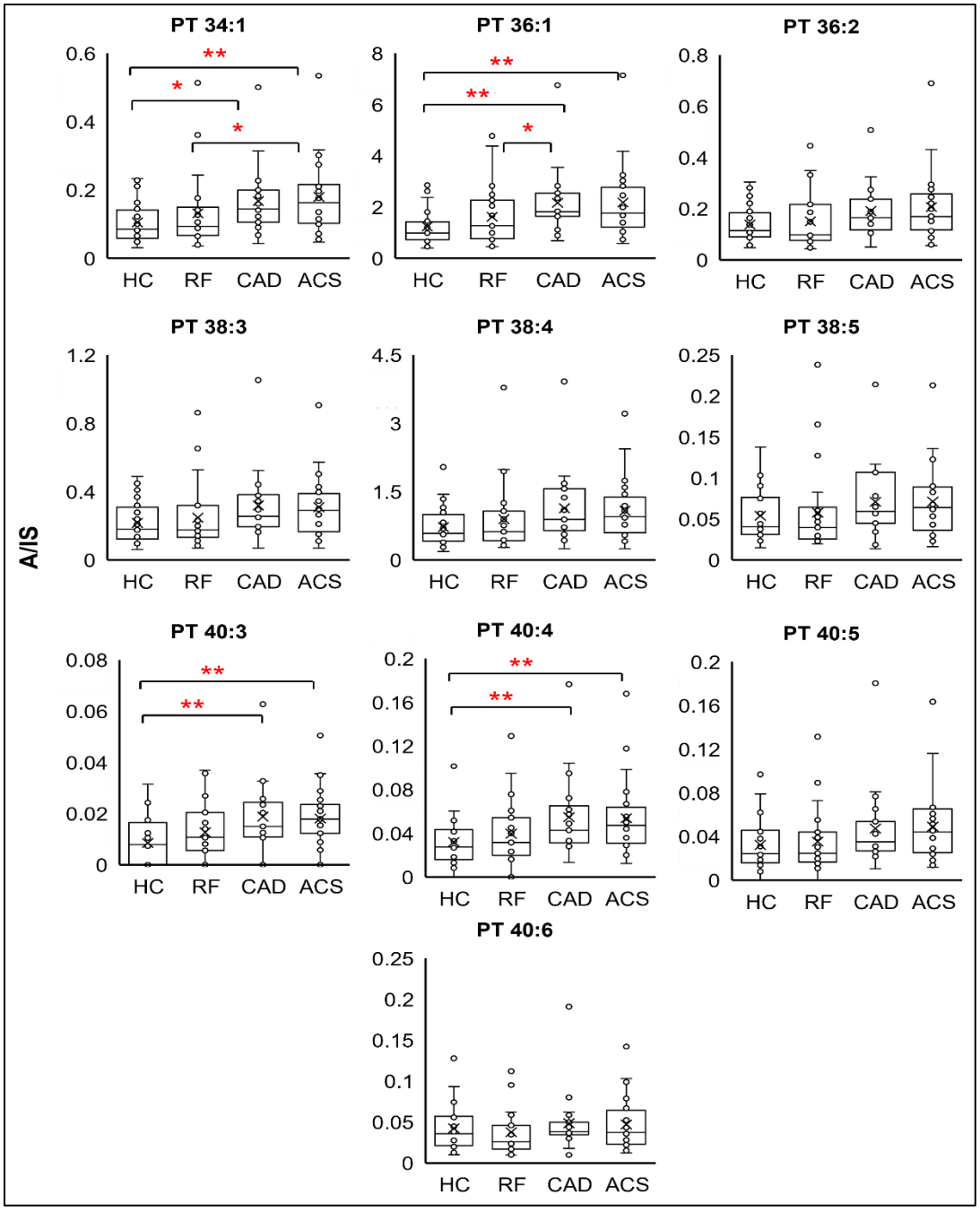


**Figure 6.2 – Some platelet PT species are significantly higher in coronary artery disease patients**

Internal standard (IS, PS 15:0/18:1-D7) was added to platelet lipid extracts from the clinical cohort then samples were analysed using targeted HILIC-LC-MS/MS, as described in **Experimental Methods**. Ratios of analytes to IS (A/IS, cps) were calculated for PT species. Data are represented as whisker plots. HC: healthy controls (n = 24), RF: risk factor (n = 23), CAD: coronary artery disease (n = 19), ACS: acute coronary syndrome (n = 24). Statistical significance was determined using the Kruskal-Wallis H test (*: $P < 0.05$, **: $P < 0.01$).

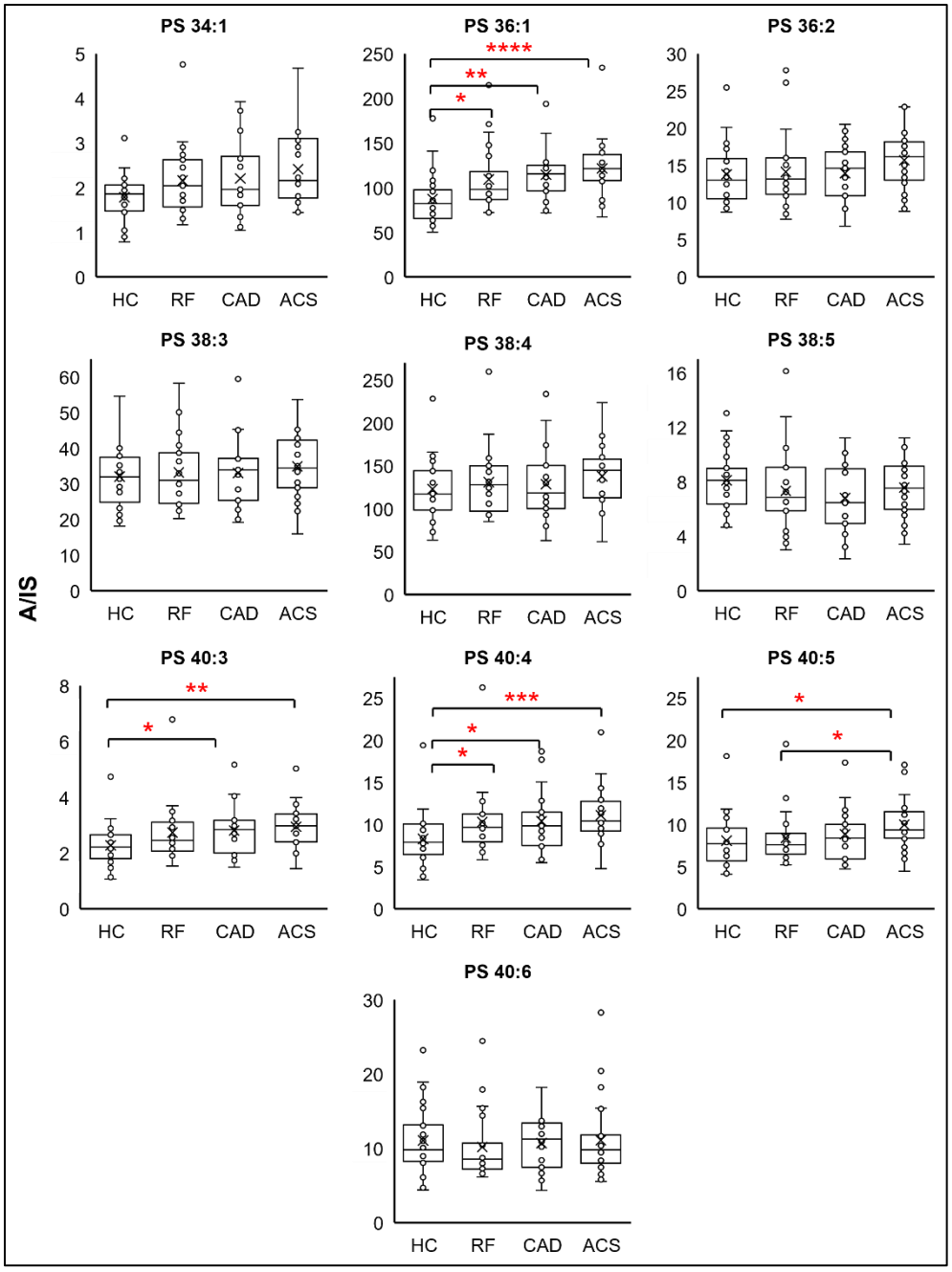


**Figure 6.3 – Some platelet PS species are significantly higher in coronary artery disease patients**

Internal standard (IS, PS 15:0/18:1-D7) was added to platelet lipid extracts from the clinical cohort then samples were analysed using targeted HILIC-LC-MS/MS, as described in **Experimental Methods**. Ratios of analytes to IS (A/IS, cps) were calculated for PS species. Data are represented as whisker plots. Statistical significance was determined using the Kruskal-Wallis H test (*: $P < 0.05$, **: $P < 0.01$, ***: $P < 0.001$).

### 6.2.2 Thrombin-activated platelets from CAD patients and RF group metabolize more PS and PT compared to healthy volunteers

Next, the impact of thrombin (0.2 U/mL at 37 °C for 30 min) on PS and PT levels was determined. PT and PS levels were reduced following thrombin of platelets from all patient groups (**Figure 6.4**). However, greater PT reductions were observed for RF and CAD groups compared to HC. PS and PT species with >2 double bonds were more impacted by thrombin activation, indicating that lipids with PUFA were more preferentially metabolized on platelet activation. Additionally, PS 36:1 and PT 36:1 were metabolized more efficiently in the CAD and RF groups compared to HC and ACS. For both PS and PT, the ACS patient platelets exhibited a lower % decrease in response to thrombin compared to other groups including HC.

Collectively, these results suggest that platelets from RF and CAD patients, but not ACS, metabolize a higher percentage of their PS and PT in response to thrombin. However, considering the increased amounts of platelet PS and PT in disease groups (RF, CAD, and ACS) compared to HC (demonstrated previously, **Figure 6.1**), it can be concluded that platelets from disease groups overall metabolize higher amounts of PS and PT compared to healthy platelets in response to thrombin.

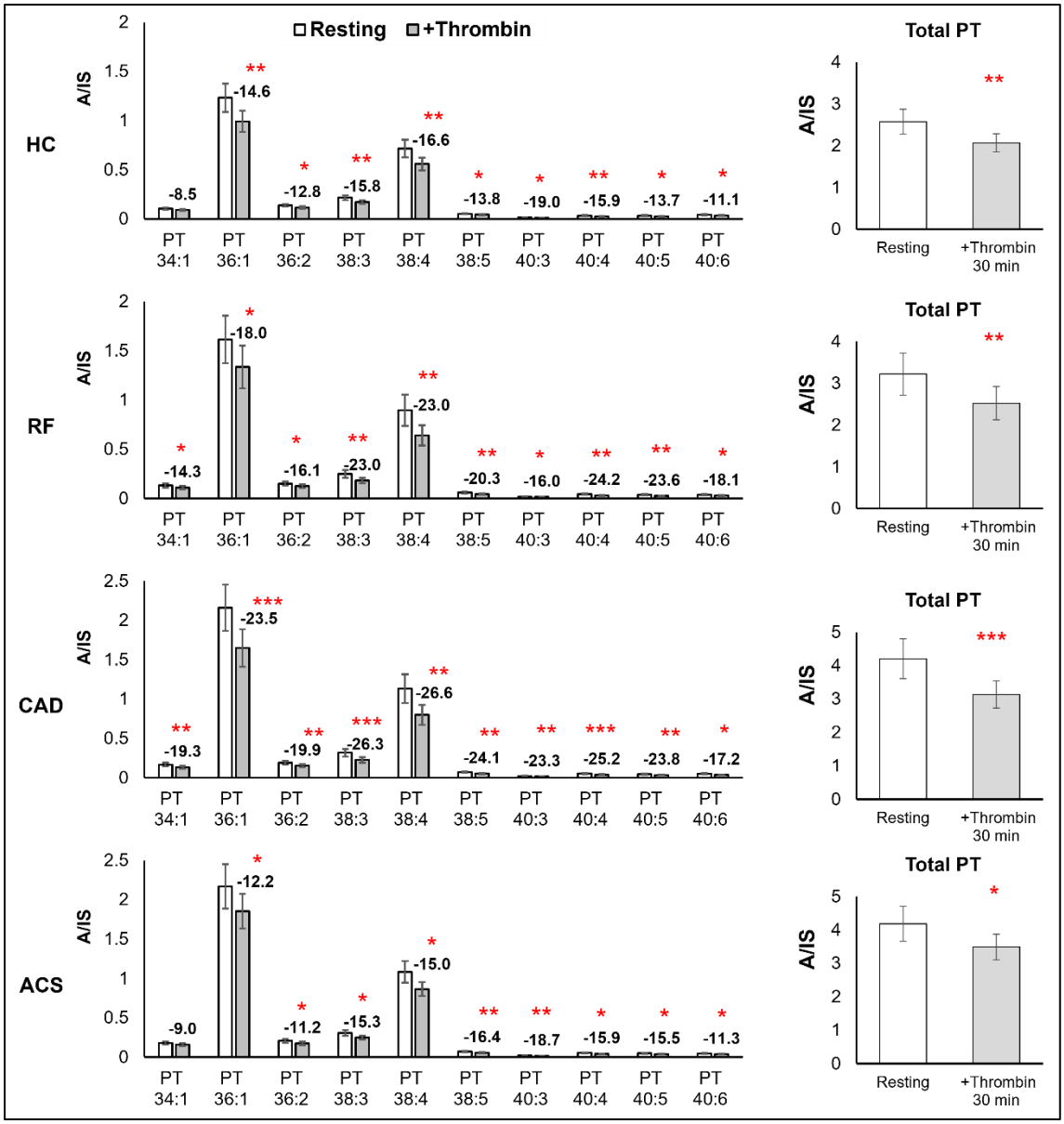


**Figure 6.4 – Thrombin activation decreases platelet PT in healthy volunteers and coronary artery disease patients**

Internal standard (IS, PS 15:0/18:1-D7) was added to resting or thrombin-activated (0.2 U/mL at 37 °C for 30 min) platelets from the clinical cohort. Extracts were then analysed using targeted HILIC-LC-MS/MS, as described in **Experimental Methods**. Ratios of analytes to IS (A/IS, cps) were calculated for PT species. Data are represented as means ± SEM. Total PT was calculated by adding A/IS values for individual species. Statistical significance was determined using paired t-tests (*: $P < 0.05$, **: $P < 0.01$, ***: $P < 0.001$).

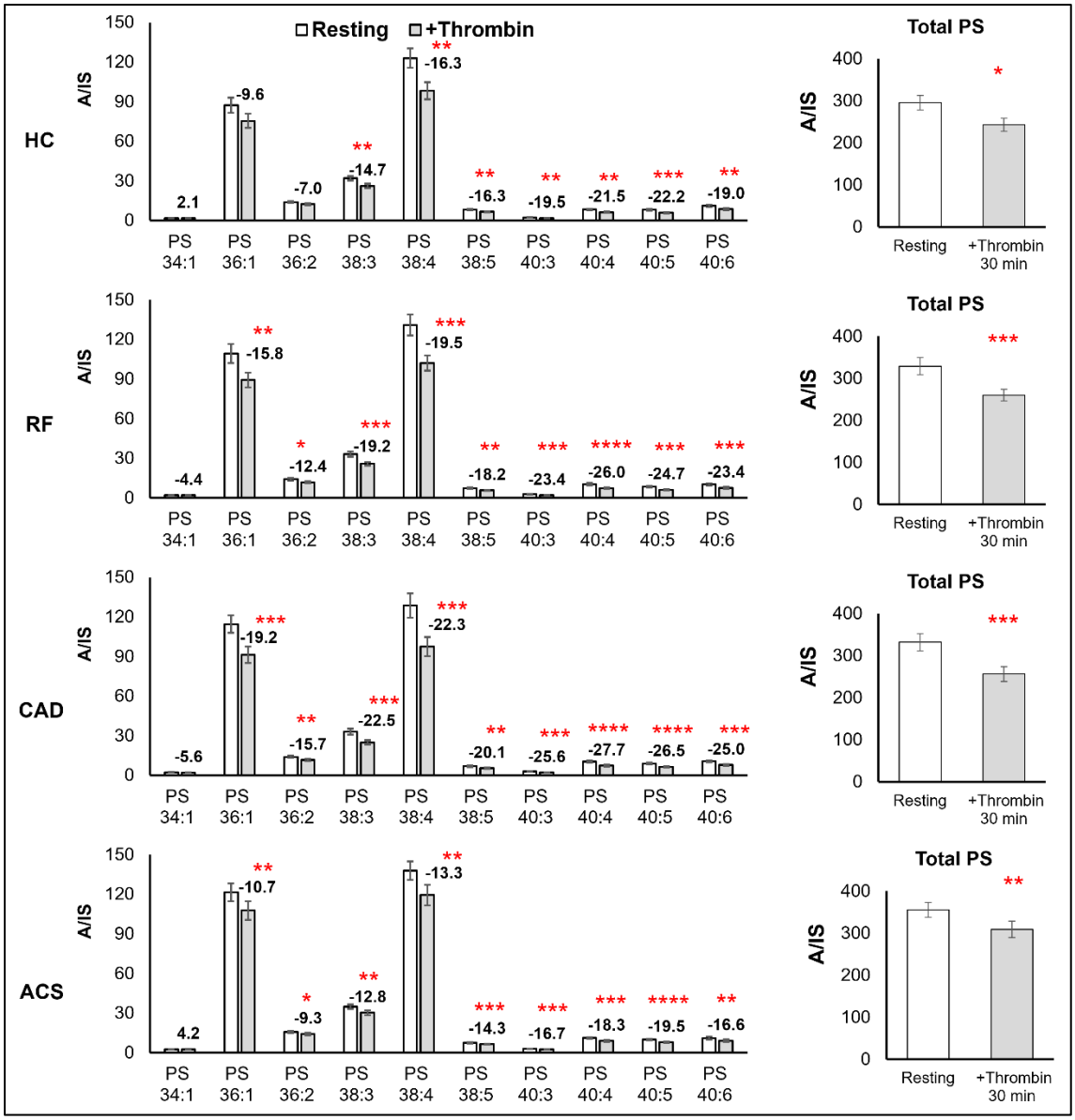


**Figure 6.5 – Thrombin activation decreases platelet PS in healthy volunteers and coronary artery disease patients**

Internal standard (IS, PS 15:0/18:1-D7) was added to resting or thrombin-activated (0.2 U/mL at 37 °C for 30 min) platelets from the clinical cohort. Extracts were then analysed using targeted HILIC-LC-MS/MS, as described in **Experimental Methods**. Ratios of analytes to IS (A/IS, cps) were calculated for PS species. Data are represented as means ± SEM. Total PS was calculated by adding A/IS values for individual species. Statistical significance was determined using paired t-tests (*: $P < 0.05$, **: $P < 0.01$, ***: $P < 0.001$, ****: $P < 0.0001$).

### 6.2.3 Extracellular vesicle PT and PS levels are significantly higher in plasma from coronary artery disease patients

An IS (PS 15:0/18:1-D7) was added to lipid extracts of extracellular vesicle (EV) isolated previously from 6 mL plasma from the four groups (HC, RF, CAD, and ACS) (54). The samples were then analysed using targeted HILIC LC-MS/MS, as described in **Experimental Methods**.

Total PT and PS were significantly higher in CAD and ACS, while RF showed an uptrend compared to HC (**Figure 6.6**). For both classes, the greatest increases were observed in CAD, closely followed by ACS, and the lowest increases (compared to HC) were in the RF group.

All measured PT species exhibited an upwards trend in disease groups compared to HC, and several species, including the two most abundant ones PT 36:1 and PT 38:4, were significantly higher in CAD and ACS groups (**Figure 6.7**). PT 40:3 was excluded from the analysis because it was detected in less than half the samples.

Similarly, all PS species measured were higher in EVs in plasma from disease groups compared to HC (**Figure 6.8**). All PS species were significantly higher in the CAD and ACS groups, and 8 out of 10 were significantly higher in the RF group compared to HC.

In summary, PS and PT are significantly higher in EVs isolated from plasma from RF, CAD, and ACS patients compared to HC. However, these lipid measurements are not normalized to EV counts, which have been shown to be higher in the disease groups (54). Thus, to address whether higher PS and PT levels in patients (compared to HC) was due to higher EV counts, PS and PT levels were normalized by EV counts reported earlier using nanoparticle tracking analysis (54). When adjusted by EV count, PT 34:1, PT 36:2, and PT 38:5 were still significantly higher in CAD and ACS patients compared to HC, whereas PT 40:4 was significantly lower in CAD compared to HC (**Figure 6.9**). Additionally, while not statistically significant, PT 36:1 (one of the two most abundant PT species) levels were higher in RF, CAD and ACS patient groups compared to HC. Similarly, several PS species were higher (albeit statistically insignificant) in the ACS group compared to HC (**Figure 6.9**). These results indicate that higher PT levels in EVs (from plasma) from coronary artery disease patients cannot be fully explained by elevated EV counts.

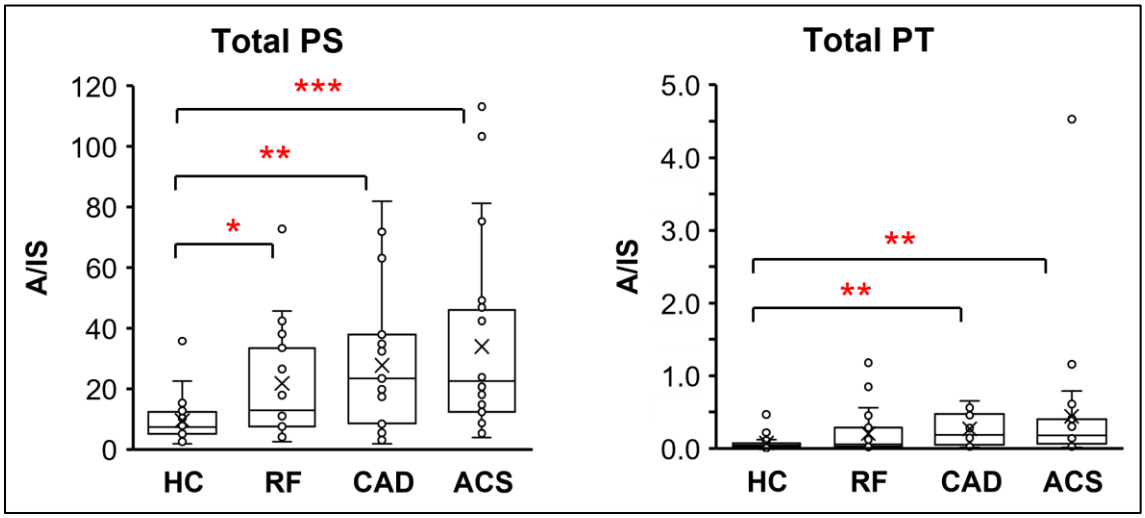


**Figure 6.6 – Total PS and PT in extracellular vesicles are significantly higher in coronary artery disease patients**

Internal standard (IS, PS 15:0/18:1-D7) was added to extracellular vesicle (EV) lipid extracts (isolated from 6 mL PPP) from the clinical cohort then samples were analysed using targeted HILIC-LC-MS/MS, as described in **Experimental Methods**. Ratios of analytes to IS (A/IS, cps) were calculated for individual PS and PT species, then A/IS values were added up to estimate total PS and PT. Data are represented as whisker plots. Statistical significance was determined using the Kruskal-Wallis H test (*: $P < 0.05$, **: $P < 0.01$, ***: $P < 0.001$).

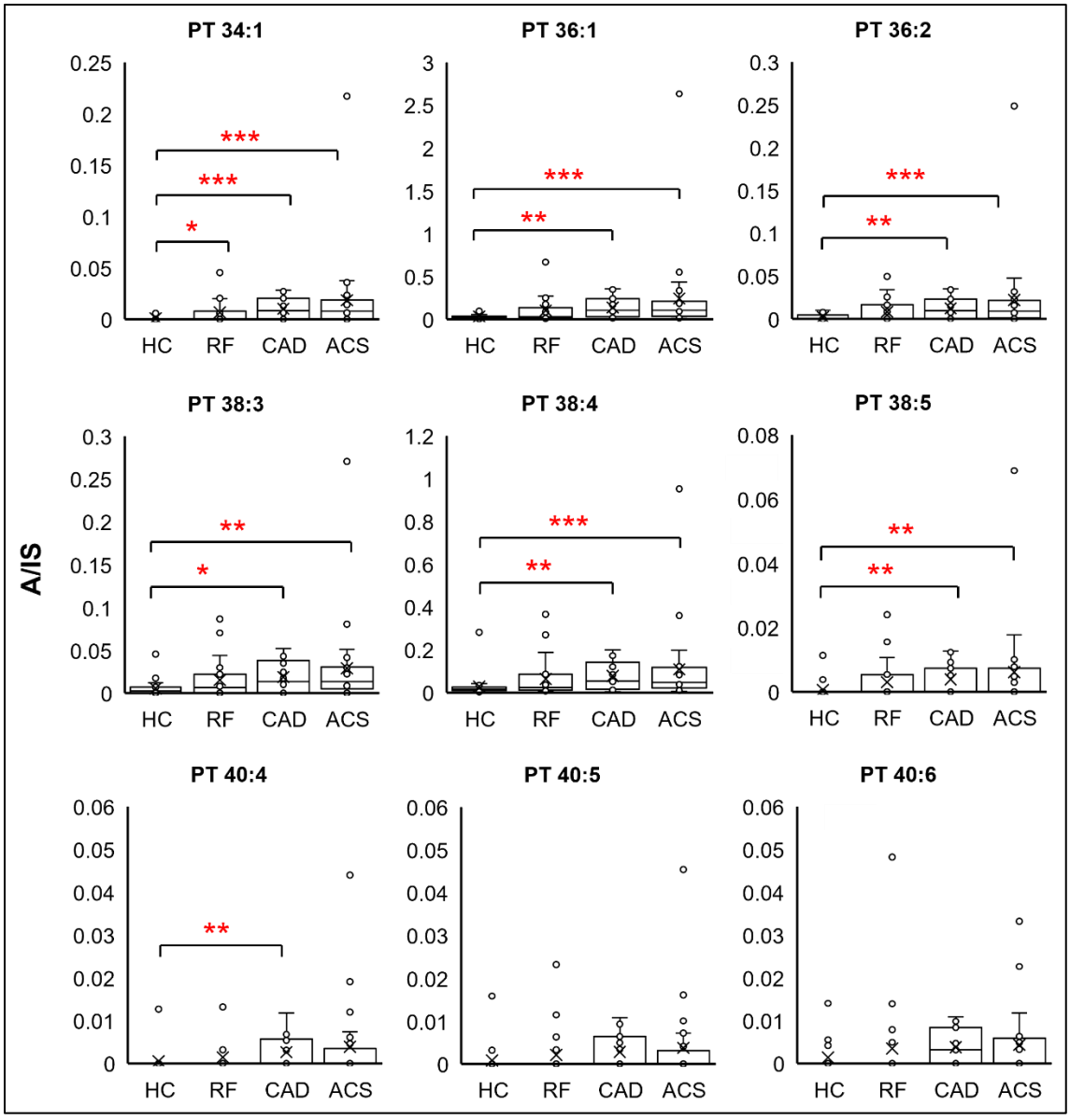


**Figure 6.7 – PT species in extracellular vesicles are significantly higher in coronary artery disease patients**

Internal standard (IS, PS 15:0/18:1-D7) was added to EV lipid extracts (isolated from 6 mL PPP) from the clinical cohort then samples were analysed using targeted HILIC-LC-MS/MS, as described in **Experimental Methods**. Ratios of analytes to IS (A/IS, cps) were calculated for PT species. Data are represented as whisker plots. Statistical significance was determined using the Kruskal-Wallis H test (*: $P < 0.05$, **: $P < 0.01$).

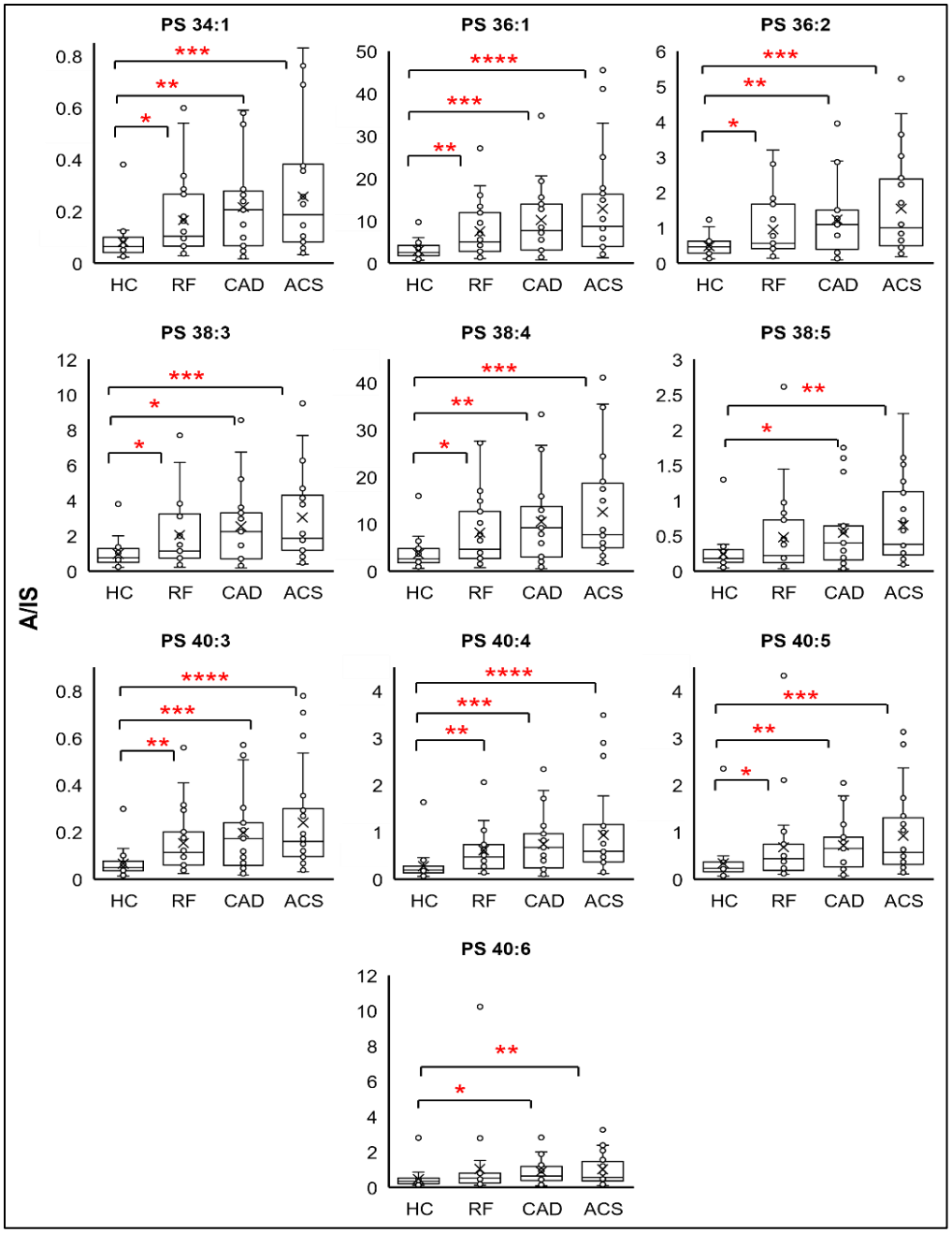


**Figure 6.8 – PS species in extracellular vesicles are significantly higher in coronary artery disease patients**

Internal standard (IS, PS 15:0/18:1-D7) was added to EV lipid extracts (isolated from 6 mL PPP) from the clinical cohort then samples were analysed using targeted HILIC-LC-MS/MS, as described in **Experimental Methods**. Ratios of analytes to IS (A/IS, cps) were calculated for PS species. Data are represented as whisker plots. Statistical significance was determined using the Kruskal-Wallis H test (*: $P < 0.05$, **: $P < 0.01$, ***: $P < 0.001$, ****: $P < 0.0001$).

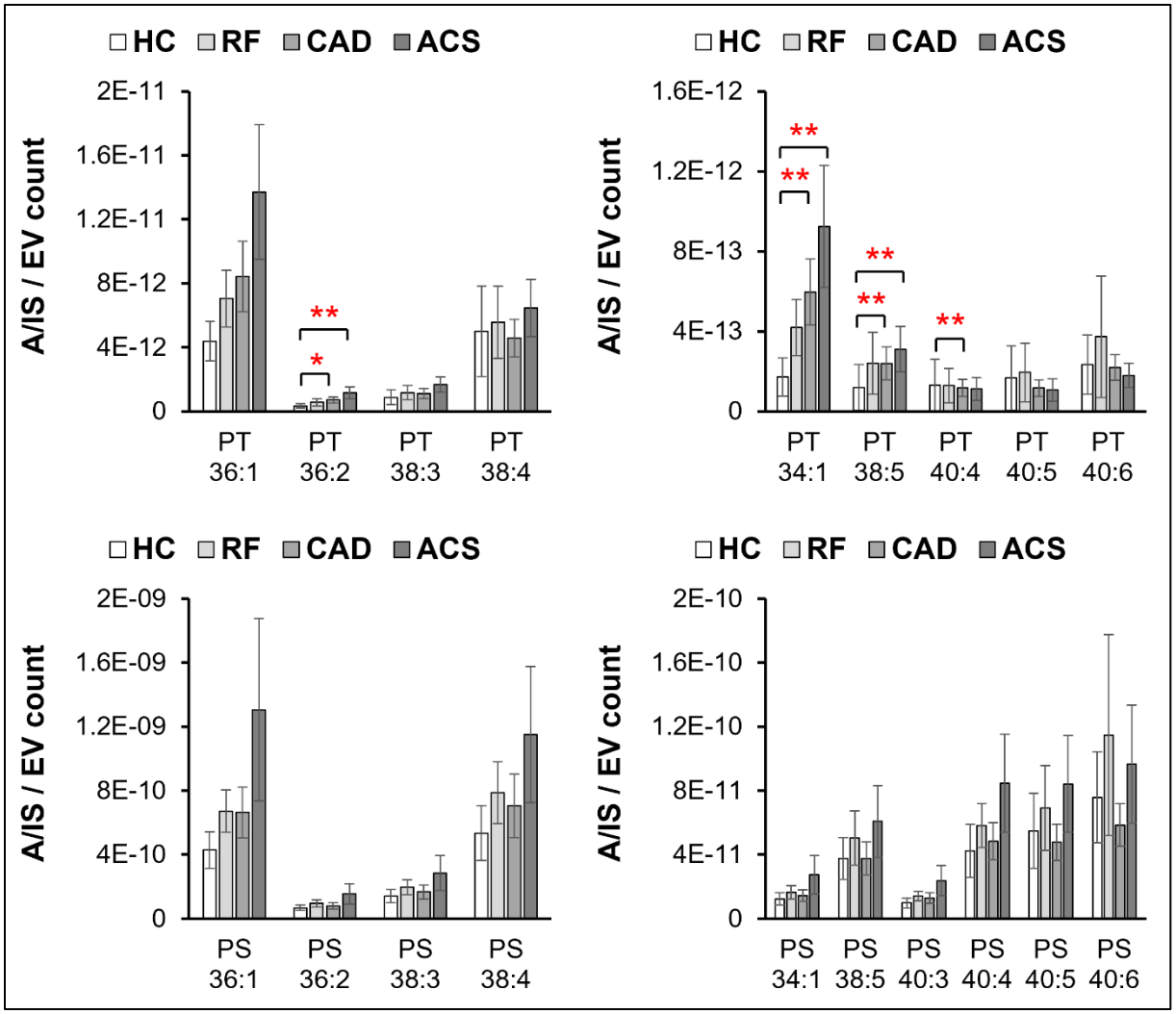


**Figure 6.9 – Several PT species are significantly altered in EVs isolated from coronary artery disease patients when adjusted by EV count**

Internal standard (IS, PS 15:0/18:1-D7) was added to EV lipid extracts (isolated from 6 mL PPP) from the clinical cohort then samples were analysed using targeted HILIC-LC-MS/MS, as described in **Experimental Methods**. Ratios of analytes to IS (A/IS, cps) were calculated for PS and PT species then normalized by EV counts obtained from (54). Data are represented as means ± SEM. Statistical significance was determined using the Kruskal-Wallis H test (*: $P < 0.05$, **: $P < 0.01$).

### 6.2.4 Leukocyte PS but not PT is decreased in coronary artery disease patients

Next, PT and PS levels were measured in leukocytes (normalized by cell count prior to lipid extract) from the four groups (HC, RF, CAD, and ACS), following the addition of internal standard (PS 15:0/18:1-D7). Non-significant trends were observed, including a slightly lower total PS and slightly higher total PT in the patient groups compared to HC (**Figure 6.10**). An upwards non-significant trend was observed for PT 36:1 and PS 36:1 levels in the patient groups compared to HC (**Figures 6.11 & 6.12**). In contrast, several PS species were significantly decreased in disease groups compared to HC, particularly species with more than 2 double bonds: PS 38:3, PS 38:4, PS 38:5, PS 40:5, and PS 40:6 (**Figure 6.12**).

Collectively, these results demonstrate there were no significant differences in leukocyte PT levels in coronary artery disease patients versus HC. However, several PUFA-containing PS species were significantly lower in patients compared to HC.

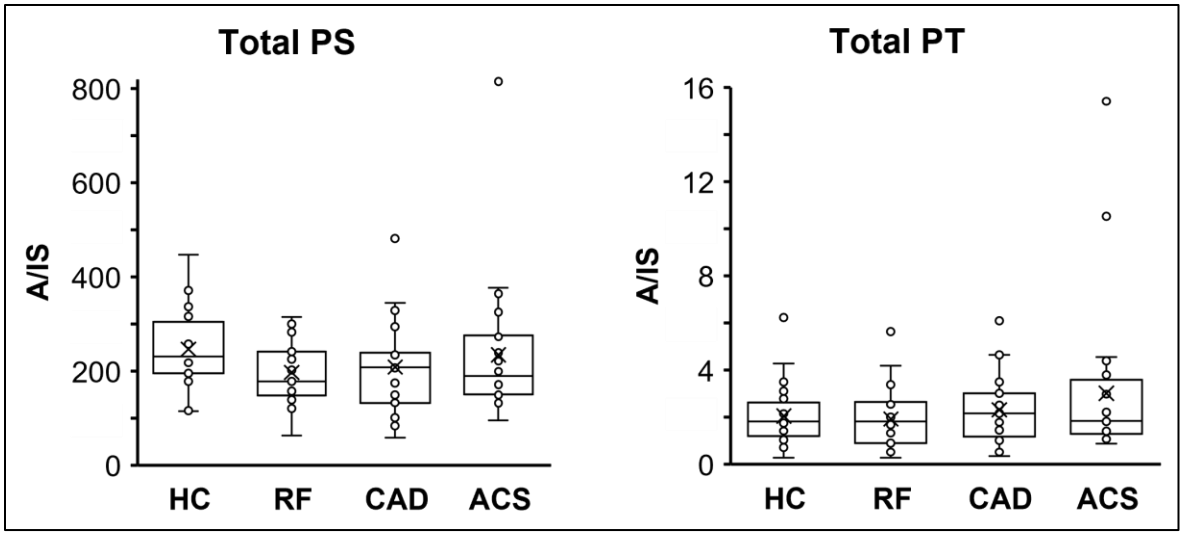


**Figure 6.10 – No significant changes in total leukocyte PS and PT in coronary artery disease patients**

Internal standard (IS, PS 15:0/18:1-D7) was added to leukocyte lipid extracts from the clinical cohort then samples were analysed using targeted HILIC-LC-MS/MS, as described in **Experimental Methods**. Ratios of analytes to IS (A/IS, cps) were calculated for individual PS and PT species, then A/IS values were added up to estimate total PS and PT. Data are represented as whisker plots. Statistical significance was determined using the Kruskal-Wallis H test.

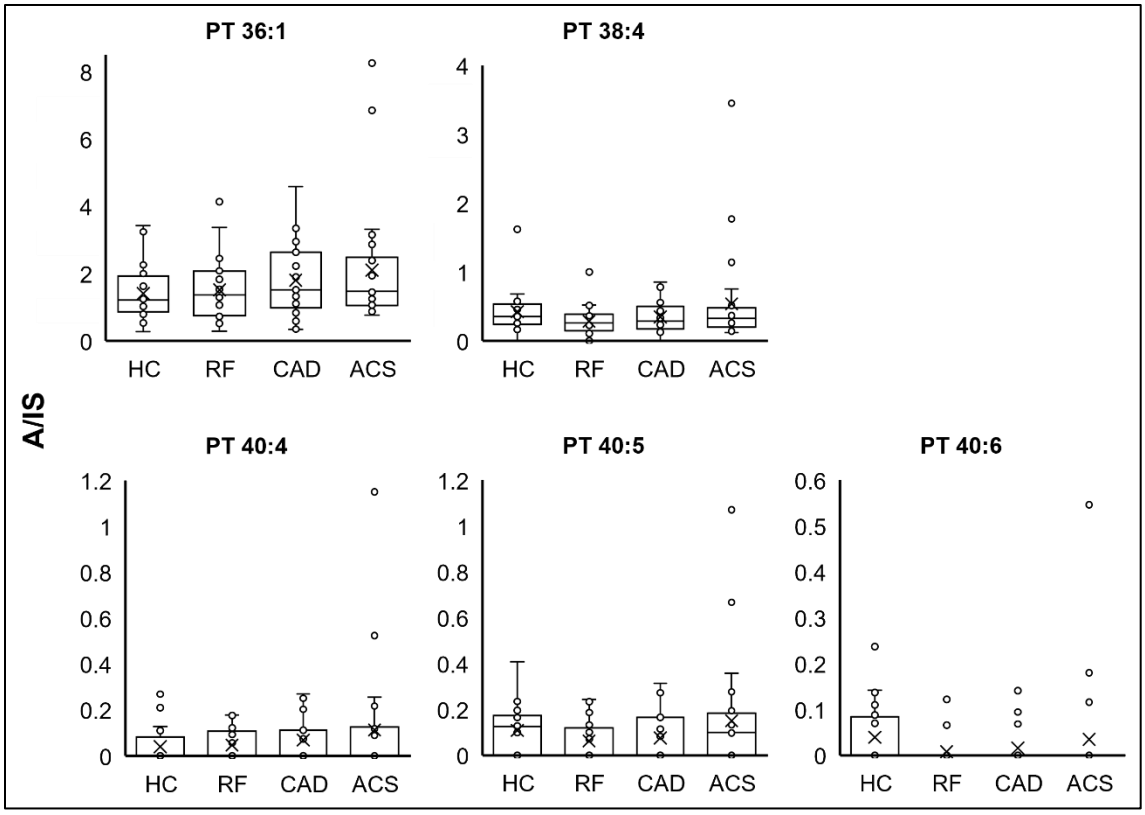


**Figure 6.11 – No significant changes to leukocyte PT in coronary artery disease patients**

Internal standard (IS, PS 15:0/18:1-D7) was added to leukocyte lipid extracts from the clinical cohort then samples were analysed using targeted HILIC-LC-MS/MS, as described in **Experimental Methods**. Ratios of analytes to IS (A/IS, cps) were calculated for PT species. Data are represented as whisker plots. Statistical significance was determined using the Kruskal-Wallis H test.

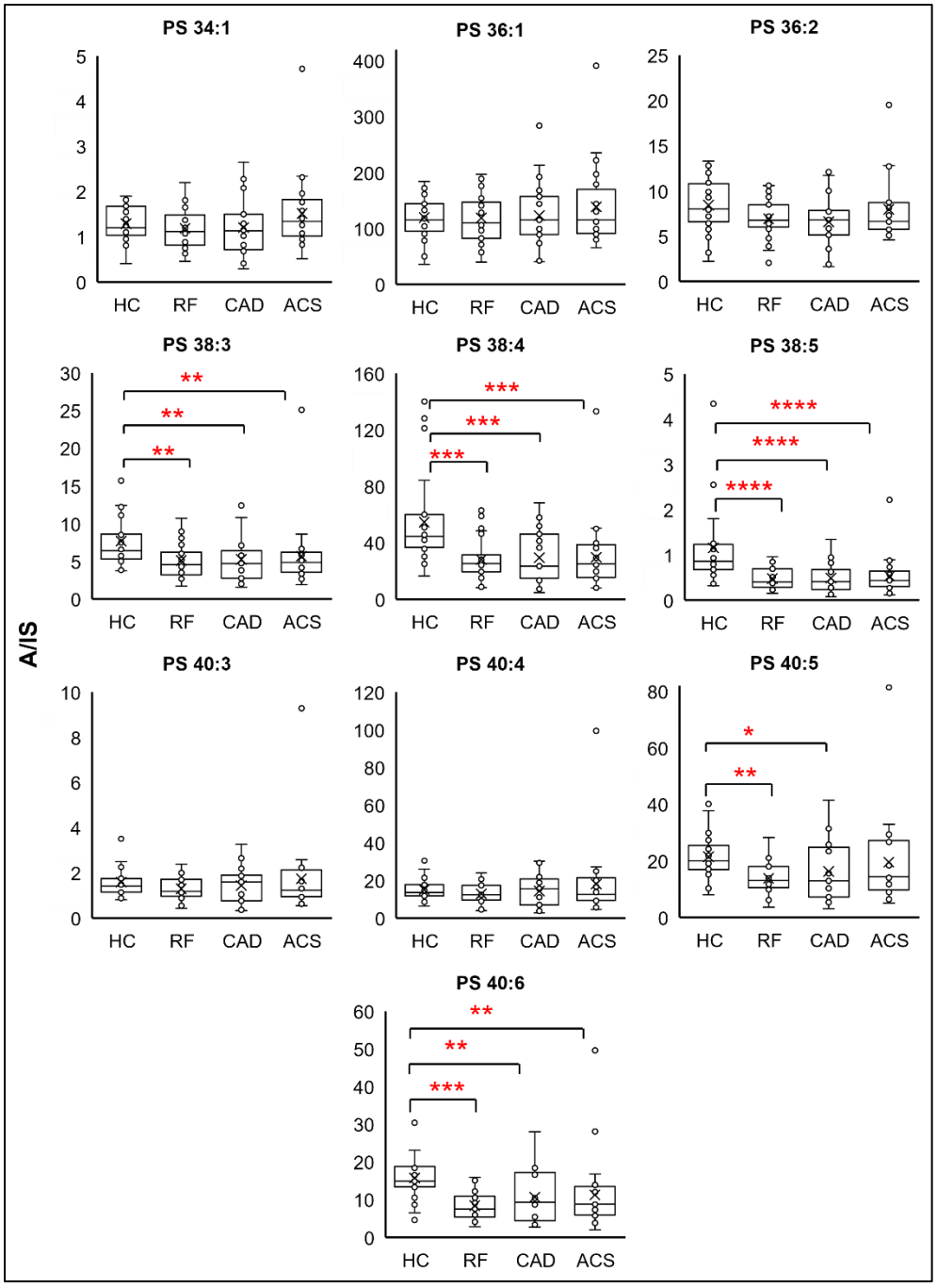


**Figure 6.12 – PUFA-containing PS species in leukocytes are decreased in coronary artery disease patients**

Internal standard (IS, PS 15:0/18:1-D7) was added to leukocyte lipid extracts from the clinical cohort then samples were analysed using targeted HILIC-LC-MS/MS, as described in **Experimental Methods**. Ratios of analytes to IS (A/IS, cps) were calculated for PS species. Data are represented as whisker plots. Statistical significance was determined using the Kruskal-Wallis H test (*: $P < 0.05$, **: $P < 0.01$, ***: $P < 0.001$, ****: $P < 0.0001$).

## 6.3 Discussion

Here, I measured PT and PS levels in platelets, EVs, and leukocytes from a clinical cohort of coronary artery disease to investigate whether the lipids are altered in patients compared to healthy volunteers.

PT and PS levels were elevated in platelets from CAD and ACS patients compared to HC. In particular, PS and PT 36:1, 40:3 and 40:4 were significantly increased, whereas several other species trended upwards without statistical significance. One possible explanation for the increase in PS and PT could be related to the morphology of the platelets. A larger immature platelet (reticulated platelet) fraction has been reported in CAD, and these immature platelets exhibit a larger cell volume (compared to mature platelets) and contain more rough ER fragments, mitochondria, alpha and dense granules (45-49). Therefore, the increased PS and PT platelets in disease groups could be due to a higher fraction of immature platelets and owing to their larger size and lipid membrane content. This hypothesis could be tested by isolating fractions of mature and immature platelets using flow cytometry then comparing their PS and PT content using LC-MS. Additionally, their sizes could be compared using automated analysers.

Immature platelets have been reported to be more reactive and exhibit a greater prothrombotic potential compared to mature platelets (113-115). In this study, platelets from the different cohort groups were activated by thrombin then PS and PT levels were measured and compared to resting platelets. Platelets from RF and CAD groups responded more vigorously to thrombin in relation to reductions in PS and PT that were seen to occur, in comparison to healthy volunteer platelets. However, this was not observed in the ACS patients' platelets, possibly due to the use of P2Y12 inhibitors or aspirin to treat those patients. In support of the former, 100% of ACS patients in the cohort were being treated with P2Y12 inhibitors, compared to 31.6% of CAD patients, 13% of RF patients and 0% of HC volunteers (54). While P2Y12 inhibitors do not directly inhibit the thrombin pathway, they inhibit the effect of ADP, which is released by activated platelets and amplifies the $Ca^{2+}$ response induced by thrombin (116). Thus, P2Y12 inhibitors may be indirectly affecting the thrombin pathway. As cytosolic phospholipase $A_2$ ($cPLA_2\alpha$) is activated by $Ca^{2+}$, the use of P2Y12 inhibitors would theoretically reduce the enzyme's activity. This could be responsible for the lower % decrease in PS and PT by the ACS platelets in response to thrombin. As for aspirin use, 100% of ACS patients in this cohort were

treated with it, compared to 73.7% of CAD patients, 87% of RF patients, and 0% of healthy volunteers (54). Aspirin is commonly used as an antiplatelet drug to manage thrombosis, and the weak activation by ACS patient platelets observed here could be due to the aspirin.

Platelets from RF and CAD groups metabolized a higher proportion of their PS and PT in response to thrombin. This, combined with the higher PS and PT contents in platelets from these patient groups (compared to HC), indicates a faster rate of PS and PT metabolism in RF and CAD platelets. That said, the metabolism of PS and PT in thrombin activated platelets is poorly understood, especially in humans. PS-specific $PLA_1$ is expressed in rat platelets but not in human platelets (22). Therefore, $PLA_2$ enzymes are mostly likely responsible for the metabolism of PS and PT in human platelets and will be the focus of this discussion. $cPLA_2\alpha$ prefers PLs with FA 20:4 in the *sn*-2 position as substrates, while calcium-independent phospholipase $A_2$ ($iPLA_2\gamma$) cleaves PLs with FA 20:4 and FA 22:6 (117-119). In this study, PS and PT species containing various PUFAs (20:3, 20:4, 22:3, 22:4, 22:5, and 22:6) and saturated FAs were analysed. PUFA-containing PS and PT appeared to be metabolised to a greater extent than those containing fewer double bonds. Platelets from the ACS group exhibited the lowest % decrease in PS and PT in response to thrombin. This could relate to administration of P2Y12 inhibitors or aspirin. For PS, there was a slight preference for metabolism of PS containing 22-carbon FAs compared other FAs. This suggests that $iPLA_2\gamma$ may be involved in PS metabolism in thrombin-activated platelets, since $cPLA_2\alpha$ prefers FA 20:4 (117). In support of this idea, a previous study on murine platelets proposed that $iPLA_2\gamma$ facilitates aggregation in response to ADP since $iPLA_2\gamma$-deficient mice showed decreased ADP-induced aggregation (119). Here, I observed reduced PS and PT metabolism in thrombin-activated platelets from ACS patients. This could be attributed to the P2Y12 inhibitors, i.e., the inhibition of the ADP pathway resulted in decreased $iPLA_2\gamma$ activity. As such, $iPLA_2\gamma$ activity could be related to the hyperactivity of platelets in coronary artery disease, but this requires further investigation. Additionally, contributions from $cPLA_2\alpha$ cannot be fully ruled out. That said, PUFAs liberated from PS and PT pools upon platelet activation could have been used for the synthesis of oxylipins via 12-lipoxygenase and cyclooxygenase-1, but this requires experimental proof with labelled (e.g., deuterated) phospholipids (90, 120). Additionally, free oxylipins could have been incorporated into PE to form enzymatically

oxidized PE, as demonstrated in a previous study (90). However, it is currently unknown if oxylipins are also incorporated into PS or PT in platelets.

RF and CAD patient platelets metabolised more PS and PT 36:1 (FA composition: 18:0_18:1) compared to HC and ACS. Assuming the lipids were metabolized by a $PLA_2$, this would release higher levels of FA 18:1 in the RF and CAD groups. Several studies reported that FA 18:1 inhibits platelet aggregation (121-123). Its mechanism of action involves blocking the rise in intracellular $Ca^{2+}$ (122). As such, the liberation of FA 18:1 from PS and PT pools in platelets from RF and CAD patients could be a homeostatic mechanism that reverses aggregation. Platelets from the ACS group had decreased FA 18:1 release, presumably due to a weaker activation. The role of FA 18:1 in platelet activation requires further investigation.

In addition to releasing FAs, the hydrolysis of PS and PT by $PLA_2$ would generate 1-lysoPS and 1-lysoPT, respectively. Both lysoPS and lysoPT have been previously shown to induce mast cell degranulation in murine models (70, 71). LysoPS also triggers the degranulation of human eosinophils (124). LysoPS levels were found to be higher in mouse serum than in plasma, suggesting they may be generated during coagulation (125). Whether they play a role in blood coagulation is currently unknown. Importantly, while my data shows a decrease in PS and PT in activated platelets, no measurements of lysoPS or lysoPT were carried out. Therefore, the generation of lysoPT by activated platelets requires further characterisation.

Total PS and PT were significantly higher in EVs from CAD and ACS groups compared to HC, and total PS levels were also significantly higher in the RF group. Overall, levels of most molecular species measured were higher in the patient groups compared to HC. Upon correcting lipid signals (A/IS) by EV count using nanoparticle tracking analysis data by Protty (54), increases in all PS and several PT molecular species lost statistical significance, but upwards trends remained. This suggests that EV counts do not fully account for the higher PT levels in EVs from patient groups. Additionally, adjusting for EV count does not represent physiological conditions, since higher EV counts (per mL plasma) are characteristic of several diseases. For example, a 2.5-fold increase in EV count was reported in ACS patients compared to healthy volunteers (53). In the cohort studied in this chapter, EV counts were significantly higher in CAD patients, and upward trends were observed for RF and ACS compared to HC (54). Additionally, EVs from disease groups (RF, CAD, and ACS) supported more thrombin

generation compared to HC (9). A positive correlation was demonstrated between EV count and thrombin generation, but thrombin generation was no longer significantly higher when it was normalized by EV count (54). The higher EV count in the disease groups partly explains the higher PS/PT levels reported here and the greater thrombin generation reported earlier by Protty (54). This also suggests a link between the PS/PT levels and thrombin generation. In support of this, one study reported higher procoagulant PS-containing EV counts in ACS compared to healthy volunteers (126). However, there is one inconsistency regarding the ACS group, where EV PS/PT levels were as high as the CAD group, but EV counts and thrombin generation were lower. The activation of P2Y12 receptors is known to promote EV release from platelets (127). Therefore, the lower EV counts in ACS patients (compared to CAD patients) could also be due to the greater use of P2Y12 inhibitors on the former.

Leukocyte PS, but not PT, was significantly decreased in the disease groups compared to HC. Notably, the lowest levels in PS were observed for PUFA-containing species, specifically those containing FA 20:4 and FA 22:6. There are several possible explanations for this. One involves non-enzymatic lipid peroxidation, which targets PUFAs in membrane PS and leads to decreased PUFA-containing PS species in disease. A non-enzymatic mechanism is unlikely to discriminate between PL classes. However, no significant decreases were observed in PUFA-containing PT species. Additionally, this would not explain the preference for PS species with FA 20:4 or FA 22:6. As such, a more likely explanation involves enzymes that specifically target PUFA-containing PS. In this cohort, leukocytes were isolated from RBCs and platelets but were not further fractionated. This makes it difficult to speculate on the pathway responsible as different leukocyte populations possess distinct enzyme profiles. That said, neutrophils are the most common leukocytes in blood, and the decrease in PS could be due to phospholipases hydrolysing PUFA for the biosynthesis of oxylipins through 5-lipoxygenase (5-LOX) (128, 129). Activated neutrophils generate 5-hydroperoxyeicosatetraenoic acid (5-HpETE) from arachidonic acid (FA 20:4(5Z,8Z,11Z,14Z)) through the action of 5-LOX. This can then be incorporated into PC and PE via Lands cycle enzymes (128). On the other hand, 15-LOX, found in eosinophils, generates 15-HpETE from arachidonic acid, but the enzyme can oxygenate free FA 22:6 and intact PLs containing FA 20:4 (130).

## 6.4 Conclusion

In conclusion, PT and PS levels were found to be higher in platelets and EVs isolated from patients with vascular disease (RF, CAD, and ACS) compared to healthy volunteers (HC). Increased platelet PS and PT in patient groups could be due to a higher proportion of immature platelets, while increased PS and PT levels in EVs are partly due to a higher EV count in disease groups. Platelets from the RF and CAD groups responded more vigorously (compared to HC) to thrombin activation by metabolising a higher % of their PS and PT. This was not observed in the ACS group, possibly due to the use of P2Y12 inhibitors. Leukocyte PS (particularly PUFA-containing molecular species) but not PT was significantly lower in patient groups compared to HC. The reason behind this is unknown. The results presented here shed a glimpse of light on PS, PT, and their metabolism in coronary artery disease. However, throughout the course of this chapter, more questions have been asked than answered. Further work is required to elucidate the links between the lipids of interest and coronary artery disease.

# CHAPTER 7 General Discussion

## 7.1 Significance and implications

The findings of this thesis have several implications ranging from basic research questions to clinical research. This is the first report of PT in humans and could revive interest in this neglected phospholipid. However, it remains unclear whether PT has distinct functions in animal tissues, or it is generated as a side product by PS synthase enzymes. PT may potentially function in coagulation and apoptosis owing to its structural similarity to PS and intracellular membrane trafficking due to its ability to bind calcium ions. The ability of PT to enhance prothrombinase activity but not extrinsic tenase activity could prompt research into the mechanism of its procoagulant properties. This could lead to a better understanding of the role of anionic phospholipids in mediating coagulation reactions.

The occurrence of PT in human tissues also raises questions about its metabolism and possible metabolic products, particularly lysophosphatidylthreonine (LysoPT) which has been shown to induce degranulation in murine mast cells (70, 71). LysoPT could exhibit a similar activity in humans. This study could also drive interest in other minor phospholipids that have been reported in the literature with no follow-up studies, such as phosphatidylaspartate and phosphatidylglutamate, which have been reported in mammalian brains (65).

Regarding the clinical implications, the higher PT levels in coronary artery disease (CAD) patients compared to healthy volunteers could stimulate research to understand the relation between the lipid and vascular disease. I found that PT levels were higher in both platelets and EV. In EVs, this was predominantly due to the higher numbers of EV in plasma. However, in platelets, the higher levels of PT per platelet number indicated enrichment of the phospholipid in platelet membranes. Here, I hypothesize that higher PT levels in platelets might result from an increased fraction of immature platelets in the circulation of CAD patients, which has been previously reported in the literature (46), and the higher PT levels in immature platelets could be due to their larger size and higher intracellular membranes (ER, mitochondria) content compared to mature platelets (45-49). This requires investigation of the lipidomics of mature and immature platelets, which could lead to a better understanding of the role of procoagulant lipids in CAD.

## 7.2 Limitations

There are some limitations in the work described in this thesis. In **Chapters 3 & 4**, PS and PT species were measured using head group MRM transitions (product ions resulting from loss of 87 or 101 Da from precursor ions). While the head group transition is highly selective for PT and confers high sensitivity to the assay, it does not allow annotation of the FA composition. As demonstrated by the $MS^3$ scans, some native PS and PT species comprised different compositions of FAs. In other words, some precursor ions were comprised of more than one molecular species of PT, with different FA compositions. Unfortunately, measuring PT using FA product ion transitions is hindered by interference from coeluting odd-chained PS species. For example, an MRM transition targeting the precursor ion of PT 36:1 and its product ion FA 18:1 will also detect PS 37:1 containing FA 17:0 and FA 18:1. Given the considerably higher abundance of PS to PT, rarer, odd chain FA containing species were seen to interfere with the $MS^2$ scans in **Chapter 3**, necessitating the use of $MS^3$ scans for the determination of FA compositions. Therefore, it would be better to first optimize the chromatography to fully resolve PS and PT, as then FA transitions could be used to measure isomeric species separately.

In **Chapters 4 & 6**, internal standards for PT/PS could not be added prior to lipid extraction and thus the samples could not be used for absolute PS/PT quantitation. This is because the cohort had been recruited for a previous study by another investigator, and the lipid extracts had already been prepared with different IS added. As such, absolute quantification of PT was not possible and relative quantification was employed instead, and I was unable to correct for extraction variations. However, despite this, I saw significant differences in PT and PS levels between the clinical cohort groups.

Throughout the thesis, lipids were extracted using acidified hexane isopropanol, which poorly recovers acidic lysoPLs. This hindered the detection of lysoPS and lysoPT due to the poor extraction efficiency. Instead, extraction methods that are suitable for acidic lysoPLs such as acidified Bligh and Dyer or methanol precipitation could be tested (131). Furthermore, platelet activation was achieved using one stimulus (agonist) and monitored at one timepoint. To better understand the metabolism of PS and PT in activated cells, several additional platelet activators (ADP, thrombin, and collagen) could be tested, measuring lysoPLs at several timepoints following activation, and in the presence and absence of specific phospholipase inhibitors. The

use of isoform-specific PLA inhibitors would assist in determining the isoforms responsible for the degradation of PT and PS during platelet activations, and activation with different ligands could reveal functional differences between PLA isoforms. Additionally, leukocytes were not isolated into individual cell populations prior to lipid extraction. Consequently, the PT profiles of individual leukocyte populations were not determined, and lipidomic differences between healthy volunteers and disease groups could be designated to specific leukocyte populations.

In **Chapter 5**, the coagulation assays involved the use of liposomes, which are simplified membranes comprising defined compositions of lipids. In contrast, biological membranes contain a large variety of lipids (classes, species) and proteins, with extensive glycosylation. Mimicking the lipid composition of biological membranes is unfeasible due to high costs or commercial unavailability of lipid standards. The difficulty is compounded when proteins are considered. Additionally, biological membranes comprise organized structures such as lipid rafts, exhibit asymmetry between leaflets, and form complex structures to support specific functions. For example, procoagulant lipids have been shown to concentrate in cap structures on platelets, which increases their local concentrations for binding of coagulation factors (37). This contrasts the homogenous distribution of lipids in spherical liposomes. As such, results from liposome experiments should be interpreted with caution, and future efforts should go into the development of more accurate models for biological membranes.

## 7.3 Future directions

### 7.3.1 Structural characterization of PT

Although several approaches were used for the structural characterization of PT in **Chapter 3**, there was no direct evidence for the location of the methyl functionality in the lipid's head group. Several approaches could be used to locate the methyl group in PT, including nuclear magnetic resonance, infrared spectroscopy, and alternative MS/MS fragmentation techniques such as ultraviolet photodissociation (UVPD). The former two options generally require pure samples in relatively high concentrations, and this is unfeasible for PT due to its low abundance *in vivo*. Therefore, the ideal approach would be UVPD MS. The experiment would involve electrospray ionization, quadrupole isolation of PT precursor ions, then fragmentation using UV lasers (193 nm or 213 nm), which fragment ions adjacent to double bonds and branching points (132-134). A collaboration with Professor Peter O'Connor (Warwick University) has been established to structurally characterize PT using UVPD ion cyclotron resonance MS.

### 7.3.2 Determining the enzymatic origin of PT

PT biosynthesis is proposed to be catalysed by PSS, but the isoform responsible is not known. The results in **Chapter 4** suggest that PSS1 synthesizes PT more efficiently compared to PSS2. However, this requires further confirmation. To address this question, it is recommended to overexpress and purify human PSS1 and PSS2 enzymes (e.g., using a mammalian protein expression system) then carry out activity assays *in vitro*. An alternate approach involves the generation of cell lines with PSS1 or PSS2 then testing their PT biosynthetic capability using stable isotope lipids and targeted lipidomics (63, 135, 136).

### 7.3.3 Characterising the metabolic products of PT

Activation of platelets with thrombin resulted in a decrease in PT, as demonstrated in **Chapters 4 & 6**. One possible PT metabolic product is lysoPT, which I propose is generated by phospholipases *in vivo*. One way to investigate this is to incubate activate platelets with thrombin then carry out lipid extractions (using an appropriate method for lysophospholipids) and MS analysis. Additionally, using specific inhibitors for $cPLA_2$ and $iPLA_2$ could help delineate the

specific enzymes involved in PT degradation. Primary targets for the study include cPLA$_2\alpha$ and iPLA$_2\gamma$ since they are found in platelets and play roles in activation (119, 137). Fortunately, specific inhibitors for both enzymes are available commercially (138, 139).

Another possible PT metabolic product is phosphatidylisopropanolamine, which is synthesized (inefficiently) by PS decarboxylase in mitochondria. This lipid has been detected in a hamster kidney cell line, but it is unknown if it is present in humans (63). Its detection in human tissues will present a challenge due to the low levels of PT combined with the low activity of PS decarboxylase with PT as a substrate. In addressing this question, it is recommended to use mitochondria-rich tissues such as heart and liver. However, acquisition of those tissues from humans will be challenging. Instead, preliminary experiments could be carried out on heart or liver cell lines using cell culture techniques or porcine tissues from an abattoir.

### 7.3.4 Investigating the interactions of PT with proteins

PT promotes coagulation *in vitro* through prothrombinase but not extrinsic tenase, as shown in **Chapter 5**. The mechanistic details behind this are unclear but could involve interactions between PT and Gla domains or C2 domains of proteins. This could be investigated using lipid nanodiscs and surface plasmon resonance, which allows for the determination of binding constants between lipids and proteins (12). A collaboration with Professor James Morrissey (University of Michigan) has been established to study the binding of PT to coagulation factors.

### 7.3.5 Characterising lipidomic differences between mature and immature platelets

In **Chapter 6**, the increased PT content of platelets from CAD patients (compared to healthy volunteers) was proposed to be potentially due to a higher fraction of immature platelets in the disease groups. To study this, platelets need to be fractionated based on their age. Immature platelets contain higher amounts of RNA, which is stainable with fluorescent RNA-binding dyes. This makes it possible to separate immature and mature platelets using flow cytometry as a preparative step for lipidomic analysis (140).

### 7.3.6 Investigating the potential function of PT in apoptosis and phagocytosis

This thesis focused primarily on the role of PT in blood coagulation. However, owing to its structural similarity to PS, PT could also be involved in apoptosis and phagocytosis. Specifically, PT on apoptotic cell surfaces (or pathogens) could be recognized by phagocytes for clearance. In support of this hypothesis, several parasitic bacteria and eukaryotes have evolved to synthesize PT, and deletion of PT synthase in *T. gondii* impairs virulence (67-69). Thus, the presence of PT in parasitic microorganisms could be a form of apoptotic mimicry in which the parasite imitates apoptotic cells to invade host cells. This indirectly suggests a function for endogenous PT in apoptotic cell recognition and engulfment.

In **Chapter 4**, I showed that PT is enriched in the inner plasma membrane leaflet of resting platelets and externalised upon thrombin activation. However, it is unknown whether PT is also externalised in response to apoptotic signals, and if so whether it is recognized by phagocytes for engulfment. These questions could be addressed using cell culture apoptosis models in combination with NHS-biotin derivatisation LC-MS/MS and macrophage uptake assays using PT liposomes.

## 7.4 Conclusion

The body of work presented in this thesis aimed to characterise PT in human blood cells and investigate its possible function in blood coagulation and its implication in coronary artery disease (CAD). Evidently, PT was detected in human whole blood, platelets, extracellular vesicles (EV), and leukocytes. The PT profiles of different cell types were distinct. In platelets, PT was enriched in the inner membranes but got externalised in response to thrombin. However, total platelet PT levels decreased following thrombin treatment. PT supported coagulation *in vitro* through enhancing prothrombinase activity but not extrinsic tenase activity. Additionally, PT was significantly higher in platelets and EVs from CAD patients compared to healthy volunteers. Collectively, the results demonstrate that PT is endogenous to human blood cells, possesses procoagulant properties, and could be involved in blood coagulation (*in vivo*) and the progression of coronary artery disease. However, many aspects of PT's biochemistry require further investigation, including its metabolism, the mechanistic details of its procoagulant properties, and its potential role in the pathophysiology of coronary heart disease.

# CHAPTER 8 References


1. Liebisch G, Fahy E, Aoki J, Dennis EA, Durand T, Ejsing CS, Fedorova M, Feussner I, Griffiths WJ, Kofeler H, Merrill AH, Jr., Murphy RC, O'Donnell VB, Oskolkova O, Subramaniam S, Wakelam MJO, Spener F. Update on LIPID MAPS classification, nomenclature, and shorthand notation for MS-derived lipid structures. J Lipid Res. 2020;61(12):1539-55. doi: 10.1194/jlr.S120001025
2. Chatgilialoglu C, Ferreri C, Melchiorre M, Sansone A, Torreggiani A. Lipid geometrical isomerism: from chemistry to biology and diagnostics. Chem Rev. 2014;114(1):255-84. doi: 10.1021/cr4002287
3. Daleke DL. Regulation of transbilayer plasma membrane phospholipid asymmetry. J Lipid Res. 2003;44(2):233-42. doi: 10.1194/jlr.R200019-JLR200
4. Sang Y, Roest M, de Laat B, de Groot PG, Huskens D. Interplay between platelets and coagulation. Blood Rev. 2021;46:100733. doi: 10.1016/j.blre.2020.100733
5. Li W. Eat-me signals: keys to molecular phagocyte biology and "appetite" control. J Cell Physiol. 2012;227(4):1291-7. doi: 10.1002/jcp.22815
6. Gailani D, Renne T. The intrinsic pathway of coagulation: a target for treating thromboembolic disease? J Thromb Haemost. 2007;5(6):1106-12. doi: 10.1111/j.1538-7836.2007.02446.x
7. Smith SA, Travers RJ, Morrissey JH. How it all starts: Initiation of the clotting cascade. Crit Rev Biochem Mol Biol. 2015;50(4):326-36. doi: 10.3109/10409238.2015.1050550
8. Grover SP, Mackman N. Intrinsic Pathway of Coagulation and Thrombosis. Arterioscler Thromb Vasc Biol. 2019;39(3):331-8. doi: 10.1161/ATVBAHA.118.312130
9. Ariens RA, Lai TS, Weisel JW, Greenberg CS, Grant PJ. Role of factor XIII in fibrin clot formation and effects of genetic polymorphisms. Blood. 2002;100(3):743-54. doi: 10.1182/blood.v100.3.743
10. Hoffman M. A cell-based model of coagulation and the role of factor VIIa. Blood Rev. 2003;17 Suppl 1:S1-5. doi: 10.1016/s0268-960x(03)90000-2
11. Smith SA. The cell-based model of coagulation. J Vet Emerg Crit Care (San Antonio). 2009;19(1):3-10. doi: 10.1111/j.1476-4431.2009.00389.x
12. Medfisch SM, Muehl EM, Morrissey JH, Bailey RC. Phosphatidylethanolamine-phosphatidylserine binding synergy of seven coagulation factors revealed using Nanodisc arrays on silicon photonic sensors. Sci Rep. 2020;10(1):17407. doi: 10.1038/s41598-020-73647-3
13. Vance JE. Phospholipid synthesis and transport in mammalian cells. Traffic. 2015;16(1):1-18. doi: 10.1111/tra.12230

14. Stone SJ, Vance JE. Phosphatidylserine synthase-1 and -2 are localized to mitochondria-associated membranes. J Biol Chem. 2000;275(44):34534-40. doi: 10.1074/jbc.M002865200
15. Sturbois-Balcerzak B, Stone SJ, Sreenivas A, Vance JE. Structure and expression of the murine phosphatidylserine synthase-1 gene. J Biol Chem. 2001;276(11):8205-12. doi: 10.1074/jbc.M009776200
16. Bergo MO, Gavino BJ, Steenbergen R, Sturbois B, Parlow AF, Sanan DA, Skarnes WC, Vance JE, Young SG. Defining the importance of phosphatidylserine synthase 2 in mice. J Biol Chem. 2002;277(49):47701-8. doi: 10.1074/jbc.M207734200
17. Eisenberg E, Levanon EY. Human housekeeping genes, revisited. Trends Genet. 2013;29(10):569-74. doi: 10.1016/j.tig.2013.05.010
18. Tomohiro S, Kawaguti A, Kawabe Y, Kitada S, Kuge O. Purification and characterization of human phosphatidylserine synthases 1 and 2. Biochem J. 2009;418(2):421-9. doi: 10.1042/BJ20081597
19. Kimura AK, Kim HY. Phosphatidylserine synthase 2: high efficiency for synthesizing phosphatidylserine containing docosahexaenoic acid. J Lipid Res. 2013;54(1):214-22. doi: 10.1194/jlr.M031989
20. Hovius R, Faber B, Brigot B, Nicolay K, de Kruijff B. On the mechanism of the mitochondrial decarboxylation of phosphatidylserine. J Biol Chem. 1992;267(24):16790-5.
21. Aoki J, Nagai Y, Hosono H, Inoue K, Arai H. Structure and function of phosphatidylserine-specific phospholipase A1. Biochim Biophys Acta. 2002;1582(1-3):26-32. doi: 10.1016/s1388-1981(02)00134-8
22. Nagai Y, Aoki J, Sato T, Amano K, Matsuda Y, Arai H, Inoue K. An alternative splicing form of phosphatidylserine-specific phospholipase A1 that exhibits lysophosphatidylserine-specific lysophospholipase activity in humans. J Biol Chem. 1999;274(16):11053-9. doi: 10.1074/jbc.274.16.11053
23. van der Meijden PEJ, Heemskerk JWM. Platelet biology and functions: new concepts and clinical perspectives. Nat Rev Cardiol. 2019;16(3):166-79. doi: 10.1038/s41569-018-0110-0
24. Ghoshal K, Bhattacharyya M. Overview of platelet physiology: its hemostatic and nonhemostatic role in disease pathogenesis. ScientificWorldJournal. 2014;2014:781857. doi: 10.1155/2014/781857
25. Kahn ML, Nakanishi-Matsui M, Shapiro MJ, Ishihara H, Coughlin SR. Protease-activated receptors 1 and 4 mediate activation of human platelets by thrombin. J Clin Invest. 1999;103(6):879-87. doi: 10.1172/JCI6042

26. Peng B, Geue S, Coman C, Munzer P, Kopczynski D, Has C, Hoffmann N, Manke MC, Lang F, Sickmann A, Gawaz M, Borst O, Ahrends R. Identification of key lipids critical for platelet activation by comprehensive analysis of the platelet lipidome. Blood. 2018;132(5):e1-e12. doi: 10.1182/blood-2017-12-822890
27. Suzuki J, Umeda M, Sims PJ, Nagata S. Calcium-dependent phospholipid scrambling by TMEM16F. Nature. 2010;468(7325):834-8. doi: 10.1038/nature09583
28. Sims PJ, Wiedmer T, Esmon CT, Weiss HJ, Shattil SJ. Assembly of the platelet prothrombinase complex is linked to vesiculation of the platelet plasma membrane. Studies in Scott syndrome: an isolated defect in platelet procoagulant activity. J Biol Chem. 1989;264(29):17049-57.
29. Ohkubo YZ, Tajkhorshid E. Distinct structural and adhesive roles of Ca2+ in membrane binding of blood coagulation factors. Structure. 2008;16(1):72-81. doi: 10.1016/j.str.2007.10.021
30. Tavoosi N, Davis-Harrison RL, Pogorelov TV, Ohkubo YZ, Arcario MJ, Clay MC, Rienstra CM, Tajkhorshid E, Morrissey JH. Molecular determinants of phospholipid synergy in blood clotting. J Biol Chem. 2011;286(26):23247-53. doi: 10.1074/jbc.M111.251769
31. Tavoosi N, Smith SA, Davis-Harrison RL, Morrissey JH. Factor VII and protein C are phosphatidic acid-binding proteins. Biochemistry. 2013;52(33):5545-52. doi: 10.1021/bi4006368
32. Falls LA, Furie BC, Jacobs M, Furie B, Rigby AC. The omega-loop region of the human prothrombin gamma-carboxyglutamic acid domain penetrates anionic phospholipid membranes. J Biol Chem. 2001;276(26):23895-902. doi: 10.1074/jbc.M008332200
33. Gilbert GE, Drinkwater D. Specific membrane binding of factor VIII is mediated by O-phospho-L-serine, a moiety of phosphatidylserine. Biochemistry. 1993;32(37):9577-85. doi: 10.1021/bi00088a009
34. Comfurius P, Smeets EF, Willems GM, Bevers EM, Zwaal RF. Assembly of the prothrombinase complex on lipid vesicles depends on the stereochemical configuration of the polar headgroup of phosphatidylserine. Biochemistry. 1994;33(34):10319-24. doi: 10.1021/bi00200a012
35. Hibbard LS, Mann KG. The calcium-binding properties of bovine factor V. J Biol Chem. 1980;255(2):638-45.
36. Macedo-Ribeiro S, Bode W, Huber R, Quinn-Allen MA, Kim SW, Ortel TL, Bourenkov GP, Bartunik HD, Stubbs MT, Kane WH, Fuentes-Prior P. Crystal structures of the membrane-binding C2 domain of human coagulation factor V. Nature. 1999;402(6760):434-9. doi: 10.1038/46594
37. Podoplelova NA, Sveshnikova AN, Kotova YN, Eckly A, Receveur N, Nechipurenko DY, Obydennyi SI, Kireev, II, Gachet C, Ataullakhanov FI, Mangin PH, Panteleev MA. Coagulation factors bound to

procoagulant platelets concentrate in cap structures to promote clotting. Blood. 2016;128(13):1745-55. doi: 10.1182/blood-2016-02-696898

38. Slatter DA, Percy CL, Allen-Redpath K, Gajsiewicz JM, Brooks NJ, Clayton A, Tyrrell VJ, Rosas M, Lauder SN, Watson A, Dul M, Garcia-Diaz Y, Aldrovandi M, Heurich M, Hall J, Morrissey JH, Lacroix-Desmazes S, Delignat S, Jenkins PV, Collins PW, O'Donnell VB. Enzymatically oxidized phospholipids restore thrombin generation in coagulation factor deficiencies. JCI Insight. 2018;3(6) doi: 10.1172/jci.insight.98459
39. Bernstein FC, Koetzle TF, Williams GJB, Meyer EF, Brice MD, Rodgers JR, Kennard O, Shimanouchi T, Tasumi M. The protein data bank: A computer-based archival file for macromolecular structures. Journal of Molecular Biology. 1977;112(3):535-42. doi: 10.1016/s0022-2836(77)80200-3
40. Steg PG, Bhatt DL, Wilson PW, D'Agostino R, Sr., Ohman EM, Rother J, Liau CS, Hirsch AT, Mas JL, Ikeda Y, Pencina MJ, Goto S, Investigators RR. One-year cardiovascular event rates in outpatients with atherothrombosis. JAMA. 2007;297(11):1197-206. doi: 10.1001/jama.297.11.1197
41. Ault KA, Cannon CP, Mitchell J, McCahan J, Tracy RP, Novotny WF, Reimann JD, Braunwald E. Platelet activation in patients after an acute coronary syndrome: results from the TIMI-12 trial. Thrombolysis in Myocardial Infarction. J Am Coll Cardiol. 1999;33(3):634-9. doi: 10.1016/s0735-1097(98)00635-4
42. Fuchs I, Frossard M, Spiel A, Riedmuller E, Laggner AN, Jilma B. Platelet function in patients with acute coronary syndrome (ACS) predicts recurrent ACS. J Thromb Haemost. 2006;4(12):2547-52. doi: 10.1111/j.1538-7836.2006.02239.x
43. Cesari F, Marcucci R, Caporale R, Paniccia R, Romano E, Gensini GF, Abbate R, Gori AM. Relationship between high platelet turnover and platelet function in high-risk patients with coronary artery disease on dual antiplatelet therapy. Thromb Haemost. 2008;99(11):930-5.
44. Larsen SB, Grove EL, Hvas AM, Kristensen SD. Platelet turnover in stable coronary artery disease - influence of thrombopoietin and low-grade inflammation. PLoS One. 2014;9(1):e85566. doi: 10.1371/journal.pone.0085566
45. Huang HL, Chen CH, Kung CT, Li YC, Sung PH, You HL, Lin YH, Huang WT. Clinical utility of mean platelet volume and immature platelet fraction in acute coronary syndrome. Biomed J. 2019;42(2):107-15. doi: 10.1016/j.bj.2018.12.005
46. Lakkis N, Dokainish H, Abuzahra M, Tsyboulev V, Jorgensen J, De Leon AP, Saleem A. Reticulated platelets in acute coronary syndrome: a marker of platelet activity. J Am Coll Cardiol. 2004;44(10):2091-3. doi: 10.1016/j.jacc.2004.05.033

47. Sansanayudh N, Anothaisintawee T, Muntham D, McEvoy M, Attia J, Thakkinstian A. Mean platelet volume and coronary artery disease: a systematic review and meta-analysis. Int J Cardiol. 2014;175(3):433-40. doi: 10.1016/j.ijcard.2014.06.028
48. Corpataux N, Franke K, Kille A, Valina CM, Neumann FJ, Nuhrenberg T, Hochholzer W. Reticulated Platelets in Medicine: Current Evidence and Further Perspectives. J Clin Med. 2020;9(11):3737. doi: 10.3390/jcm9113737
49. Hille L, Lenz M, Vlachos A, Gruning B, Hein L, Neumann FJ, Nuhrenberg TG, Trenk D. Ultrastructural, transcriptional, and functional differences between human reticulated and non-reticulated platelets. J Thromb Haemost. 2020;18(8):2034-46. doi: 10.1111/jth.14895
50. Hamad MA, Schanze N, Schommer N, Nuhrenberg T, Duerschmied D. Reticulated Platelets-Which Functions Have Been Established by In Vivo and In Vitro Data? Cells. 2021;10(5):1172. doi: 10.3390/cells10051172
51. Berckmans RJ, Nieuwland R, Boing AN, Romijn FP, Hack CE, Sturk A. Cell-derived microparticles circulate in healthy humans and support low grade thrombin generation. Thromb Haemost. 2001;85(4):639-46.
52. Nielsen T, Kristensen AF, Pedersen S, Christiansen G, Kristensen SR. Investigation of procoagulant activity in extracellular vesicles isolated by differential ultracentrifugation. J Extracell Vesicles. 2018;7(1):1454777. doi: 10.1080/20013078.2018.1454777
53. Liu Y, He Z, Zhang Y, Dong Z, Bi Y, Kou J, Zhou J, Shi J. Dissimilarity of increased phosphatidylserine-positive microparticles and associated coagulation activation in acute coronary syndromes. Coron Artery Dis. 2016;27(5):365-75. doi: 10.1097/MCA.0000000000000368
54. Protty MB. Characterising the role of inflammatory procoagulant phospholipids in arterial thrombosis. [PhD Thesis].Cardiff University; 2021.
55. Rhodes DN, Lea CH. Phospholipids. IV. On the composition of hen's egg phospholipids. Biochem J. 1957;65(3):526-33. doi: 10.1042/bj0650526
56. Igarashi H, Zama K, Katada M. Presence of a threonine-containing phospholipid in tunny muscle. Nature. 1958;181(4618):1282-3. doi: 10.1038/1811282a0
57. Baer E, Eckstein F. Phosphatidylthreonines. I. Synthesis of distearoyl-L-alpha-glycerylphosphoryl-L-threonine. J Biol Chem. 1962;237(5):1449-53.
58. Porcellati G, di Jeso F, Malcovati M. The conversion of L-serine ethanolamine phosphate and L-threonine ethanolamine phosphate to microsomal phospholipid in brain tissue. Life Sciences. 1966;5(9):769-74. doi: 10.1016/0024-3205(66)90299-2

59. Mark-Malchoff D, Marinetti GV, Hare JD, Meisler A. Elevation of a threonine phospholipid in polyoma virus transformed hamster embryo fibroblasts. Biochem Biophys Res Commun. 1977;75(3):589-97. doi: 10.1016/0006-291x(77)91513-3
60. Mark-Malchoff D, Marinetti GV, Hare GD, Meisler A. Characterization of phosphatidylthreonine in polyoma virus transformed fibroblasts. Biochemistry. 1978;17(13):2684-8. doi: 10.1021/bi00606a035
61. Mitoma J, Kasama T, Furuya S, Hirabayashi Y. Occurrence of an unusual phospholipid, phosphatidyl-L-threonine, in cultured hippocampal neurons. Exogenous L-serine is required for the synthesis of neuronal phosphatidyl-L-serine and sphingolipids. J Biol Chem. 1998;273(31):19363-6. doi: 10.1074/jbc.273.31.19363
62. Mitoma J, Furuya S, Hirabayashi Y. A novel metabolic communication between neurons and astrocytes: non-essential amino acid L-serine released from astrocytes is essential for developing hippocampal neurons. Neurosci Res. 1998;30(2):195-9. doi: 10.1016/s0168-0102(97)00113-2
63. Heikinheimo L, Somerharju P. Translocation of phosphatidylthreonine and -serine to mitochondria diminishes exponentially with increasing molecular hydrophobicity. Traffic. 2002;3(5):367-77. doi: 10.1034/j.1600-0854.2002.30506.x
64. Ivanova PT, Milne SB, Brown HA. Identification of atypical ether-linked glycerophospholipid species in macrophages by mass spectrometry. J Lipid Res. 2010;51(6):1581-90. doi: 10.1194/jlr.D003715
65. Omori T, Honda A, Mihara H, Kurihara T, Esaki N. Identification of novel mammalian phospholipids containing threonine, aspartate, and glutamate as the base moiety. J Chromatogr B Analyt Technol Biomed Life Sci. 2011;879(29):3296-302. doi: 10.1016/j.jchromb.2011.04.033
66. Muller FD, Beck S, Strauch E, Linscheid MW. Bacterial predators possess unique membrane lipid structures. Lipids. 2011;46(12):1129-40. doi: 10.1007/s11745-011-3614-5
67. Arroyo-Olarte RD, Brouwers JF, Kuchipudi A, Helms JB, Biswas A, Dunay IR, Lucius R, Gupta N. Phosphatidylthreonine and Lipid-Mediated Control of Parasite Virulence. PLoS Biol. 2015;13(11):e1002288. doi: 10.1371/journal.pbio.1002288
68. Kong P, Lehmann MJ, Helms JB, Brouwers JF, Gupta N. Lipid analysis of Eimeria sporozoites reveals exclusive phospholipids, a phylogenetic mosaic of endogenous synthesis, and a host-independent lifestyle. Cell Discov. 2018;4(1):24. doi: 10.1038/s41421-018-0023-4
69. Kuchipudi A, Arroyo-Olarte RD, Hoffmann F, Brinkmann V, Gupta N. Optogenetic monitoring identifies phosphatidylthreonine-regulated calcium homeostasis in Toxoplasma gondii. Microb Cell. 2016;3(5):215-23. doi: 10.15698/mic2016.05.500

70. Iwashita M, Makide K, Nonomura T, Misumi Y, Otani Y, Ishida M, Taguchi R, Tsujimoto M, Aoki J, Arai H, Ohwada T. Synthesis and evaluation of lysophosphatidylserine analogues as inducers of mast cell degranulation. Potent activities of lysophosphatidylthreonine and its 2-deoxy derivative. J Med Chem. 2009;52(19):5837-63. doi: 10.1021/jm900598m
71. Kishi T, Kawana H, Sayama M, Makide K, Inoue A, Otani Y, Ohwada T, Aoki J. Identification of lysophosphatidylthreonine with an aromatic fatty acid surrogate as a potent inducer of mast cell degranulation. Biochem Biophys Rep. 2016;8:346-51. doi: 10.1016/j.bbrep.2016.09.013
72. Damnjanović J, Matsunaga N, Adachi M, Nakano H, Iwasaki Y. Facile Enzymatic Synthesis of Phosphatidylthreonine Using an Engineered Phospholipase D. European Journal of Lipid Science and Technology. 2018;120(6):1800089. doi: 10.1002/ejlt.201800089
73. Pulfer M, Murphy RC. Electrospray mass spectrometry of phospholipids. Mass Spectrom Rev. 2003;22(5):332-64. doi: 10.1002/mas.10061
74. Ho CS, Lam CW, Chan MH, Cheung RC, Law LK, Lit LC, Ng KF, Suen MW, Tai HL. Electrospray ionisation mass spectrometry: principles and clinical applications. Clin Biochem Rev. 2003;24(1):3-12.
75. Yost RA, Enke CG. Selected ion fragmentation with a tandem quadrupole mass spectrometer. Journal of the American Chemical Society. 1978;100(7):2274-5. doi: 10.1021/ja00475a072
76. Thomas CP, Clark SR, Hammond VJ, Aldrovandi M, Collins PW, O'Donnell VB. Identification and quantification of aminophospholipid molecular species on the surface of apoptotic and activated cells. Nat Protoc. 2014;9(1):51-63. doi: 10.1038/nprot.2013.163
77. Pluckthun A, Dennis EA. Acyl and phosphoryl migration in lysophospholipids: importance in phospholipid synthesis and phospholipase specificity. Biochemistry. 1982;21(8):1743-50. doi: 10.1021/bi00537a007
78. Kielbowicz G, Smuga D, Gladkowski W, Chojnacka A, Wawrzenczyk C. An LC method for the analysis of phosphatidylcholine hydrolysis products and its application to the monitoring of the acyl migration process. Talanta. 2012;94:22-9. doi: 10.1016/j.talanta.2012.01.018
79. Prinsen H, Schiebergen-Bronkhorst BGM, Roeleveld MW, Jans JJM, de Sain-van der Velden MGM, Visser G, van Hasselt PM, Verhoeven-Duif NM. Rapid quantification of underivatized amino acids in plasma by hydrophilic interaction liquid chromatography (HILIC) coupled with tandem mass-spectrometry. J Inherit Metab Dis. 2016;39(5):651-60. doi: 10.1007/s10545-016-9935-z

80. Xu M, Legradi J, Leonards P. Evaluation of LC-MS and LCxLC-MS in analysis of zebrafish embryo samples for comprehensive lipid profiling. Anal Bioanal Chem. 2020;412(18):4313-25. doi: 10.1007/s00216-020-02661-1
81. Zhao H, Hamase K, Morikawa A, Qiu Z, Zaitsu K. Determination of d- and l-enantiomers of threonine and allo-threonine in mammals using two-step high-performance liquid chromatography. J Chromatogr B Analyt Technol Biomed Life Sci. 2004;810(2):245-50. doi: 10.1016/j.jchromb.2004.08.006
82. Valentine WJ, Yanagida K, Kawana H, Kono N, Noda NN, Aoki J, Shindou H. Update and nomenclature proposal for mammalian lysophospholipid acyltransferases, which create membrane phospholipid diversity. J Biol Chem. 2022;298(1):101470. doi: 10.1016/j.jbc.2021.101470
83. Wiesner P, Leidl K, Boettcher A, Schmitz G, Liebisch G. Lipid profiling of FPLC-separated lipoprotein fractions by electrospray ionization tandem mass spectrometry. J Lipid Res. 2009;50(3):574-85. doi: 10.1194/jlr.D800028-JLR200
84. Dashti M, Kulik W, Hoek F, Veerman EC, Peppelenbosch MP, Rezaee F. A phospholipidomic analysis of all defined human plasma lipoproteins. Sci Rep. 2011;1(1):139. doi: 10.1038/srep00139
85. Christinat N, Masoodi M. Comprehensive Lipoprotein Characterization Using Lipidomics Analysis of Human Plasma. J Proteome Res. 2017;16(8):2947-53. doi: 10.1021/acs.jproteome.7b00236
86. Leidl K, Liebisch G, Richter D, Schmitz G. Mass spectrometric analysis of lipid species of human circulating blood cells. Biochim Biophys Acta. 2008;1781(10):655-64. doi: 10.1016/j.bbalip.2008.07.008
87. van Engeland M, Nieland LJ, Ramaekers FC, Schutte B, Reutelingsperger CP. Annexin V-affinity assay: a review on an apoptosis detection system based on phosphatidylserine exposure. Cytometry. 1998;31(1):1-9. doi: 10.1002/(sici)1097-0320(19980101)31:1<1::aid-cyto1>3.0.co;2-r
88. Clark SR, Thomas CP, Hammond VJ, Aldrovandi M, Wilkinson GW, Hart KW, Murphy RC, Collins PW, O'Donnell VB. Characterization of platelet aminophospholipid externalization reveals fatty acids as molecular determinants that regulate coagulation. Proc Natl Acad Sci U S A. 2013;110(15):5875-80. doi: 10.1073/pnas.1222419110
89. Skeaff CM, Holub BJ. Altered phospholipid composition of plasma membranes from thrombin-stimulated human platelets. Biochimica et Biophysica Acta (BBA) - Lipids and Lipid Metabolism. 1985;834(2):164-71. doi: 10.1016/0005-2760(85)90152-3
90. Thomas CP, Morgan LT, Maskrey BH, Murphy RC, Kuhn H, Hazen SL, Goodall AH, Hamali HA, Collins PW, O'Donnell VB. Phospholipid-esterified eicosanoids are generated in agonist-activated human

platelets and enhance tissue factor-dependent thrombin generation. J Biol Chem. 2010;285(10):6891-903. doi: 10.1074/jbc.M109.078428

91. Lewis N, Majerus PW. Lipid metabolism in human platelets. II. De novo phospholipid synthesis and the effect of thrombin on the pattern of synthesis. J Clin Invest. 1969;48(11):2114-23. doi: 10.1172/JCI106178

92. Thomas LM, Holub BJ. Eicosanoid-dependent and -independent formation of individual [14C]stearoyl-labelled lysophospholipids in collagen-stimulated human platelets. Biochim Biophys Acta. 1991;1081(1):92-8. doi: 10.1016/0005-2760(91)90255-g

93. Omi J, Kano K, Aoki J. Current Knowledge on the Biology of Lysophosphatidylserine as an Emerging Bioactive Lipid. Cell Biochem Biophys. 2021;79(3):497-508. doi: 10.1007/s12013-021-00988-9

94. Shanbhag K, Mhetre A, Khandelwal N, Kamat SS. The Lysophosphatidylserines-An Emerging Class of Signalling Lysophospholipids. J Membr Biol. 2020;253(5):381-97. doi: 10.1007/s00232-020-00133-2

95. Heijnen HF, Schiel AE, Fijnheer R, Geuze HJ, Sixma JJ. Activated platelets release two types of membrane vesicles: microvesicles by surface shedding and exosomes derived from exocytosis of multivesicular bodies and alpha-granules. Blood. 1999;94(11):3791-9. doi: 10.1182/blood.V94.11.3791

96. Sinn CG, Antonietti M, Dimova R. Binding of calcium to phosphatidylcholine–phosphatidylserine membranes. Colloids and Surfaces A: Physicochemical and Engineering Aspects. 2006;282-283:410-9. doi: 10.1016/j.colsurfa.2005.10.014

97. Martin-Molina A, Rodriguez-Beas C, Faraudo J. Effect of calcium and magnesium on phosphatidylserine membranes: experiments and all-atomic simulations. Biophys J. 2012;102(9):2095-103. doi: 10.1016/j.bpj.2012.03.009

98. Hemker HC, Giesen P, AlDieri R, Regnault V, de Smed E, Wagenvoord R, Lecompte T, Beguin S. The calibrated automated thrombogram (CAT): a universal routine test for hyper- and hypocoagulability. Pathophysiol Haemost Thromb. 2002;32(5-6):249-53. doi: 10.1159/000073575

99. Hansson KM, Nielsen S, Elg M, Deinum J. The effect of corn trypsin inhibitor and inhibiting antibodies for FXIa and FXIIa on coagulation of plasma and whole blood. J Thromb Haemost. 2014;12(10):1678-86. doi: 10.1111/jth.12707

100. Tsui FC, Ojcius DM, Hubbell WL. The intrinsic pKa values for phosphatidylserine and phosphatidylethanolamine in phosphatidylcholine host bilayers. Biophys J. 1986;49(2):459-68. doi: 10.1016/S0006-3495(86)83655-4

101. Yegneswaran S, Fernandez JA, Griffin JH, Dawson PE. Factor Va increases the affinity of factor Xa for prothrombin: a binding study using a novel photoactivable thiol-specific fluorescent probe. Chem Biol. 2002;9(4):485-94. doi: 10.1016/s1074-5521(02)00132-1

102. Pryzdial EL, Mann KG. The association of coagulation factor Xa and factor Va. J Biol Chem. 1991;266(14):8969-77.

103. Koklic T, Majumder R, Lentz BR. Ca2+ switches the effect of PS-containing membranes on Factor Xa from activating to inhibiting: implications for initiation of blood coagulation. Biochem J. 2014;462(3):591-601. doi: 10.1042/BJ20140130

104. Koklic T, Chattopadhyay R, Majumder R, Lentz BR. Factor Xa dimerization competes with prothrombinase complex formation on platelet-like membrane surfaces. Biochem J. 2015;467(1):37-46. doi: 10.1042/BJ20141177

105. Jafri L, Khan AH, Azeem S. Ionized calcium measurement in serum and plasma by ion selective electrodes: comparison of measured and calculated parameters. Indian J Clin Biochem. 2014;29(3):327-32. doi: 10.1007/s12291-013-0360-x

106. Falls LA, Furie B, Furie BC. Role of phosphatidylethanolamine in assembly and function of the factor IXa-factor VIIIa complex on membrane surfaces. Biochemistry. 2000;39(43):13216-22. doi: 10.1021/bi0009789

107. Papahadjopoulos D, Hanahan DJ. Observations on the Interaction of Phospholipids and Certain Clotting Factors in Prothrombin Activator Formation. Biochim Biophys Acta. 1964;90(2):436-9. doi: 10.1016/0304-4165(64)90220-x

108. Bom VJ, Bertina RM. The contributions of Ca2+, phospholipids and tissue-factor apoprotein to the activation of human blood-coagulation factor X by activated factor VII. Biochem J. 1990;265(2):327-36. doi: 10.1042/bj2650327

109. McCallum CD, Hapak RC, Neuenschwander PF, Morrissey JH, Johnson AE. The location of the active site of blood coagulation factor VIIa above the membrane surface and its reorientation upon association with tissue factor. A fluorescence energy transfer study. J Biol Chem. 1996;271(45):28168-75. doi: 10.1074/jbc.271.45.28168

110. Grover SP, Mackman N. Tissue Factor: An Essential Mediator of Hemostasis and Trigger of Thrombosis. Arterioscler Thromb Vasc Biol. 2018;38(4):709-25. doi: 10.1161/ATVBAHA.117.309846

111. Ohkubo YZ, Morrissey JH, Tajkhorshid E. Dynamical view of membrane binding and complex formation of human factor VIIa and tissue factor. J Thromb Haemost. 2010;8(5):1044-53. doi: 10.1111/j.1538-7836.2010.03826.x

112. Nelsestuen GL, Kisiel W, Di Scipio RG. Interaction of vitamin K dependent proteins with membranes. Biochemistry. 1978;17(11):2134-8. doi: 10.1021/bi00604a017
113. Karpatkin S. Heterogeneity of human platelets. II. Functional evidence suggestive of young and old platelets. J Clin Invest. 1969;48(6):1083-7. doi: 10.1172/JCI106064
114. Thompson CB, Jakubowski JA, Quinn PG, Deykin D, Valeri CR. Platelet size as a determinant of platelet function. J Lab Clin Med. 1983;101(2):205-13.
115. Clancy L, Beaulieu LM, Tanriverdi K, Freedman JE. The role of RNA uptake in platelet heterogeneity. Thromb Haemost. 2017;117(5):948-61. doi: 10.1160/TH16-11-0873
116. van der Meijden PE, Feijge MA, Giesen PL, Huijberts M, van Raak LP, Heemskerk JW. Platelet P2Y12 receptors enhance signalling towards procoagulant activity and thrombin generation. A study with healthy subjects and patients at thrombotic risk. Thromb Haemost. 2005;93(6):1128-36. doi: 10.1160/TH04-09-0597
117. Clark JD, Lin LL, Kriz RW, Ramesha CS, Sultzman LA, Lin AY, Milona N, Knopf JL. A novel arachidonic acid-selective cytosolic PLA2 contains a Ca(2+)-dependent translocation domain with homology to PKC and GAP. Cell. 1991;65(6):1043-51. doi: 10.1016/0092-8674(91)90556-e
118. Strokin M, Sergeeva M, Reiser G. Docosahexaenoic acid and arachidonic acid release in rat brain astrocytes is mediated by two separate isoforms of phospholipase A2 and is differently regulated by cyclic AMP and Ca2+. Br J Pharmacol. 2003;139(5):1014-22. doi: 10.1038/sj.bjp.0705326
119. Yoda E, Rai K, Ogawa M, Takakura Y, Kuwata H, Suzuki H, Nakatani Y, Murakami M, Hara S. Group VIB calcium-independent phospholipase A2 (iPLA2gamma) regulates platelet activation, hemostasis and thrombosis in mice. PLoS One. 2014;9(10):e109409. doi: 10.1371/journal.pone.0109409
120. Morgan LT, Thomas CP, Kuhn H, O'Donnell VB. Thrombin-activated human platelets acutely generate oxidized docosahexaenoic-acid-containing phospholipids via 12-lipoxygenase. Biochem J. 2010;431(1):141-8. doi: 10.1042/BJ20100415
121. Nunez D, Randon J, Gandhi C, Siafaka-Kapadai A, Olson MS, Hanahan DJ. The inhibition of platelet-activating factor-induced platelet activation by oleic acid is associated with a decrease in polyphosphoinositide metabolism. J Biol Chem. 1990;265(30):18330-8.
122. Kimoto M, Javors MA, Ekholm J, Siafaka-Kapadai A, Hanahan DJ. Dual effects of oleic acid on Ca2+ mobilization and protein phosphorylation in human platelets in presence or absence of platelet activating factor. Arch Biochem Biophys. 1992;298(2):471-9. doi: 10.1016/0003-9861(92)90437-2
123. Smal MA, Baldo BA. Inhibition of platelet-activating factor (PAF)-induced platelet aggregation by fatty acids from human saliva. Platelets. 2021:1-8. doi: 10.1080/09537104.2021.1961705

124. Hwang SM, Kim HJ, Kim SM, Jung Y, Park SW, Chung IY. Lysophosphatidylserine receptor P2Y10: A G protein-coupled receptor that mediates eosinophil degranulation. Clin Exp Allergy. 2018;48(8):990-9. doi: 10.1111/cea.13162

125. Okudaira M, Inoue A, Shuto A, Nakanaga K, Kano K, Makide K, Saigusa D, Tomioka Y, Aoki J. Separation and quantification of 2-acyl-1-lysophospholipids and 1-acyl-2-lysophospholipids in biological samples by LC-MS/MS. J Lipid Res. 2014;55(10):2178-92. doi: 10.1194/jlr.D048439

126. Wang L, Bi Y, Cao M, Ma R, Wu X, Zhang Y, Ding W, Liu Y, Yu Q, Zhang Y, Jiang H, Sun Y, Tong D, Guo L, Dong Z, Tian Y, Kou J, Shi J. Microparticles and blood cells induce procoagulant activity via phosphatidylserine exposure in NSTEMI patients following stent implantation. Int J Cardiol. 2016;223:121-8. doi: 10.1016/j.ijcard.2016.07.260

127. Gasecka A, Rogula S, Eyileten C, Postula M, Jaguszewski MJ, Kochman J, Mazurek T, Nieuwland R, Filipiak KJ. Role of P2Y Receptors in Platelet Extracellular Vesicle Release. Int J Mol Sci. 2020;21(17):6065. doi: 10.3390/ijms21176065

128. Clark SR, Guy CJ, Scurr MJ, Taylor PR, Kift-Morgan AP, Hammond VJ, Thomas CP, Coles B, Roberts GW, Eberl M, Jones SA, Topley N, Kotecha S, O'Donnell VB. Esterified eicosanoids are acutely generated by 5-lipoxygenase in primary human neutrophils and in human and murine infection. Blood. 2011;117(6):2033-43. doi: 10.1182/blood-2010-04-278887

129. Archambault AS, Turcotte C, Martin C, Provost V, Larose MC, Laprise C, Chakir J, Bissonnette E, Laviolette M, Bosse Y, Flamand N. Comparison of eight 15-lipoxygenase (LO) inhibitors on the biosynthesis of 15-LO metabolites by human neutrophils and eosinophils. PLoS One. 2018;13(8):e0202424. doi: 10.1371/journal.pone.0202424

130. Snodgrass RG, Brune B. Regulation and Functions of 15-Lipoxygenases in Human Macrophages. Front Pharmacol. 2019;10:719. doi: 10.3389/fphar.2019.00719

131. Zhao Z, Xu Y. An extremely simple method for extraction of lysophospholipids and phospholipids from blood samples. J Lipid Res. 2010;51(3):652-9. doi: 10.1194/jlr.D001503

132. Williams PE, Klein DR, Greer SM, Brodbelt JS. Pinpointing Double Bond and sn-Positions in Glycerophospholipids via Hybrid 193 nm Ultraviolet Photodissociation (UVPD) Mass Spectrometry. J Am Chem Soc. 2017;139(44):15681-90. doi: 10.1021/jacs.7b06416

133. Blevins MS, Klein DR, Brodbelt JS. Localization of Cyclopropane Modifications in Bacterial Lipids via 213 nm Ultraviolet Photodissociation Mass Spectrometry. Anal Chem. 2019;91(10):6820-8. doi: 10.1021/acs.analchem.9b01038

134. Klein DR, Blevins MS, Macias LA, Douglass MV, Trent MS, Brodbelt JS. Localization of Double Bonds in Bacterial Glycerophospholipids Using 193 nm Ultraviolet Photodissociation in the Negative Mode. Anal Chem. 2020;92(8):5986-93. doi: 10.1021/acs.analchem.0c00221

135. Qi J, Lang W, Geisler JG, Wang P, Petrounia I, Mai S, Smith C, Askari H, Struble GT, Williams R, Bhanot S, Monia BP, Bayoumy S, Grant E, Caldwell GW, Todd MJ, Liang Y, Gaul MD, Demarest KT, Connelly MA. The use of stable isotope-labeled glycerol and oleic acid to differentiate the hepatic functions of DGAT1 and -2. J Lipid Res. 2012;53(6):1106-16. doi: 10.1194/jlr.M020156

136. Dushianthan A, Cusack R, Grocott MPW, Postle AD. Abnormal liver phosphatidylcholine synthesis revealed in patients with acute respiratory distress syndrome. J Lipid Res. 2018;59(6):1034-45. doi: 10.1194/jlr.P085050

137. Wong DA, Kita Y, Uozumi N, Shimizu T. Discrete role for cytosolic phospholipase A(2)alpha in platelets: studies using single and double mutant mice of cytosolic and group IIA secretory phospholipase A(2). J Exp Med. 2002;196(3):349-57. doi: 10.1084/jem.20011443

138. Seno K, Okuno T, Nishi K, Murakami Y, Watanabe F, Matsuura T, Wada M, Fujii Y, Yamada M, Ogawa T, Okada T, Hashizume H, Kii M, Hara S, Hagishita S, Nakamoto S, Yamada K, Chikazawa Y, Ueno M, Teshirogi I, Ono T, Ohtani M. Pyrrolidine inhibitors of human cytosolic phospholipase A(2). J Med Chem. 2000;43(6):1041-4. doi: 10.1021/jm9905155

139. Jenkins CM, Han X, Mancuso DJ, Gross RW. Identification of calcium-independent phospholipase A2 (iPLA2) beta, and not iPLA2gamma, as the mediator of arginine vasopressin-induced arachidonic acid release in A-10 smooth muscle cells. Enantioselective mechanism-based discrimination of mammalian iPLA2s. J Biol Chem. 2002;277(36):32807-14. doi: 10.1074/jbc.M202568200

140. Ferreira FLB, Colella MP, Medina SS, Costa-Lima C, Fiusa MML, Costa LNG, Orsi FA, Annichino-Bizzacchi JM, Fertrin KY, Gilberti MFP, Ozelo MC, De Paula EV. Evaluation of the immature platelet fraction contribute to the differential diagnosis of hereditary, immune and other acquired thrombocytopenias. Sci Rep. 2017;7(1):3355. doi: 10.1038/s41598-017-03668-y

# CHAPTER 9 Appendices

## 9.1 Calibration curves for amino acids

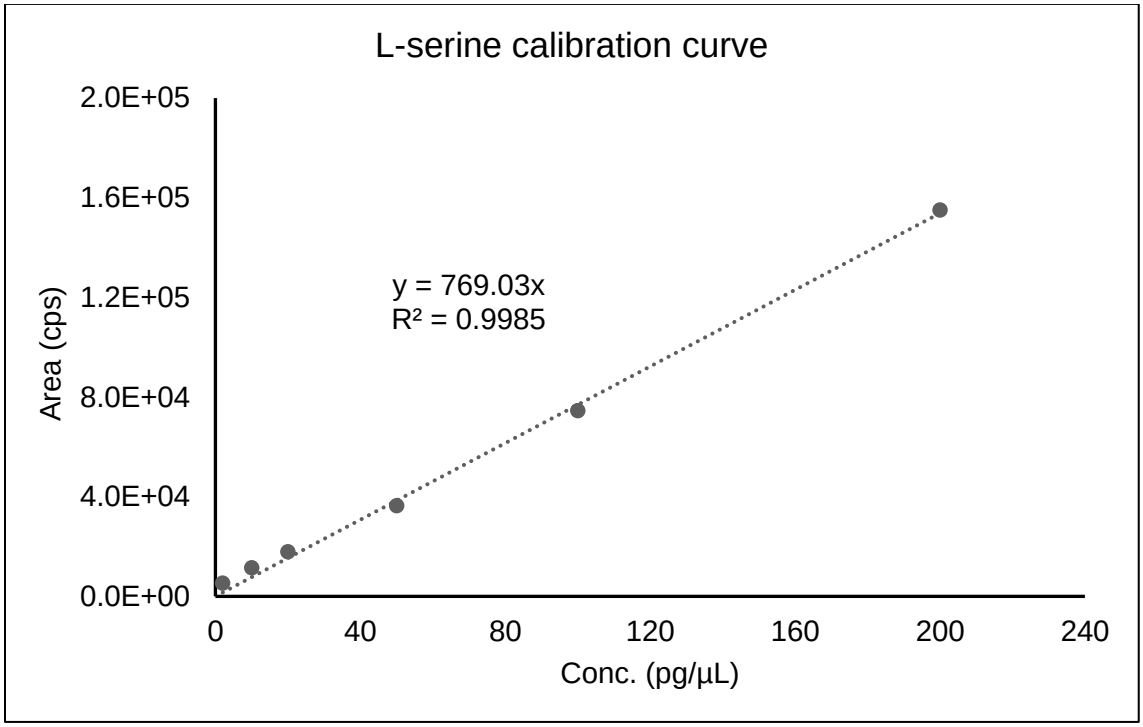


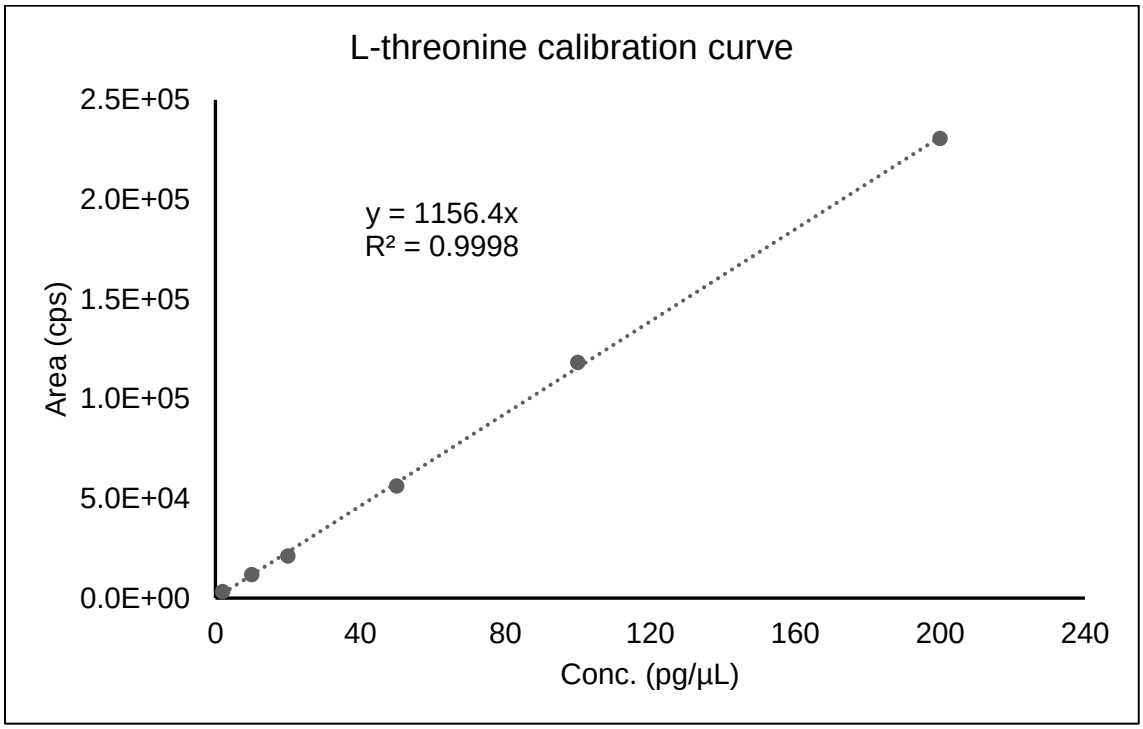

9.2 Calibration curves for phospholipids

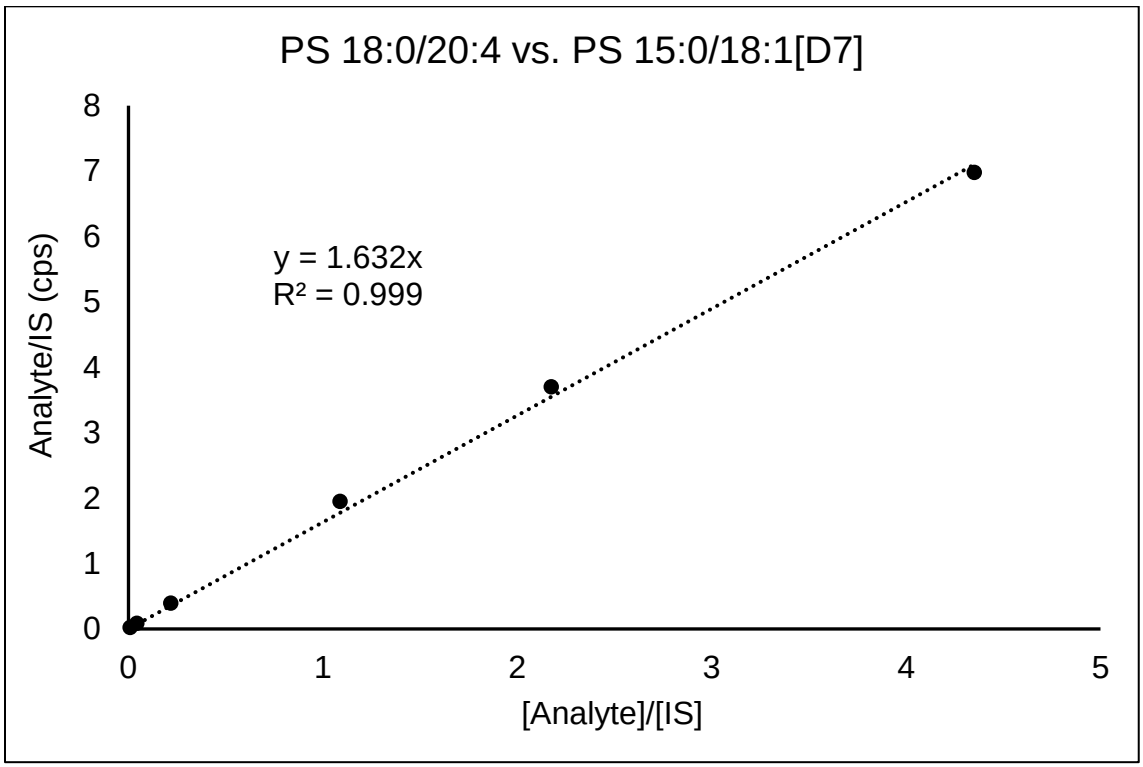


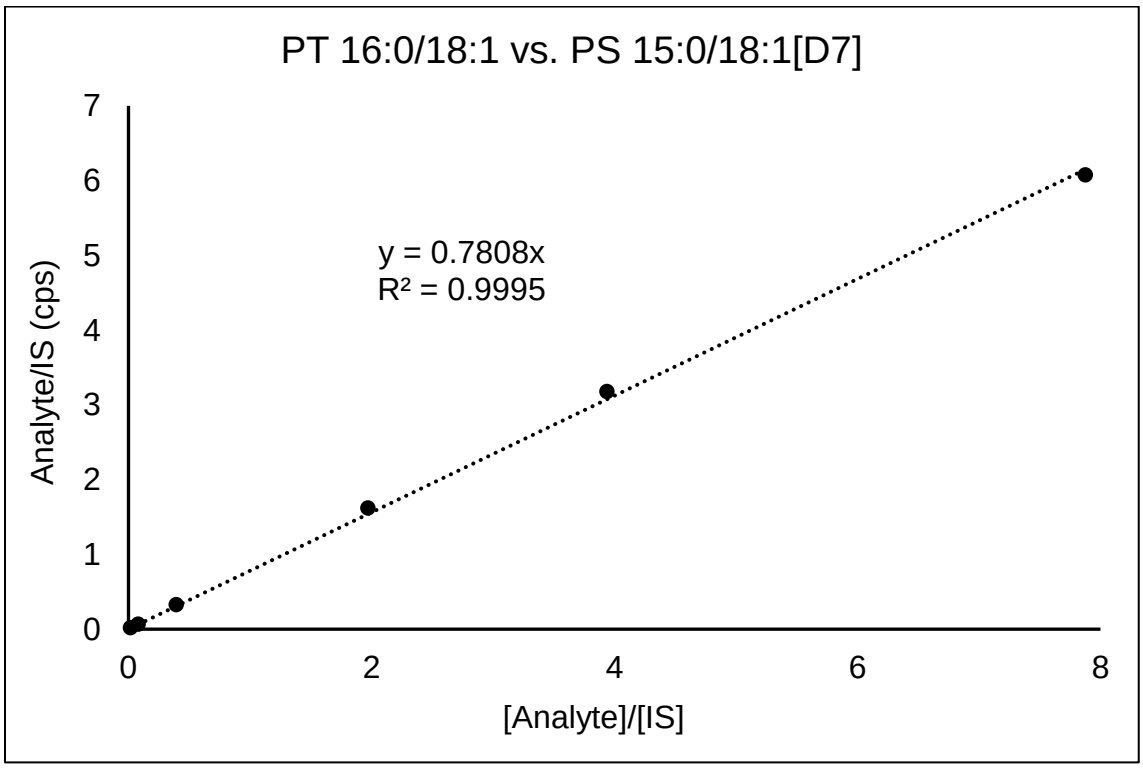

## 9.3 Representative chromatograms (HILIC-LC-MS/MS of amino acids)

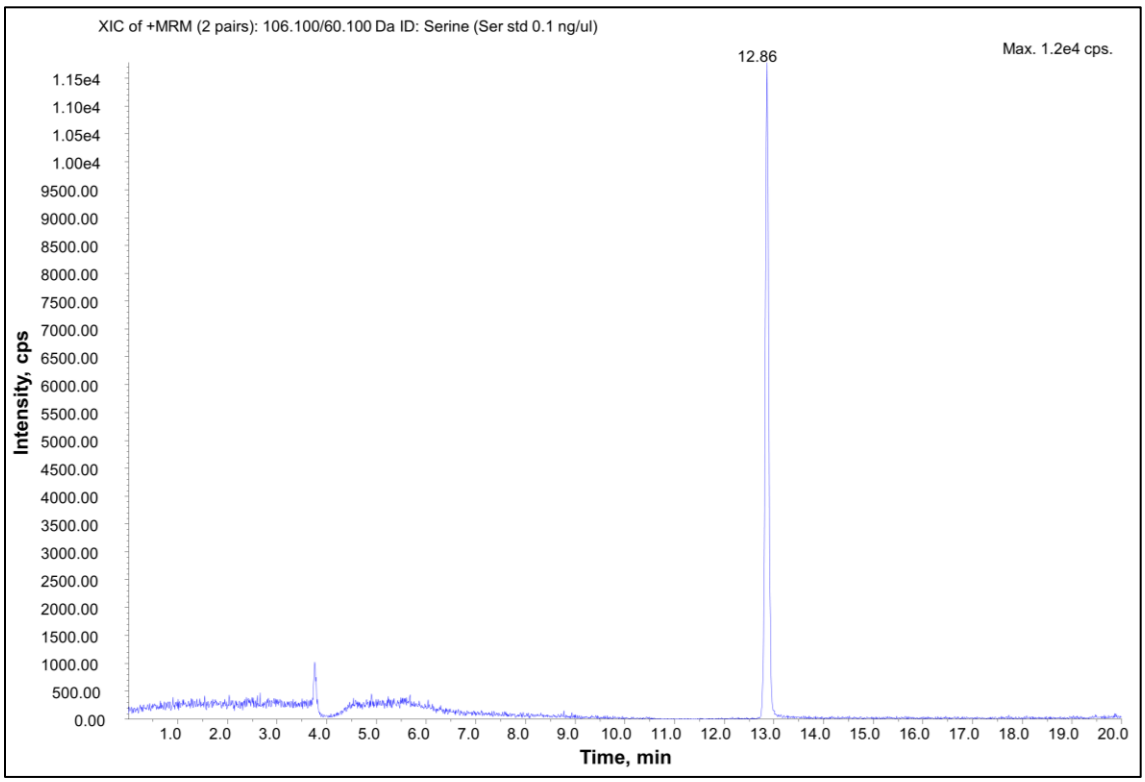


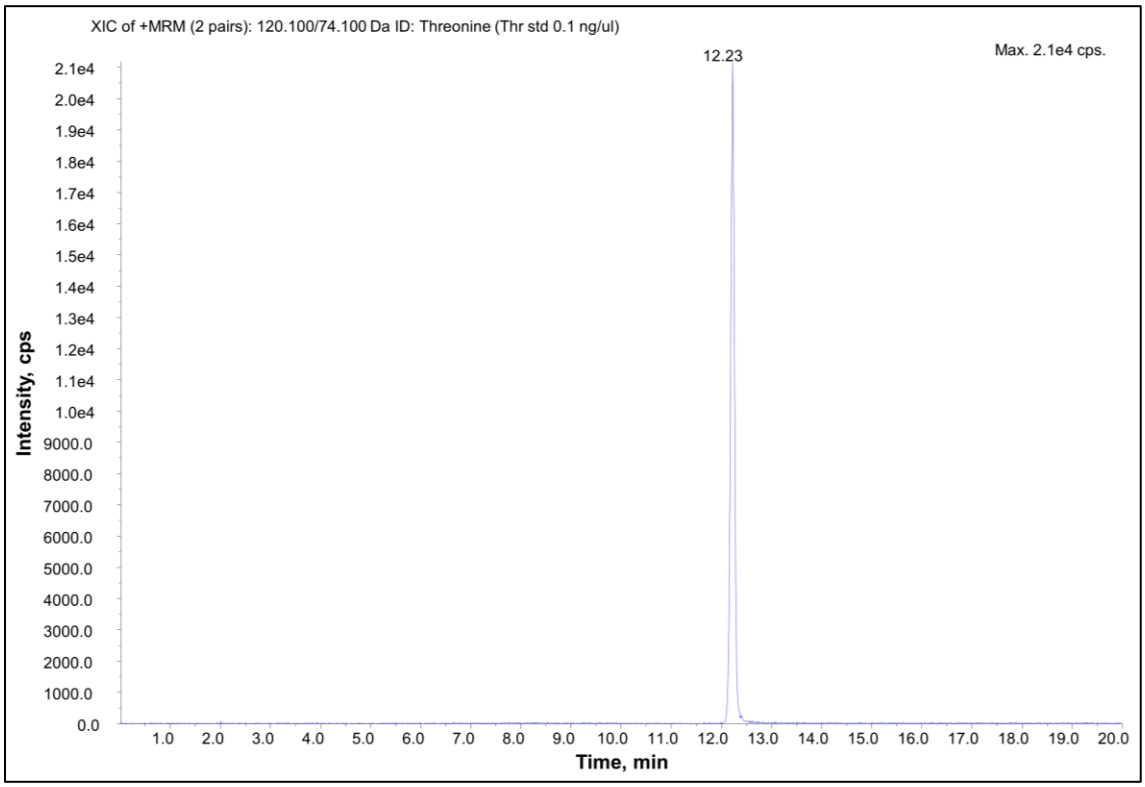

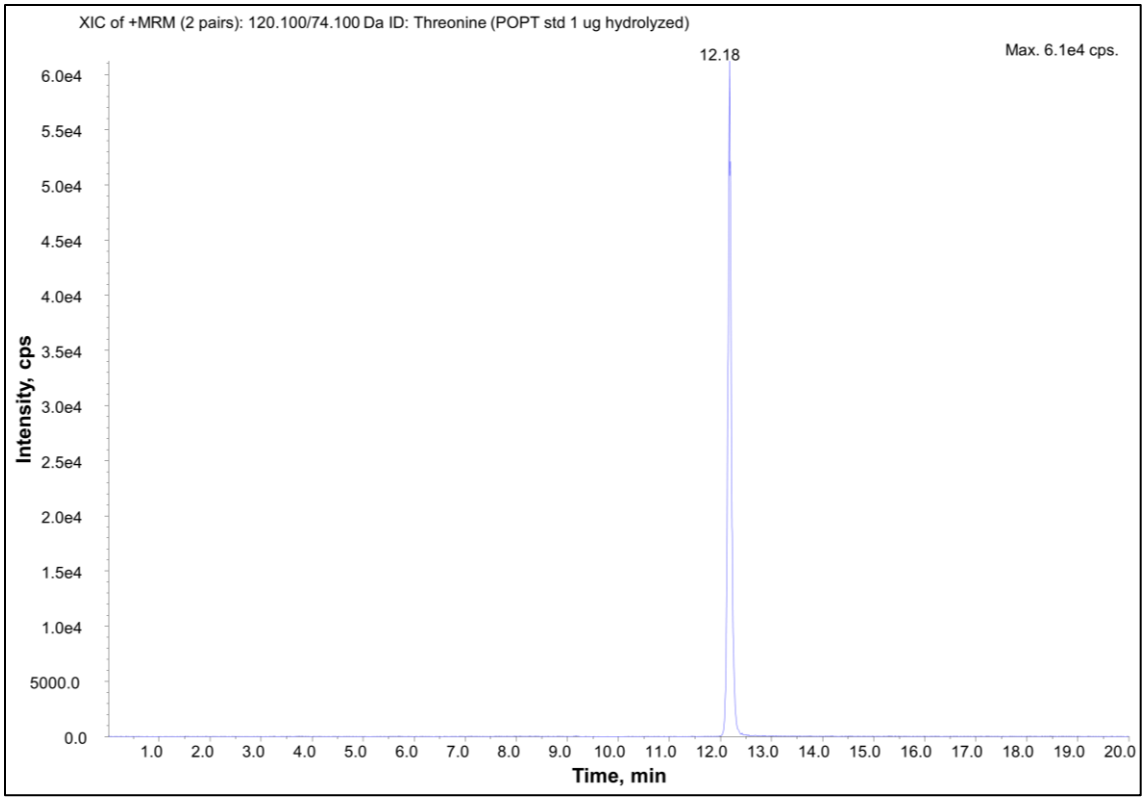
XIC of +MRM (2 pairs): 120.100/74.100 Da ID: Threonine (POPT std 1 ug hydrolyzed)
Max. 6.1e4 cps.
12.18
Intensity, cps
Time, min

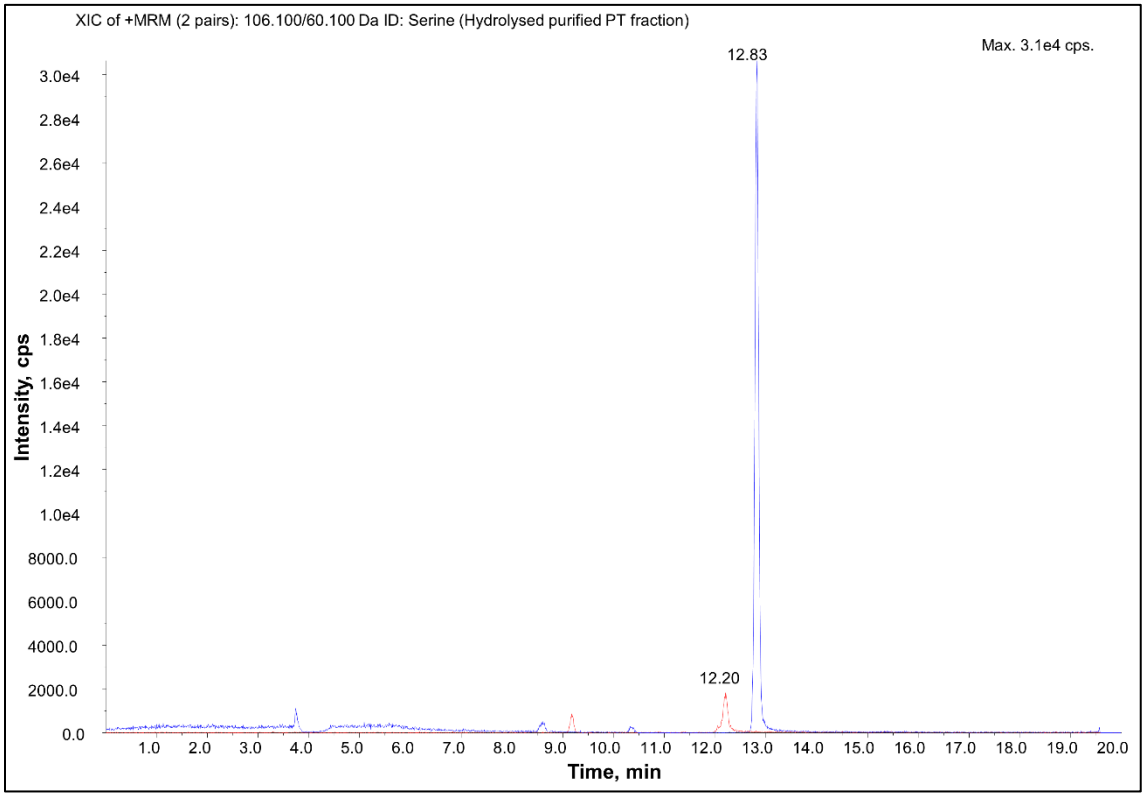
XIC of +MRM (2 pairs): 106.100/60.100 Da ID: Serine (Hydrolysed purified PT fraction)
Max. 3.1e4 cps.
12.83
12.20
Intensity, cps
Time, min

## 9.4 $MS^3$ spectra of PS & PT species from whole blood

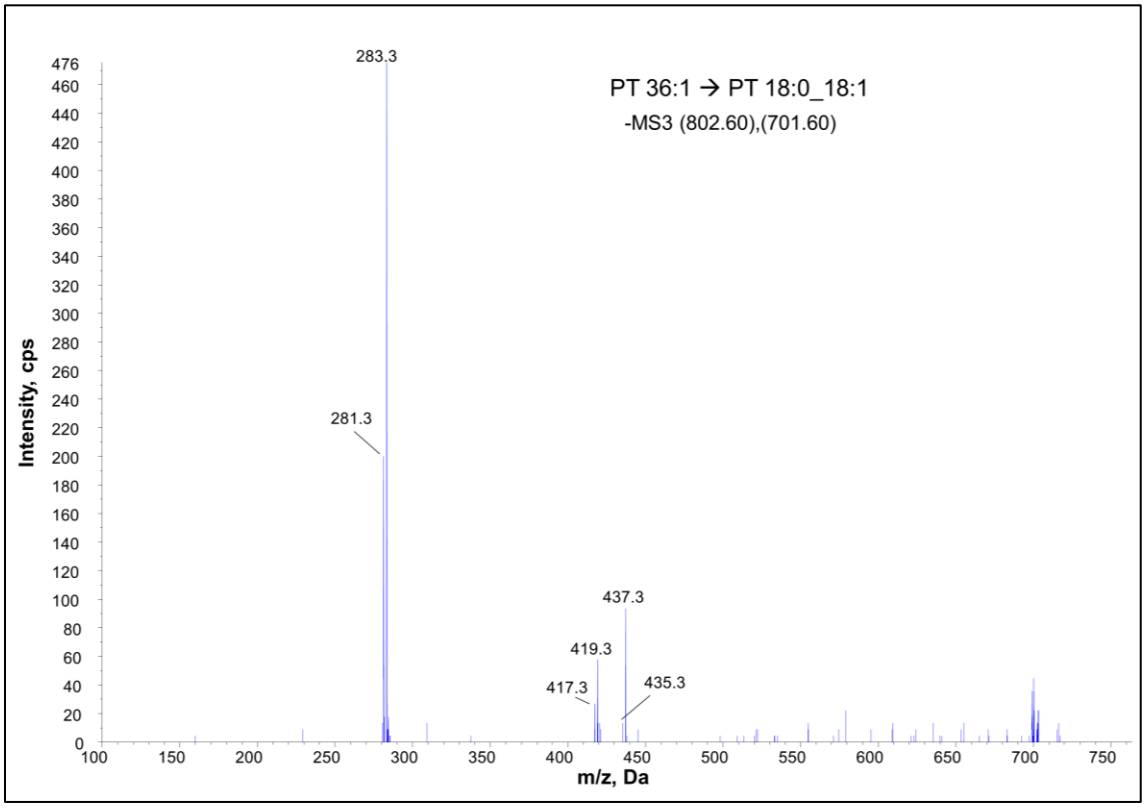


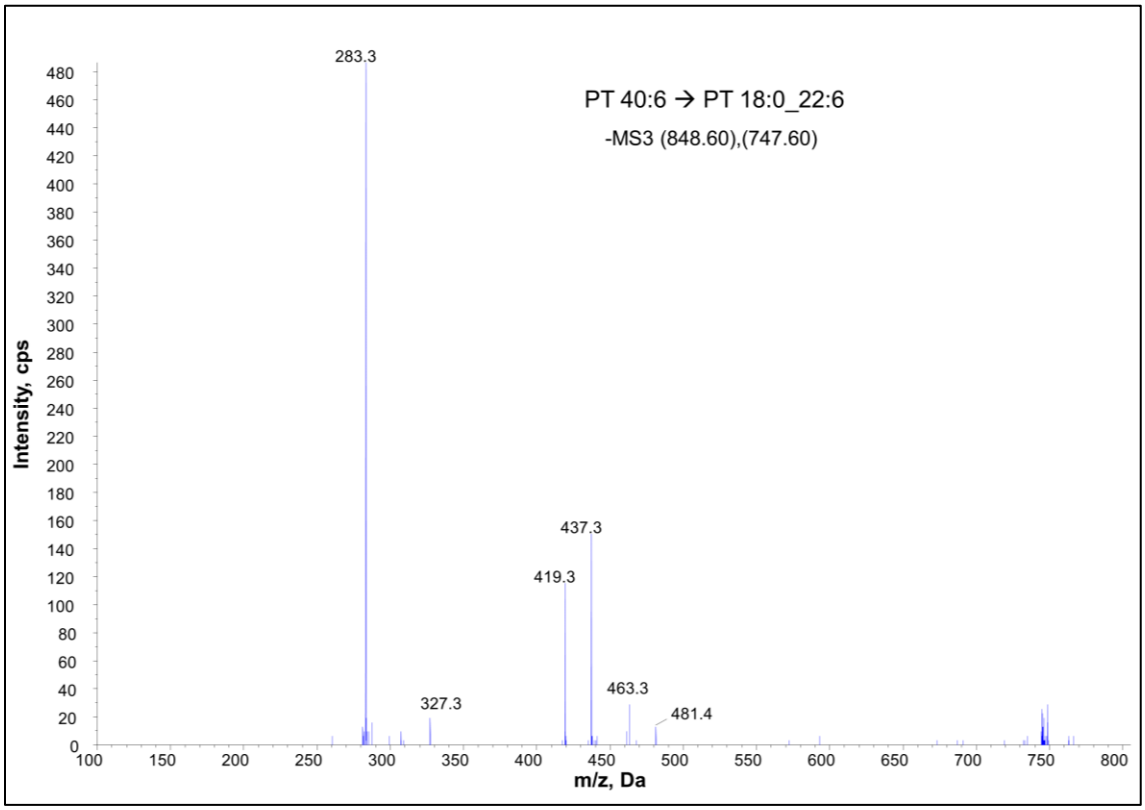

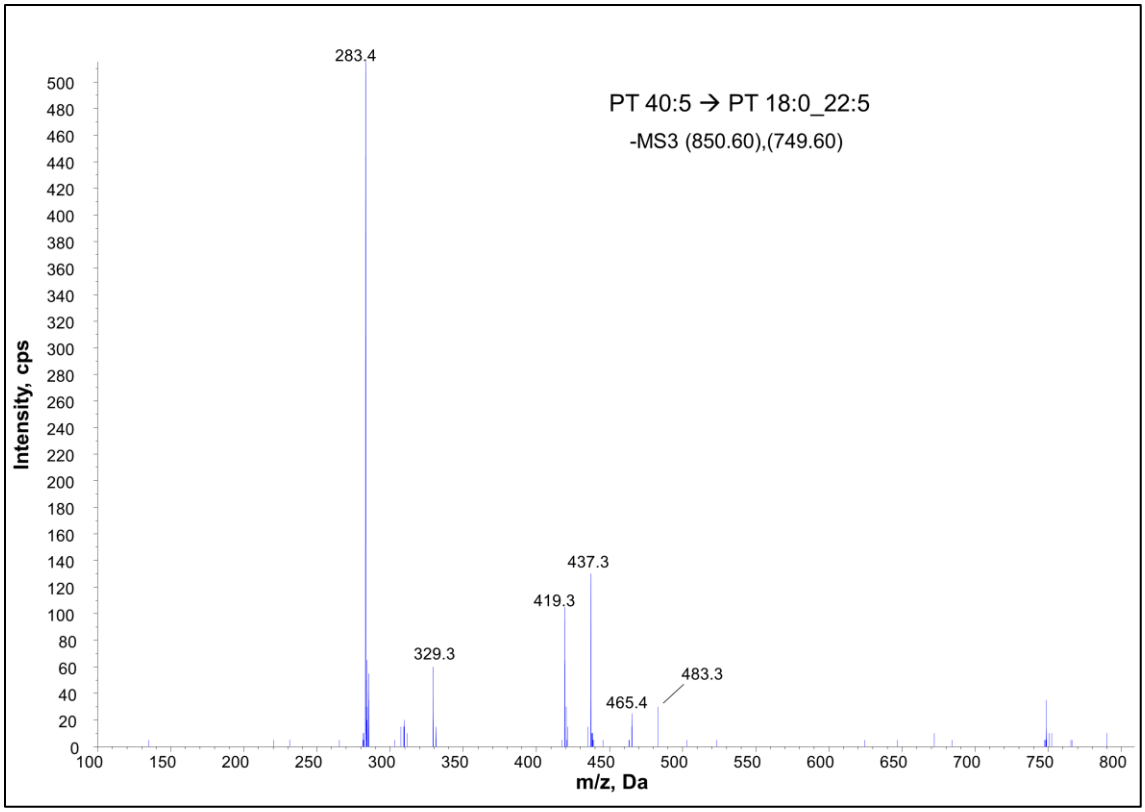
PT 40:5 → PT 18:0_22:5
-MS3 (850.60),(749.60)
283.4
437.3
419.3
329.3
483.3
465.4
Intensity, cps
m/z, Da

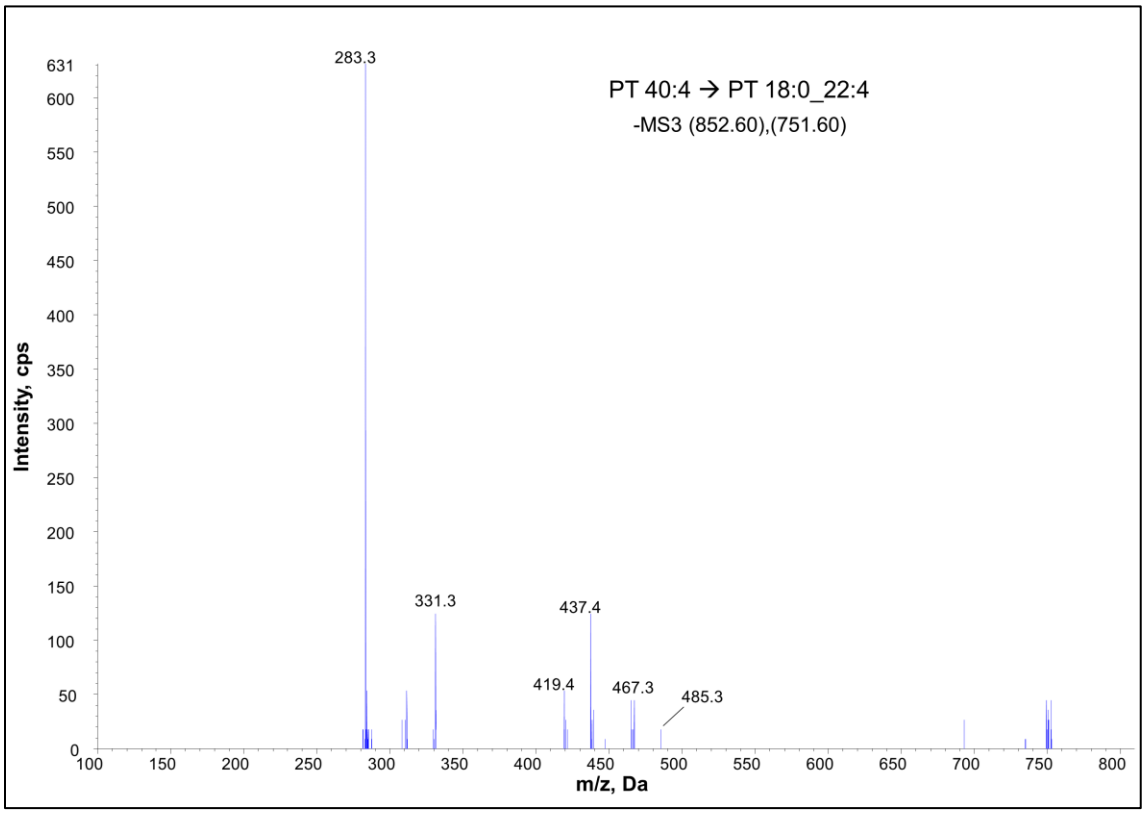
PT 40:4 → PT 18:0_22:4
-MS3 (852.60),(751.60)
283.3
331.3
437.4
419.4
467.3
485.3
Intensity, cps
m/z, Da

## 9.5 Representative chromatograms (HILIC-LC-MS/MS of lysophospholipids)

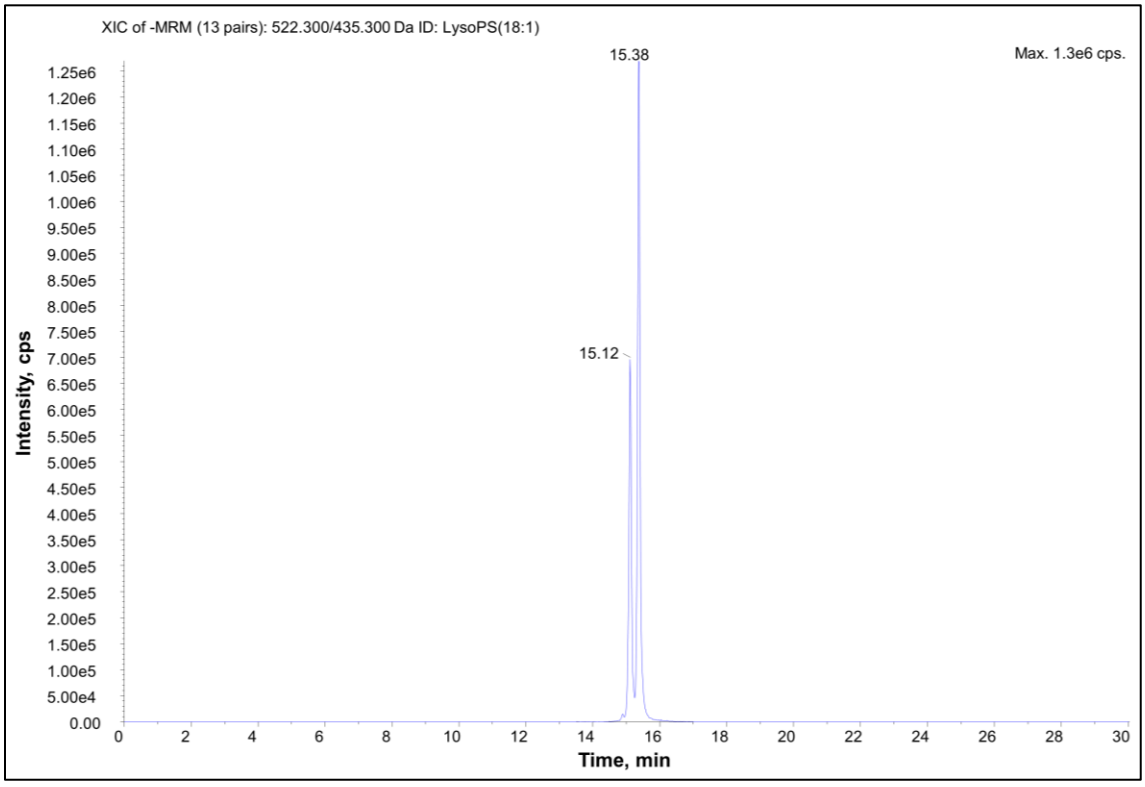


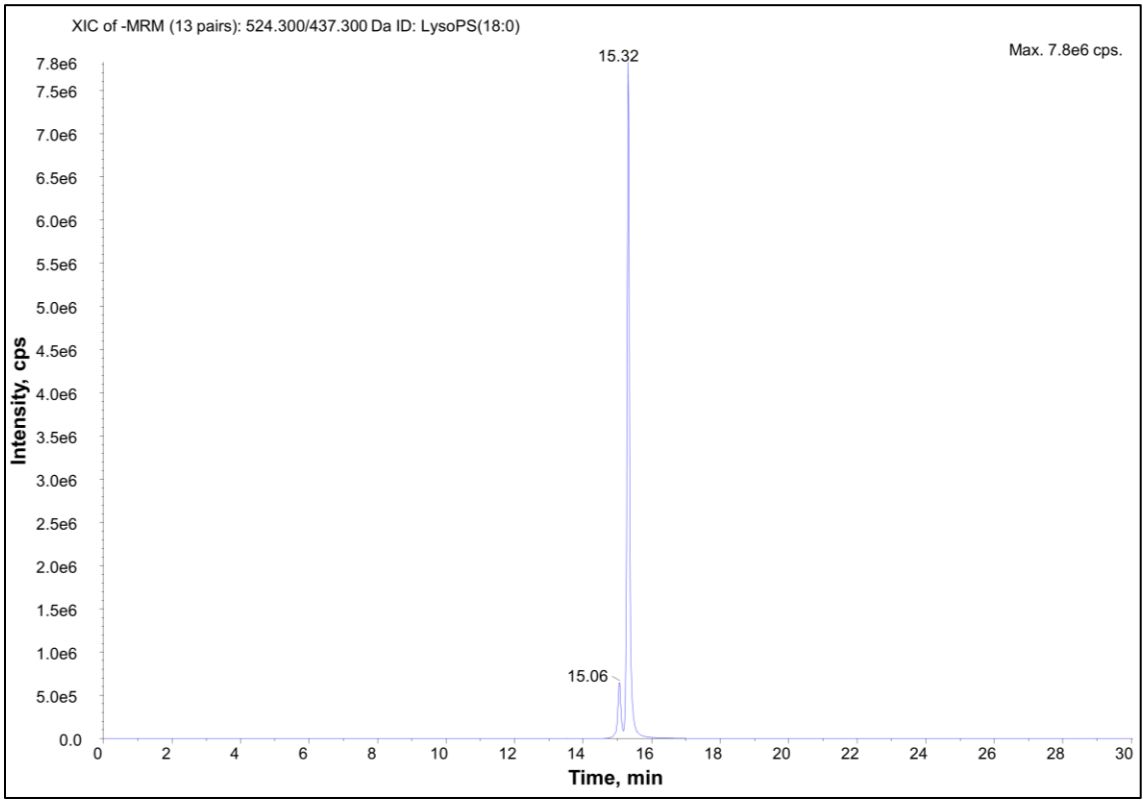

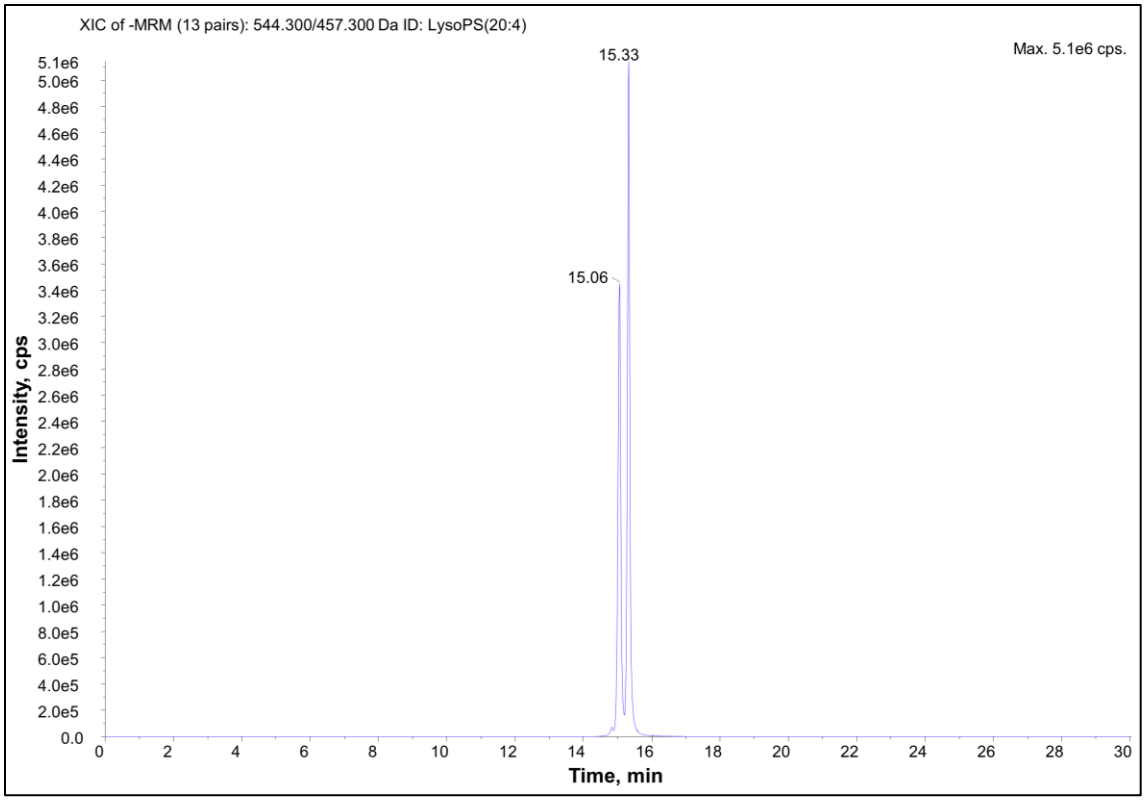
XIC of -MRM (13 pairs): 544.300/457.300 Da ID: LysoPS(20:4)
Max. 5.1e6 cps.
15.33
15.06
Intensity, cps
Time, min

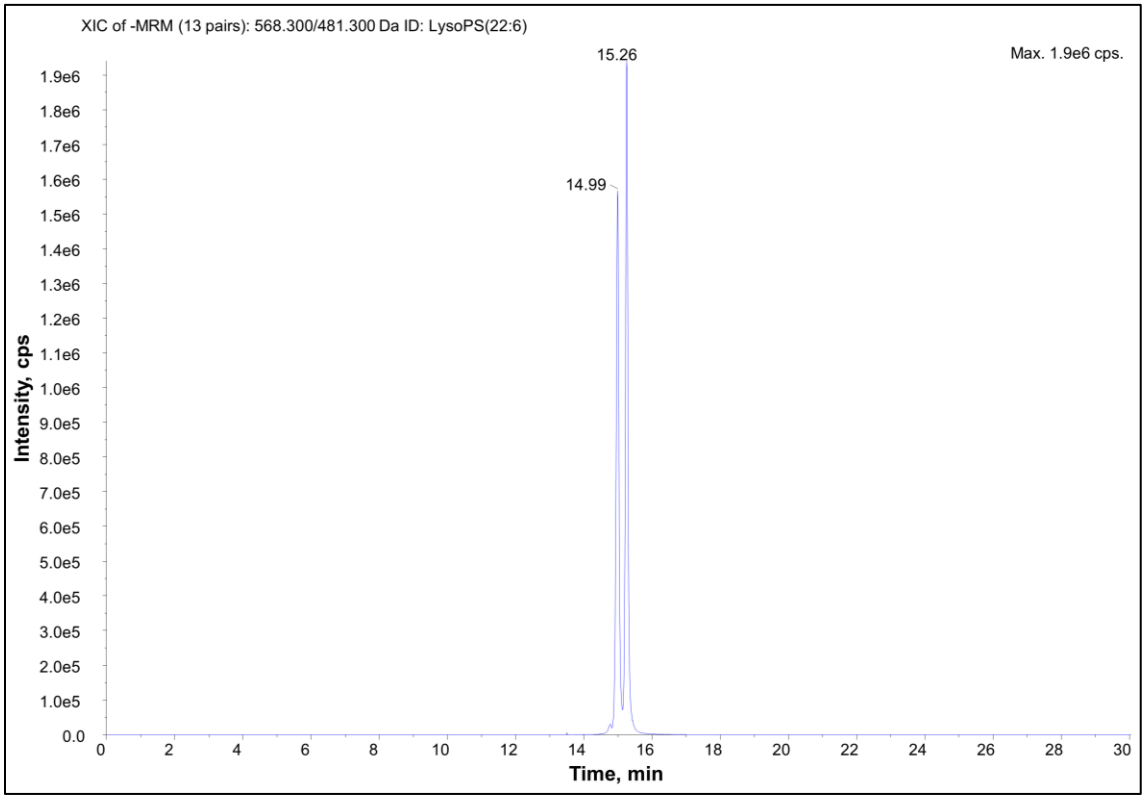
XIC of -MRM (13 pairs): 568.300/481.300 Da ID: LysoPS(22:6)
Max. 1.9e6 cps.
15.26
14.99
Intensity, cps
Time, min

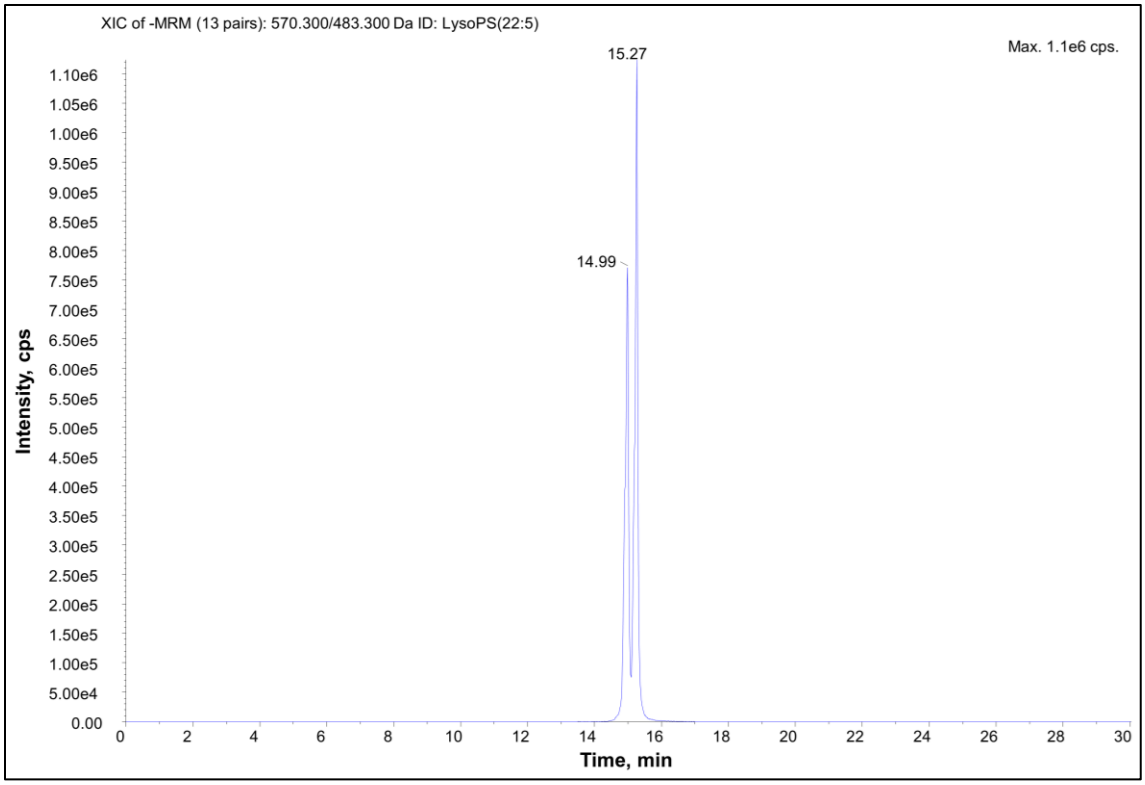
XIC of -MRM (13 pairs): 570.300/483.300 Da ID: LysoPS(22:5)
Max. 1.1e6 cps.
15.27
14.99
Intensity, cps
Time, min

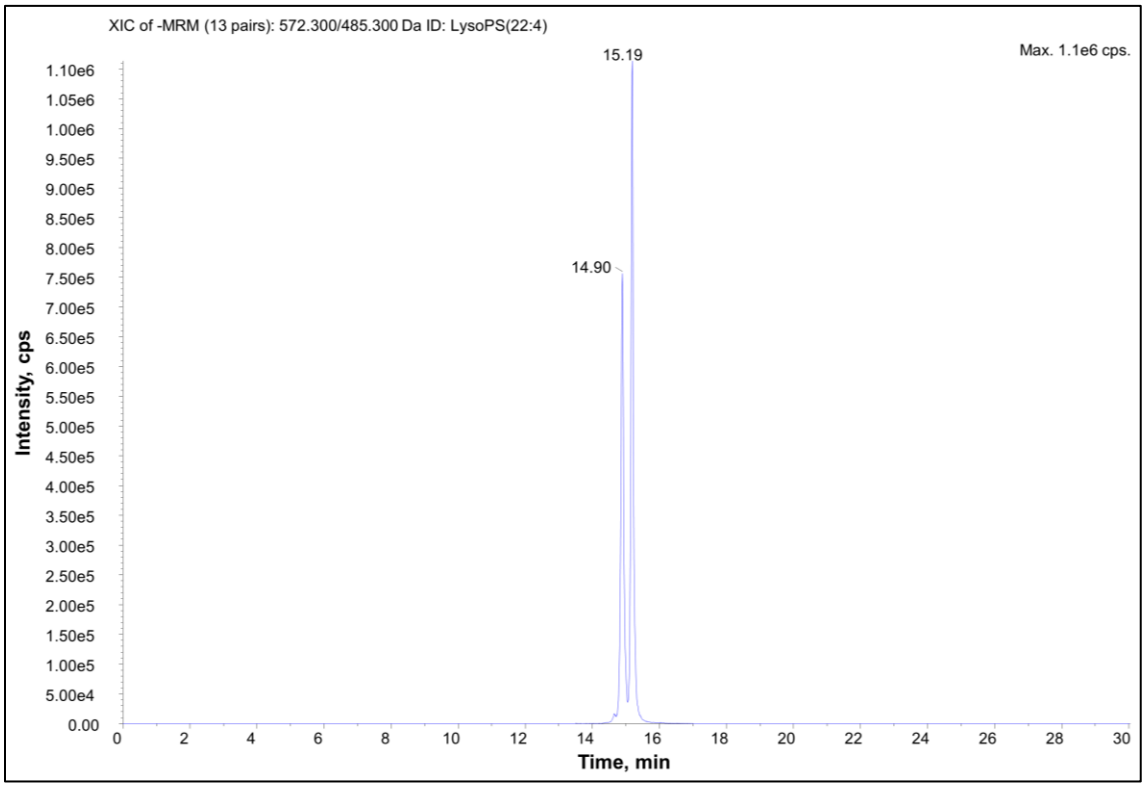
XIC of -MRM (13 pairs): 572.300/485.300 Da ID: LysoPS(22:4)
Max. 1.1e6 cps.
15.19
14.90
Intensity, cps
Time, min

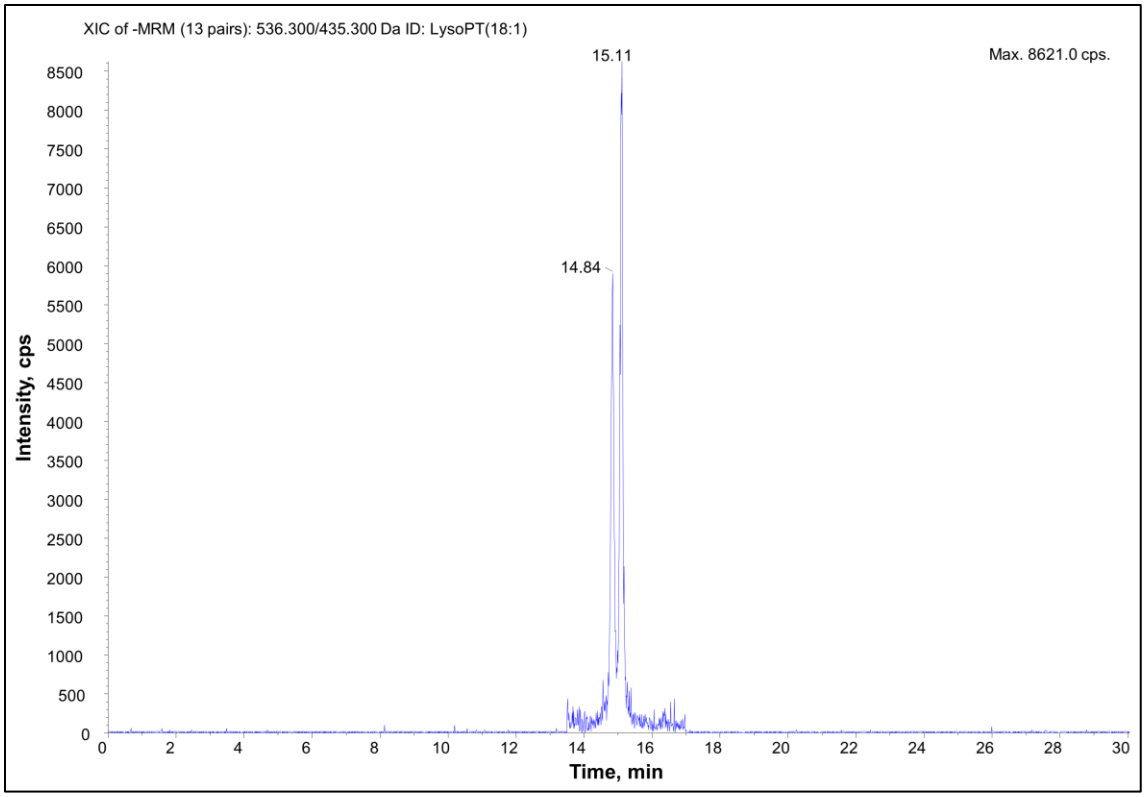
XIC of -MRM (13 pairs): 536.300/435.300 Da ID: LysoPT(18:1)
Max. 8621.0 cps.
15.11
14.84
Intensity, cps
Time, min

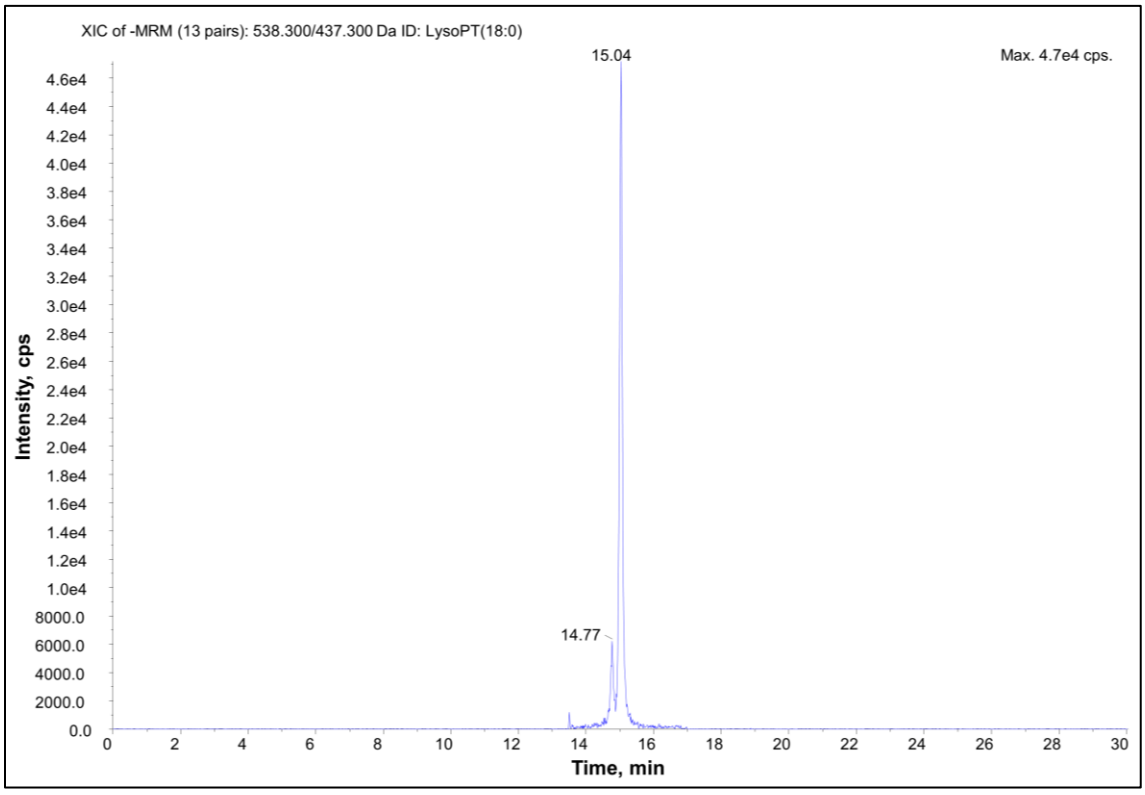
XIC of -MRM (13 pairs): 538.300/437.300 Da ID: LysoPT(18:0)
Max. 4.7e4 cps.
15.04
14.77
Intensity, cps
Time, min

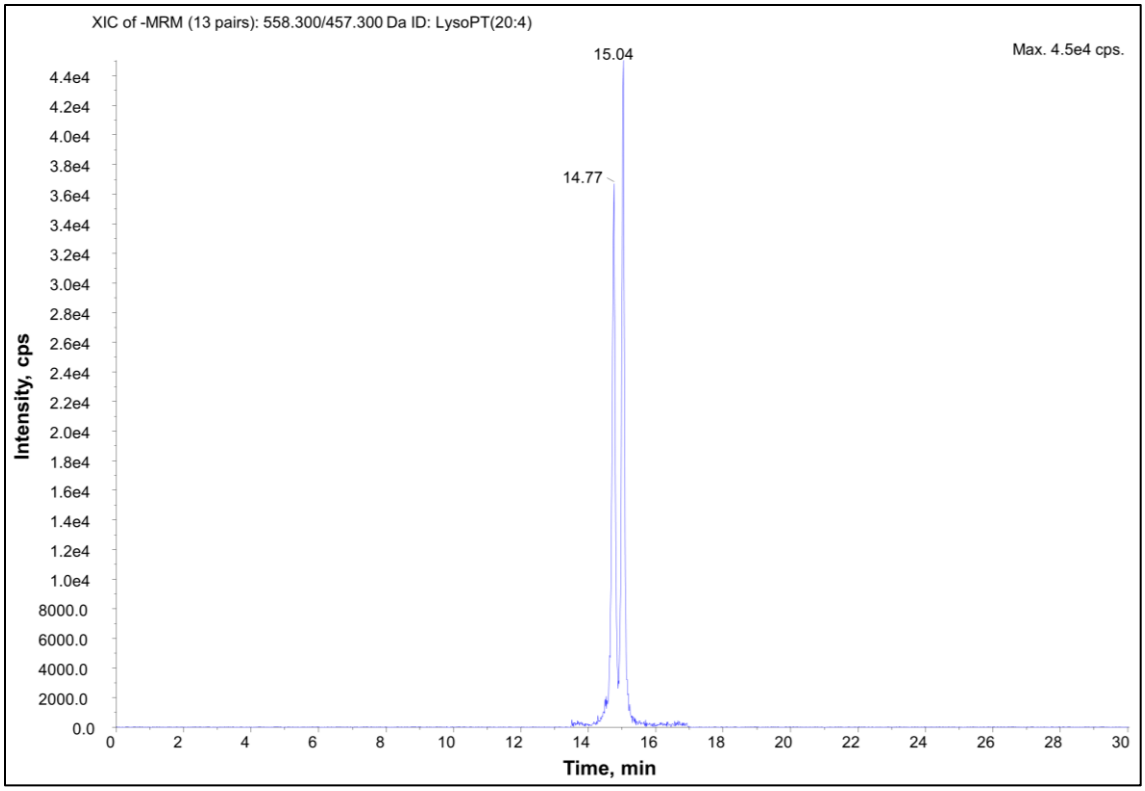
XIC of -MRM (13 pairs): 558.300/457.300 Da ID: LysoPT(20:4)
Max. 4.5e4 cps.
15.04
14.77
Intensity, cps
Time, min

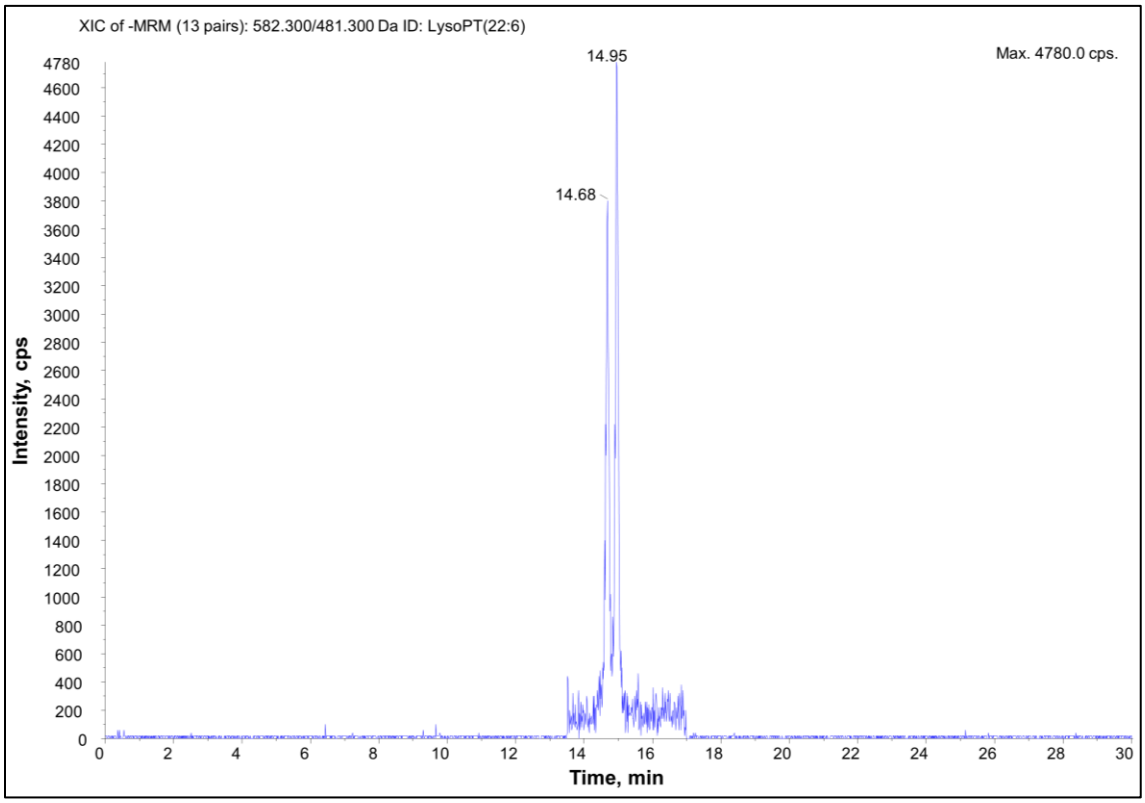
XIC of -MRM (13 pairs): 582.300/481.300 Da ID: LysoPT(22:6)
Max. 4780.0 cps.
14.95
14.68
Intensity, cps
Time, min

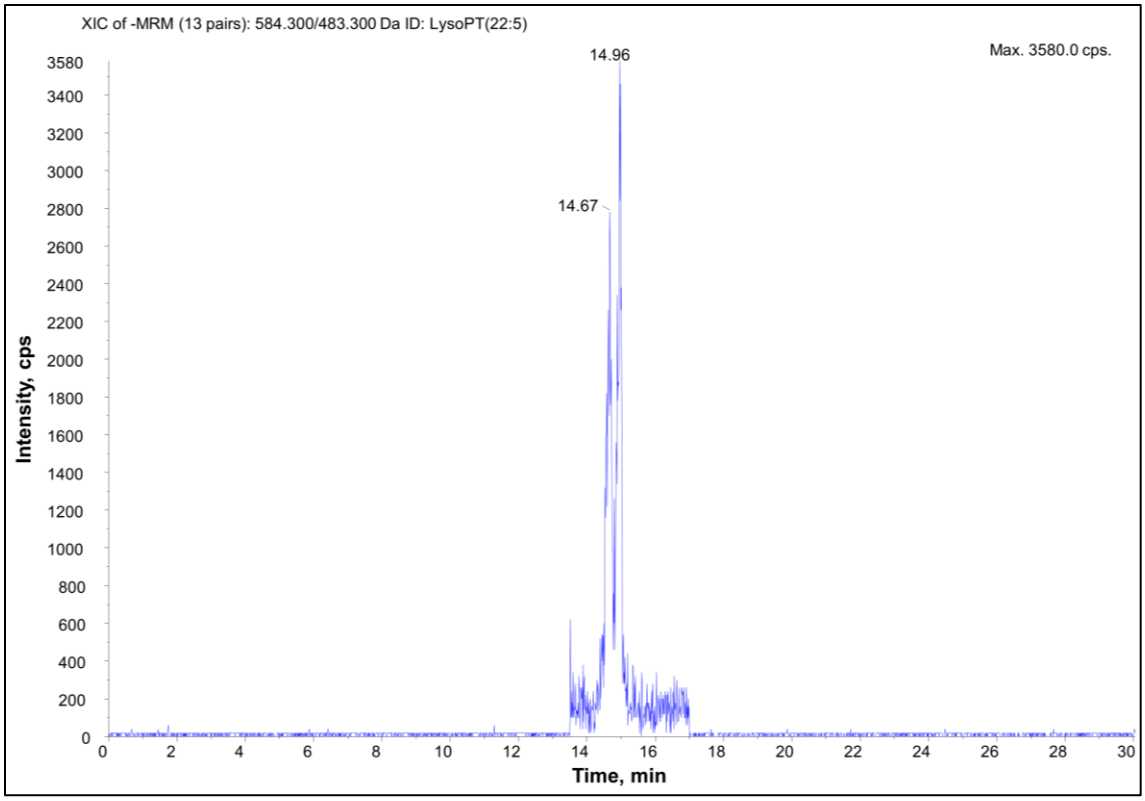
XIC of -MRM (13 pairs): 584.300/483.300 Da ID: LysoPT(22:5)
Max. 3580.0 cps.
14.96
14.67
Intensity, cps
Time, min

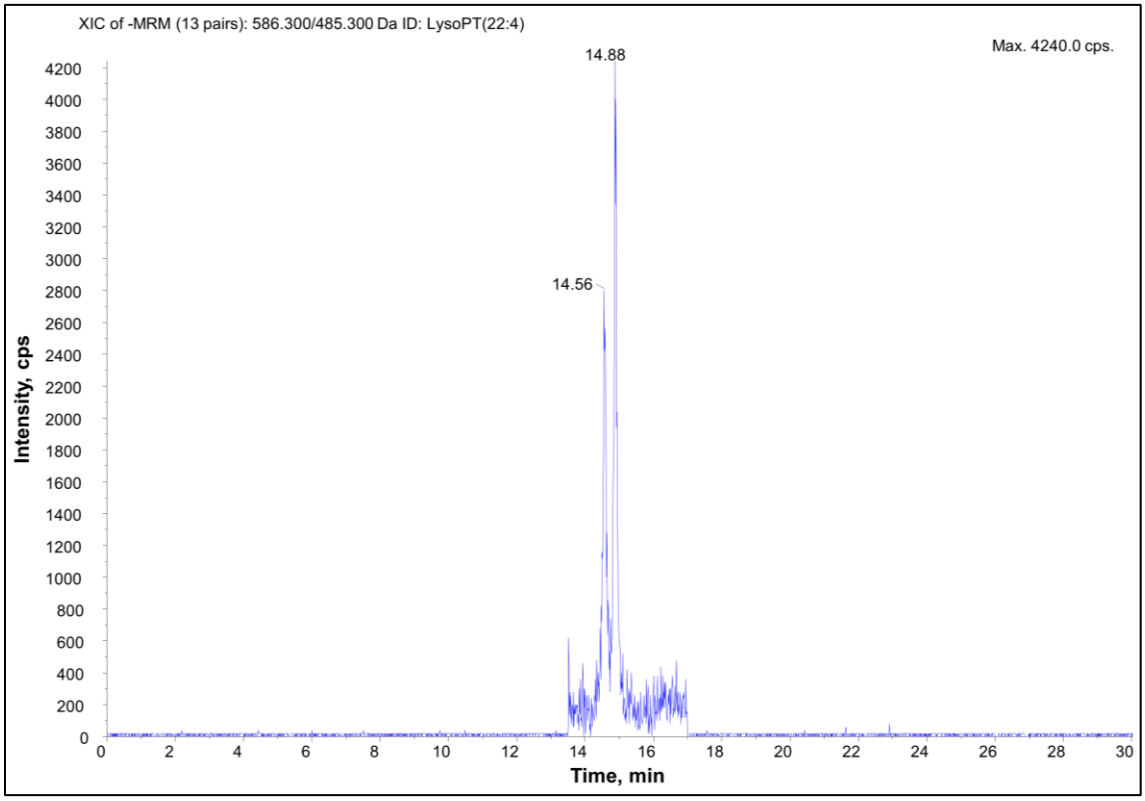
XIC of -MRM (13 pairs): 586.300/485.300 Da ID: LysoPT(22:4)
Max. 4240.0 cps.
14.88
14.56
Intensity, cps
Time, min

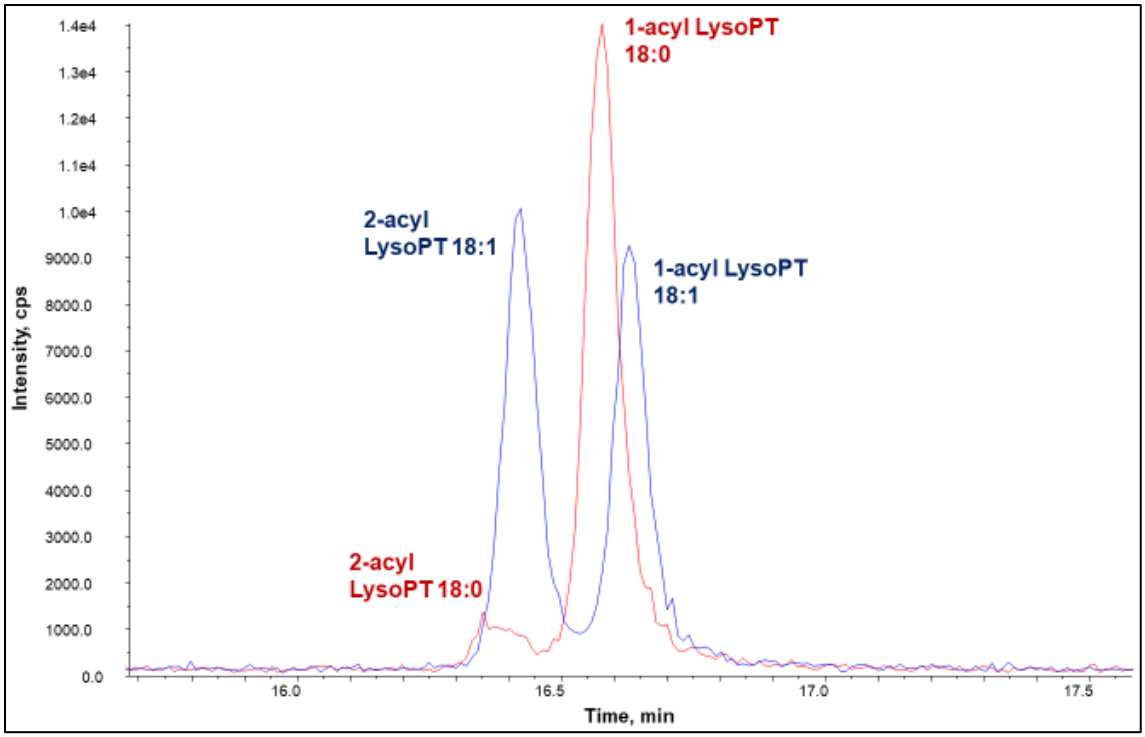
1-acyl LysoPT
18:0
2-acyl
LysoPT 18:1
1-acyl LysoPT
18:1
2-acyl
LysoPT 18:0
Intensity, cps
Time, min
1.4e4
1.3e4
1.2e4
1.1e4
1.0e4
9000.0
8000.0
7000.0
6000.0
5000.0
4000.0
3000.0
2000.0
1000.0
0.0
16.0
16.5
17.0
17.5

## 9.6 Representative chromatograms (HILIC-LC-MS/MS of biotinylated phospholipids)

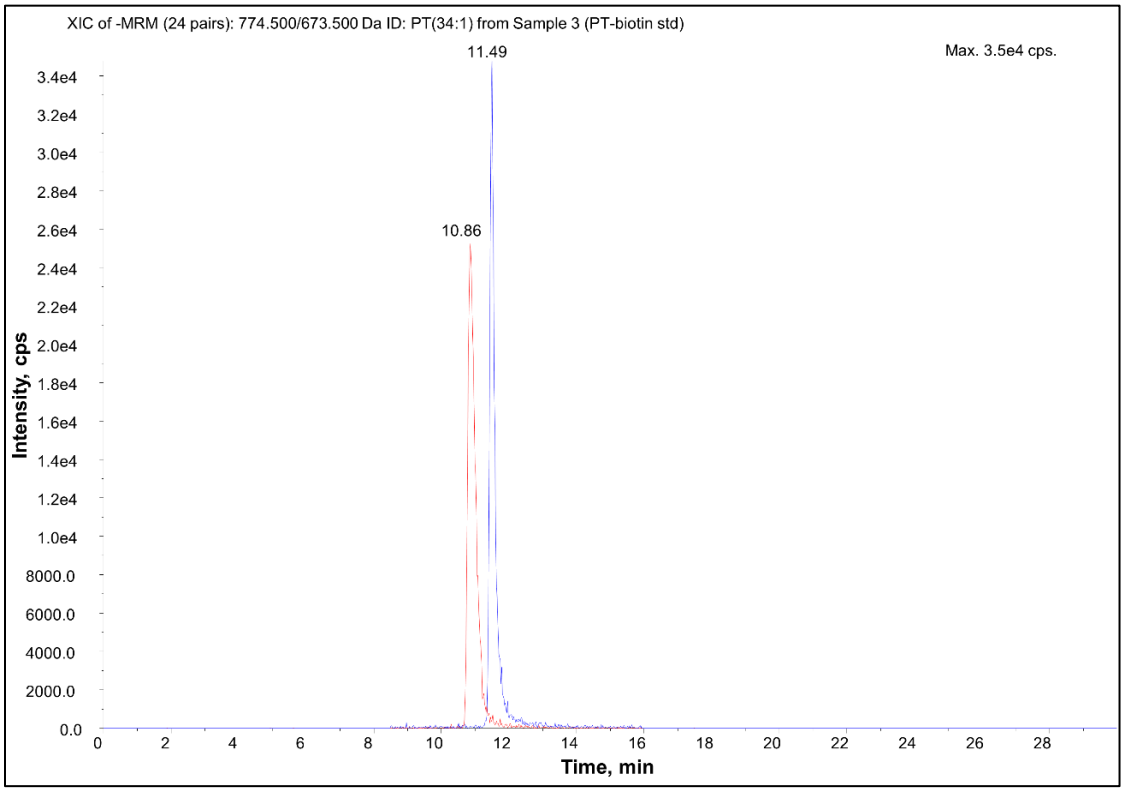


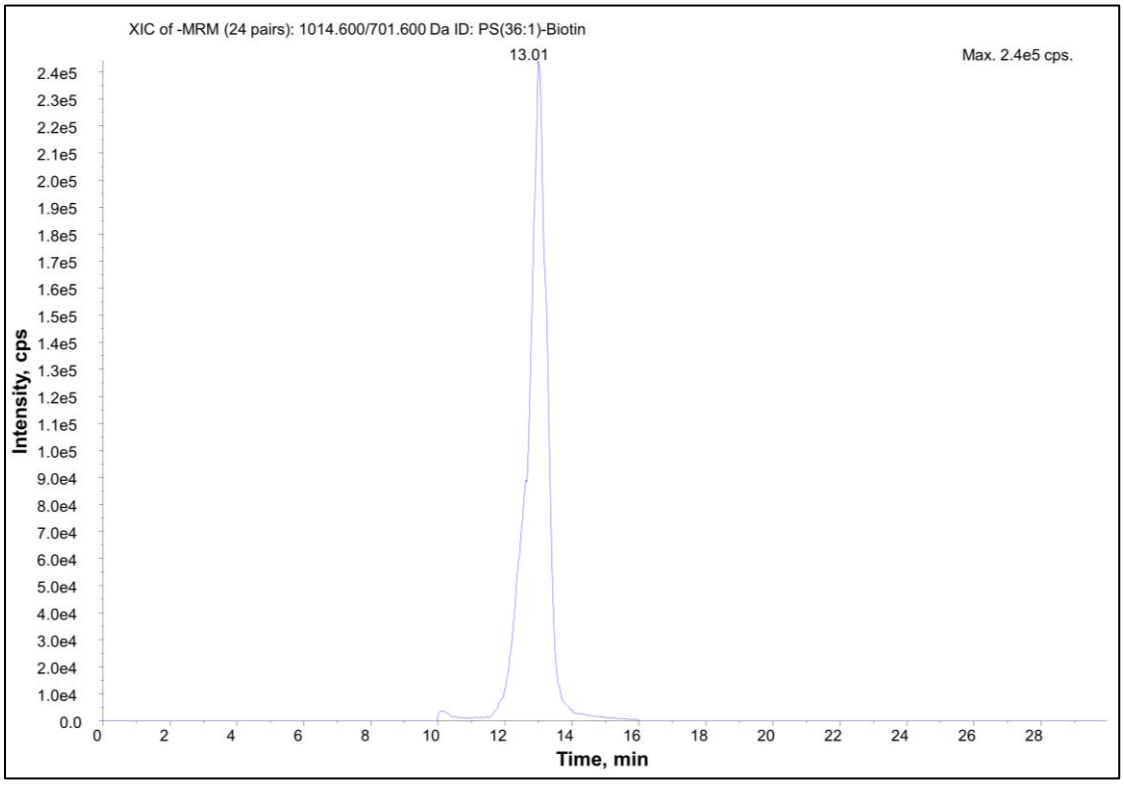

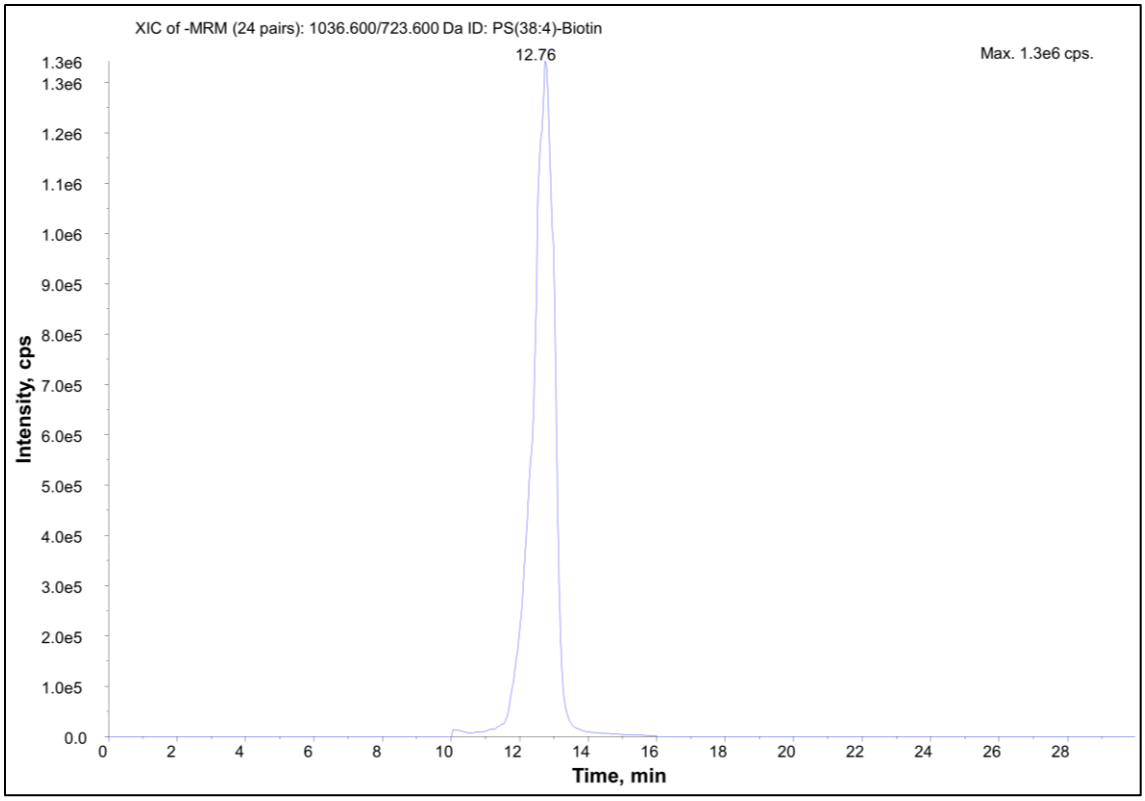
XIC of -MRM (24 pairs): 1036.600/723.600 Da ID: PS(38:4)-Biotin
12.76
Max. 1.3e6 cps.
Intensity, cps
1.3e6
1.3e6
1.2e6
1.1e6
1.0e6
9.0e5
8.0e5
7.0e5
6.0e5
5.0e5
4.0e5
3.0e5
2.0e5
1.0e5
0.0
0
2
4
6
8
10
12
14
16
18
20
22
24
26
28
Time, min

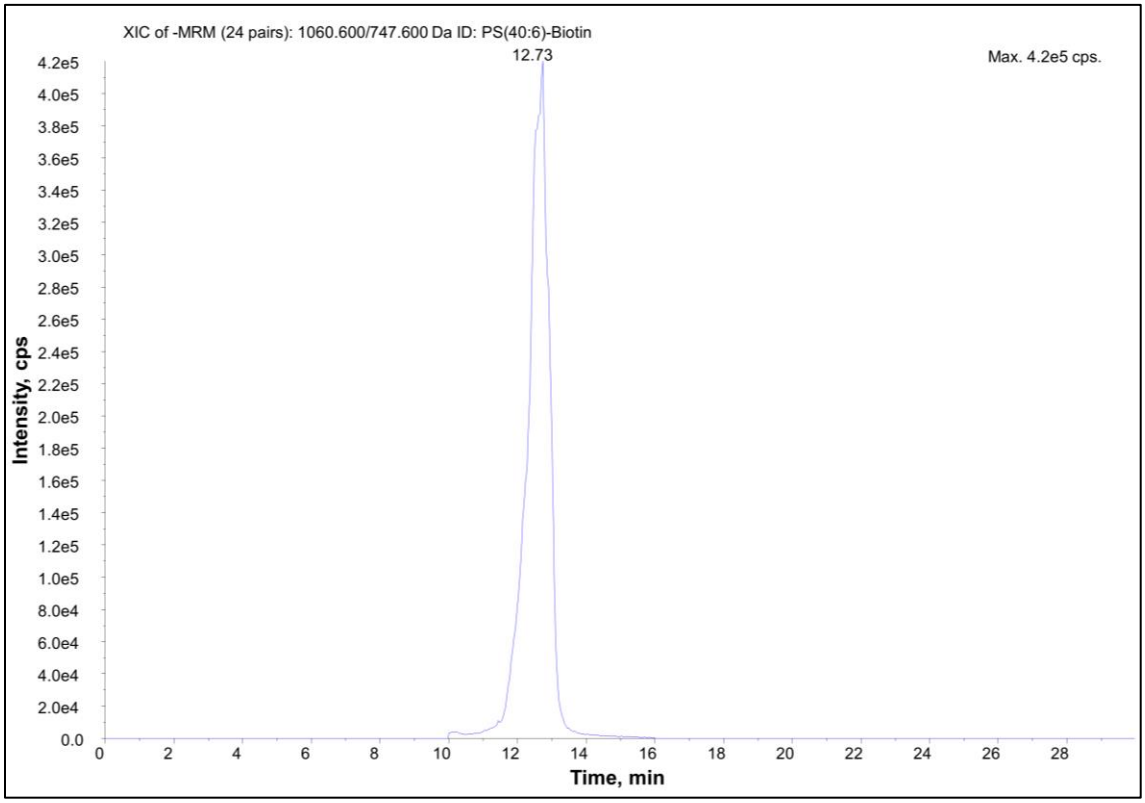
XIC of -MRM (24 pairs): 1060.600/747.600 Da ID: PS(40:6)-Biotin
12.73
Max. 4.2e5 cps.
Intensity, cps
4.2e5
4.0e5
3.8e5
3.6e5
3.4e5
3.2e5
3.0e5
2.8e5
2.6e5
2.4e5
2.2e5
2.0e5
1.8e5
1.6e5
1.4e5
1.2e5
1.0e5
8.0e4
6.0e4
4.0e4
2.0e4
0.0
0
2
4
6
8
10
12
14
16
18
20
22
24
26
28
Time, min

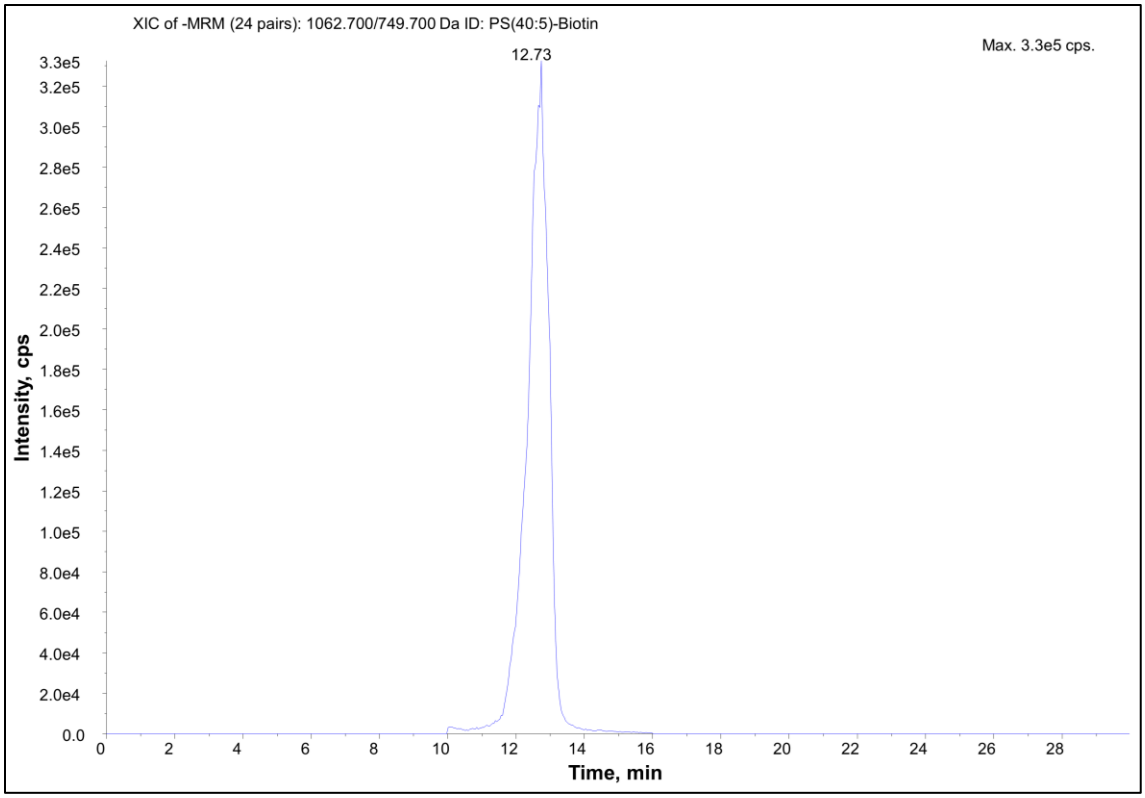
XIC of -MRM (24 pairs): 1062.700/749.700 Da ID: PS(40:5)-Biotin
Max. 3.3e5 cps.
12.73
Intensity, cps
Time, min

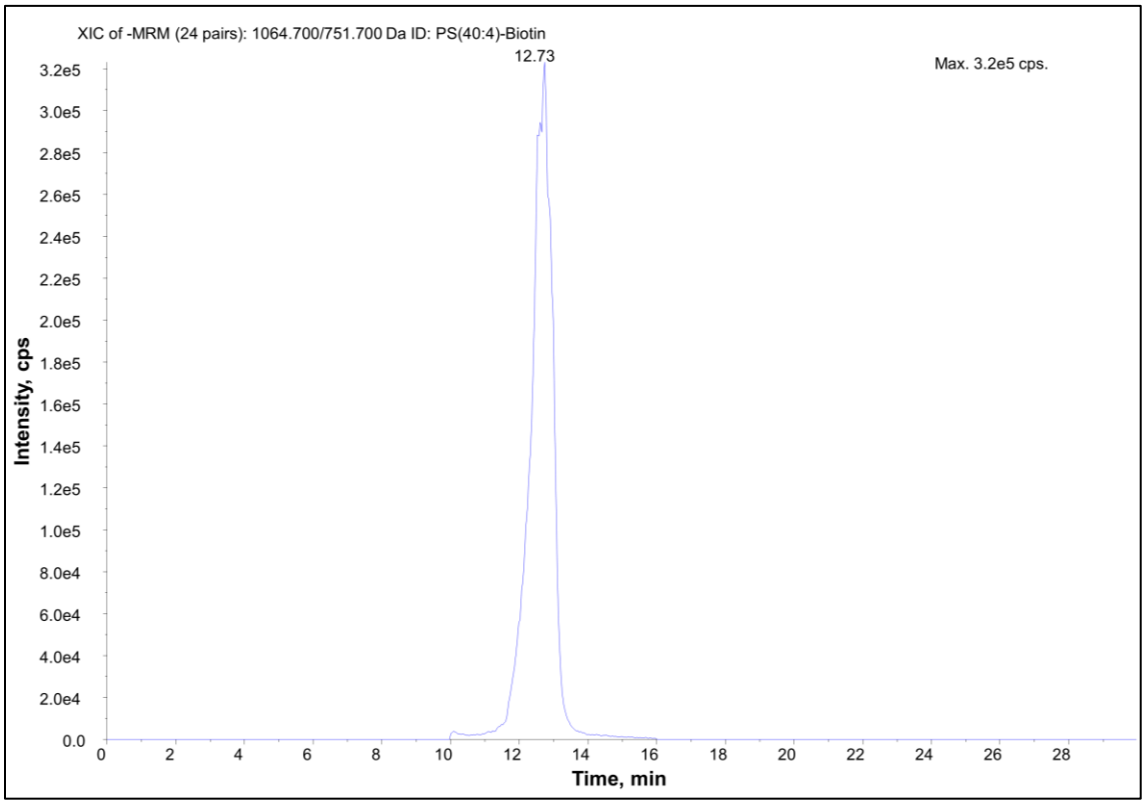
XIC of -MRM (24 pairs): 1064.700/751.700 Da ID: PS(40:4)-Biotin
Max. 3.2e5 cps.
12.73
Intensity, cps
Time, min

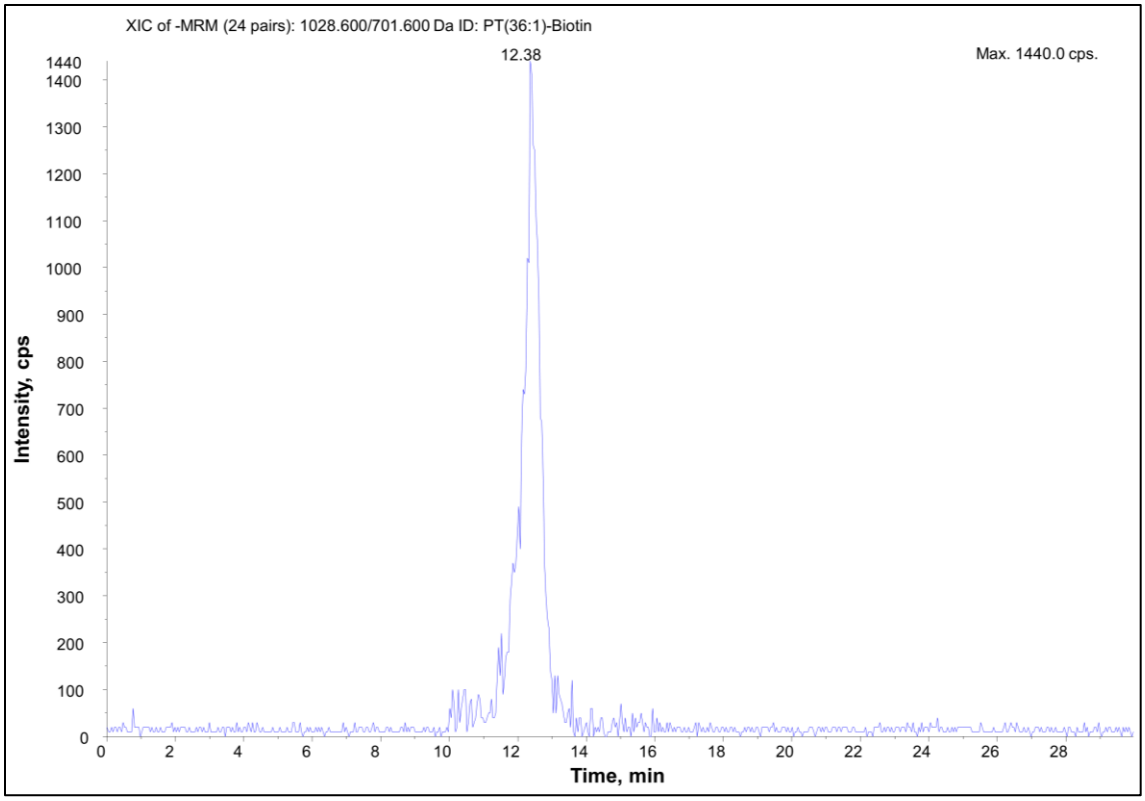
XIC of -MRM (24 pairs): 1028.600/701.600 Da ID: PT(36:1)-Biotin
12.38
Max. 1440.0 cps.
Intensity, cps
Time, min

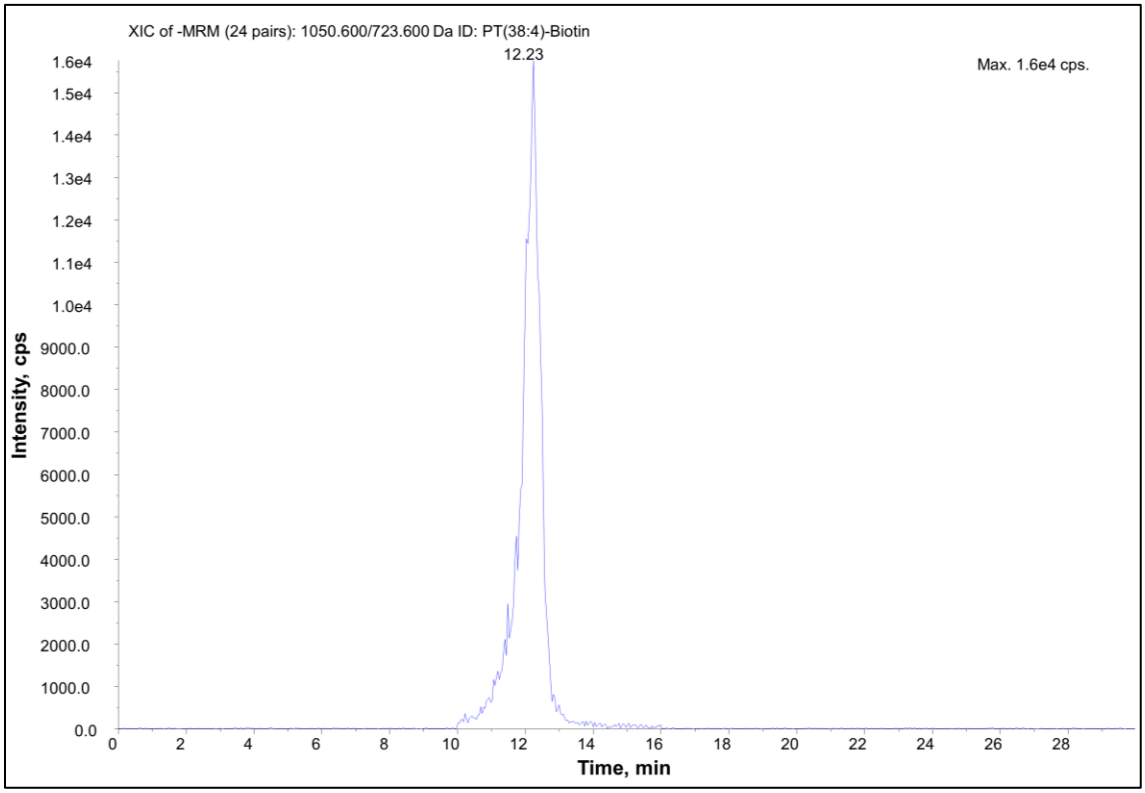
XIC of -MRM (24 pairs): 1050.600/723.600 Da ID: PT(38:4)-Biotin
12.23
Max. 1.6e4 cps.
Intensity, cps
Time, min

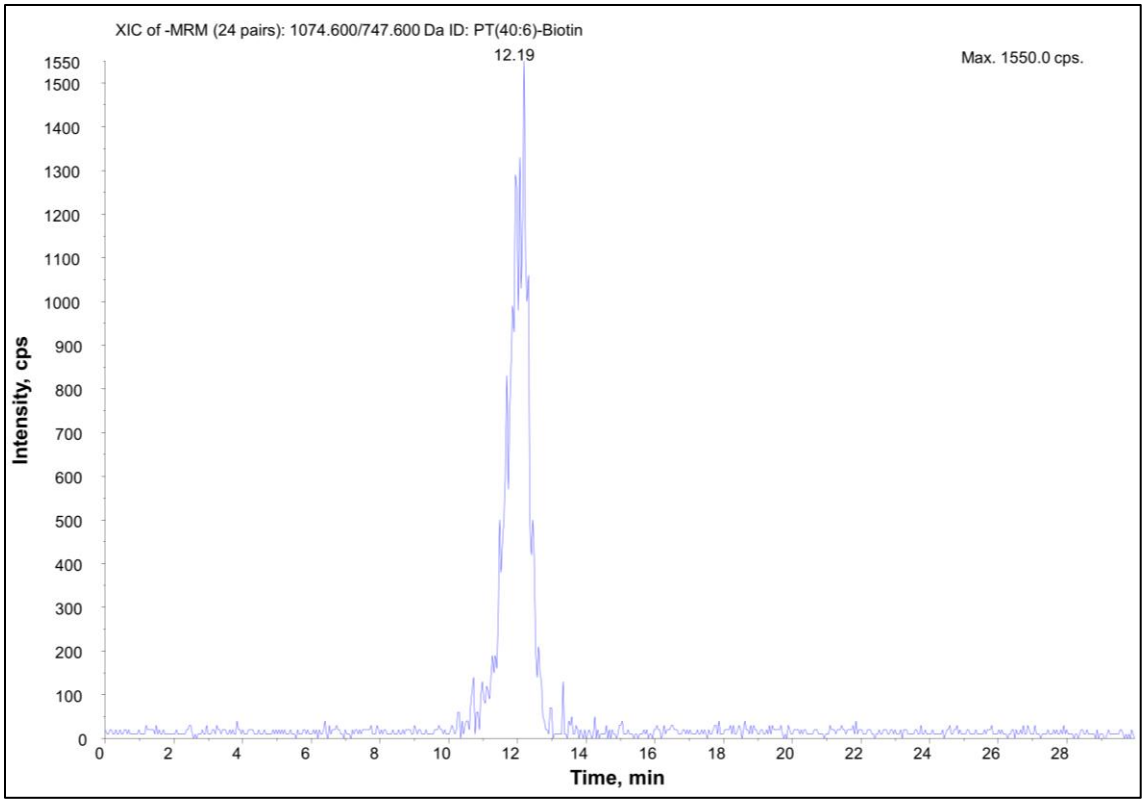
XIC of -MRM (24 pairs): 1074.600/747.600 Da ID: PT(40:6)-Biotin
12.19
Max. 1550.0 cps.
Intensity, cps
Time, min

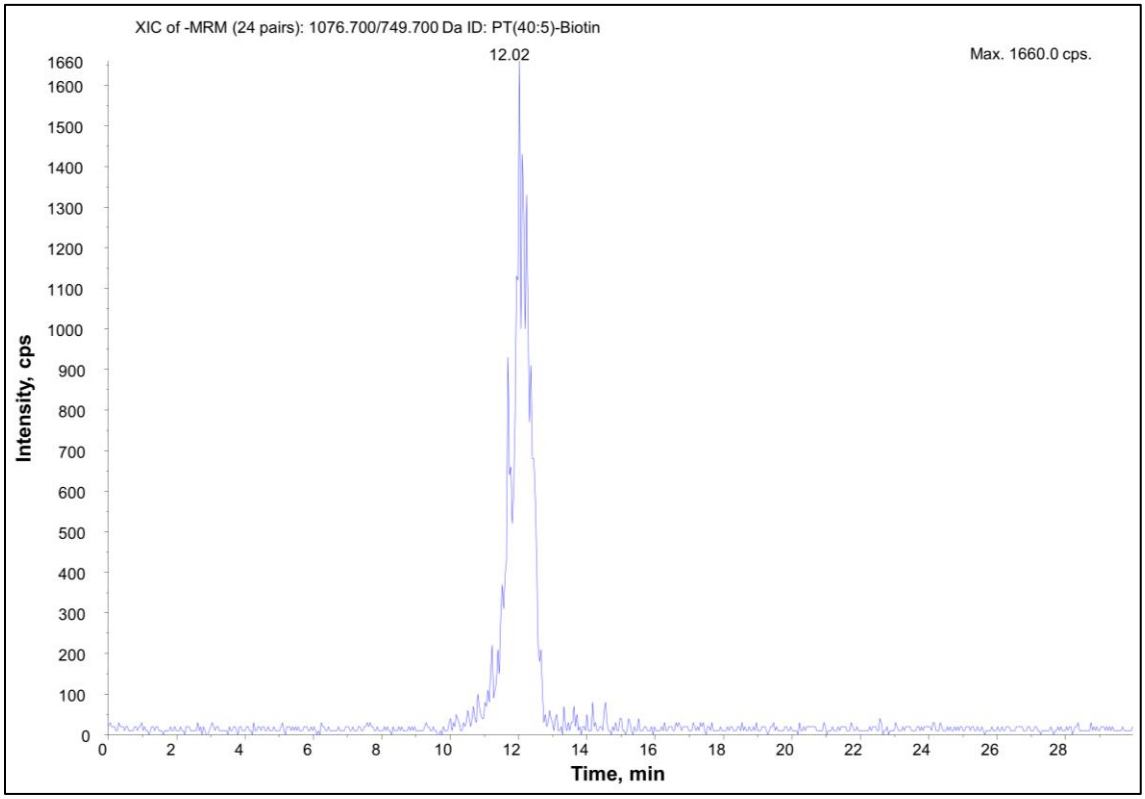
XIC of -MRM (24 pairs): 1076.700/749.700 Da ID: PT(40:5)-Biotin
12.02
Max. 1660.0 cps.
Intensity, cps
Time, min

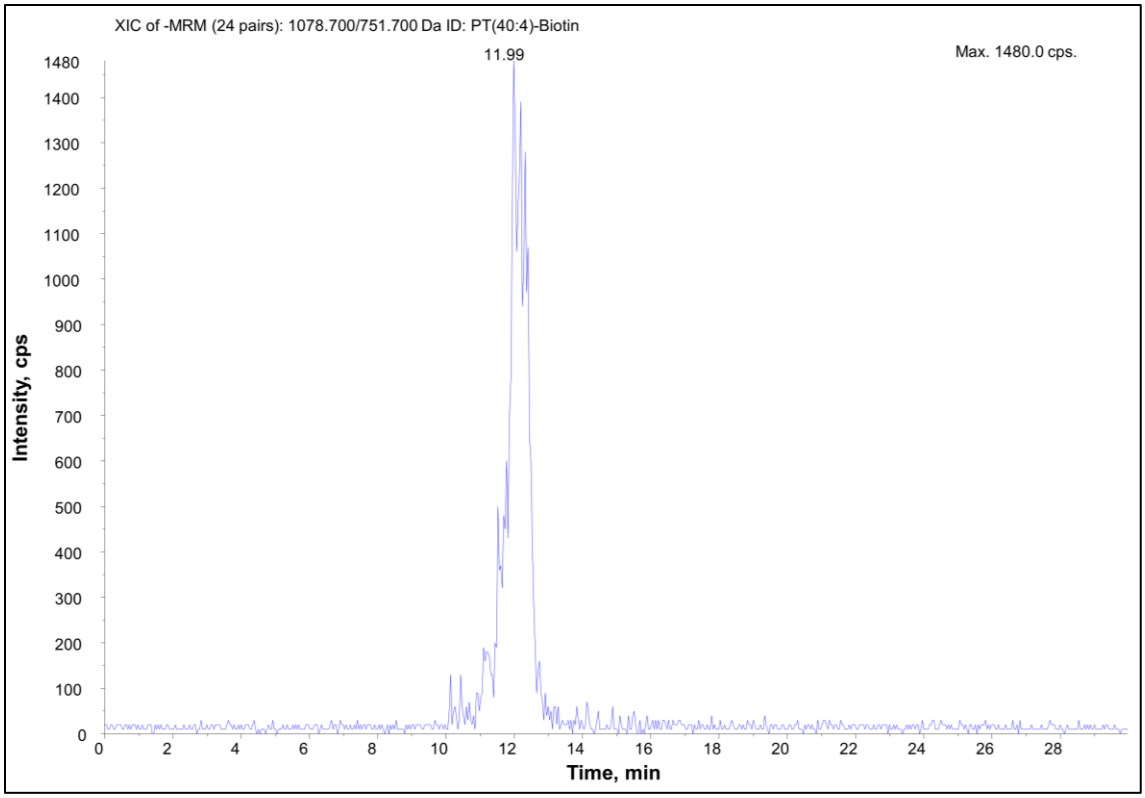
XIC of -MRM (24 pairs): 1078.700/751.700 Da ID: PT(40:4)-Biotin
11.99
Max. 1480.0 cps.
Intensity, cps
Time, min
0
100
200
300
400
500
600
700
800
900
1000
1100
1200
1300
1400
1480
0
2
4
6
8
10
12
14
16
18
20
22
24
26
28

## 9.7 Representative chromatograms (HILIC-LC-MS/MS of phospholipids)

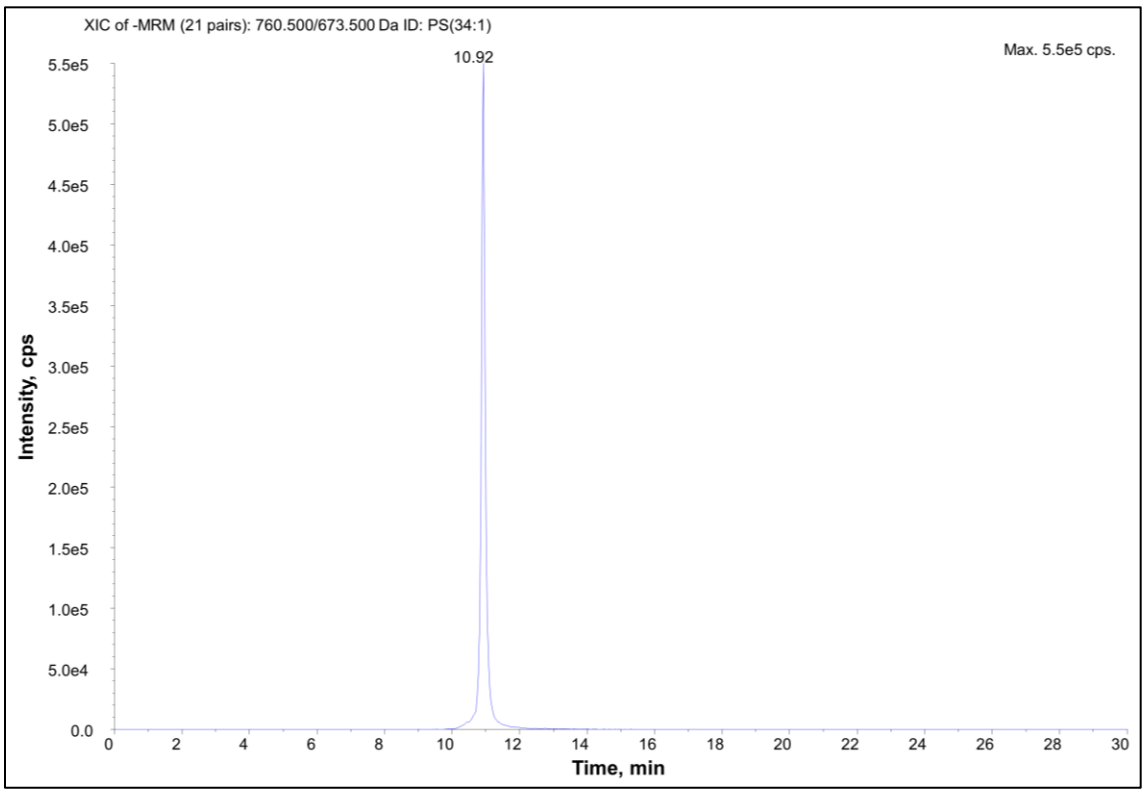


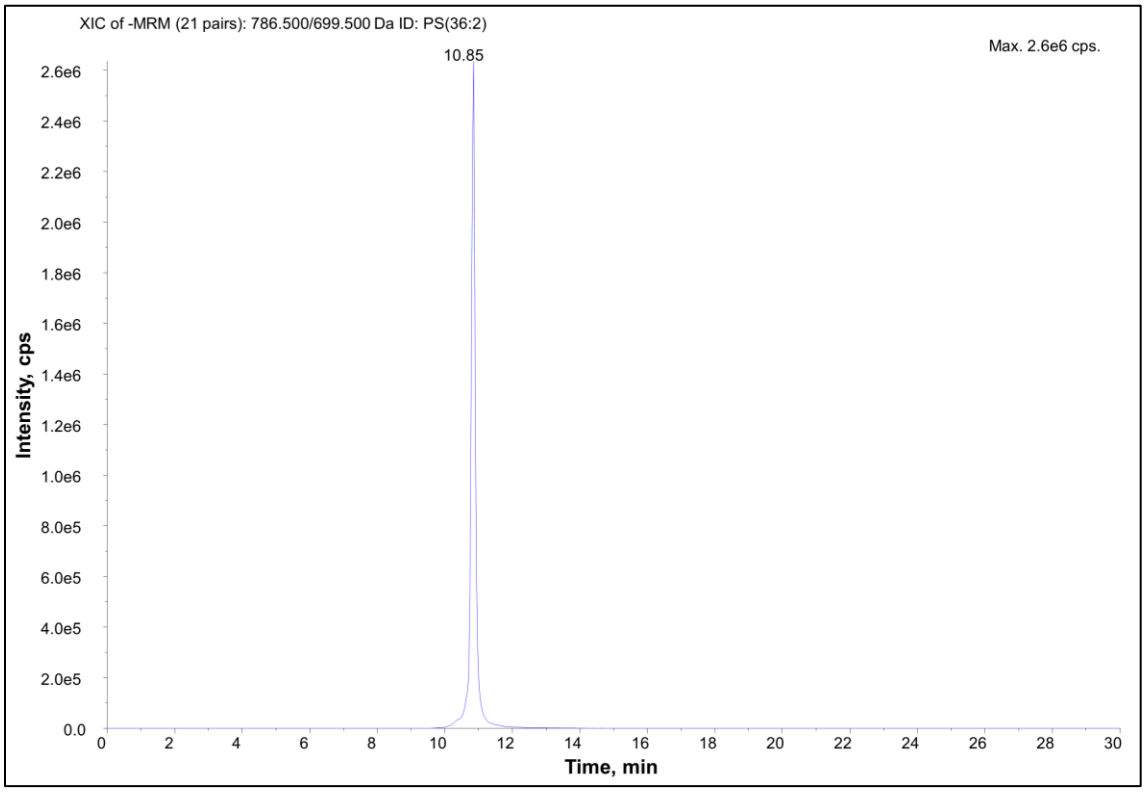

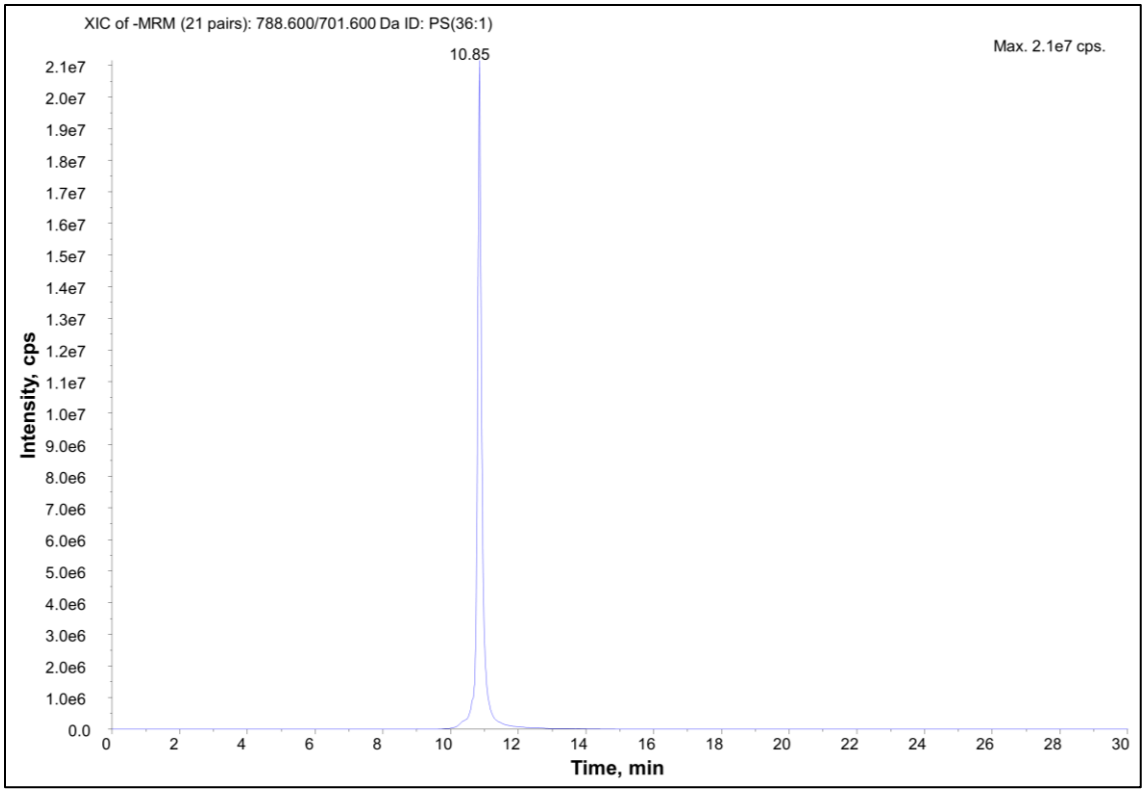
XIC of -MRM (21 pairs): 788.600/701.600 Da ID: PS(36:1)
Max. 2.1e7 cps.
10.85
Intensity, cps
Time, min

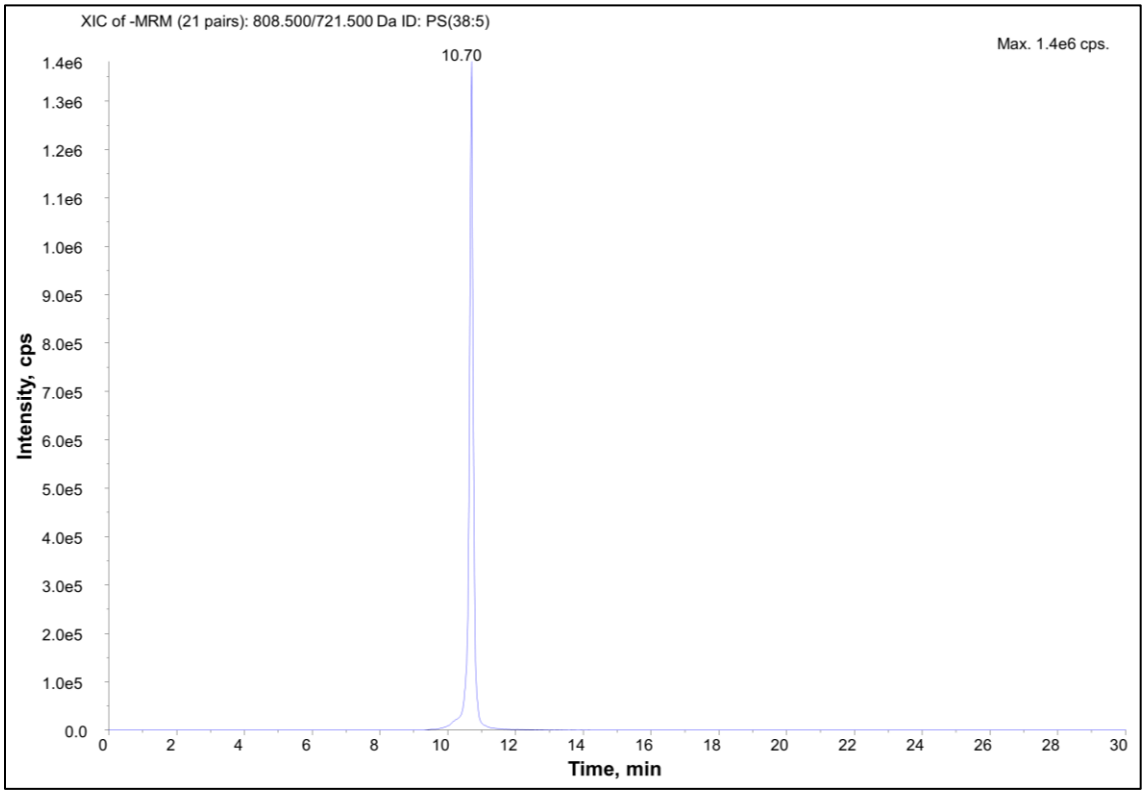
XIC of -MRM (21 pairs): 808.500/721.500 Da ID: PS(38:5)
Max. 1.4e6 cps.
10.70
Intensity, cps
Time, min

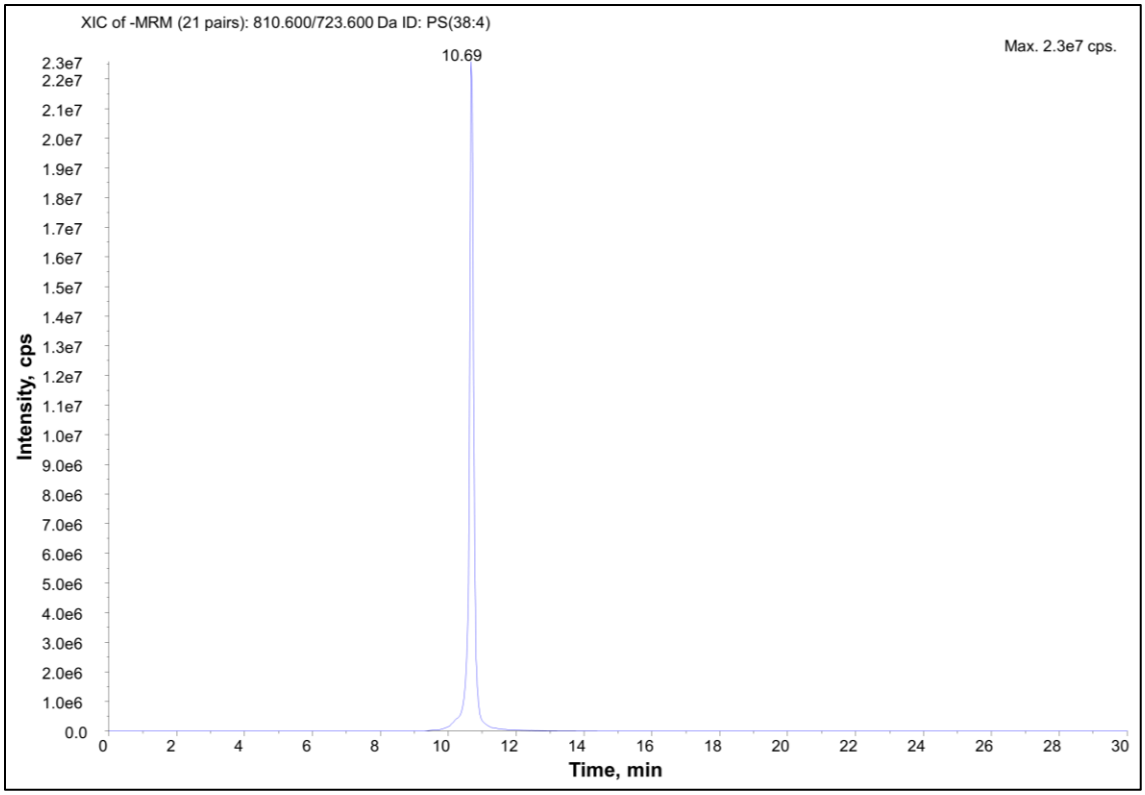
XIC of -MRM (21 pairs): 810.600/723.600 Da ID: PS(38:4)
Max. 2.3e7 cps.
10.69
Intensity, cps
Time, min

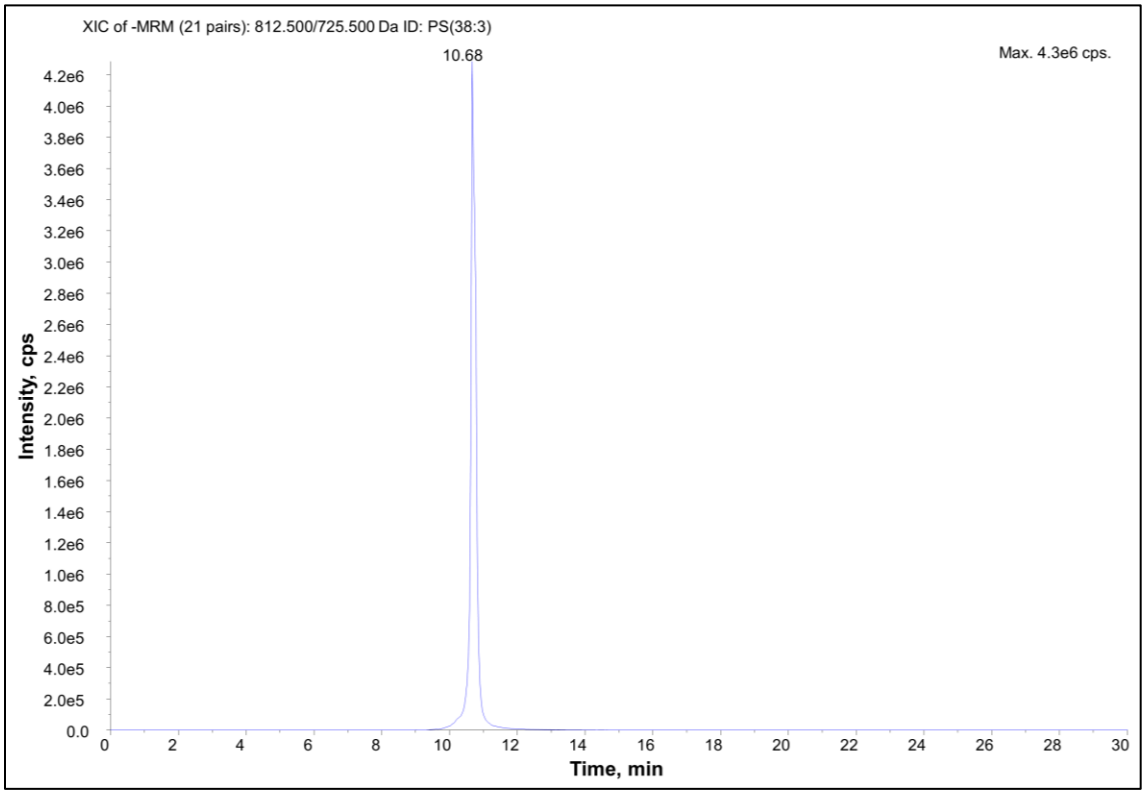
XIC of -MRM (21 pairs): 812.500/725.500 Da ID: PS(38:3)
Max. 4.3e6 cps.
10.68
Intensity, cps
Time, min

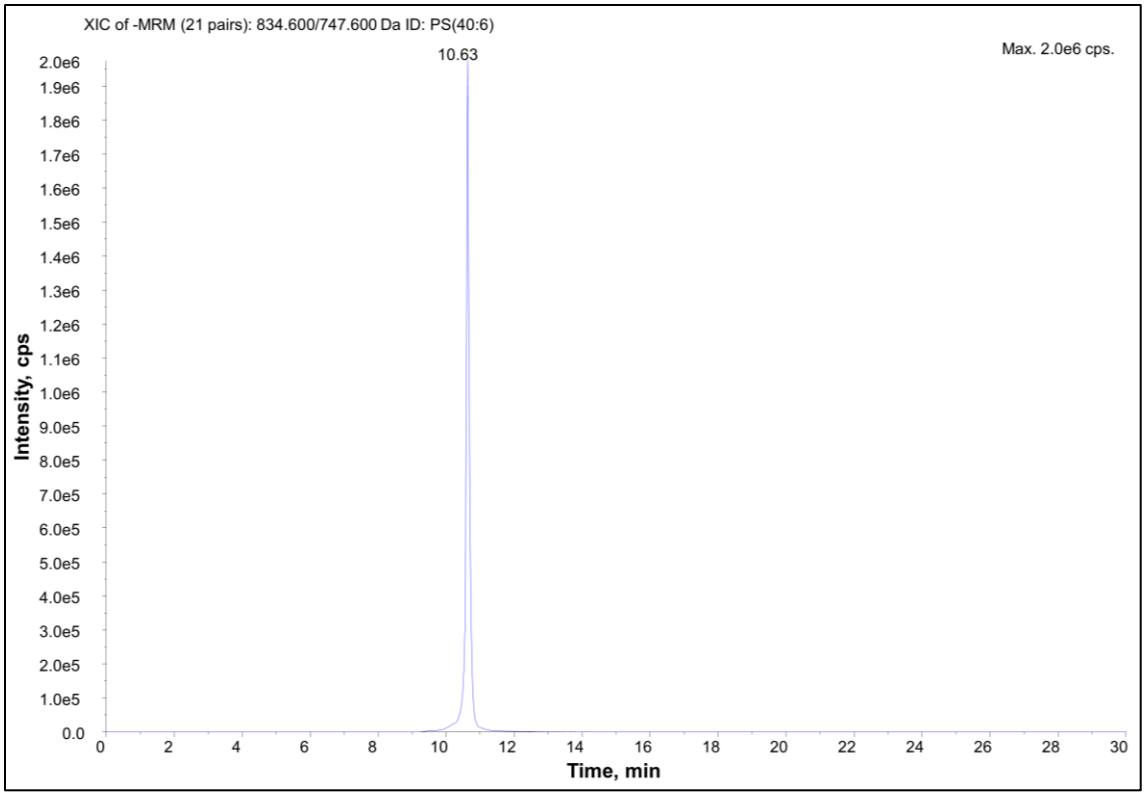
XIC of -MRM (21 pairs): 834.600/747.600 Da ID: PS(40:6)
Max. 2.0e6 cps.
10.63
Intensity, cps
Time, min

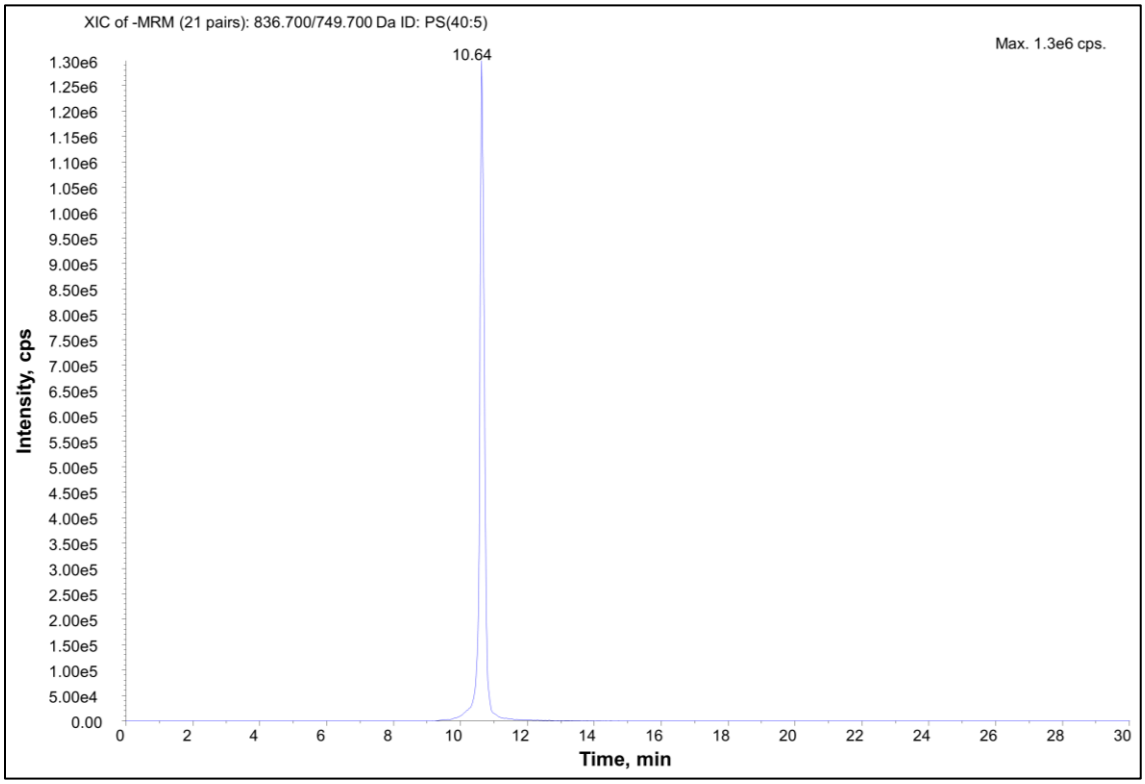
XIC of -MRM (21 pairs): 836.700/749.700 Da ID: PS(40:5)
Max. 1.3e6 cps.
10.64
Intensity, cps
Time, min

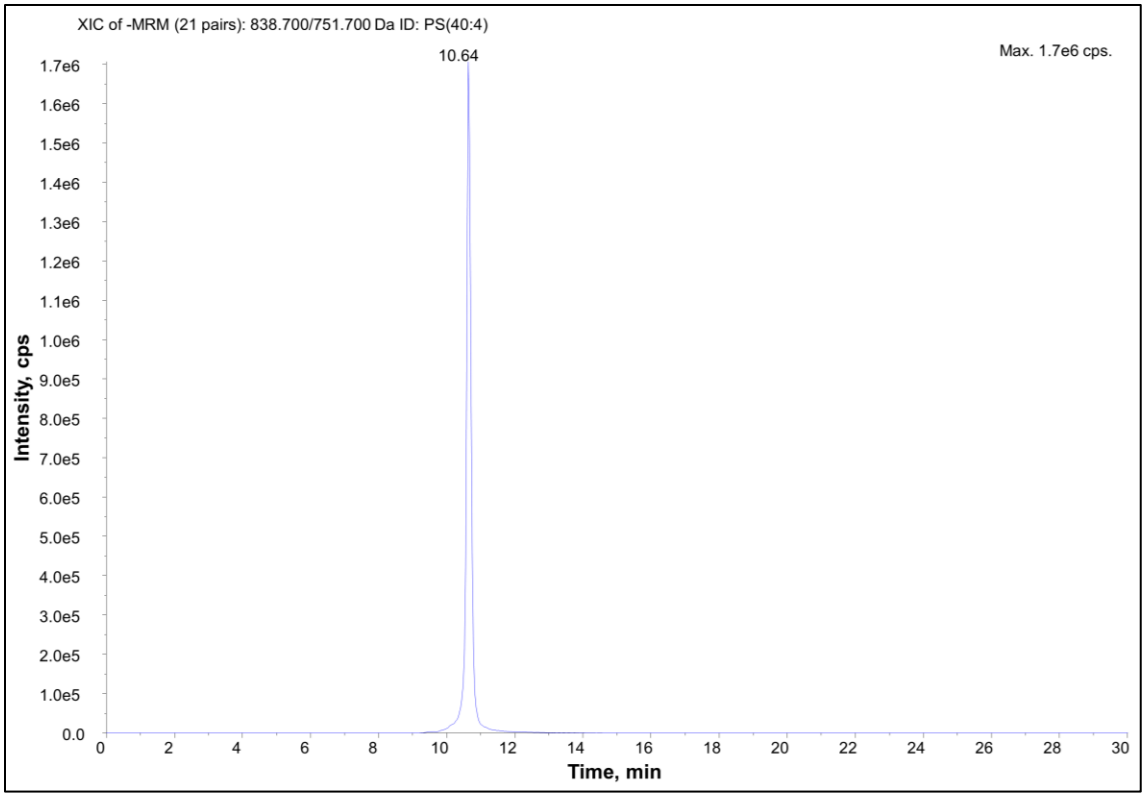
XIC of -MRM (21 pairs): 838.700/751.700 Da ID: PS(40:4)
Max. 1.7e6 cps.
10.64
Intensity, cps
1.7e6
1.6e6
1.5e6
1.4e6
1.3e6
1.2e6
1.1e6
1.0e6
9.0e5
8.0e5
7.0e5
6.0e5
5.0e5
4.0e5
3.0e5
2.0e5
1.0e5
0.0
0
2
4
6
8
10
12
14
16
18
20
22
24
26
28
30
Time, min

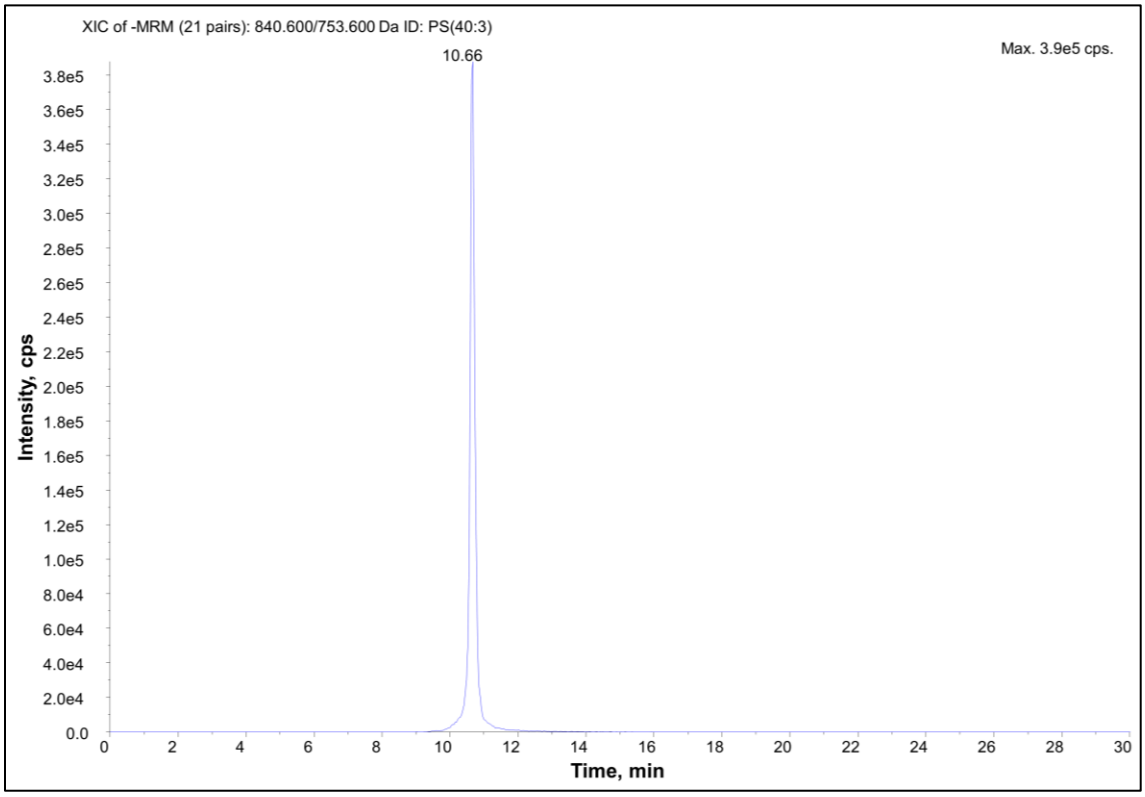
XIC of -MRM (21 pairs): 840.600/753.600 Da ID: PS(40:3)
Max. 3.9e5 cps.
10.66
Intensity, cps
3.8e5
3.6e5
3.4e5
3.2e5
3.0e5
2.8e5
2.6e5
2.4e5
2.2e5
2.0e5
1.8e5
1.6e5
1.4e5
1.2e5
1.0e5
8.0e4
6.0e4
4.0e4
2.0e4
0.0
0
2
4
6
8
10
12
14
16
18
20
22
24
26
28
30
Time, min

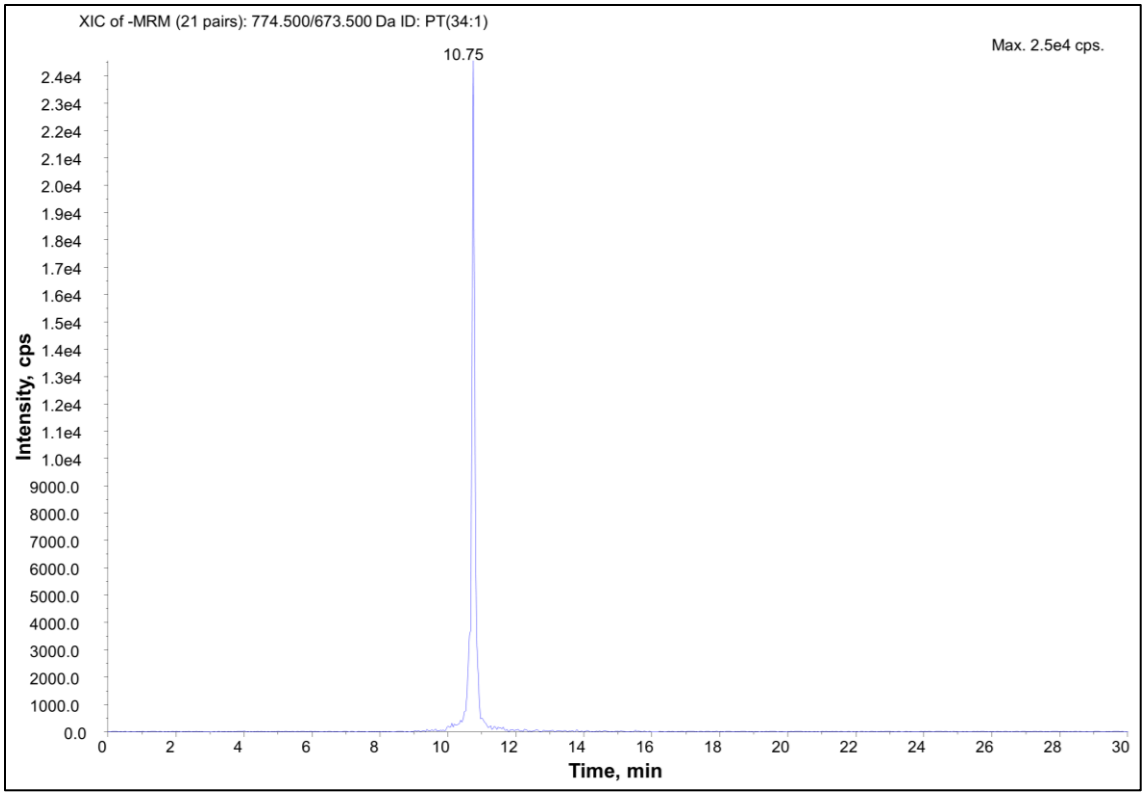
XIC of -MRM (21 pairs): 774.500/673.500 Da ID: PT(34:1)
Max. 2.5e4 cps.
10.75
Intensity, cps
Time, min

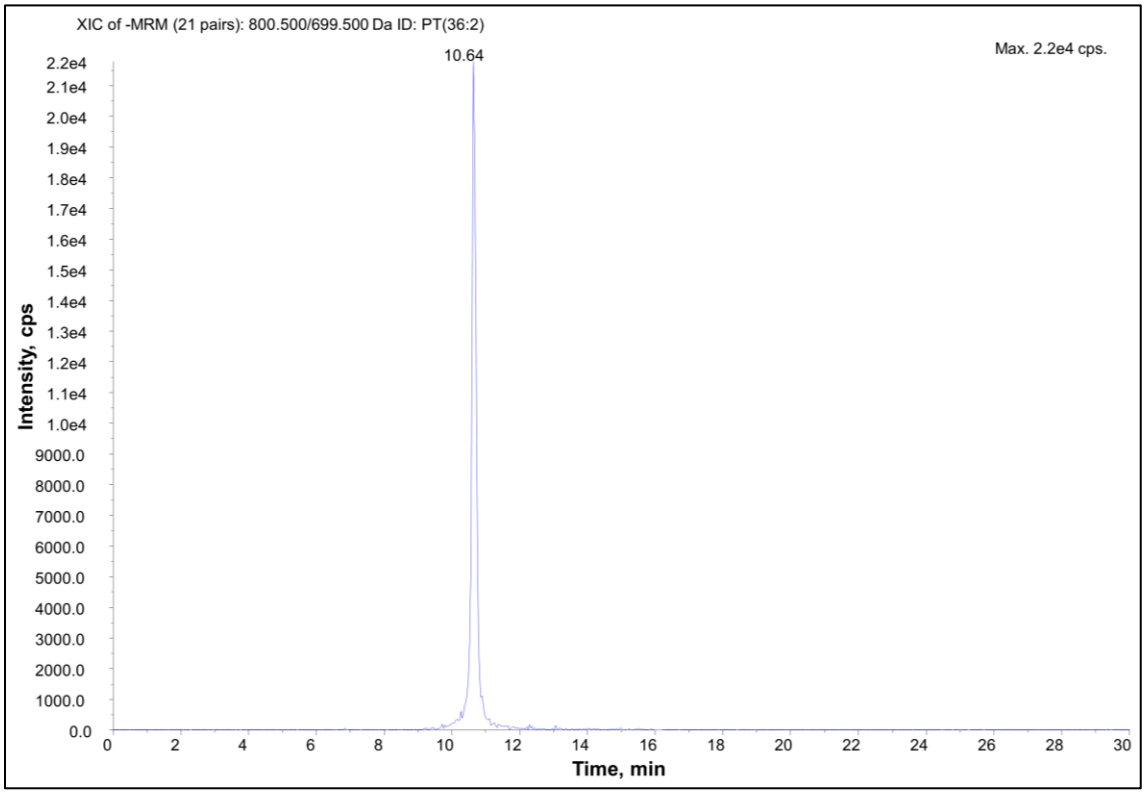
XIC of -MRM (21 pairs): 800.500/699.500 Da ID: PT(36:2)
Max. 2.2e4 cps.
10.64
Intensity, cps
Time, min

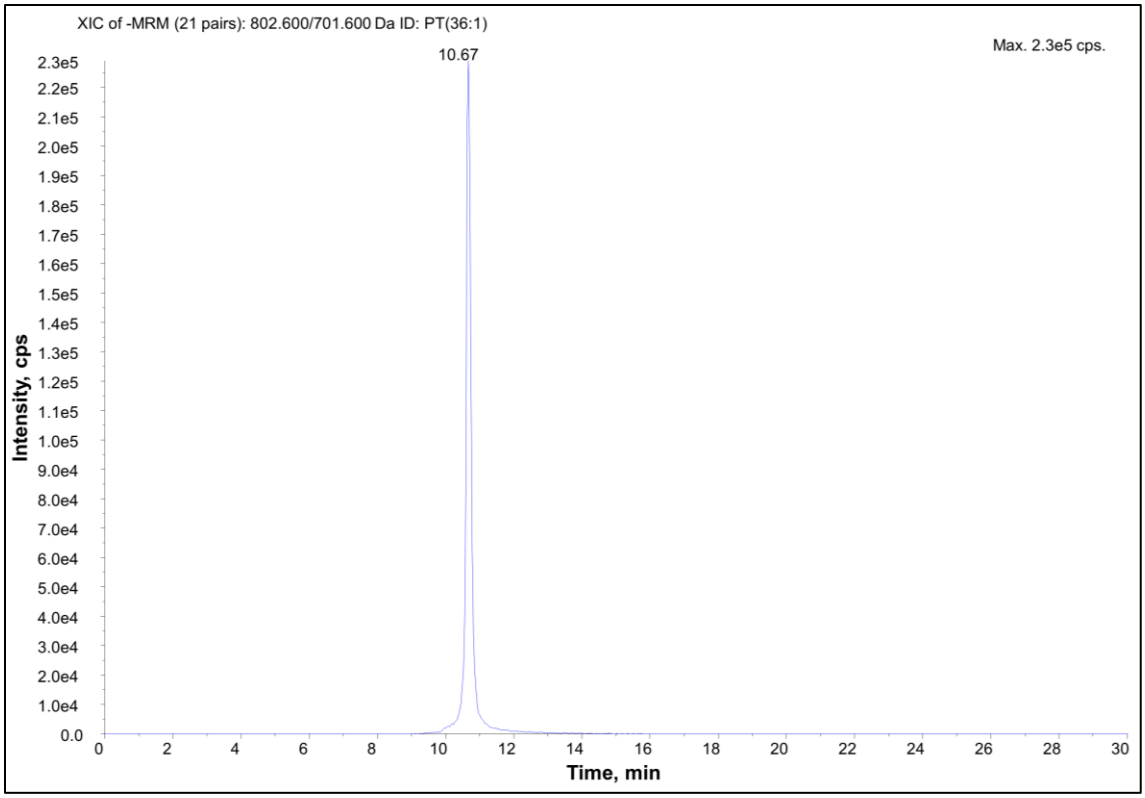
XIC of -MRM (21 pairs): 802.600/701.600 Da ID: PT(36:1)
Max. 2.3e5 cps.
10.67
Intensity, cps
Time, min

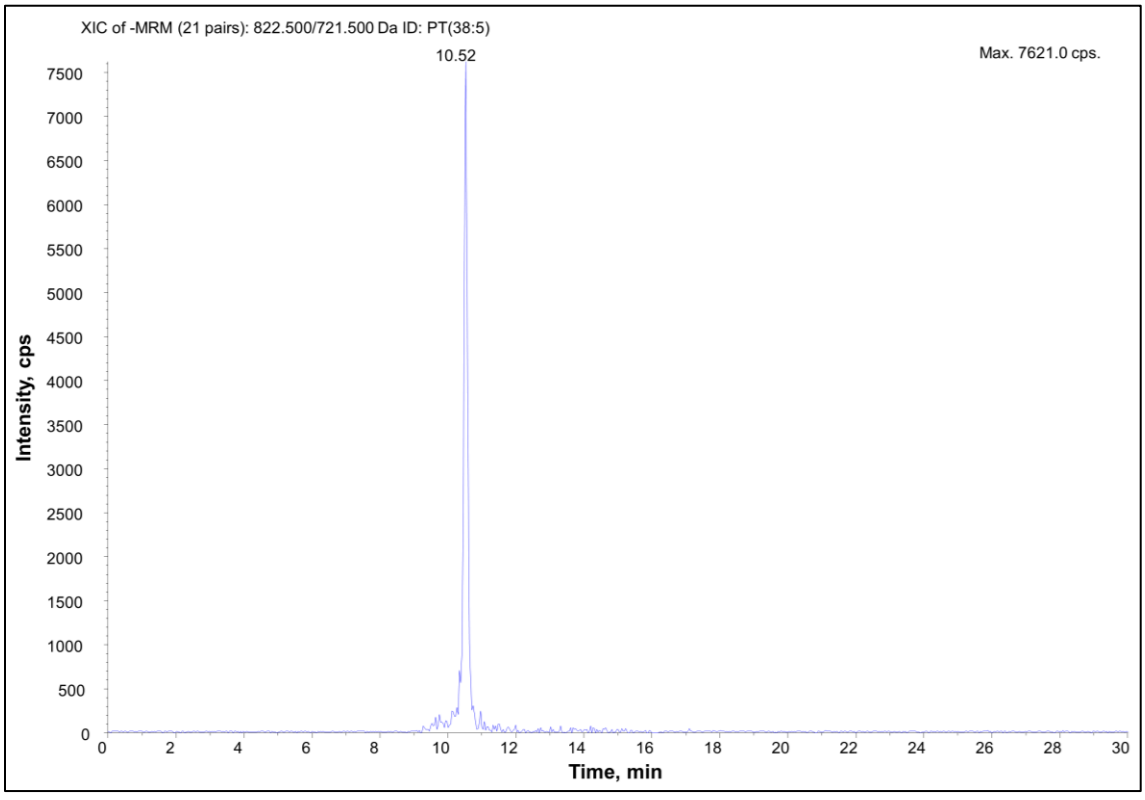
XIC of -MRM (21 pairs): 822.500/721.500 Da ID: PT(38:5)
Max. 7621.0 cps.
10.52
Intensity, cps
Time, min

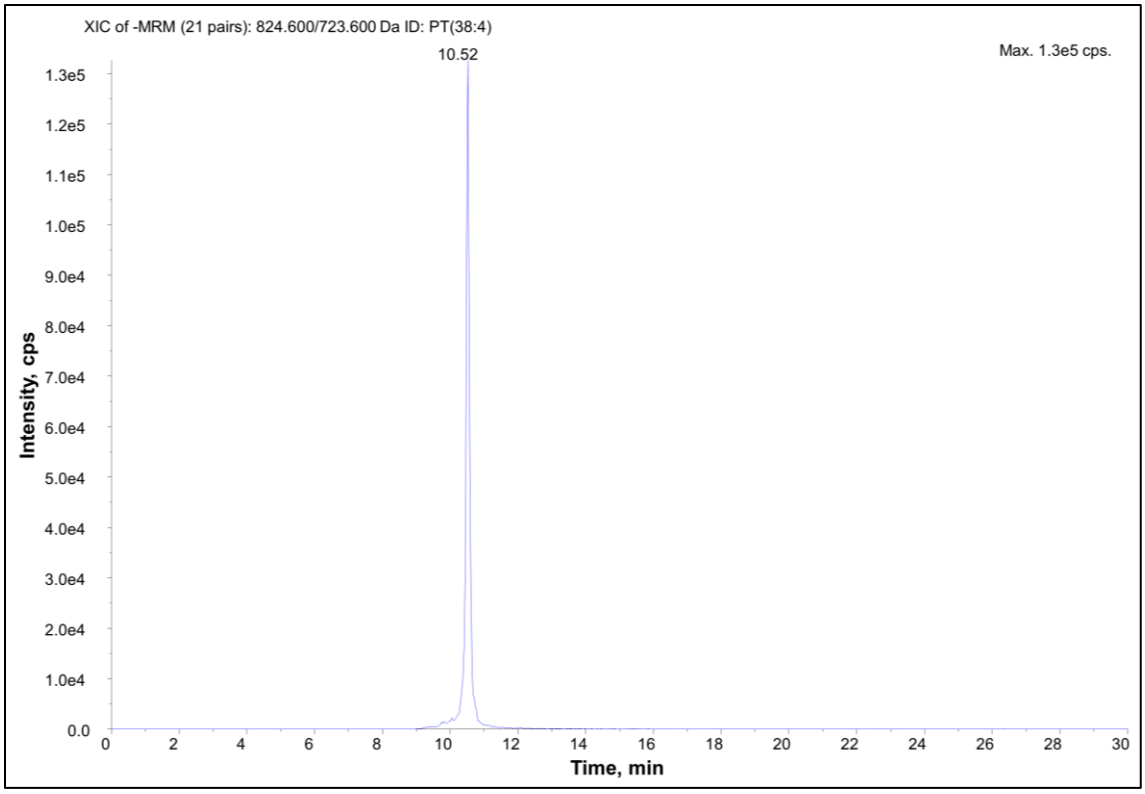
XIC of -MRM (21 pairs): 824.600/723.600 Da ID: PT(38:4)
10.52
Max. 1.3e5 cps.
Intensity, cps
1.3e5
1.2e5
1.1e5
1.0e5
9.0e4
8.0e4
7.0e4
6.0e4
5.0e4
4.0e4
3.0e4
2.0e4
1.0e4
0.0
0 2 4 6 8 10 12 14 16 18 20 22 24 26 28 30
Time, min

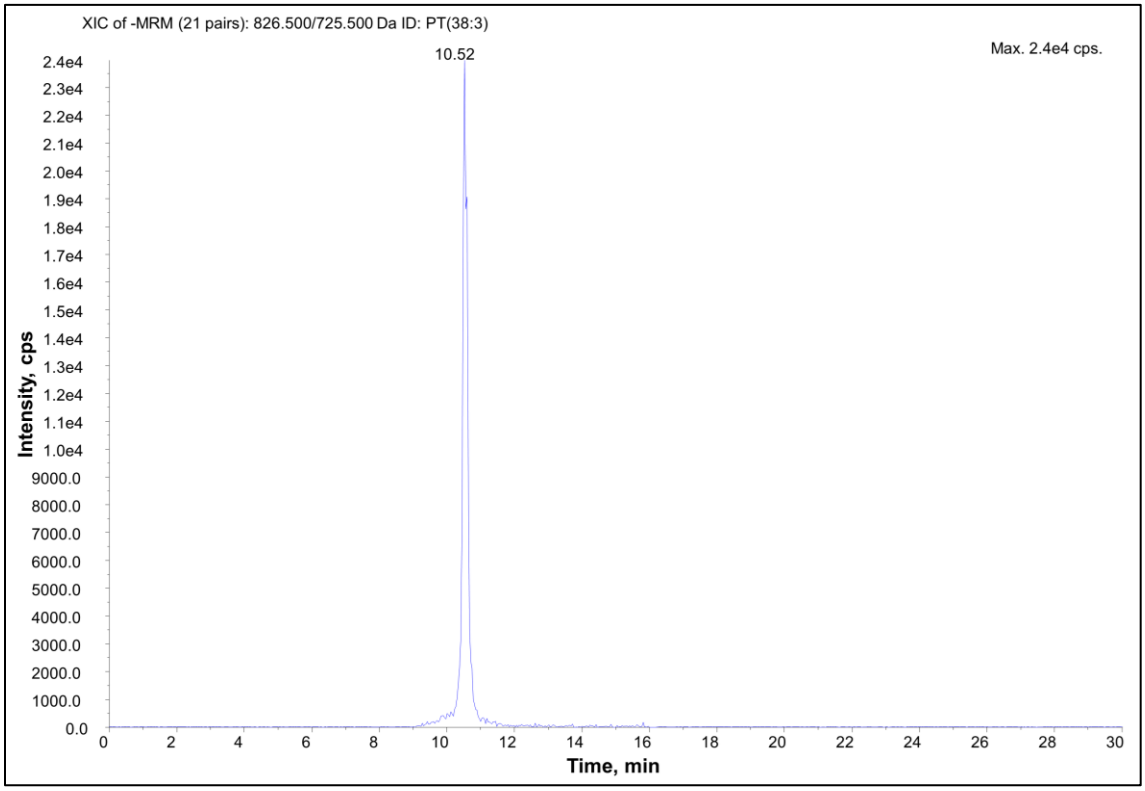
XIC of -MRM (21 pairs): 826.500/725.500 Da ID: PT(38:3)
10.52
Max. 2.4e4 cps.
Intensity, cps
2.4e4
2.3e4
2.2e4
2.1e4
2.0e4
1.9e4
1.8e4
1.7e4
1.6e4
1.5e4
1.4e4
1.3e4
1.2e4
1.1e4
1.0e4
9000.0
8000.0
7000.0
6000.0
5000.0
4000.0
3000.0
2000.0
1000.0
0.0
0 2 4 6 8 10 12 14 16 18 20 22 24 26 28 30
Time, min

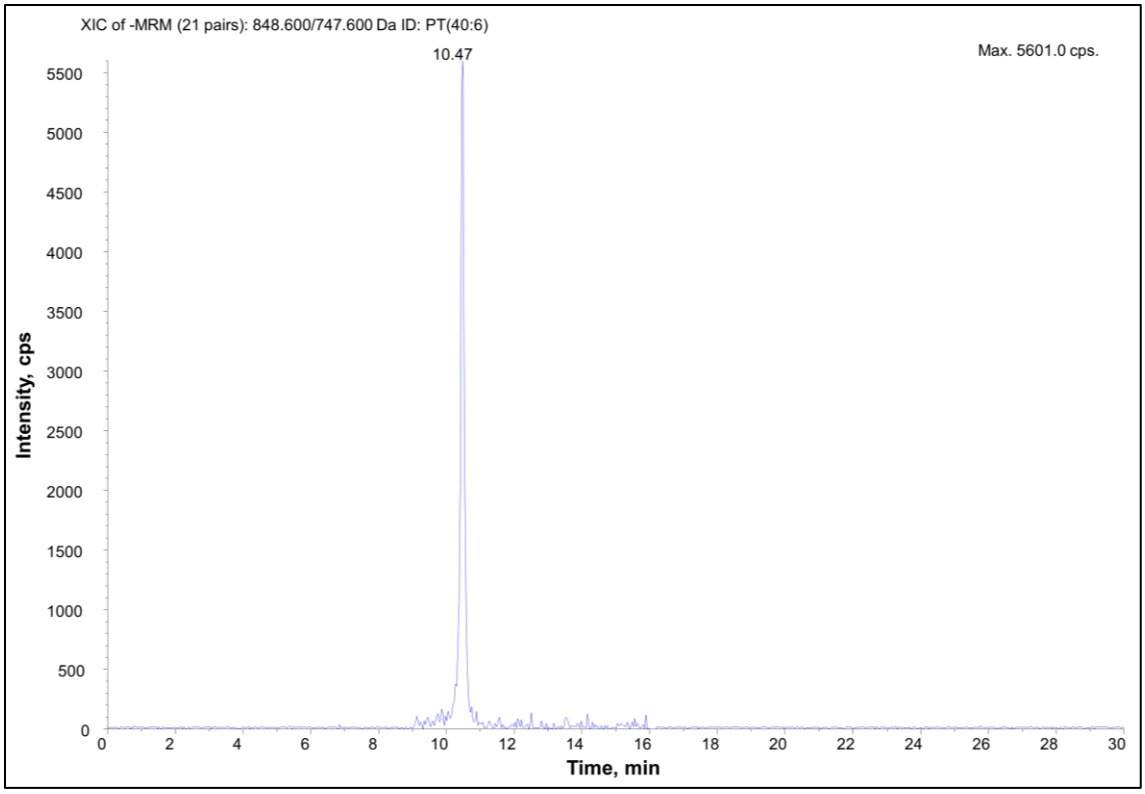
XIC of -MRM (21 pairs): 848.600/747.600 Da ID: PT(40:6)
10.47
Max. 5601.0 cps.
Intensity, cps
Time, min

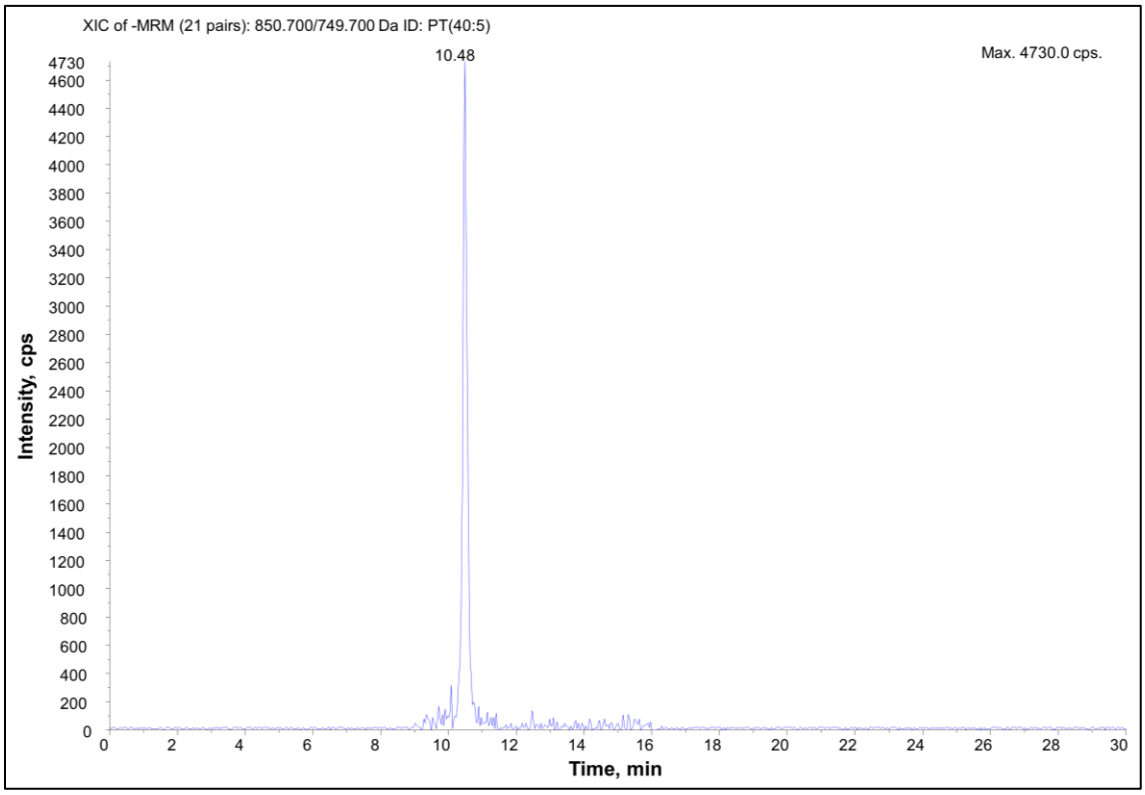
XIC of -MRM (21 pairs): 850.700/749.700 Da ID: PT(40:5)
10.48
Max. 4730.0 cps.
Intensity, cps
Time, min

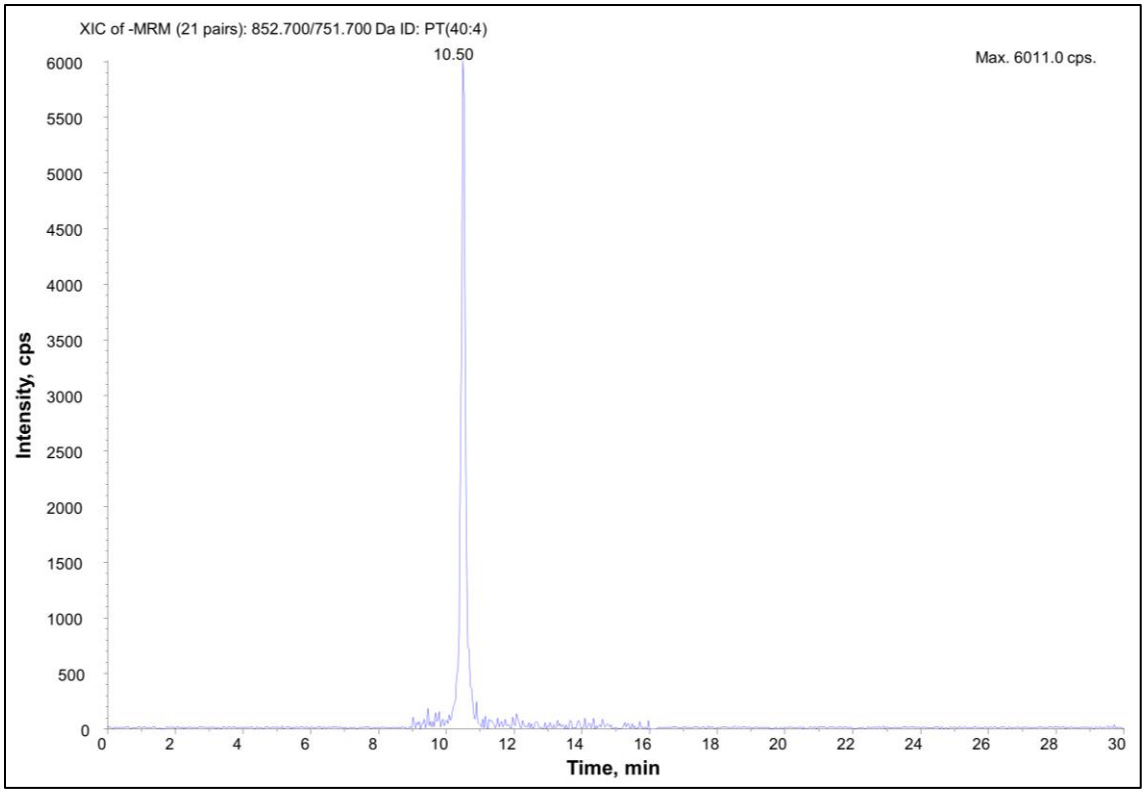
XIC of -MRM (21 pairs): 852.700/751.700 Da ID: PT(40:4)
10.50
Max. 6011.0 cps.
Intensity, cps
Time, min

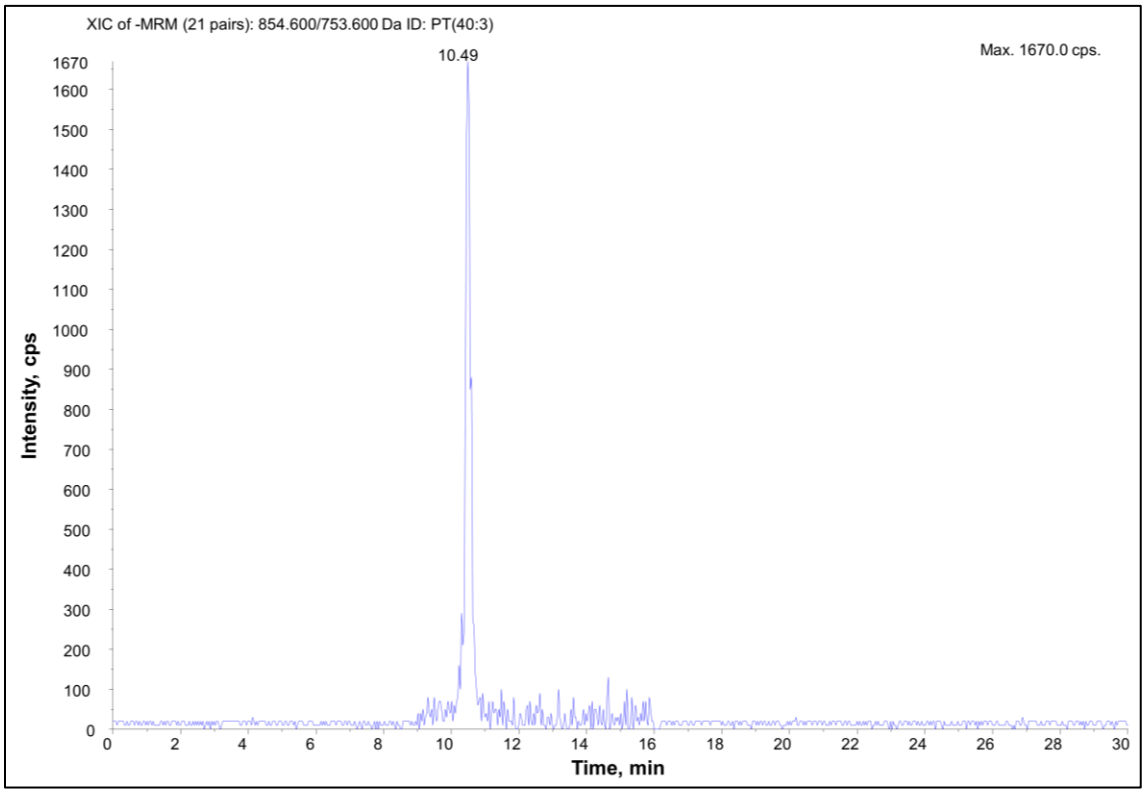
XIC of -MRM (21 pairs): 854.600/753.600 Da ID: PT(40:3)
10.49
Max. 1670.0 cps.
Intensity, cps
Time, min

## 9.8 Representative chromatograms (RP-LC-MS/MS of biotinylated phospholipids)

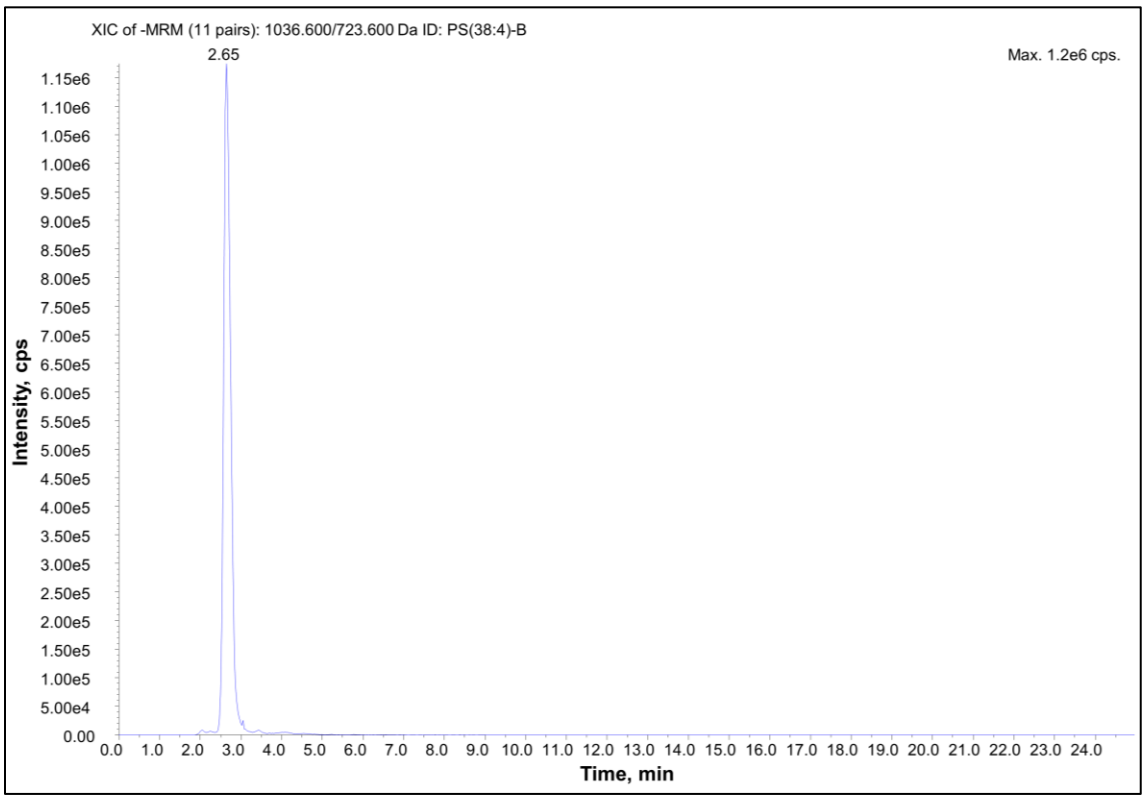


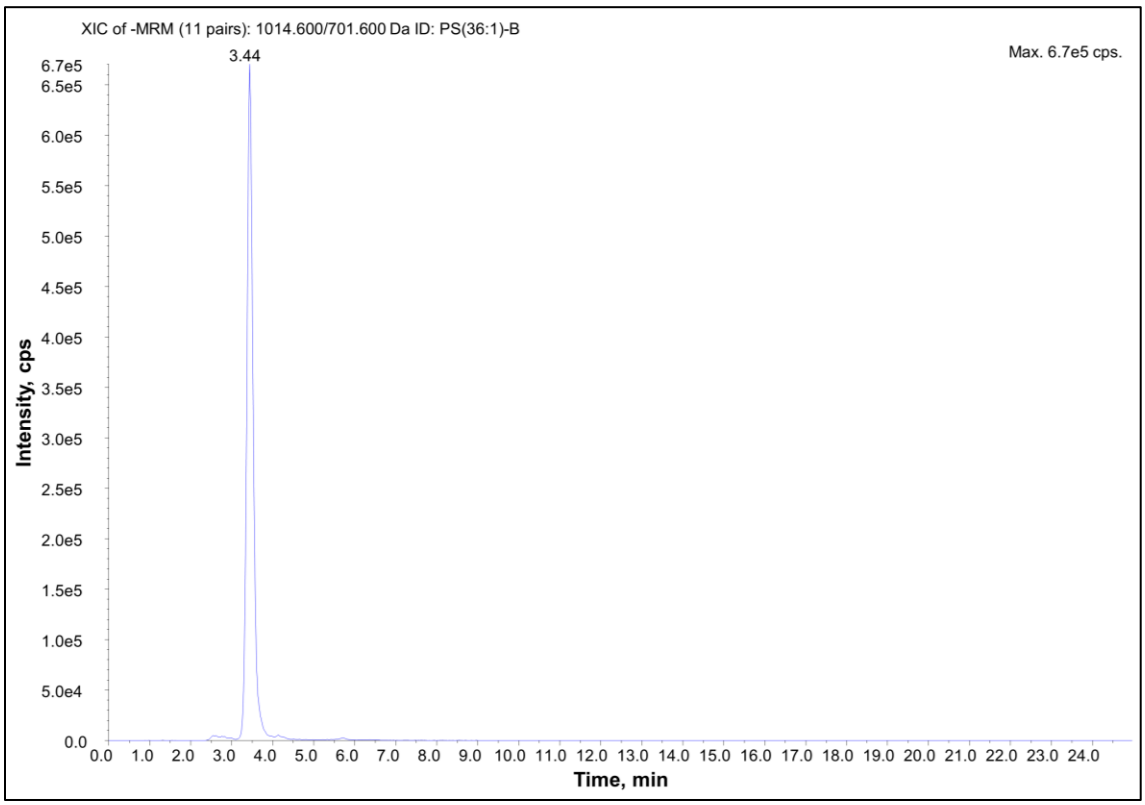

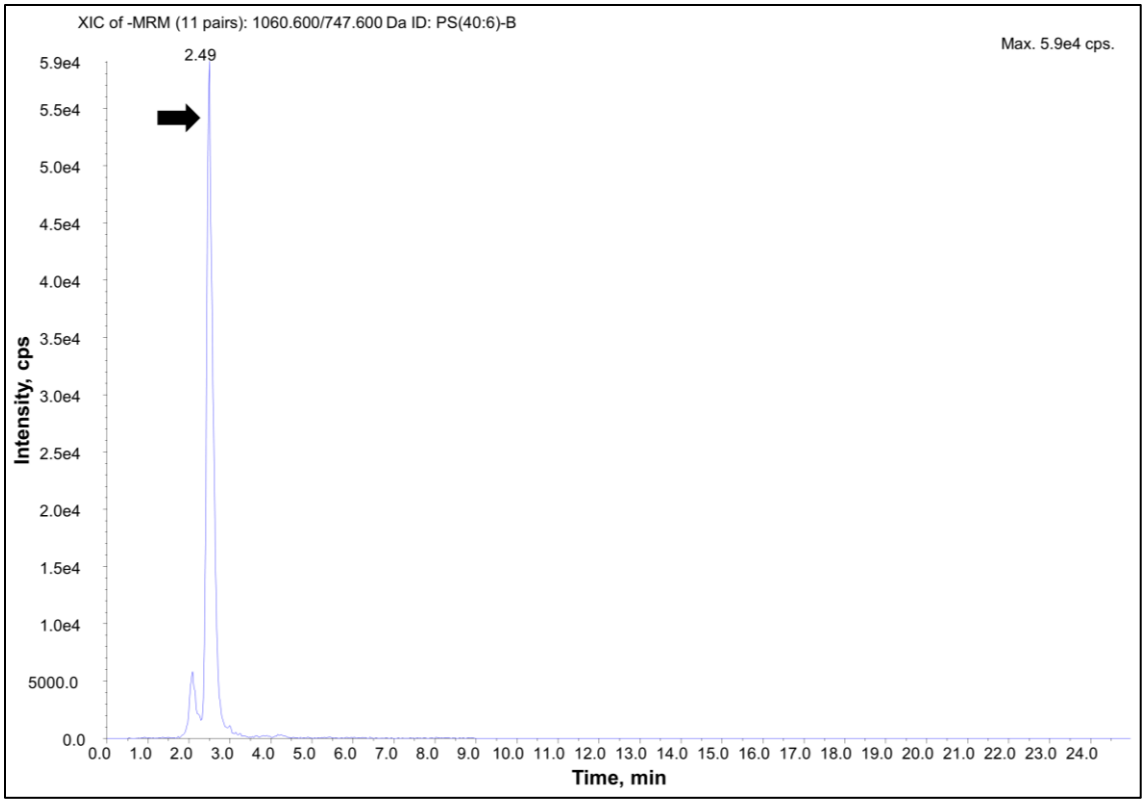
XIC of -MRM (11 pairs): 1060.600/747.600 Da ID: PS(40:6)-B
Max. 5.9e4 cps.
2.49
Intensity, cps
Time, min

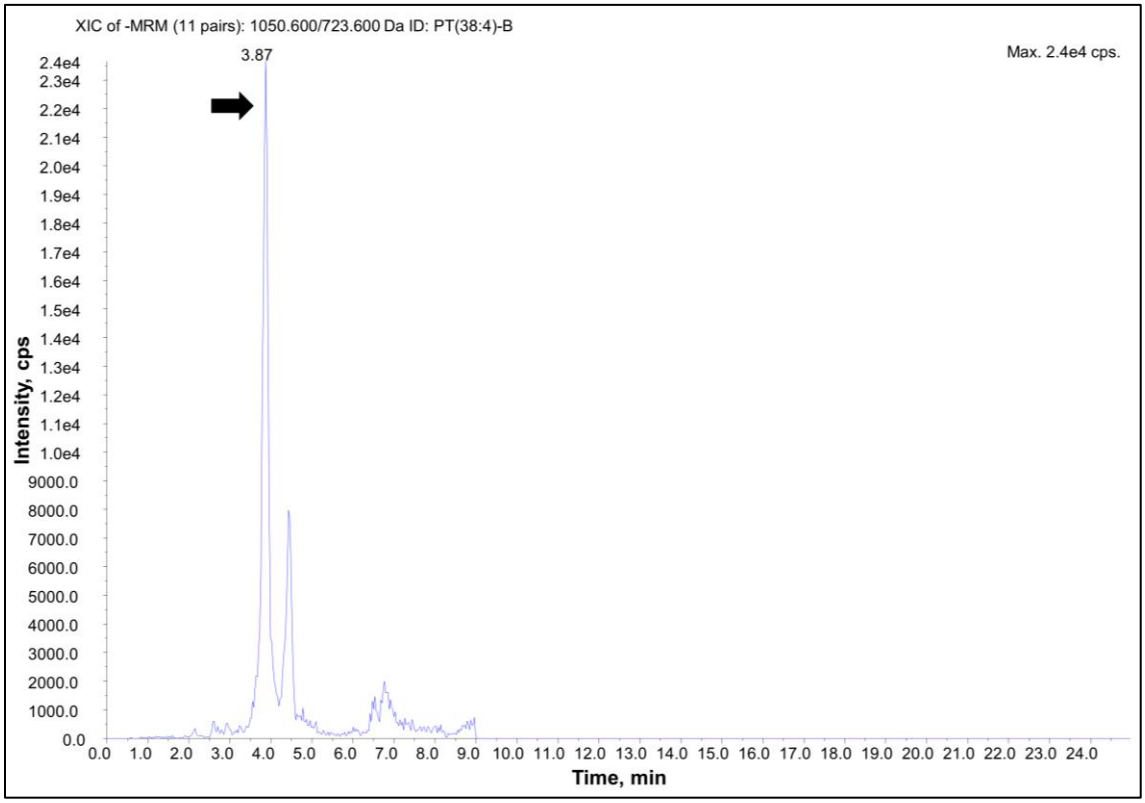
XIC of -MRM (11 pairs): 1050.600/723.600 Da ID: PT(38:4)-B
Max. 2.4e4 cps.
3.87
Intensity, cps
Time, min

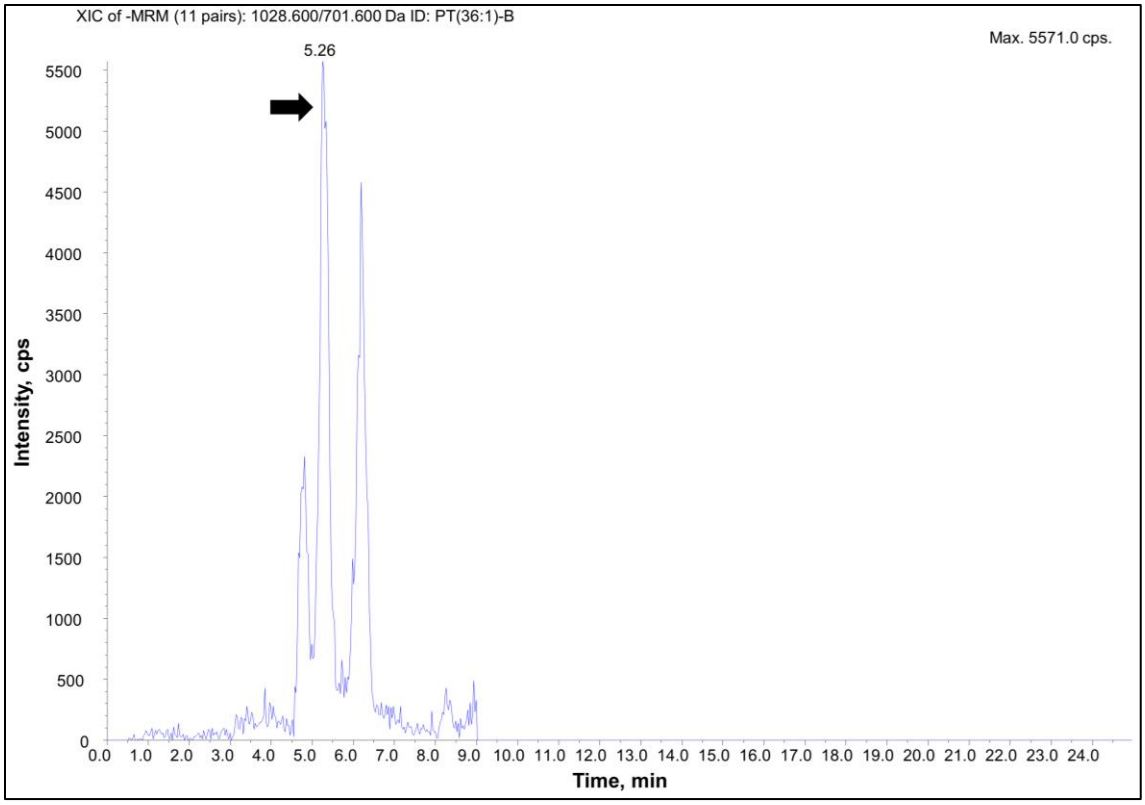
XIC of -MRM (11 pairs): 1028.600/701.600 Da ID: PT(36:1)-B
Max. 5571.0 cps.
5.26
Intensity, cps
Time, min

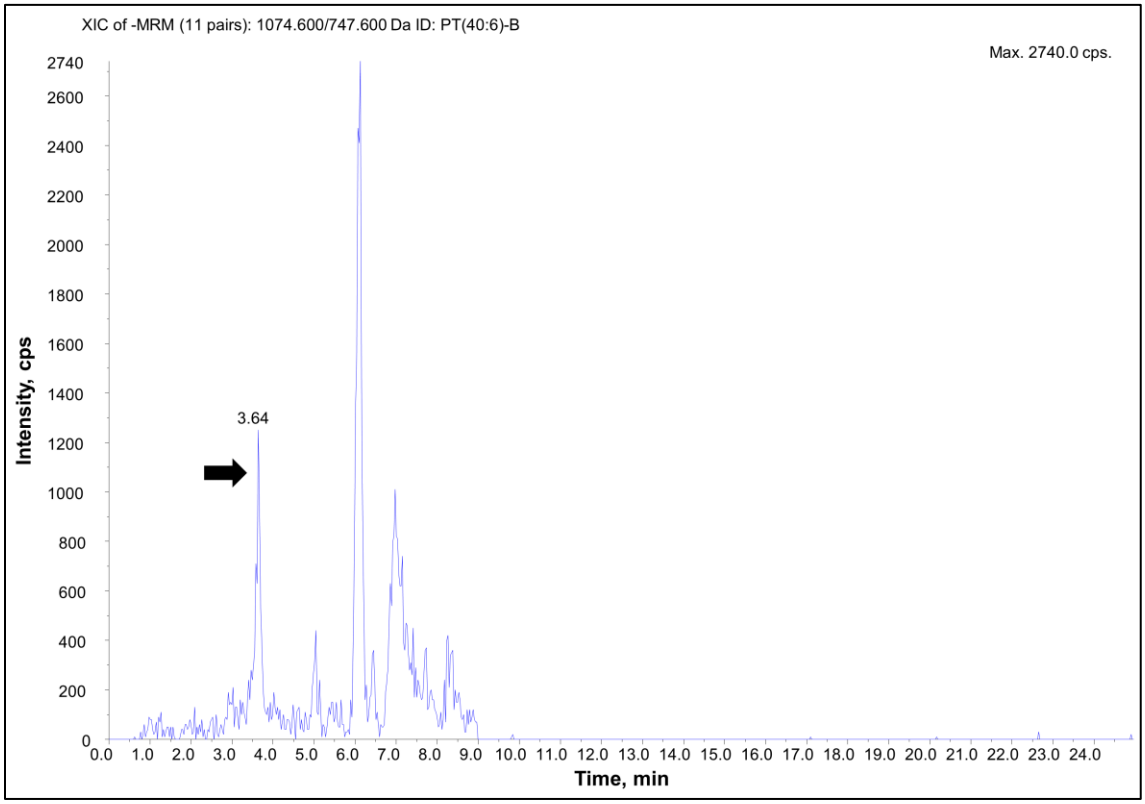
XIC of -MRM (11 pairs): 1074.600/747.600 Da ID: PT(40:6)-B
Max. 2740.0 cps.
3.64
Intensity, cps
Time, min

## 9.9 $MS^2$ & $MS^3$ spectra of PS & PT species from platelets

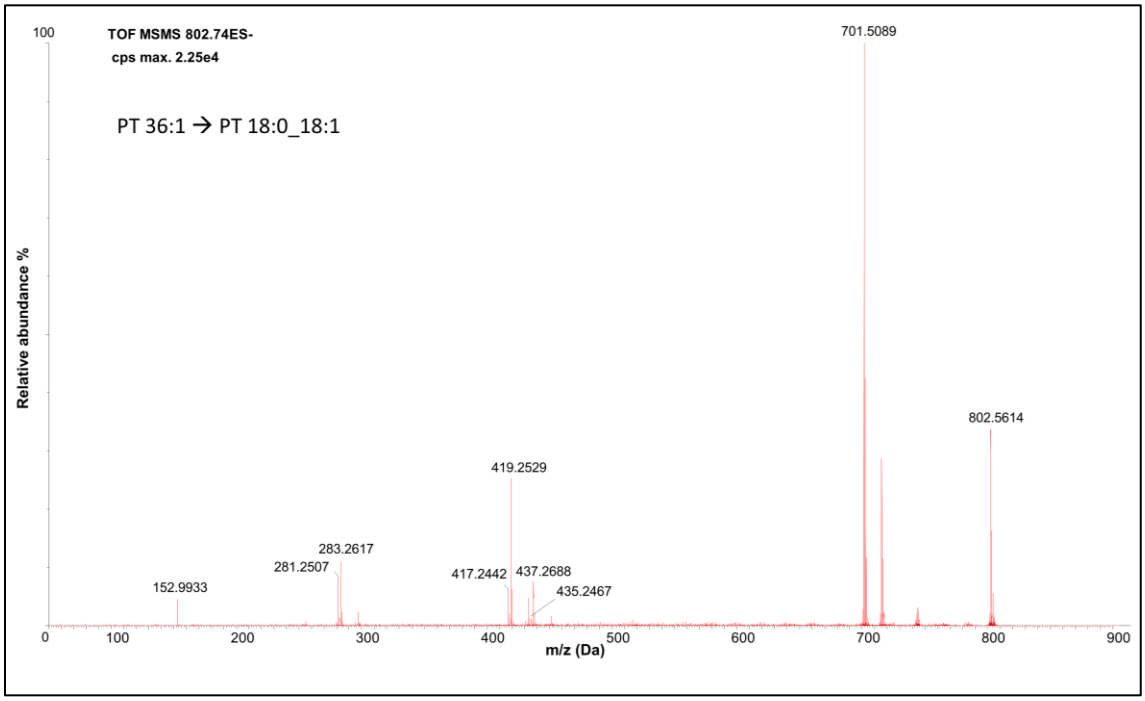


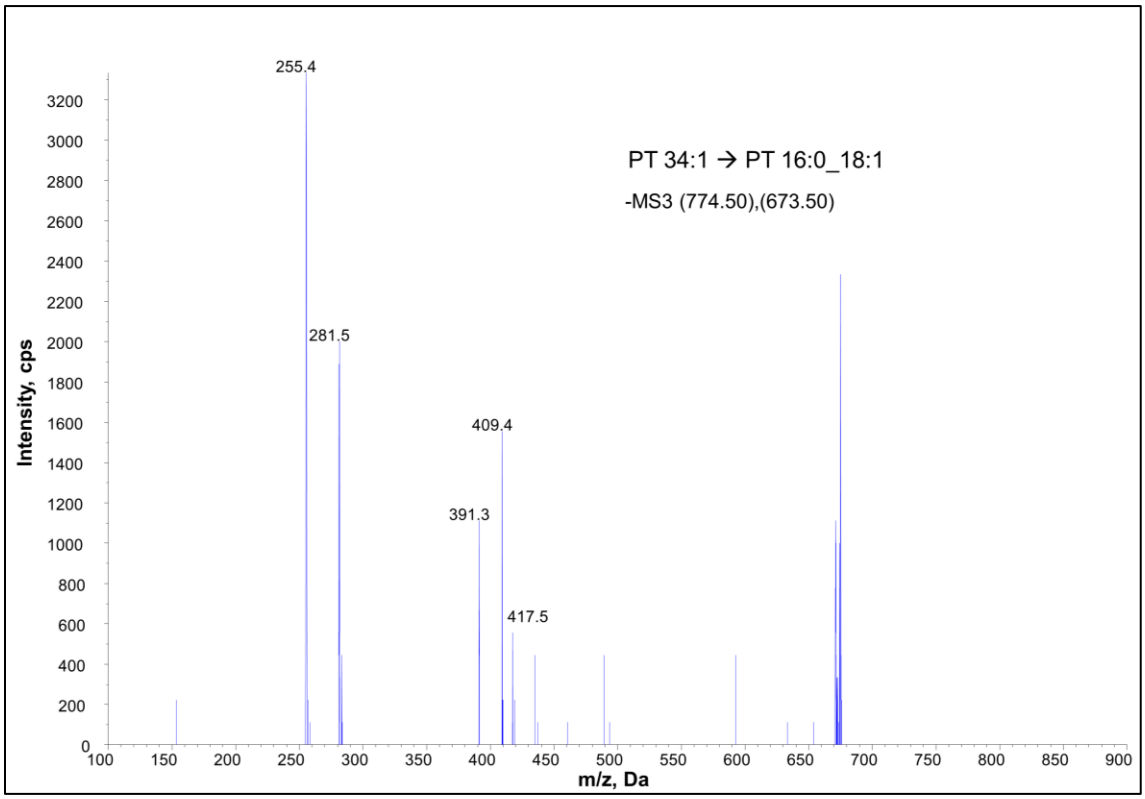

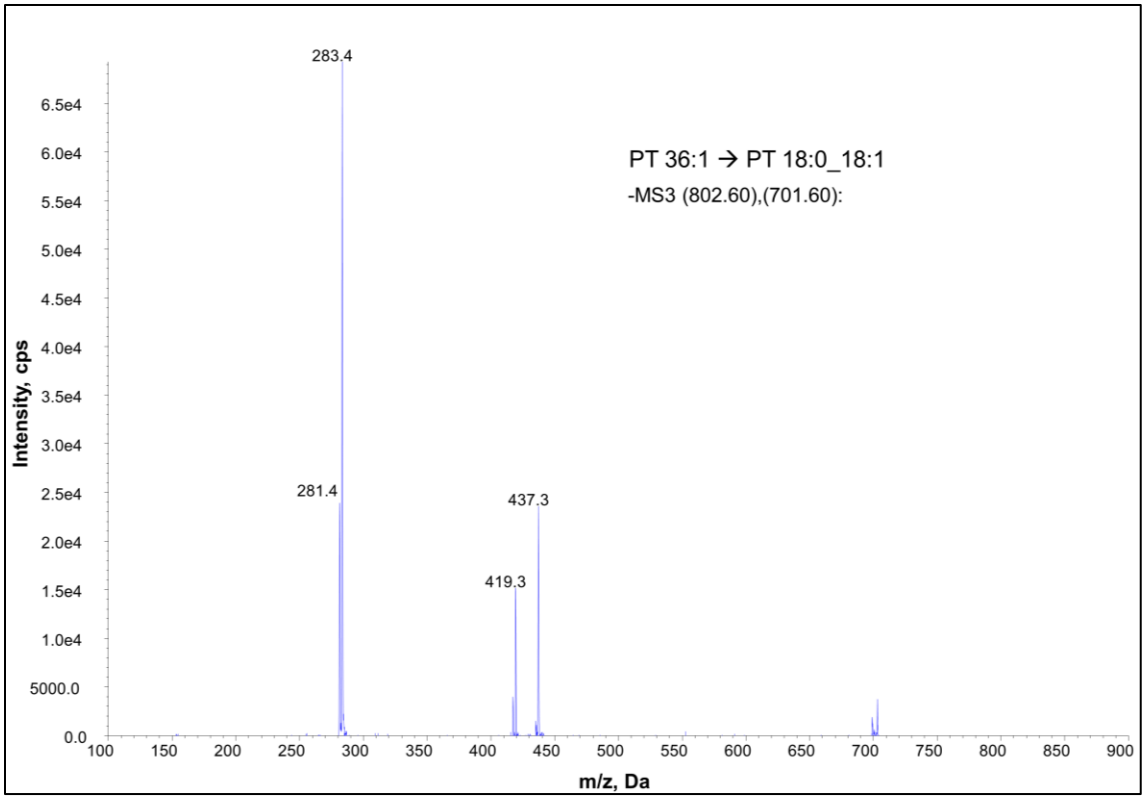
283.4
PT 36:1 → PT 18:0_18:1
-MS3 (802.60),(701.60):
281.4
437.3
419.3
Intensity, cps
m/z, Da

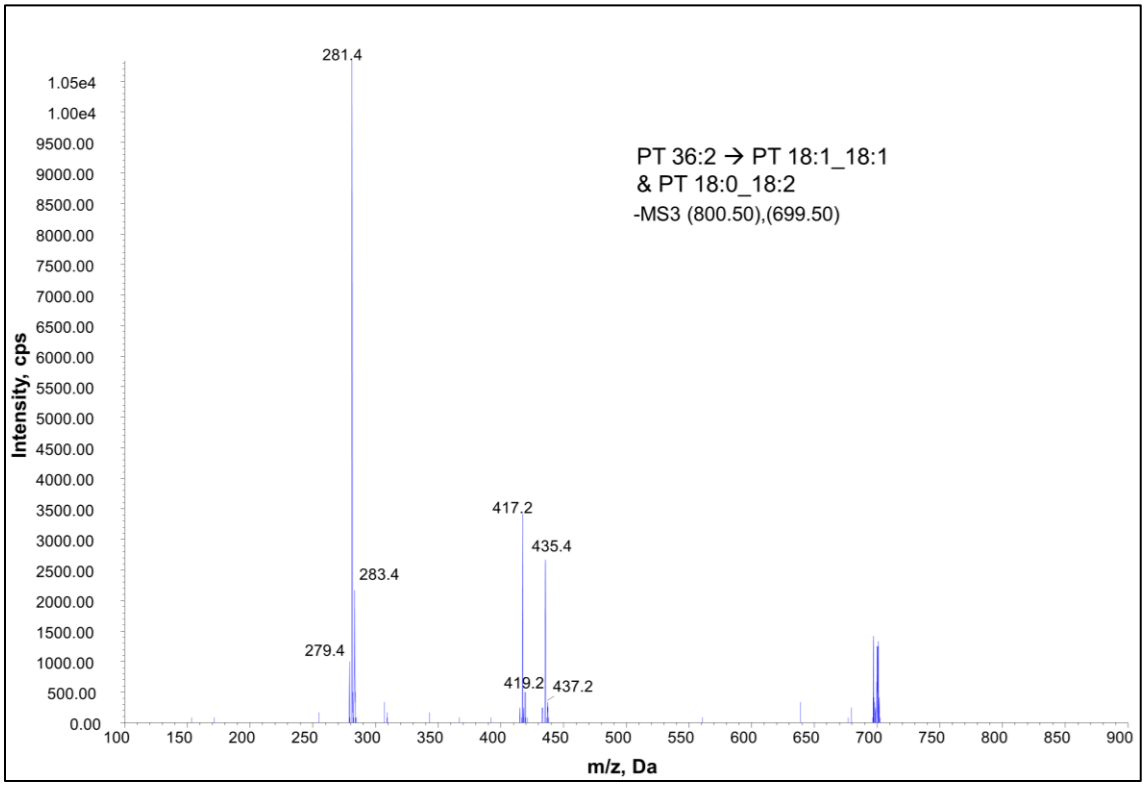
281.4
PT 36:2 → PT 18:1_18:1
& PT 18:0_18:2
-MS3 (800.50),(699.50)
417.2
435.4
283.4
279.4
419.2
437.2
Intensity, cps
m/z, Da

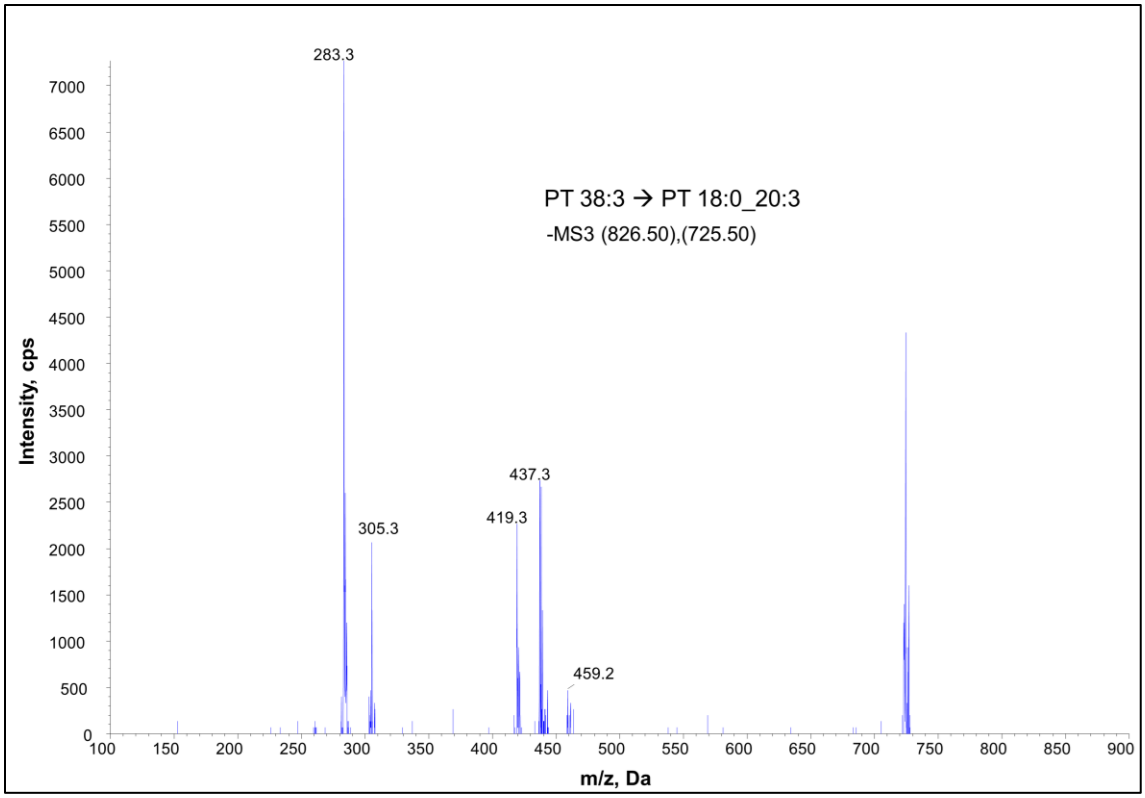
283.3
PT 38:3 → PT 18:0_20:3
-MS3 (826.50),(725.50)
437.3
419.3
305.3
459.2
Intensity, cps
m/z, Da

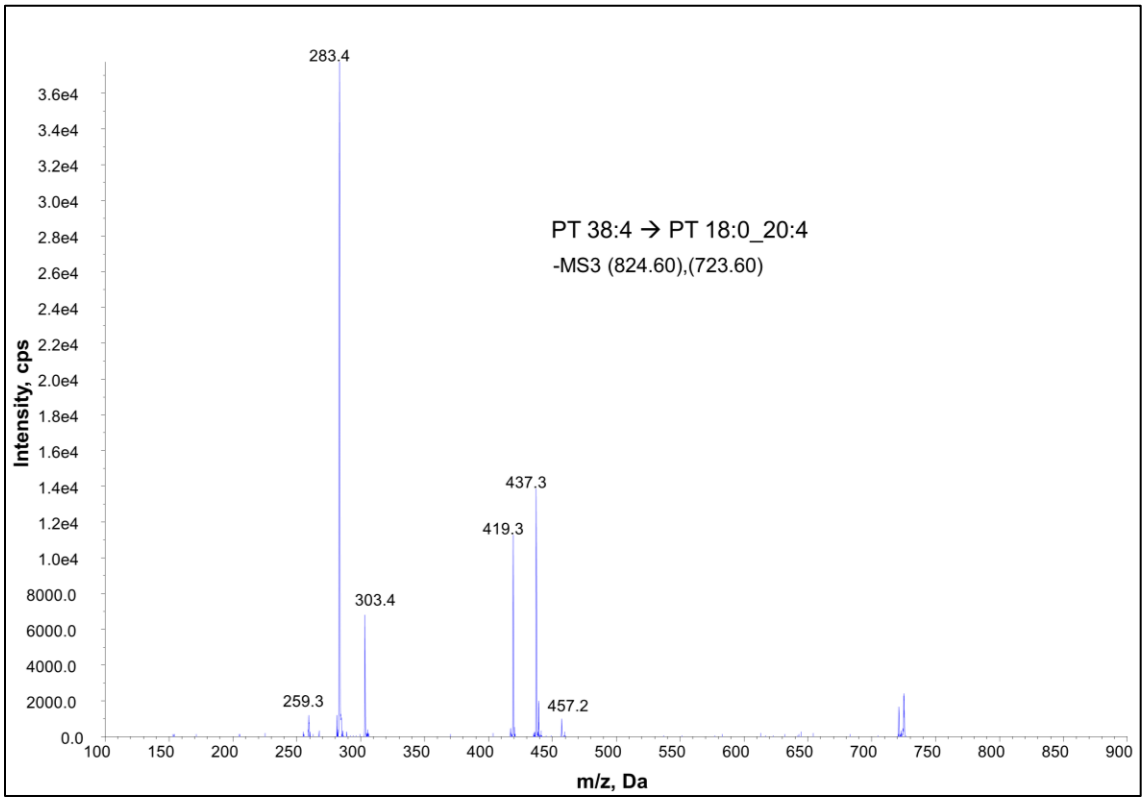
283.4
PT 38:4 → PT 18:0_20:4
-MS3 (824.60),(723.60)
437.3
419.3
303.4
259.3
457.2
Intensity, cps
m/z, Da

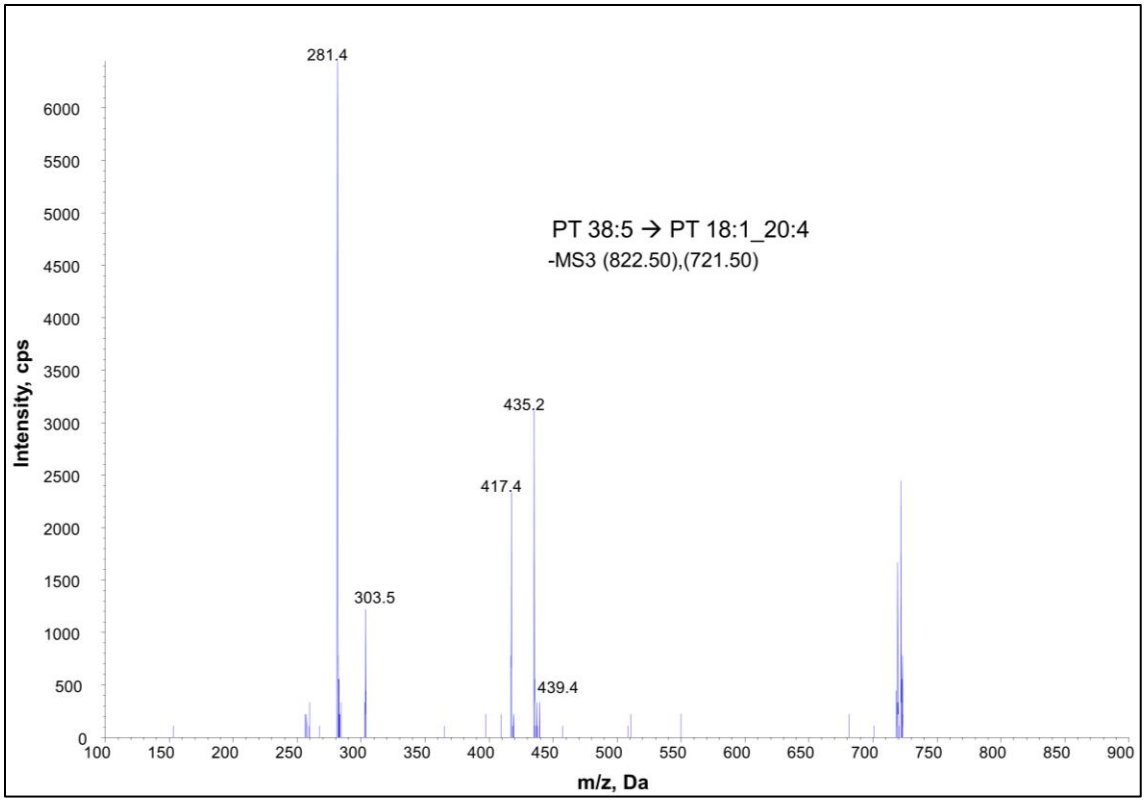
281.4
PT 38:5 → PT 18:1_20:4
-MS3 (822.50),(721.50)
435.2
417.4
303.5
439.4
Intensity, cps
m/z, Da

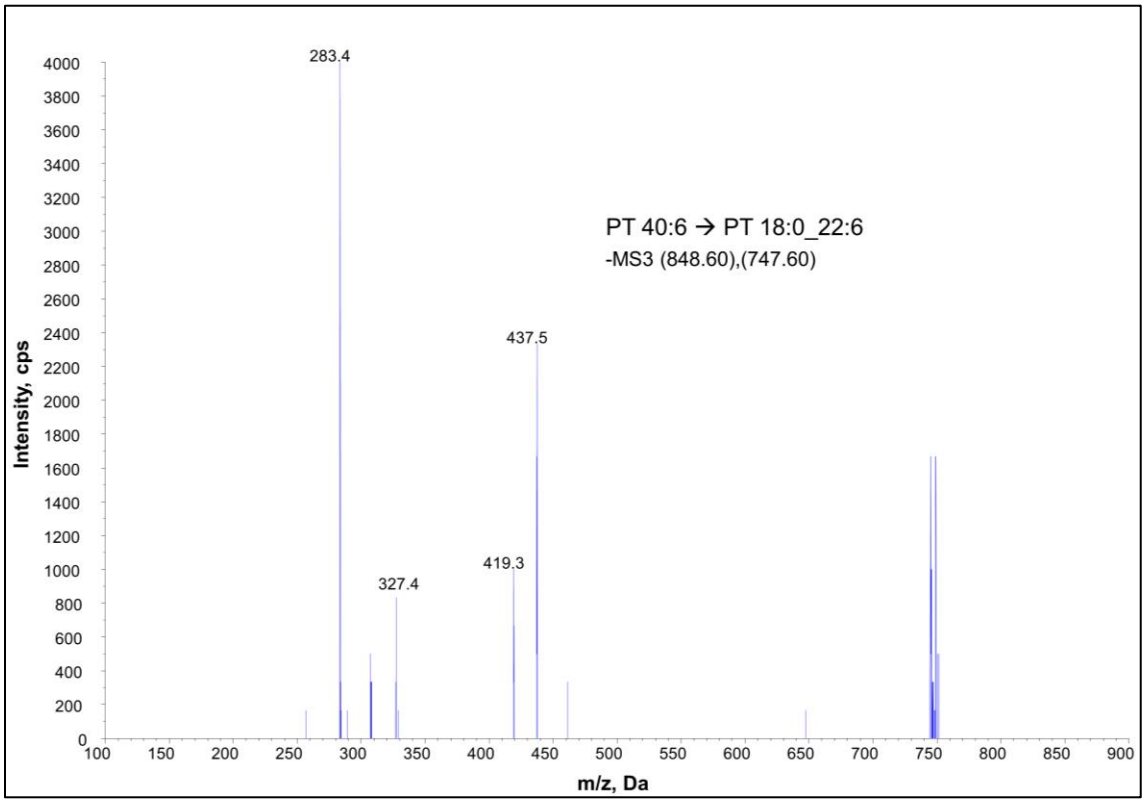
283.4
PT 40:6 → PT 18:0_22:6
-MS3 (848.60),(747.60)
437.5
419.3
327.4
Intensity, cps
m/z, Da

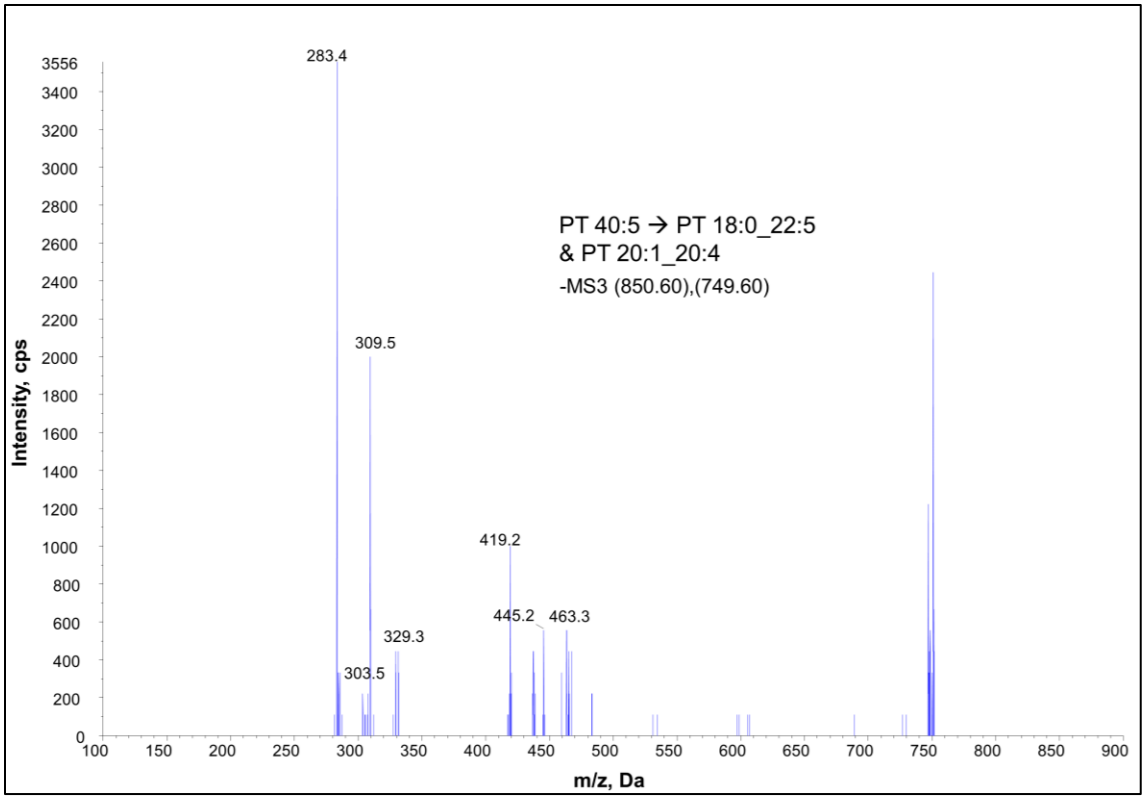
283.4
309.5
419.2
445.2
463.3
329.3
303.5
PT 40:5 → PT 18:0_22:5
& PT 20:1_20:4
-MS3 (850.60),(749.60)
Intensity, cps
m/z, Da

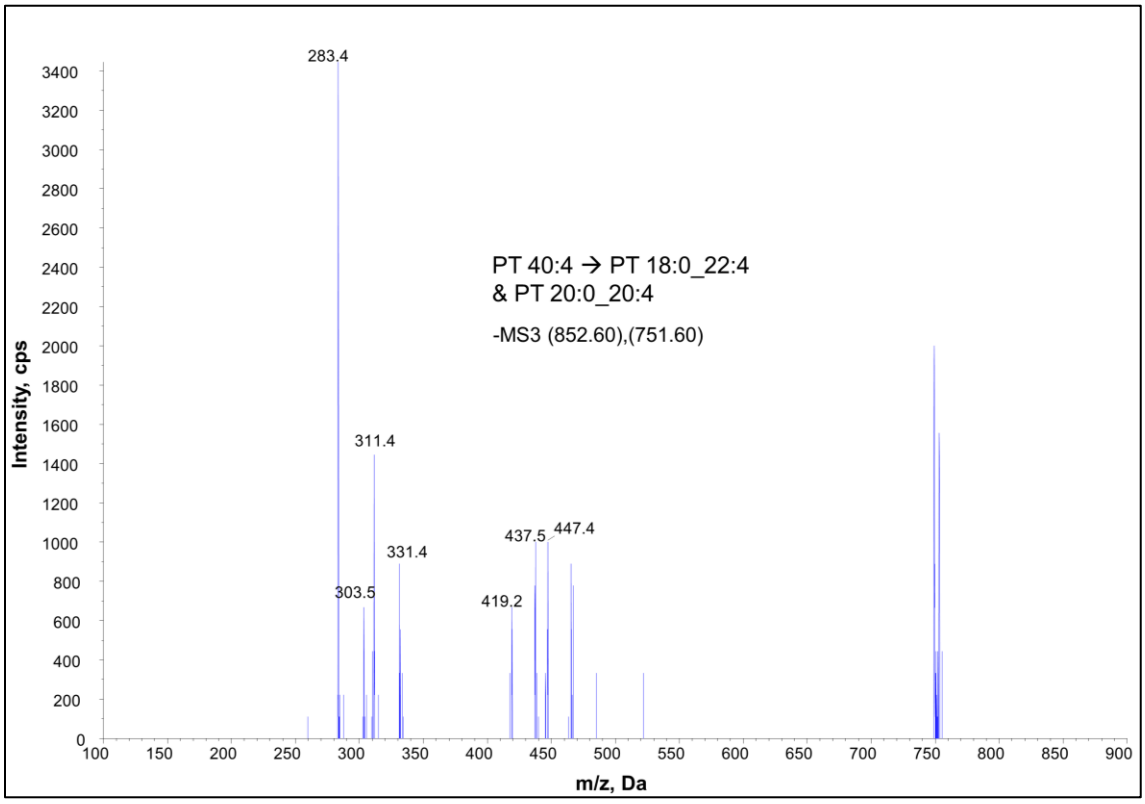
283.4
311.4
331.4
303.5
437.5
447.4
419.2
PT 40:4 → PT 18:0_22:4
& PT 20:0_20:4
-MS3 (852.60),(751.60)
Intensity, cps
m/z, Da

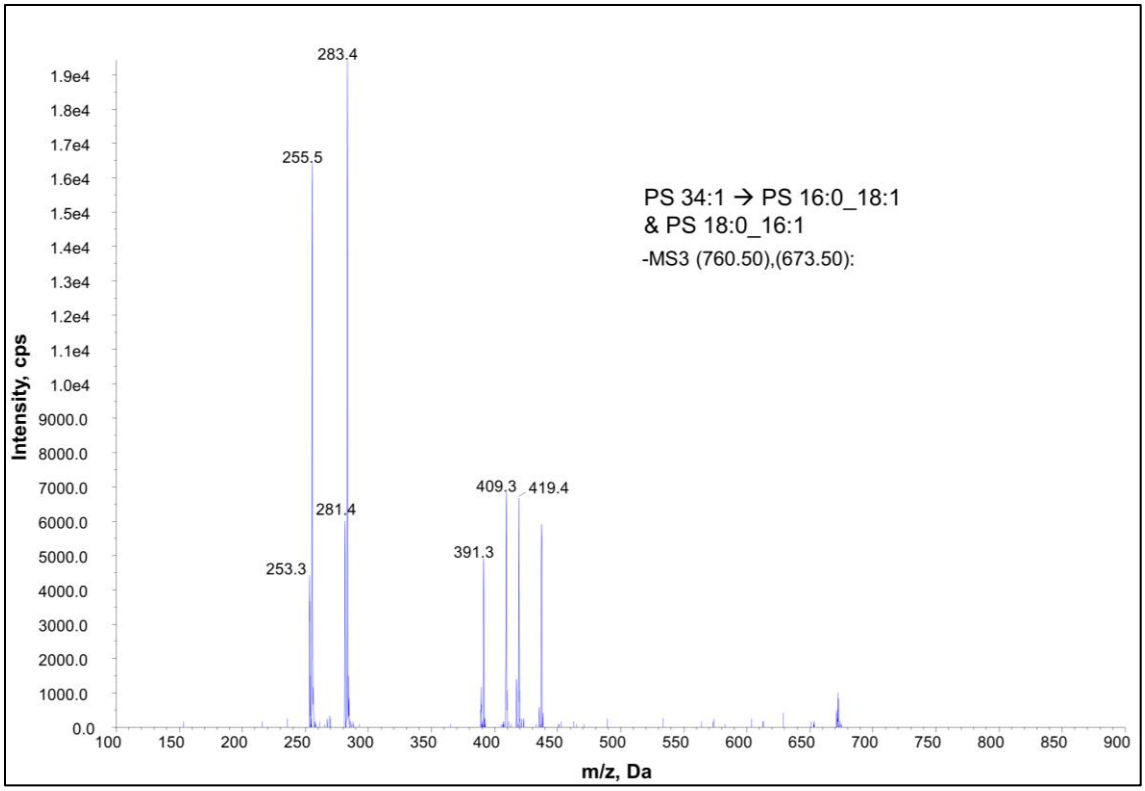
283.4
255.5
PS 34:1 → PS 16:0_18:1
& PS 18:0_16:1
-MS3 (760.50),(673.50):
409.3
419.4
281.4
391.3
253.3
Intensity, cps
m/z, Da

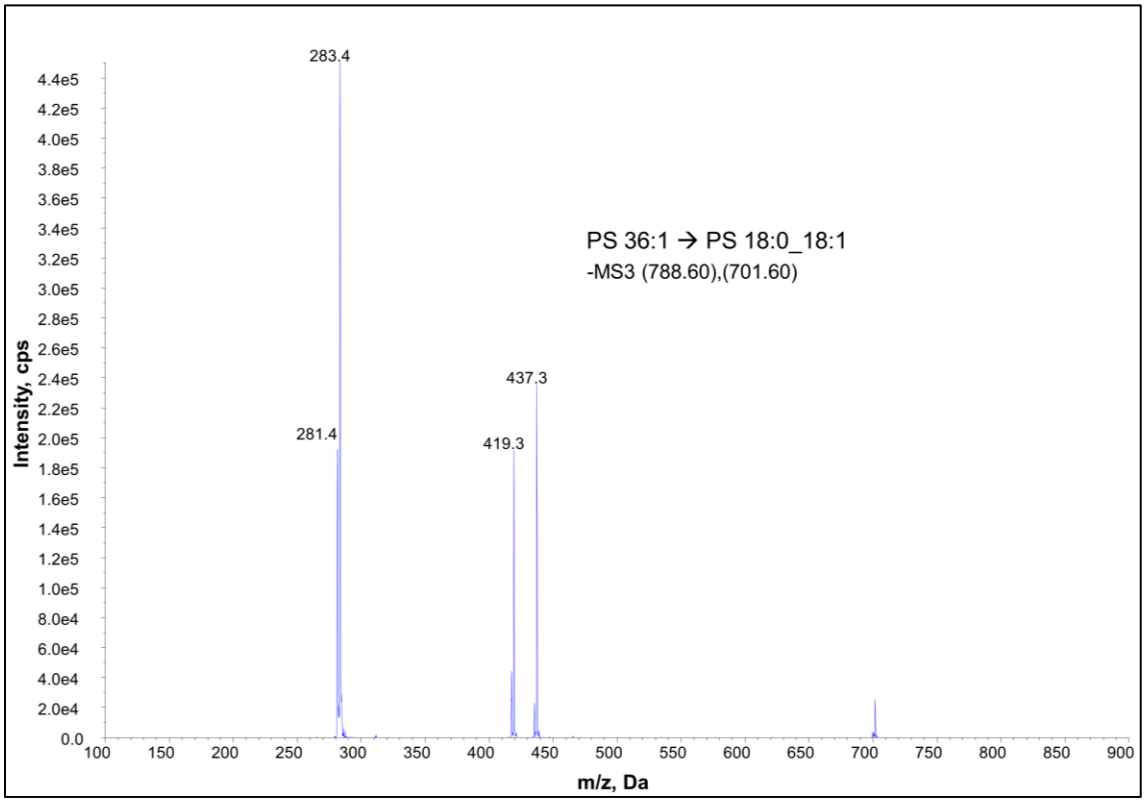
283.4
PS 36:1 → PS 18:0_18:1
-MS3 (788.60),(701.60)
437.3
281.4
419.3
Intensity, cps
m/z, Da

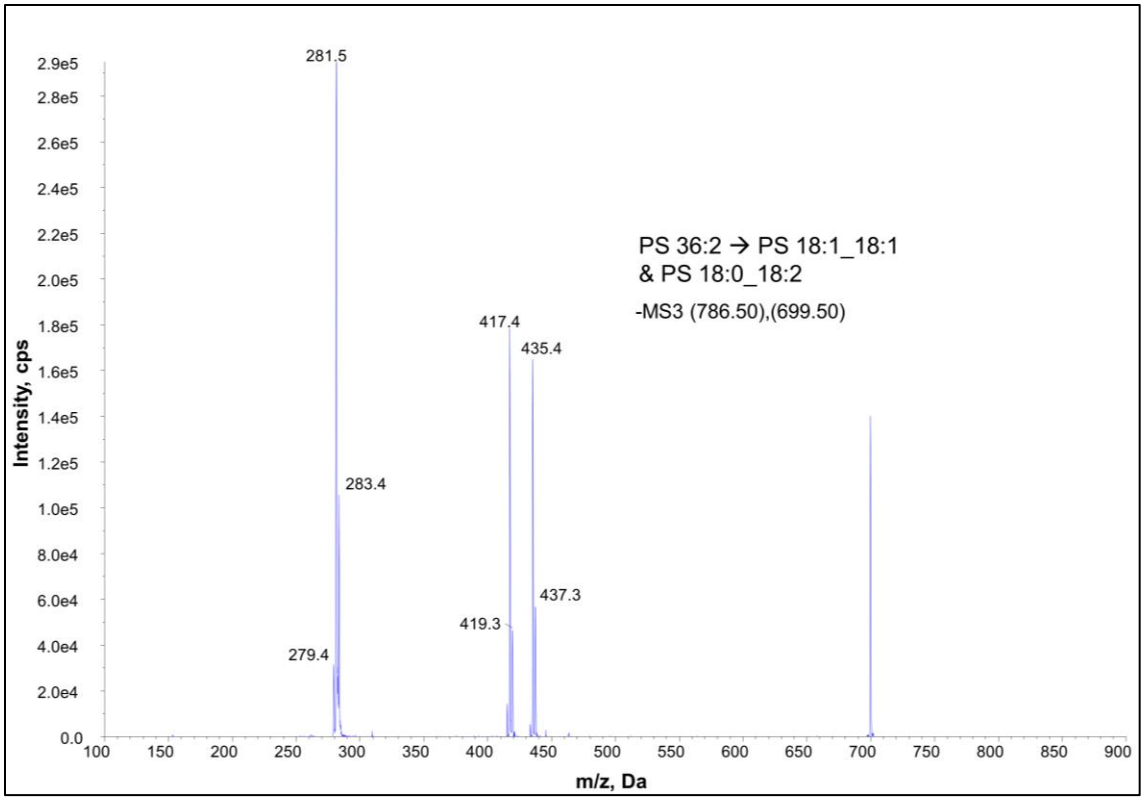
281.5
417.4
435.4
283.4
437.3
419.3
279.4
PS 36:2 → PS 18:1_18:1
& PS 18:0_18:2
-MS3 (786.50),(699.50)
Intensity, cps
m/z, Da

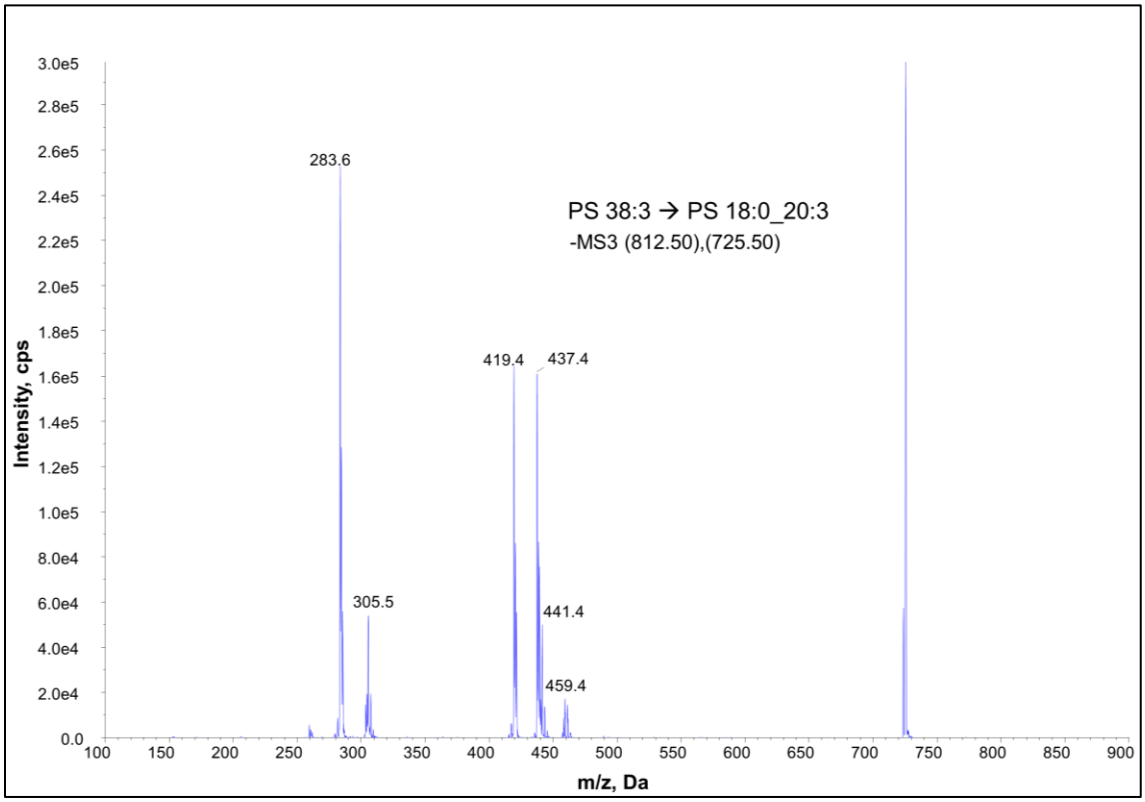
283.6
419.4
437.4
305.5
441.4
459.4
PS 38:3 → PS 18:0_20:3
-MS3 (812.50),(725.50)
Intensity, cps
m/z, Da

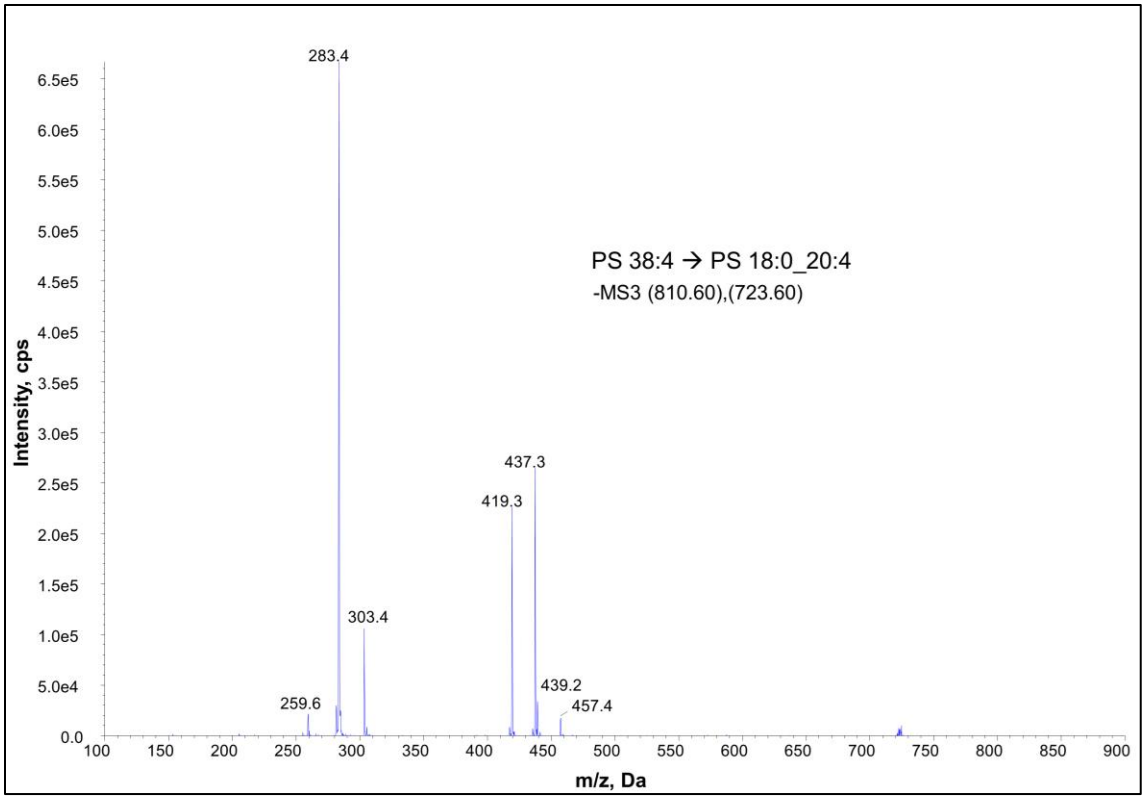
283.4
PS 38:4 → PS 18:0_20:4
-MS3 (810.60),(723.60)
437.3
419.3
303.4
439.2
259.6
457.4
Intensity, cps
m/z, Da

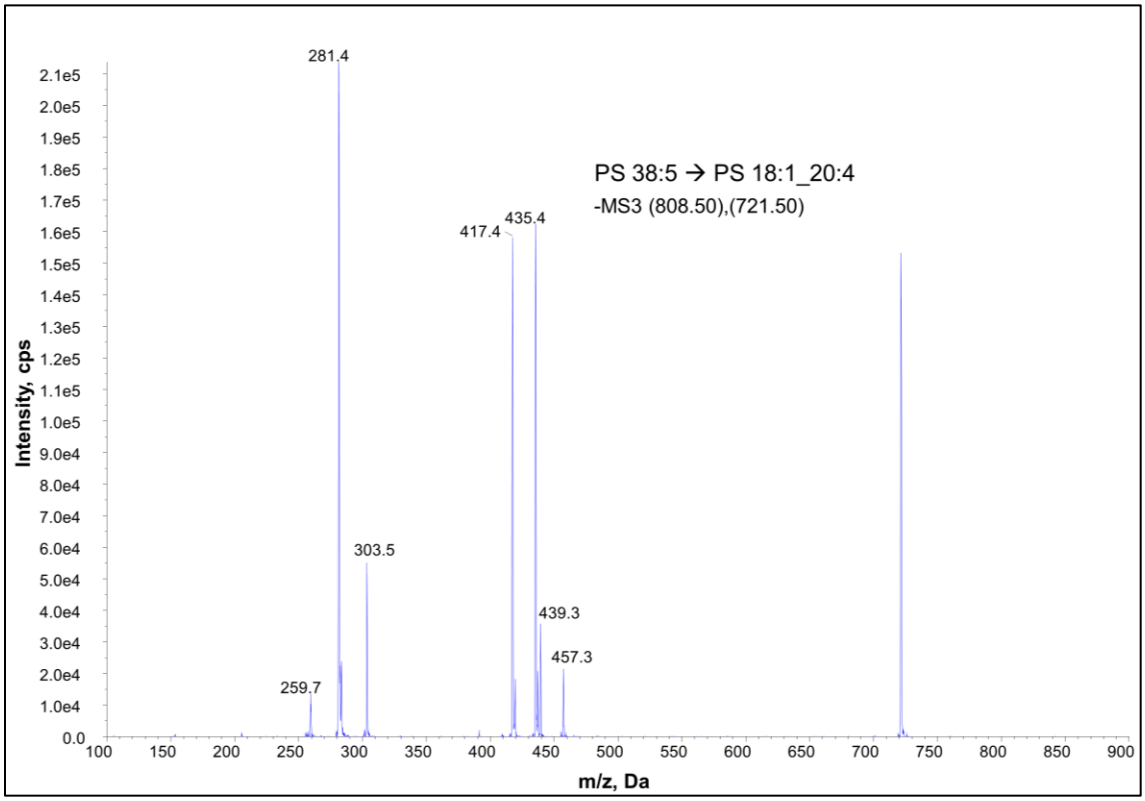
281.4
PS 38:5 → PS 18:1_20:4
-MS3 (808.50),(721.50)
435.4
417.4
303.5
439.3
457.3
259.7
Intensity, cps
m/z, Da

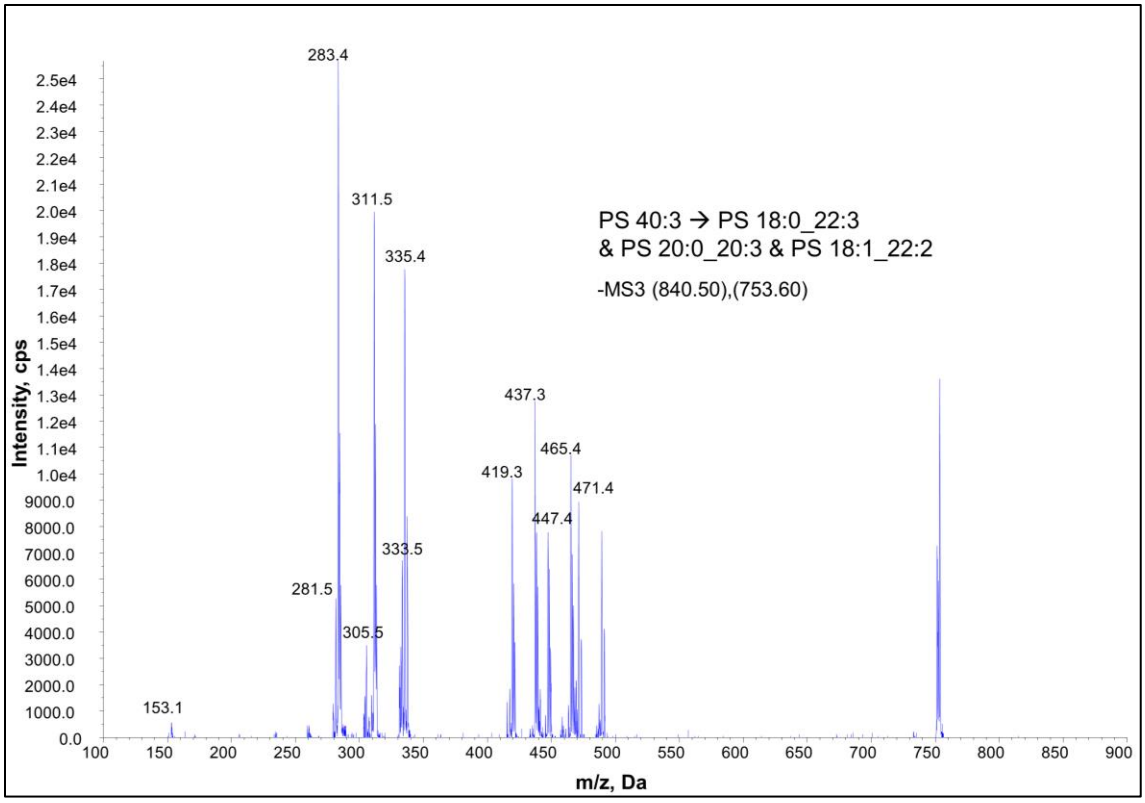
PS 40:3 → PS 18:0_22:3
& PS 20:0_20:3 & PS 18:1_22:2
-MS3 (840.50),(753.60)
Intensity, cps
m/z, Da
283.4
311.5
335.4
437.3
465.4
419.3
471.4
447.4
333.5
281.5
305.5
153.1

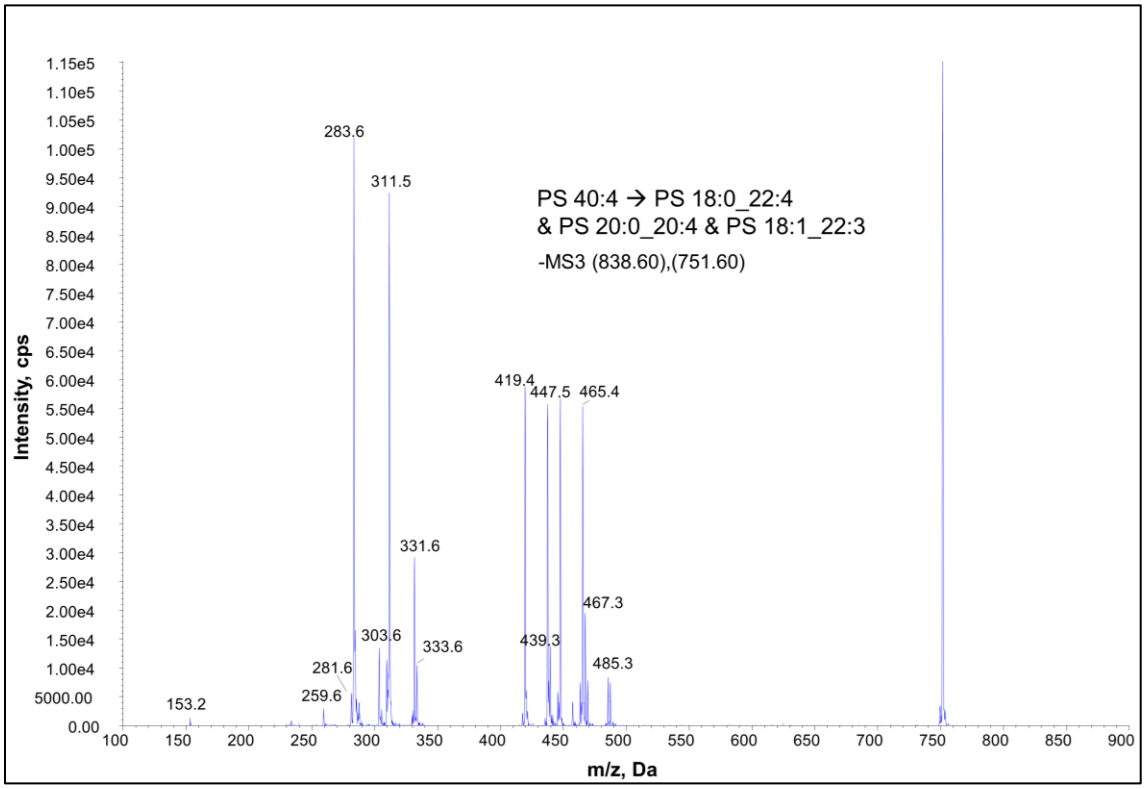
PS 40:4 → PS 18:0_22:4
& PS 20:0_20:4 & PS 18:1_22:3
-MS3 (838.60),(751.60)
Intensity, cps
m/z, Da
283.6
311.5
419.4
447.5
465.4
331.6
467.3
303.6
333.6
439.3
485.3
281.6
259.6
153.2

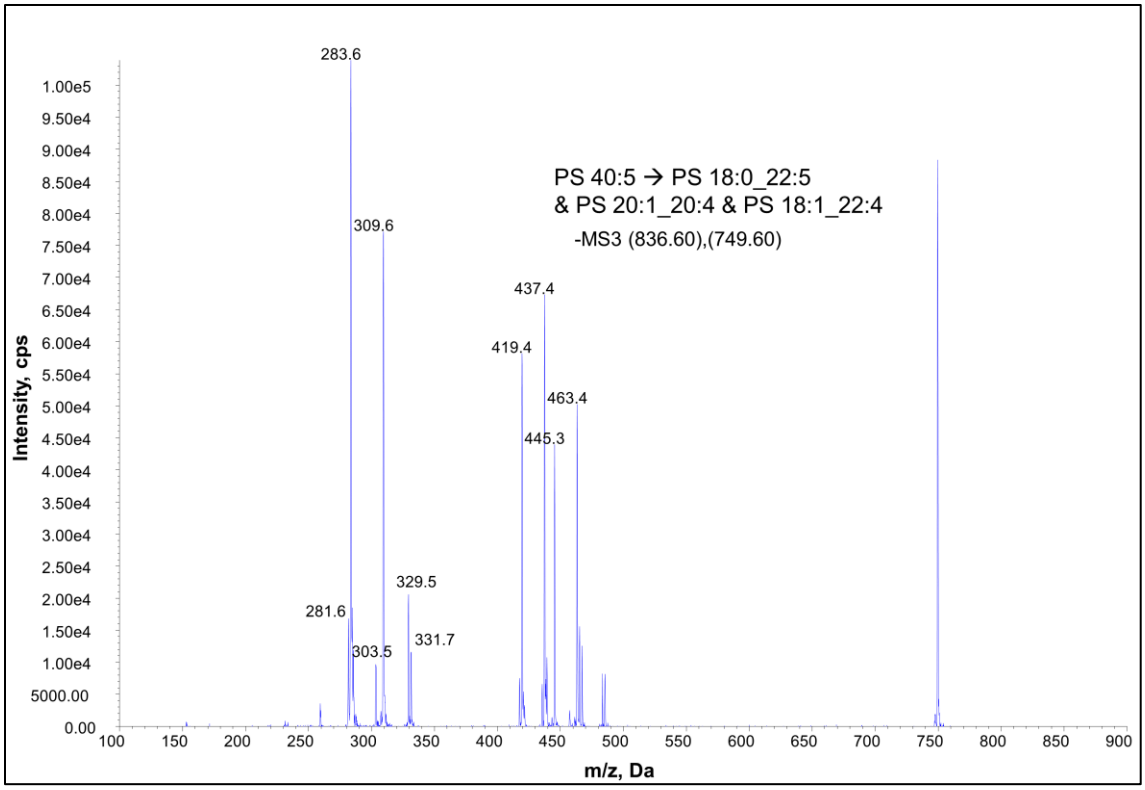
283.6
309.6
437.4
419.4
463.4
445.3
329.5
281.6
331.7
303.5
PS 40:5 → PS 18:0_22:5
& PS 20:1_20:4 & PS 18:1_22:4
-MS3 (836.60),(749.60)
Intensity, cps
m/z, Da

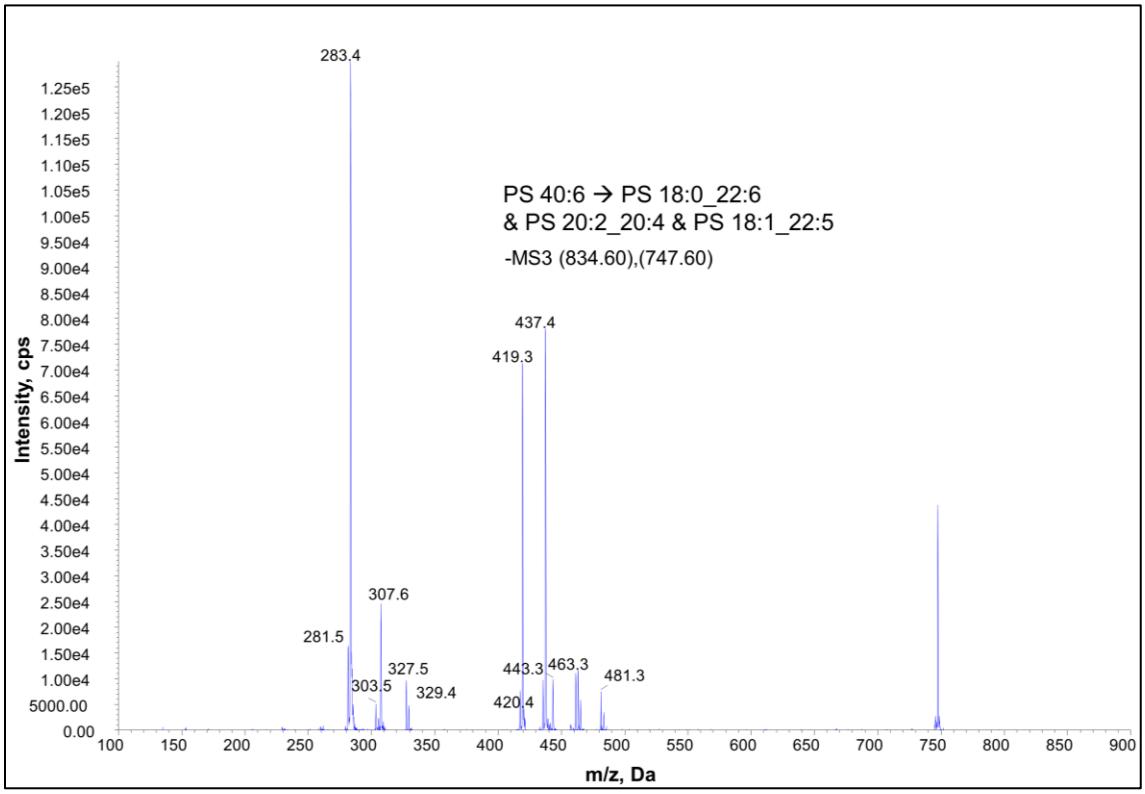
283.4
437.4
419.3
307.6
281.5
327.5
303.5
329.4
443.3
463.3
481.3
420.4
PS 40:6 → PS 18:0_22:6
& PS 20:2_20:4 & PS 18:1_22:5
-MS3 (834.60),(747.60)
Intensity, cps
m/z, Da

## 9.10 $MS^3$ spectra of PS & PT species from leukocytes

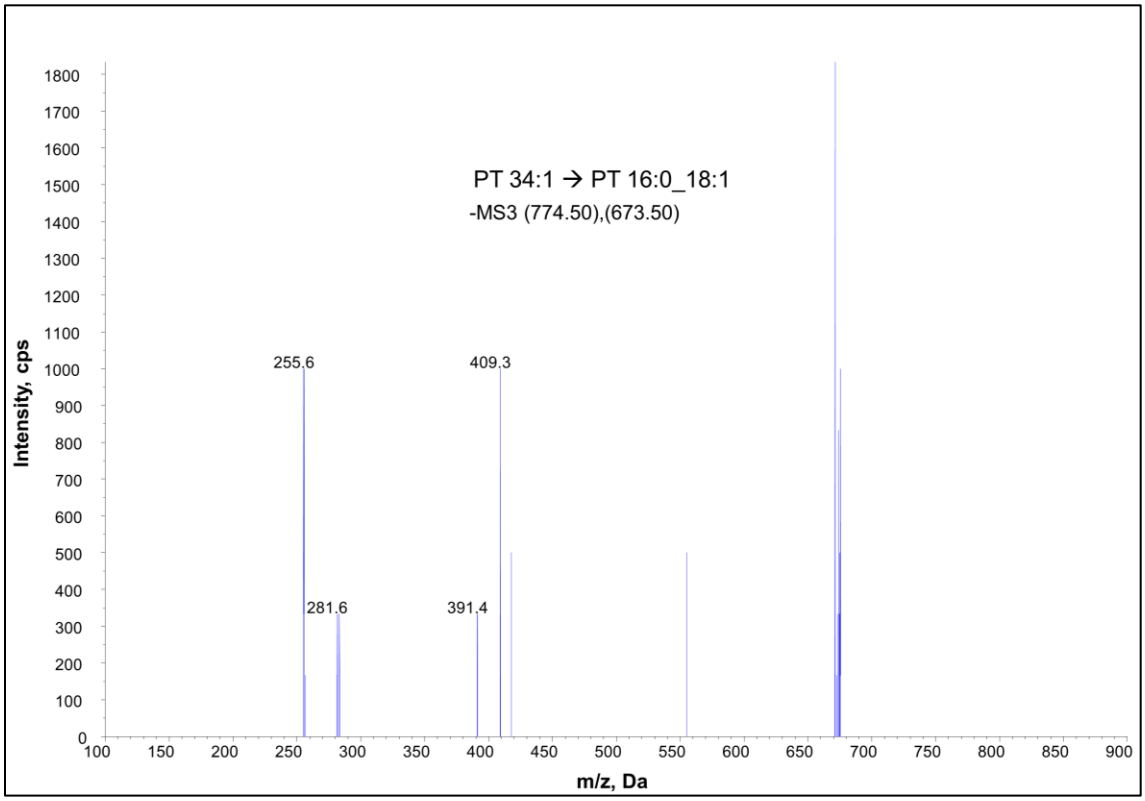


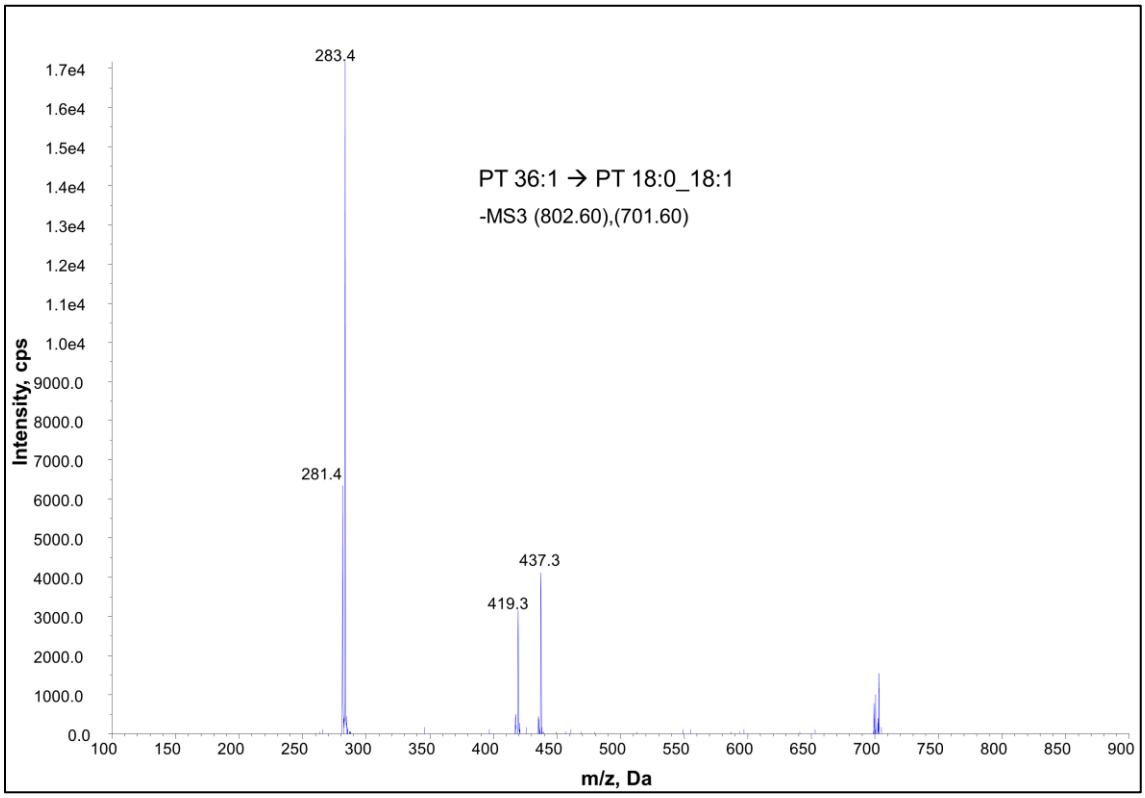

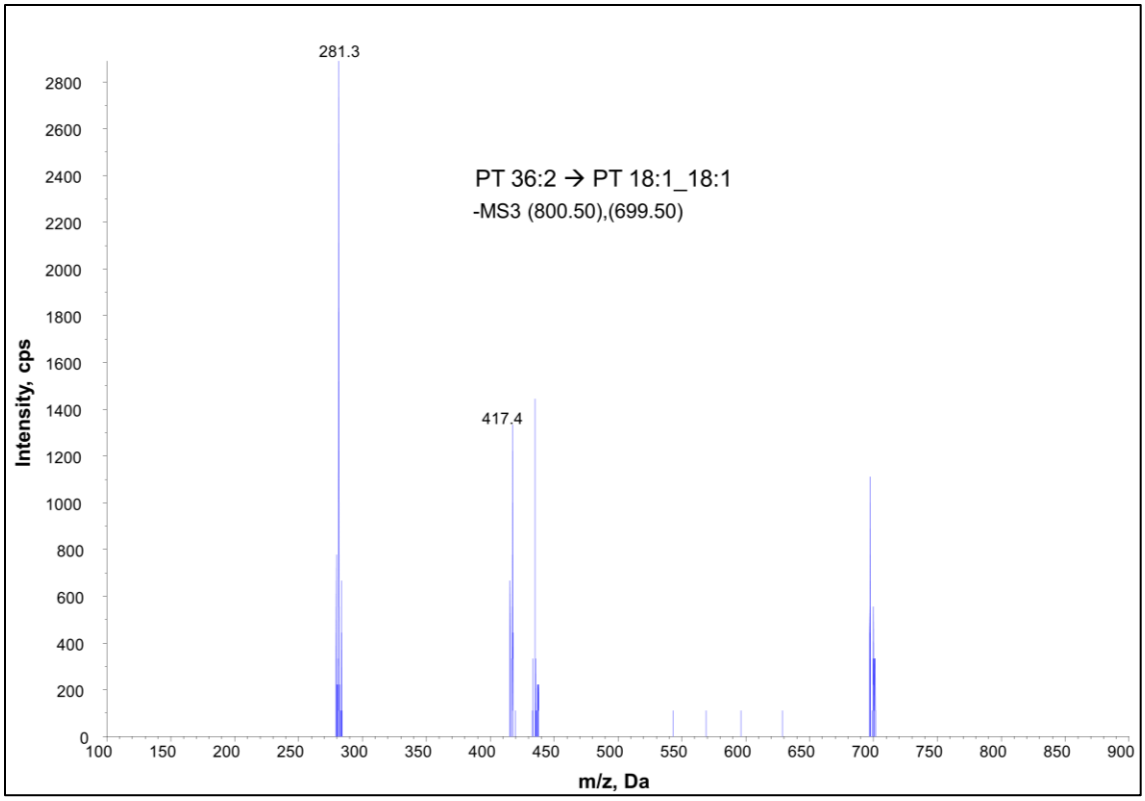
281.3
PT 36:2 → PT 18:1_18:1
-MS3 (800.50),(699.50)
417.4
Intensity, cps
m/z, Da

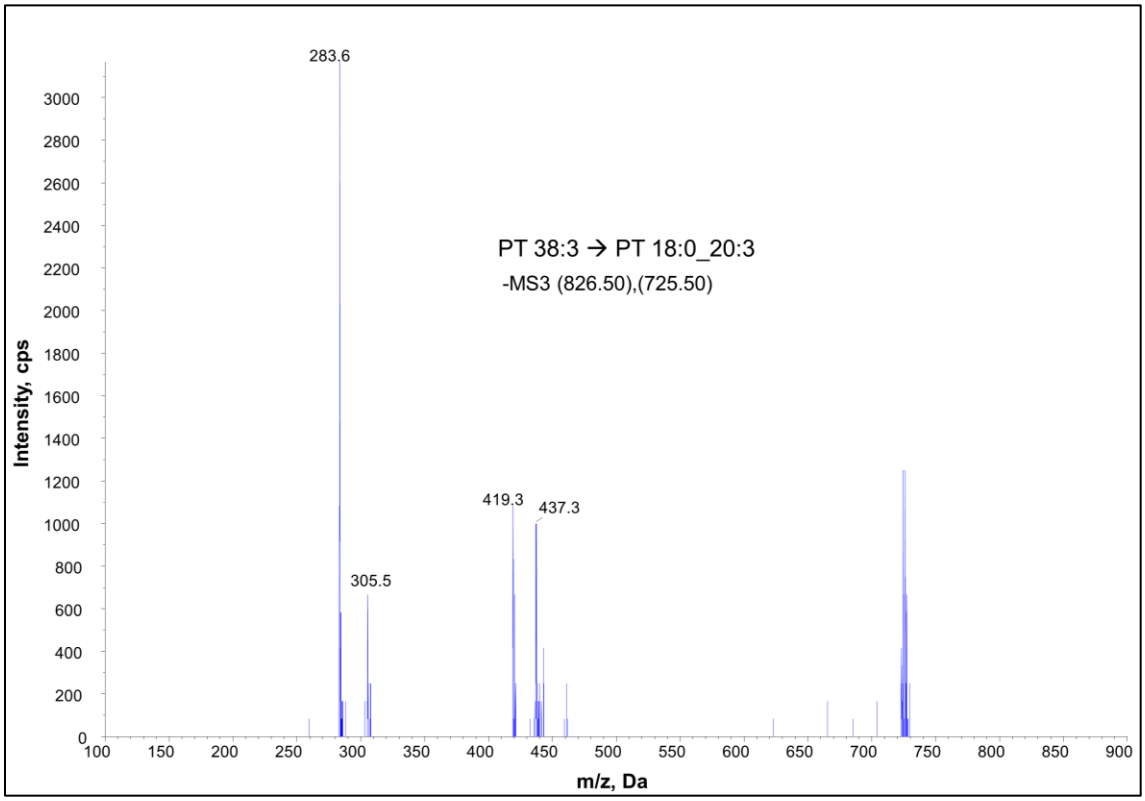
283.6
PT 38:3 → PT 18:0_20:3
-MS3 (826.50),(725.50)
419.3
437.3
305.5
Intensity, cps
m/z, Da

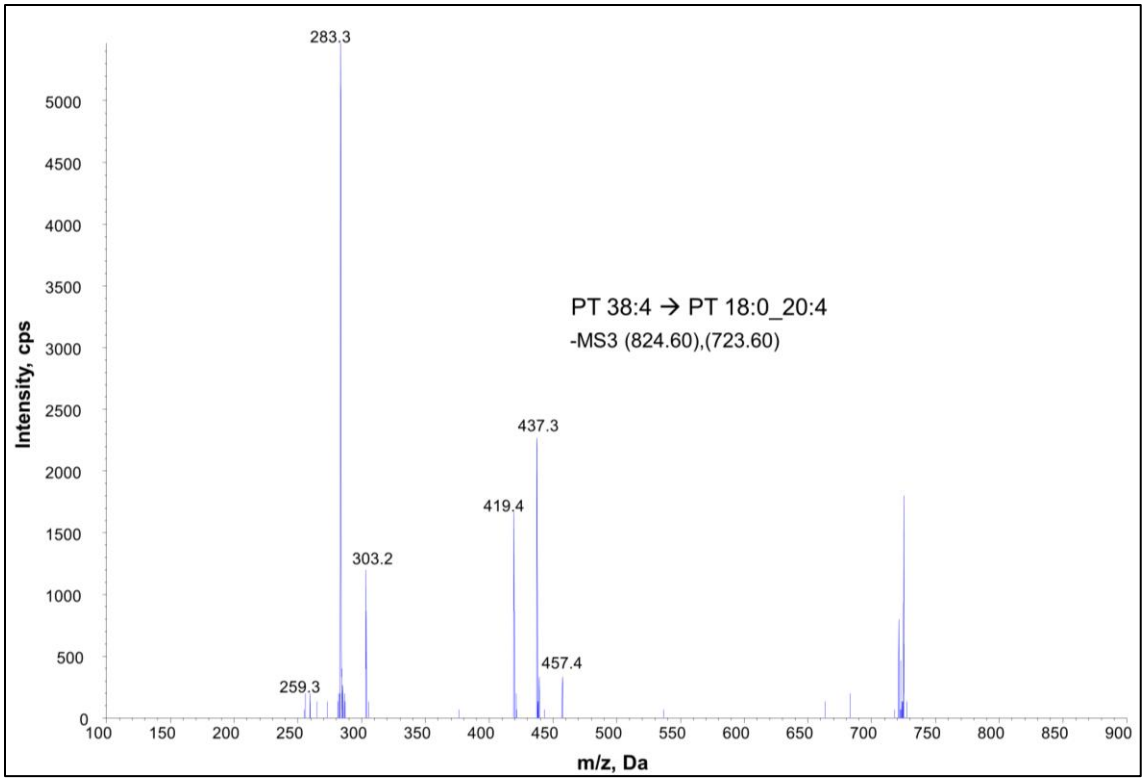
283.3
437.3
419.4
303.2
457.4
259.3
PT 38:4 → PT 18:0_20:4
-MS3 (824.60),(723.60)
Intensity, cps
m/z, Da

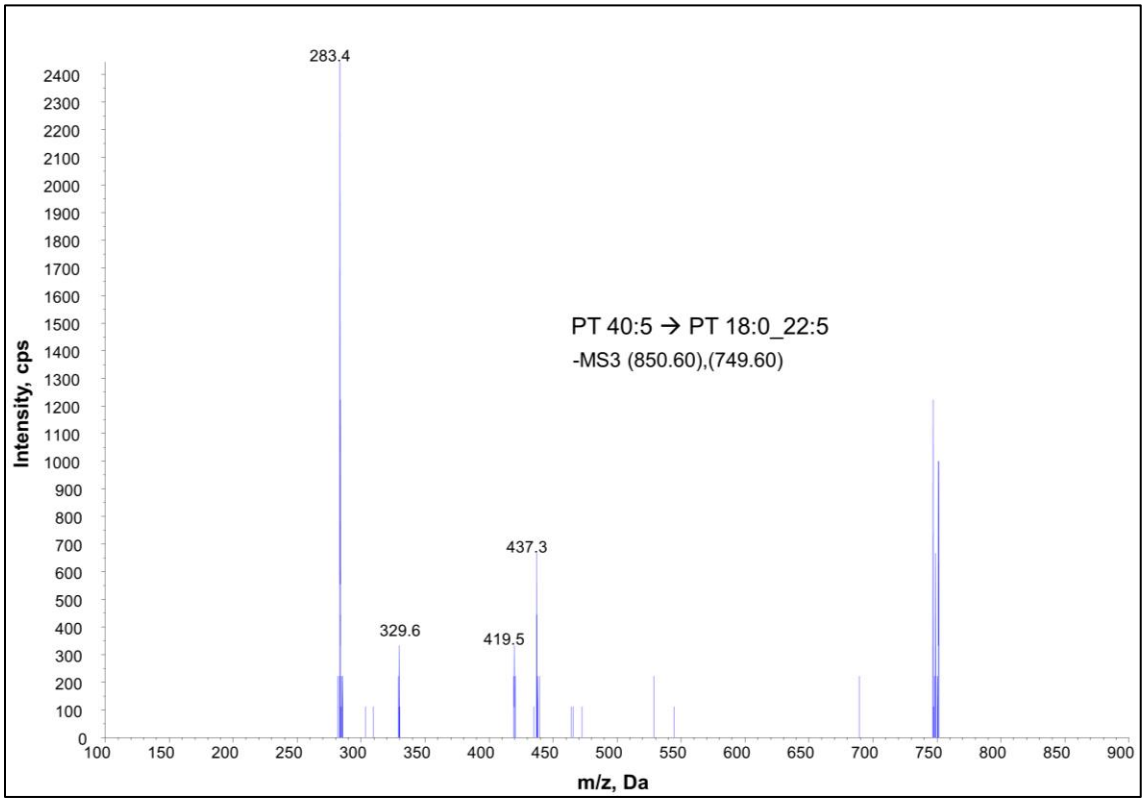
283.4
437.3
329.6
419.5
PT 40:5 → PT 18:0_22:5
-MS3 (850.60),(749.60)
Intensity, cps
m/z, Da

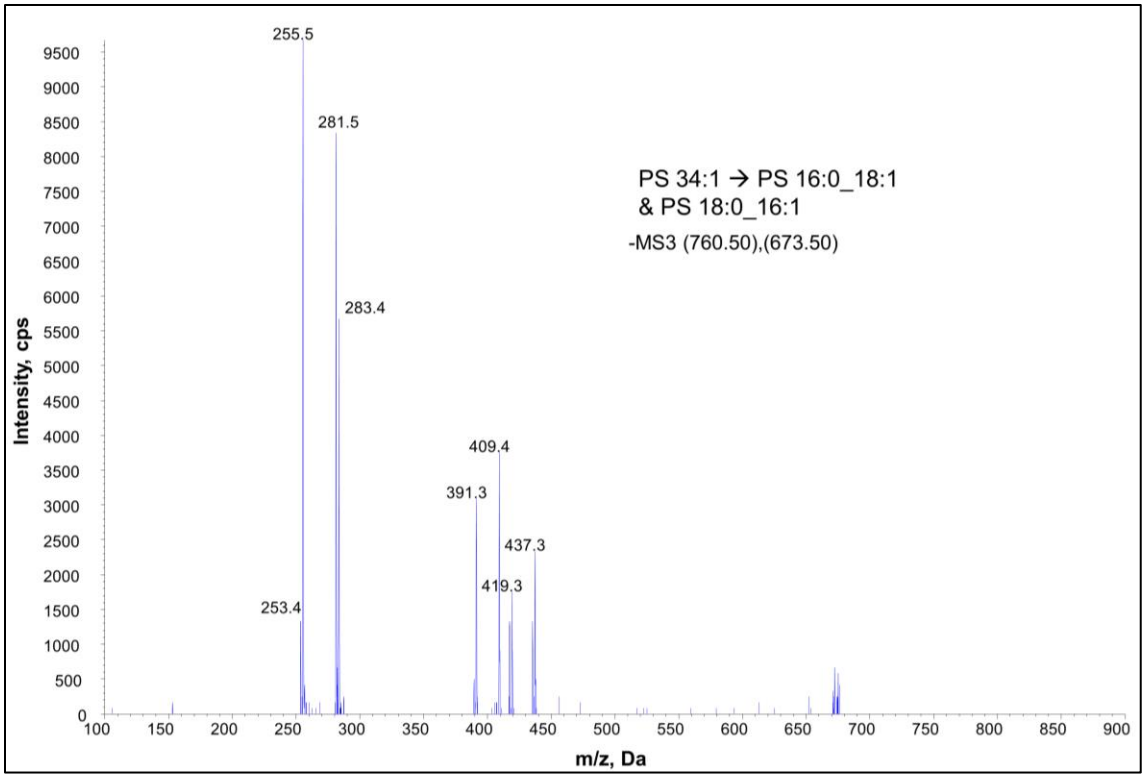
255.5
281.5
283.4
409.4
391.3
437.3
419.3
253.4
PS 34:1 → PS 16:0_18:1
& PS 18:0_16:1
-MS3 (760.50),(673.50)
Intensity, cps
m/z, Da

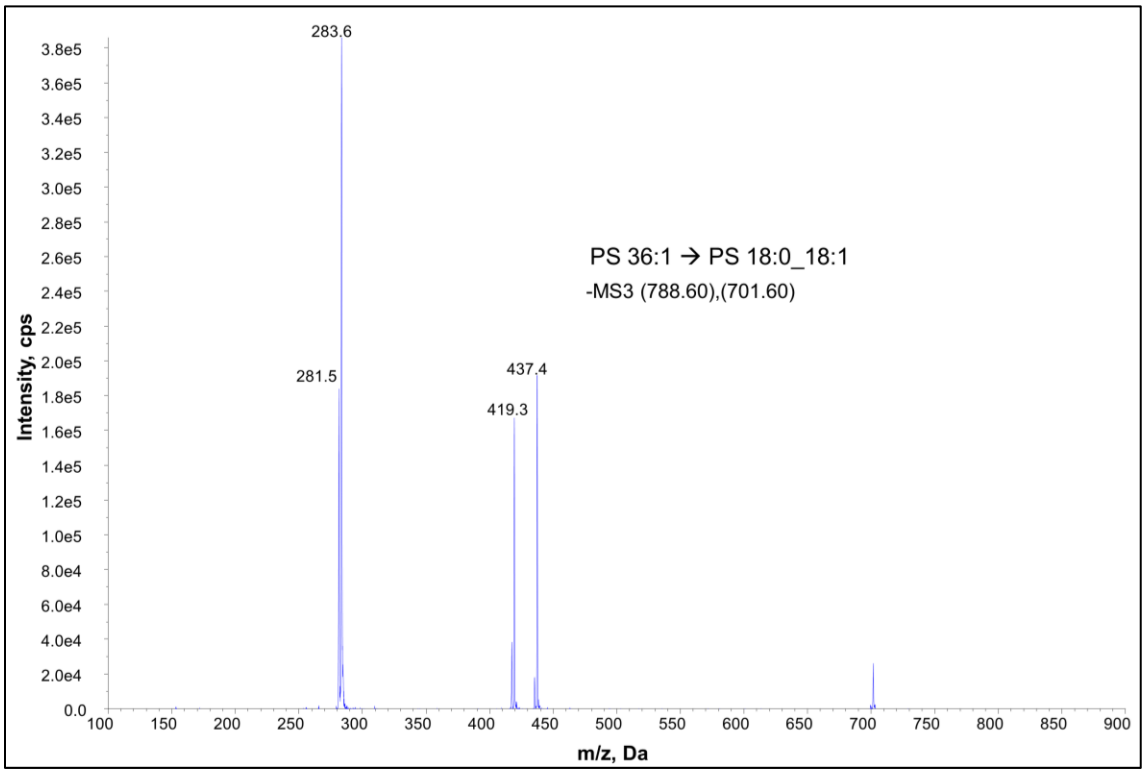
283.6
281.5
437.4
419.3
PS 36:1 → PS 18:0_18:1
-MS3 (788.60),(701.60)
Intensity, cps
m/z, Da

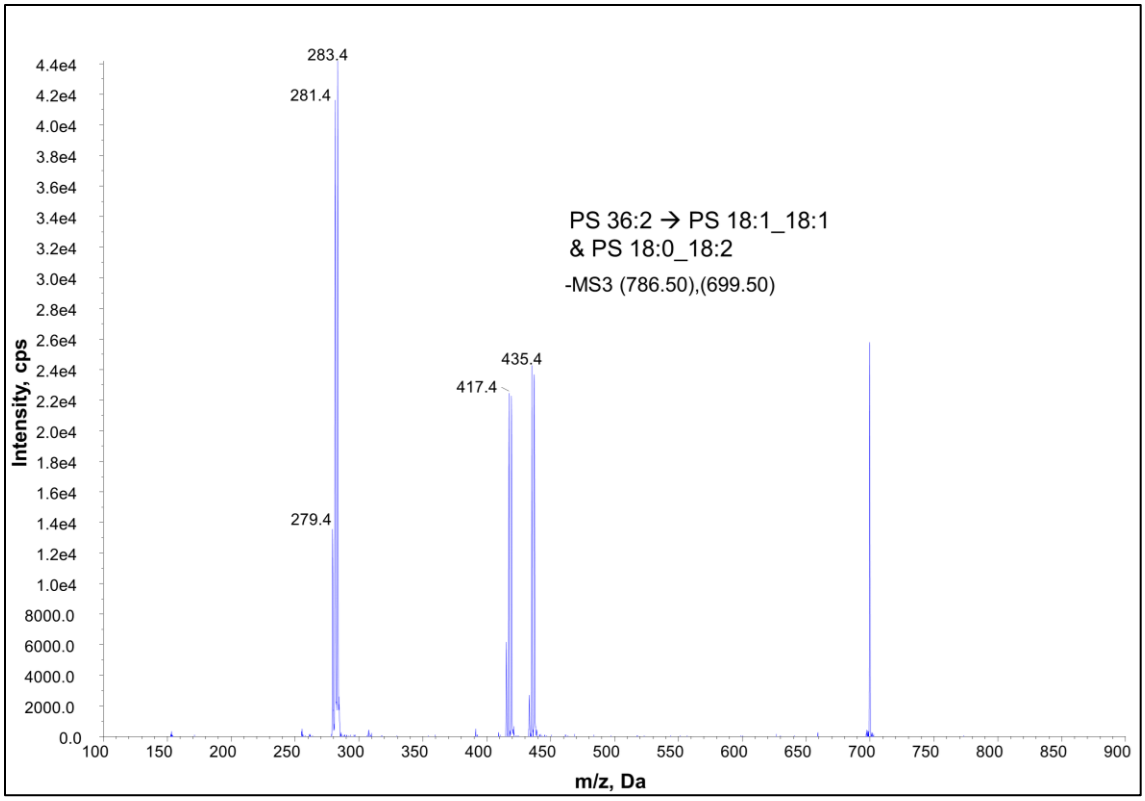
283.4
281.4
435.4
417.4
279.4
PS 36:2 → PS 18:1_18:1
& PS 18:0_18:2
-MS3 (786.50),(699.50)
Intensity, cps
m/z, Da

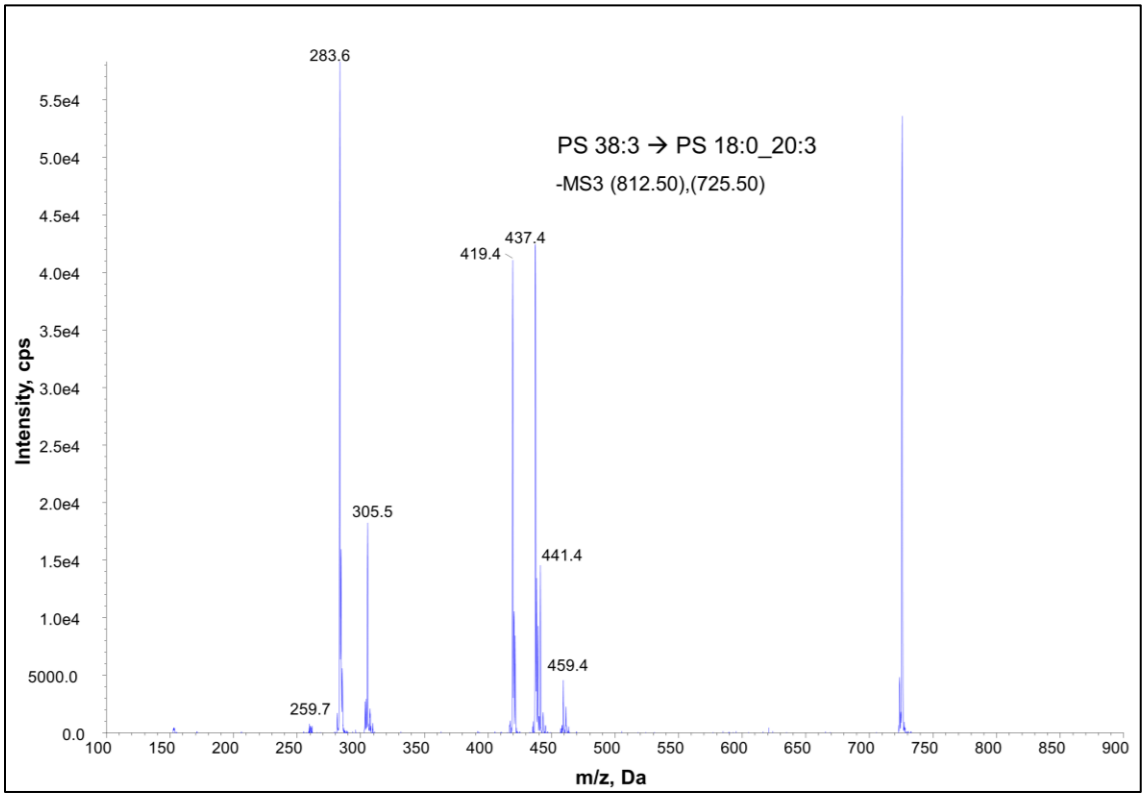
283.6
437.4
419.4
305.5
441.4
459.4
259.7
PS 38:3 → PS 18:0_20:3
-MS3 (812.50),(725.50)
Intensity, cps
m/z, Da

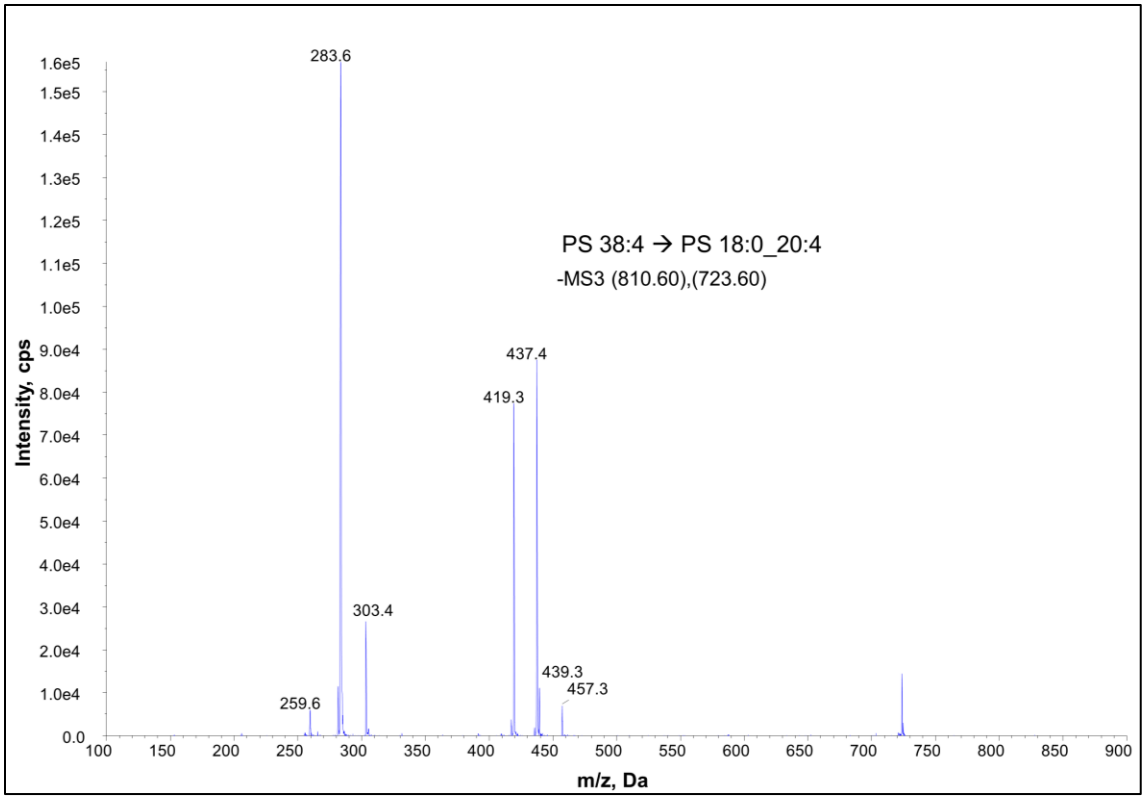
PS 38:4 → PS 18:0_20:4
-MS3 (810.60),(723.60)
283.6
437.4
419.3
303.4
439.3
457.3
259.6
Intensity, cps
m/z, Da

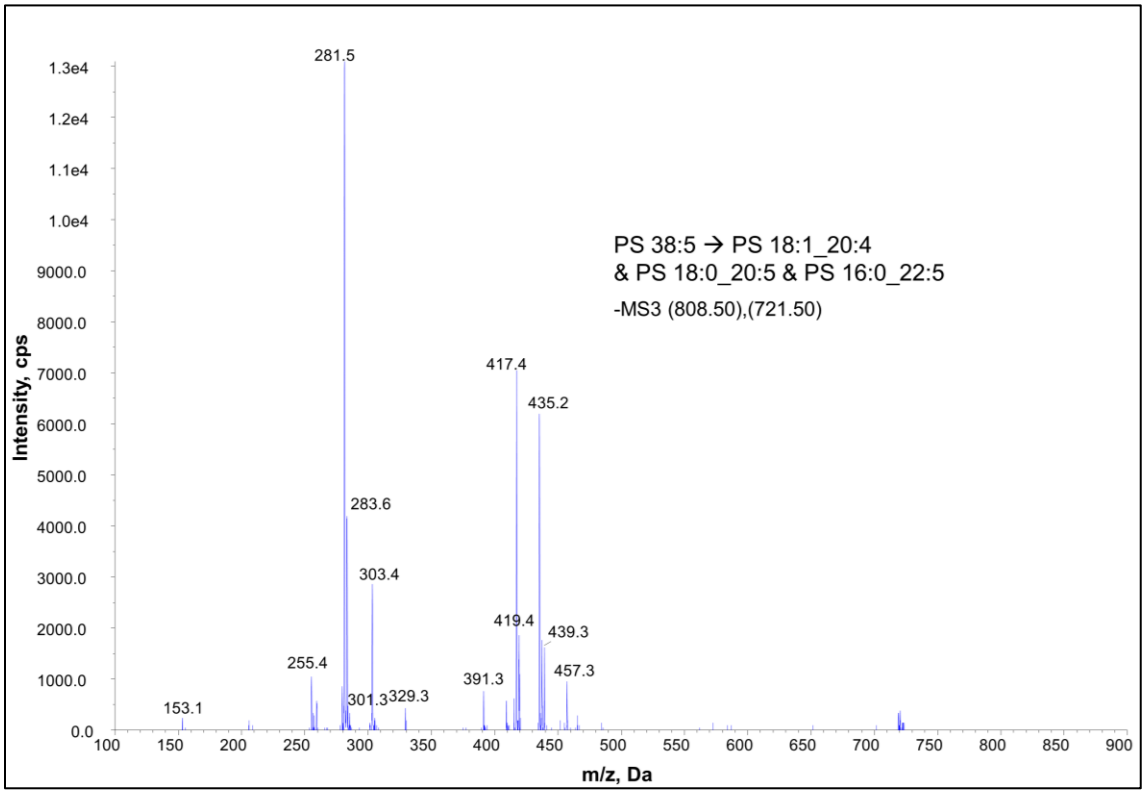
PS 38:5 → PS 18:1_20:4
& PS 18:0_20:5 & PS 16:0_22:5
-MS3 (808.50),(721.50)
281.5
417.4
435.2
283.6
303.4
419.4
439.3
255.4
457.3
391.3
301.3
329.3
153.1
Intensity, cps
m/z, Da

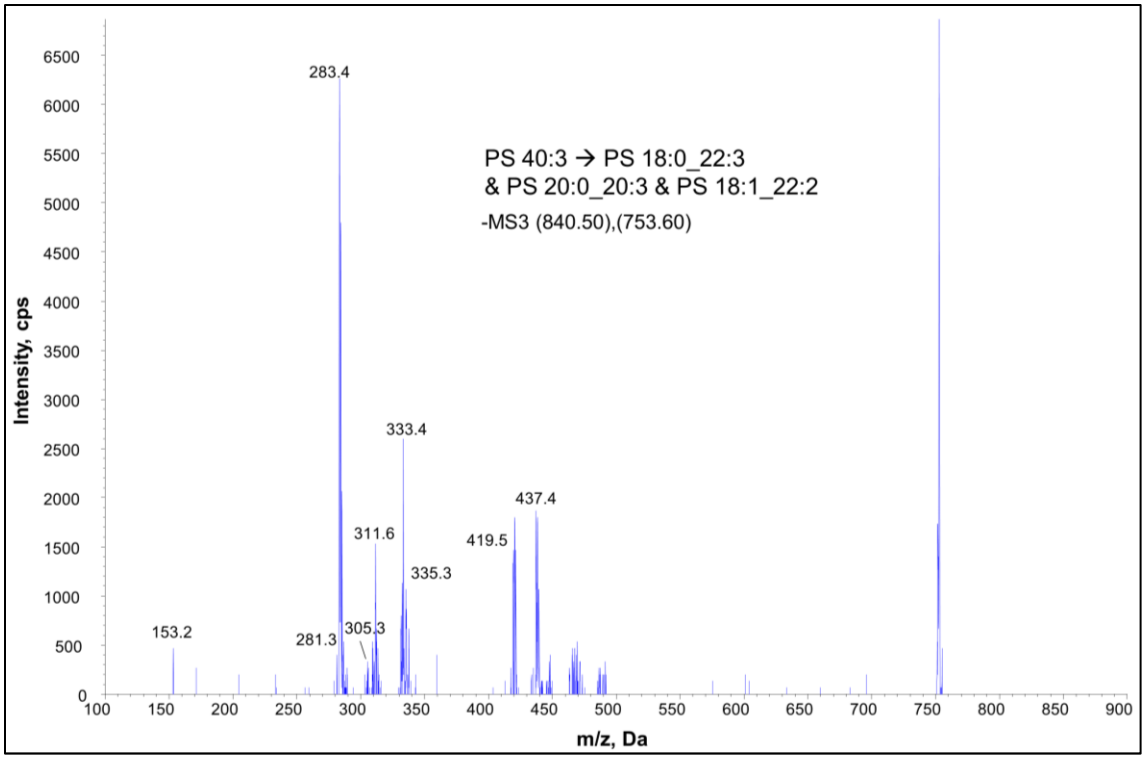
PS 40:3 → PS 18:0_22:3
& PS 20:0_20:3 & PS 18:1_22:2
-MS3 (840.50),(753.60)
283.4
333.4
437.4
311.6
419.5
335.3
153.2
281.3
305.3
Intensity, cps
m/z, Da

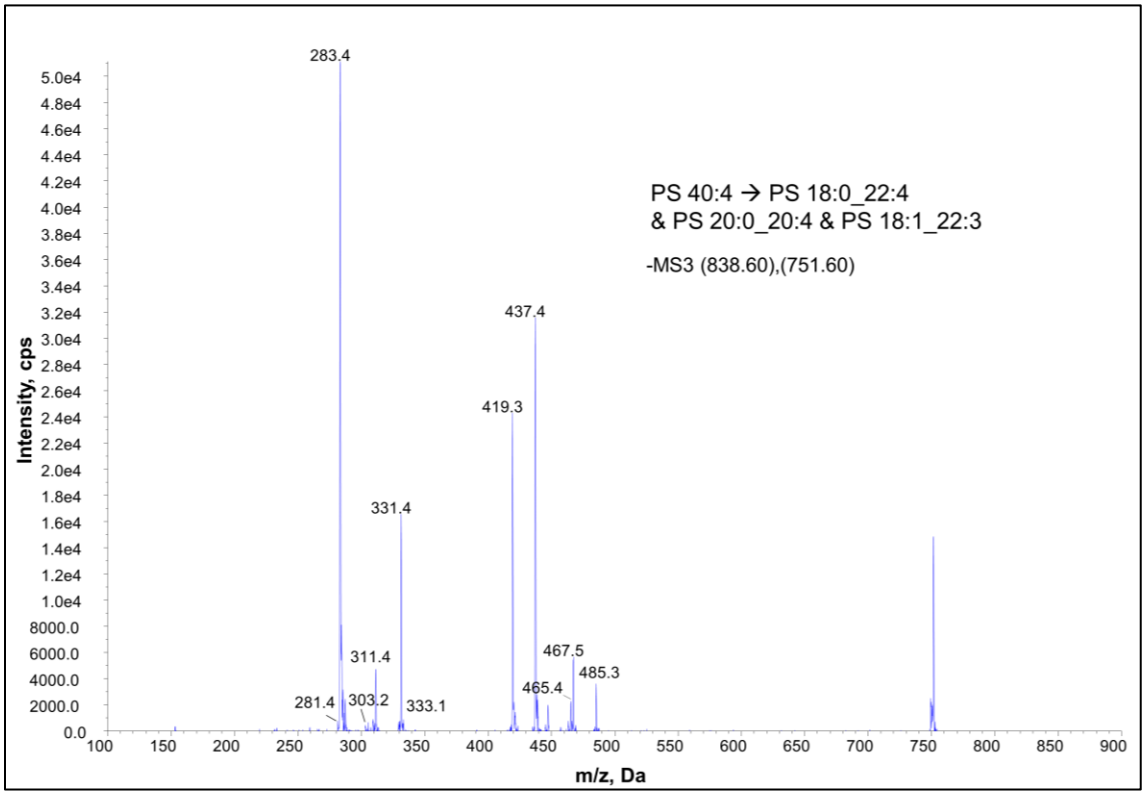
PS 40:4 → PS 18:0_22:4
& PS 20:0_20:4 & PS 18:1_22:3
-MS3 (838.60),(751.60)
283.4
437.4
419.3
331.4
311.4
467.5
485.3
465.4
281.4
303.2
333.1
Intensity, cps
m/z, Da

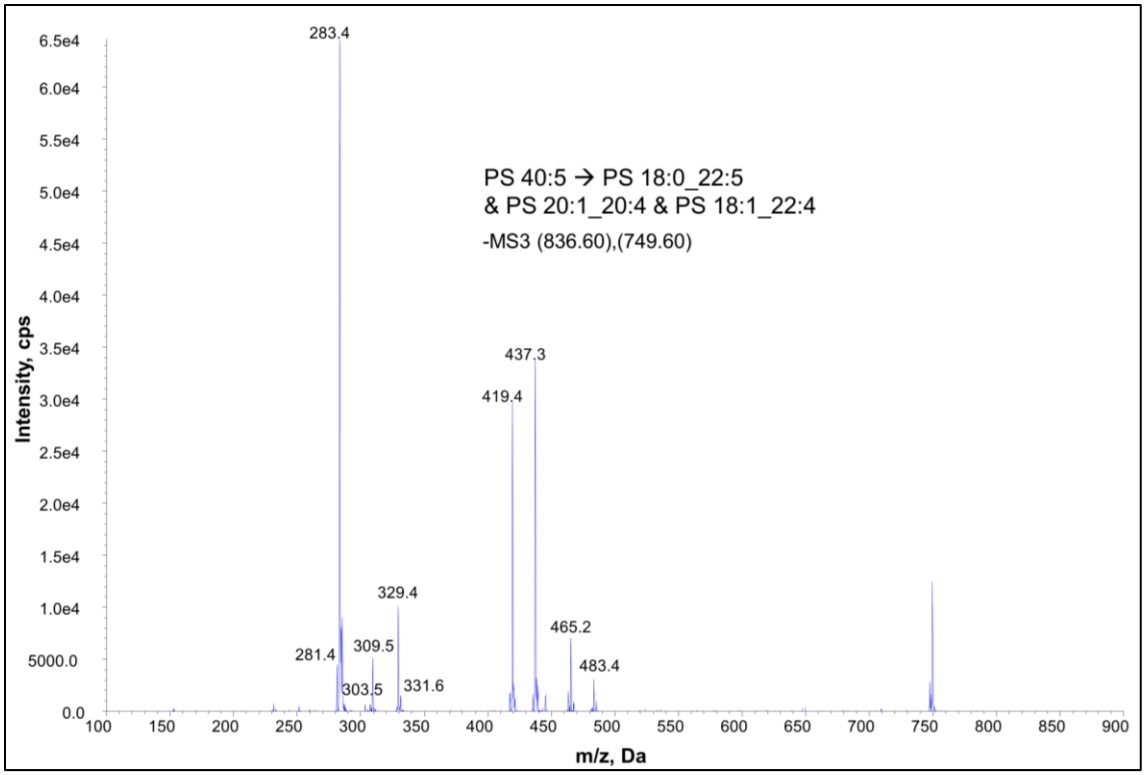
PS 40:5 → PS 18:0_22:5
& PS 20:1_20:4 & PS 18:1_22:4
-MS3 (836.60),(749.60)
283.4
437.3
419.4
329.4
465.2
309.5
281.4
483.4
303.5
331.6
Intensity, cps
m/z, Da

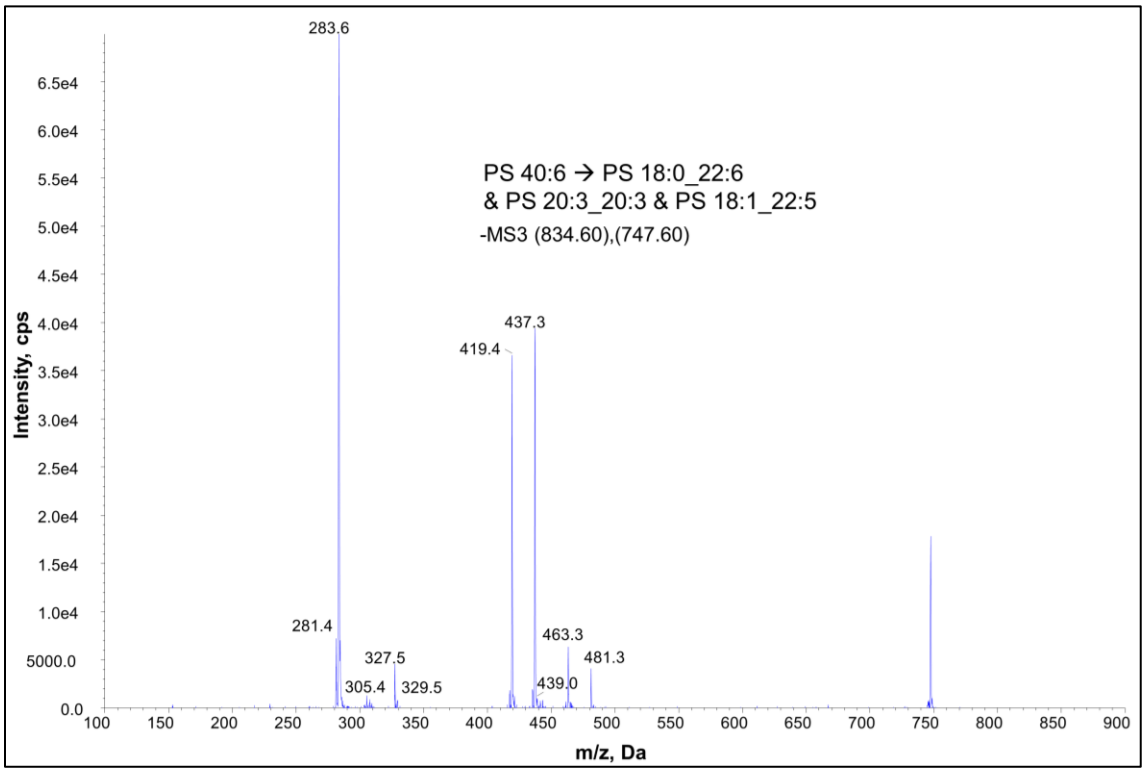
PS 40:6 → PS 18:0_22:6
& PS 20:3_20:3 & PS 18:1_22:5
-MS3 (834.60),(747.60)
283.6
437.3
419.4
463.3
281.4
481.3
327.5
305.4
329.5
439.0
Intensity, cps
m/z, Da